universität wien

DISSERTATION

Titel der Dissertation

Macroscopic Quantum Systems and Gravitational Phenomena

Verfasser

Dipl.-Phys. Igor Pikovski

angestrebter akademischer Grad

Doktor der Naturwissenschaften (Dr. rer. nat.)

Wien, 2014

Studienkennzahl lt. Studienblatt:	A 091 411
Dissertationsgebiet lt. Studienblatt:	Physik
Betreuer:	Univ.-Prof. Mag. Dr. Časlav Brukner

Contents

Abstract

In the past 30 years, crucial techniques have been developed to manipulate and to control physical systems on the quantum scale. The theoretical and experimental developments in quantum optics opened new research directions in quantum foundations and for technological applications on the single quantum level. Recently, quantum physics at larger scales has become increasingly accessible in experiments. Matter waves can now be controlled over large distances and quantum interference experiments can be performed with complex molecules. The interaction of light with a mechanical resonator can today be used to study and to manipulate the quantum properties of nano- and micro-scale mechanical devices, with masses ranging from picogram to kilogram scales. With new light-matter interactions, the ability to control quantum systems in new physical regimes and to perform high precision measurements opens the route to probe our current understanding of physics.

In this thesis, large quantum systems are theoretically studied in light of possible experiments to test the interplay between quantum theory and general relativity [1–5]. To this end, the work includes two main lines of research. In the first line of research, new interaction regimes of opto-mechanical systems are studied. It is shown that pulsed opto-mechanics can be used to prepare quantum states of massive mechanical resonators by measurements of light, and that pulsed opto-mechanics also offers the ability to perform full quantum state tomography of the resonator [1]. A scheme based on the pulsed interaction regime is then presented, which allows for experimental tests of some phenomenological models of quantum gravity: possible deformations of the canonical commutator of the center-of-mass mode of the mechanical resonator can be probed to very high accuracy [2]. Such deformations may occur for quantum systems due to possible quantum gravity induced modifications of the Heisenberg uncertainty relation. It is shown that the proposed experiment could put stringent bounds on such models for massive quantum systems.

The second line of research presented in this thesis is the study of general

relativistic time dilation within low-energy quantum theory [3–5]. It is shown that general relativistic corrections to Newtonian gravity, that stem from time dilation, lead to entirely new effects in quantum theory with no classical analogue. The slowdown of the time evolution of internal states of a quantum system in a gravitational field causes entanglement of the internal states to the position of the system. This results in periodic reduction and revival of quantum interference for matter-wave interference experiments that include internal clock-states [3]. A similar phenomenon for quantum states of light can be probed due to the Shapiro delay of single photons [4]. In addition, it is shown that the time-dilation-induced entanglement between internal states and the position causes universal decoherence of all composite quantum systems [5]. The thermal oscillations within any composite particle will cause its position degree-of-freedom to become classical. Thus time dilation causes the transition to classicality and the decoherence on Earth takes place on time scales that could in principle be observed in matter-wave experiments with large molecules or with microspheres.

The results of this thesis show that new phenomena arise when gravity is considered in quantum theory. Various quantum systems are considered which operate in new parameter regimes in terms of mass and size, and how they can be used for testing low energy quantum theory on a fixed background space-time and quantum gravity phenomenology. Thus it is shown that precision measurements in quantum theory allow for tests of the interplay between quantum theory and general relativity.

Zusammenfassung

In den letzten 30 Jahren wurden neue Möglichkeiten entwickelt physikalische Systeme auf der Quantenskala zu kontrollieren und zu manipulieren. Theoretische und experimentelle Entwicklungen in der Quantenoptik haben neue Wege für Grundlagenforschung und technologische Anwendungen eröffnet. Vor Kurzem wurde es möglich, Quantenmechanik auf grösseren Skalen zu erforschen. Materiewellen können heute über grössere Distanzen kontrolliert werden und Quanteninterferenzexperimente mit komplexen Molekülen sind möglich. Ausserdem kann die Wechselwirkung zwischen Licht und einem Spiegel dazu genutzt werden, die Quanteneigenschaften eines nano- oder mikro-Spiegels zu erforschen und zu manipulieren. Dieses neue Forschungsfeld der Optomechanik ermöffnet den Zugang zu Quantenphänomenen auf makroskopischen Grössenordnungen und wird in verschiedenen Experimenten erforscht, von pico-gram Resonatoren bis zu kg-Spiegeln. Mit den neuen Materie-Licht-Wechselwirkungen und den damit verbundenen neuen Methoden der Quantenkontrolle werden neue Möglichkeiten eröffnet, unser derzeitiges Verständnis der Physik zu testen. Obwohl die Quantentheorie auf kleinen Skalen sehr genau überprüft ist, ist der Übergang zur klassischen Physik und vor allem die Wechselwirkung mit der Gravitation weitgehend unerforscht.

In dieser Dissertation werden grosse Quantensysteme theoretisch studiert, um vor allem neue Möglichkeiten zu finden, die Wechselwirkung zwischen Quantenmechanik und der allgemeinen Relativitätstheorie experimentell zu erforschen [1–5]. Die Arbeit umfasst zwei Hauptforschungsrichtungen. Zum einen wird ein neues Regime der opto-mechanischen Wechselwirkung untersucht. Es wird gezeigt, dass gepulste opto-mechanische Systeme dazu genutzt werden können, Quantenzustände eines massiven Spiegels durch Messungen des Lichts zu präparieren, und dass das gepulste Regime eine vollständige Tomographie des mechanischen Zustands ermöglicht [1]. Aufbauend auf der gepulsten opto-mechanischen Wechselwirkung wird gezeigt, dass bestimmte phänomenologische Modelle der Quantengravitation experimentell überprüft werden können [2]. Solche Modelle umfassen mögliche Modifikationen des kanonischen Kommutators, die aufgrund einer Modifikation der

Heisenberg'schen Unschärferelation auftreten können. Es wird gezeigt, dass für die Schwerpunktskoordinaten des massiven Spiegels diese Quantengravitationsmodelle sehr genau gemessen werden können.

Als zweite Hauptforschungsrichtung wird die gravitative Zeitdilatation in niedrig-Energie Quantensystemen studiert. Die Zeitdilatation ist für klassische Systeme genau gemessen, in der Quantenmechanik jedoch wurde bis jetzt nur die Newtonische Gravitation beobachtet. Es wird gezeigt, dass relativistische Korrekturen der Newtonischen Gravitation aufgrund der Zeitdilatation zu neuen Effekten in der Quantentheorie führen, ohne Analogon in der klassischen Theorie. Die Verlangsamung der Zeit im Gravitationsfeld führt zu der Verschränkung zwischen internen Freiheitsgraden eines Quantensystems und seiner Trajektorie im Raum. Dies führt zur periodischen Verringerung und zum Wiederkehren der Quanteninterferenz für Materiewellen mit internen Freiheitsgraden [3]. Ein ähnlicher Effekt kann in Quanteninterferenzexperimenten mit Licht aufgrund der Shapiro-Verlangsamung von einzelnen Photonen beobachtet werden [4]. Als wichtigstes Resultat dieser Forschungsrichtung wird gezeigt, dass jegliches zusammengesetztes Quantensystem im Gravitationsfeld der Erde dekohäriert, aufgrund der Zeitdilatationsinduzierten Verschränkung zwischen Poisition und internen Freiheitsgraden [5]. Die Zeitdilatation der thermischen Oszillationen innerhalb eines zusammengesetzten Systems bewirkt die Dekohärenz der Position des Teilchens. Die Zeitskala dieser Dekohärenz auf der Erde ist gross genug, dass sie prinzipiell in Quanteninterferenzexperimenten mit grossen Molekülen oder mikro-Kugeln nachgewiesen werden könnte.

Die Ergebnisse dieser Dissertation zeigen, dass neue Effekte auftreten, wenn die Gravitation in der Quantenmechanik berücksichtigt wird. Sogar schwache Gravitationsfelder wirken sich auf Quantensysteme aus, sodass Experimente in naher Zukunft möglich sein sollten, das Zusammenspiel zwischen den zwei Theorien zu testen.

Chapter 1

Introduction

1.1 Quantum mechanics and gravity

With the development of modern physical theories in the 20th century, the description of physical laws has fundamentally changed. The theory of general relativity explains the emergence of the gravitational interaction as a manifestation of space-time geometry. Quantum theory, on the other hand, describes interactions through the exchange of particles and is inherently probabilistic. These two fundamental theories have very different underlying concepts and give rise to distinct phenomena. Until today, no unified framework has been fully developed. Such a unified theory is expected to describe gravity as a quantum theory, but a major difficulty is the lack of experiments on the overlap between these two theories.

In non-relativistic quantum mechanics, a physical system is described by a wave function $|\,\Psi\rangle$, the dynamics of which is described by the Schrödinger equation

$$i\hbar\frac{\partial}{\partial t}|\,\psi\rangle = H|\,\psi\rangle\,. \tag{1.1}$$

The wave function evolves in time according to the Hamiltonian H of the system. The predictions of quantum theory have a fundamentally probabilistic nature. Only the probability of an experimental outcome can be predicted, given by the Born rule: The probability of finding a system in some specific state $|\,\mathcal{S}\rangle$ is given by $|\langle\mathcal{S}\,|\,\psi\rangle|^2$. According to the superposition principle the state $|\,\psi\rangle$ can be written as a linear combination in terms of any other basis, which gives rise to quantum interference phenomena. For composite systems, the superposition principle gives rise to entanglement, correlations that are stronger than classically possible. At high velocities or high energies, a relativistic description of quantum systems becomes necessary and quantum theory is fully consistent with special relativity. Relativistic equations

of motion are the Klein-Gordon and the Dirac equations, which describe spin-0 and spin-1/2 particles, respectively. With the development of quantum field theory, a full quantum mechanical description of electro-magnetic interactions was realized. Since then, the standard model was able to explain all particles and all fundamental interactions have been successfully incorporated into quantum theory, except for gravity.

Gravitational interactions are described by the theory of general relativity. In general relativity, the central quantity is the space-time metric $g_{\mu\nu}$, which describes the geometry of space and time. The equation of motion for physical systems is a generalized version of the free motion in Newtonian physics, free particles move along geodesics and their four-vector x^μ obeys the geodesic equation

$$\frac{d^2x^\mu}{d\tau^2} + \Gamma^\mu_{\rho\nu}\frac{dx^\rho}{d\tau}\frac{dx^\nu}{d\tau} = 0\,, \tag{1.2}$$

where $\Gamma^\lambda_{\mu\nu} = \frac{1}{2}g^{\lambda\rho}(\partial_\mu g_{\nu\rho} + \partial_\nu g_{\rho\mu} - \partial_\rho g_{\mu\nu})$ is the Christoffel connection of the metric $g_{\mu\nu}$ and τ is the proper time. The metric $g_{\mu\nu}$ thus governs the motion of particles and effects of gravity are manifestation of such geodesic motion in a four-dimensional space-time. On the other hand, the curvature itself depends on the matter content, captured by the stress-energy tensor $T_{\mu\nu}$. The change in geometry is governed by Einstein's equations

$$R_{\mu\nu} - \frac{1}{2}g_{\mu\nu}R + g_{\mu\nu}\Lambda = \frac{8\pi G}{c^4}T_{\mu\nu}\,, \tag{1.3}$$

where Λ is the cosmological constant and $R_{\mu\nu} = R^\rho_{\mu\rho\nu}$ is the Ricci-tensor derived from the Riemann tensor $R^\rho_{\sigma\mu\nu} = \partial_\mu\Gamma^\rho_{\nu\sigma} - \partial_\nu\Gamma^\rho_{\mu\sigma} + \Gamma^\rho_{\mu\omega}\Gamma^\omega_{\nu\sigma} - \Gamma^\rho_{\nu\omega}\Gamma^\omega_{\mu\sigma}$. Eq. (1.3) shows how physical content alters the geometry of space-time, whereas eq. (1.2) governs how space-time geometry affects the dynamics of matter. These two equations are the cornerstones of the theory of general relativity, but they are inherently classical. It is, however, possible to describe quantum theory on a fixed, curved background space time. In such a case, the possible quantum nature of eq. (1.3) is neglected and the dynamics of particles, eq. (1.2), is incorporated into quantum theory through covariant derivatives. On the other hand, phenomenological models of quantum gravity can be constructed, where instead of quantizing eq. (1.3), some specific aspects of the theory and their possible modifications are considered. Figure 1.1 shows a schematic overview of the development of physical theories and the interrelation between gravitational and quantum phenomena.

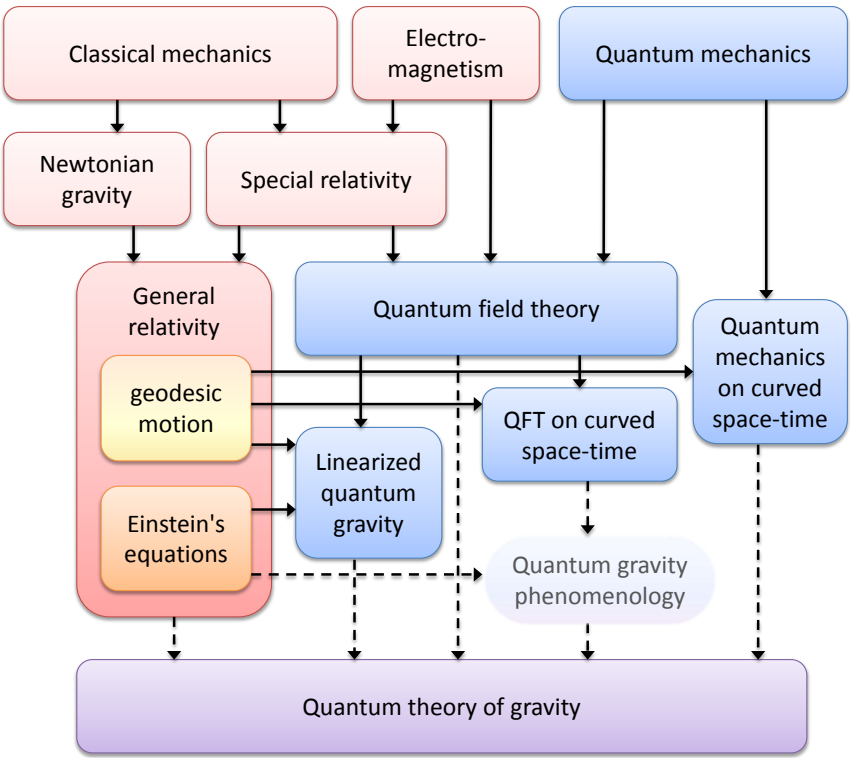

Figure 1.1: Schematic diagram of the development and unification of physical theories, inspired by Bronstein's work [6, 7] and Okun's cube of physical theories [8]. Classical theories are highlighted in red, while quantum theories are highlighted in blue. The arrows correspond to the development of the theories and dashed arrows represent currently unknown relations. For clarity, general relativity is shown to include two separate conceptual pillars: dynamics of physical systems on a background metric and dynamics of the metric itself (corresponding to eqs. (1.2) and (1.3), respectively). The former can be included into quantum theory, thus low-energy quantum mechanics and quantum field theory can be formulated on a fixed, possibly curved, background space-time. However, no complete theory of quantum gravity that includes quantization of gravity beyond the linear approximation is currently known. Quantum gravity phenomenology may allow for the possibility of testing possible aspects of quantum gravity by modelling some expected behaviour. The research focus in this thesis is on low-energy quantum systems (at non-relativistic velocities), which can be controlled with very high precision and which allow for tests of quantum theory at novel scales in terms of mass and size. It is shown that quantum mechanics in the presence of general relativistic time dilation, as well as possible quantum gravity phenomenology, can become accessible with such systems.

1.2 This thesis

In this thesis, low-energy quantum systems are studied and how they can be used to probe the interplay between quantum theory and general relativity. The results of the thesis are laid out in the publications [1–5]. Here an introduction and summary of the results is presented. In chapter 2, opto-mechanical systems are studied and a pulsed interaction regime is proposed and investigated. It is shown that the pulsed interaction regime allows for the preparation and read-out of quantum states of a massive mechanical resonator. Chapter 3 shows how the pulsed opto-mechanical interaction can be used to probe some phenomenological models of quantum gravity. It is shown that possible modifications of the canonical commutator of the center-of-mass of the mechanical state can be probed to very high accuracy. Chapter 4 deals with time dilation in low-energy quantum theory and how Earth-based quantum interference experiments are affected. Universal decoherence due to time dilation is derived, which affects coherence in position of any composite system. In chapter 5 short summaries and the reprints of the corresponding publications are given, in which more detailed elaborations on the results can be found.

The results of this thesis demonstrate that the interplay between quantum theory and general relativity affects even low-energy quantum systems and that it offers novel phenomena. It is shown that quantum optical experiments which are conceivable in the near future can be used to probe the interplay between these two theories.

Chapter 2

Pulsed quantum opto-mechanics

The study of the interaction between light and matter has been of crucial importance for quantum foundations and quantum technologies. Quantum theory originated from the necessity to explain the statistical properties of thermal emission of radiation [9]. Thereafter, observations of the absorption and emission spectra of atoms have triggered the development of the Bohr model [10] of the atom and the subsequent development of quantum theory. The precision measurement of the Lamb shift [11] in hydrogen has been critical for the development and verification of relativistic quantum mechanics [12, 13]. After the full formulation of quantum theory, light-matter interactions became the focus of studying coherent quantum phenomena. After the study of the interaction of atoms with semi-classical optical fields, Glauber's development of a quantum description of optics [14] paved the way for maser and laser technology, opening the rote for the study of coherent interaction between light and matter. The Jaynes-Cummings model [15] is until today the most widely studied model for the interaction between a single photon and matter. It was formulated to approximate the quantum electrodynamic interaction between photons and a single atom by modeling the latter as a two-level system [16]. Based on these theoretical developments, crucial techniques have been developed in the past few decades to observe and to maintain quantum behavior of various physical systems [17, 18]. More recently, a different form of light matter interaction has been the focus of intensive research: in opto-mechanics the radiation pressure interaction between electromagnetic radiation and the collective mode of a mechanical resonator is studied [19–24]. In a typical opto-mechanical system, a small mirror is displaced via radiation pressure of light inside an optical Fabry-Perot cavity [25–27]. Other setups include microwave resonators [28–30], driven piezo-

electric crystals [31], whispering gallery modes in toroidal structures [32–34], photonic crystals [35] and micro-mechanical membranes [36], to name a few. Some example structures are shown in Fig. 2.1. Initially, opto-mechanical systems have been studied for its use in gravitational wave detectors [37–40]. The mechanical mirror serves as a sensitive force sensor which is read out via the continuously interacting laser field [41–43], which is the key component of interferometric gravitational wave detectors. Much work has also been done in studying how a movable mirror can be used to prepare and measure quantum states of light [44–47]. However, in recent years the quantum nature of the mechanical resonator itself has moved into the focus of research [48–57].

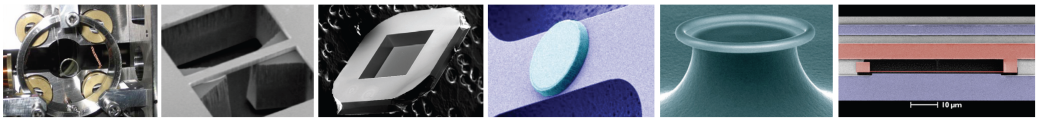

Figure 2.1: Opto-mechanical systems can be engineered in a wide range of mass and size. The pictures are showing some examples of opto-mechanical systems, taken from Ref. [20]. From left to right, respectively: A suspended 1 g mirror as part of a Fabry-Perot cavity [40], a micro-mirror etched on a silicon resonator [26], a 50 nm thick dielectric membrane inside a cavity [36], a micromechanical resonator with an attached μm-scale mirror [27], a silica microtoroid that couples optical whispering-gallery modes to mechanical radial-breathing modes [33] and a nanomechanical oscillator coupled to a superconducting microwave cavity [28].

2.1 Description of opto-mechanical systems

In this chapter the focus will be on optical fields that interact with a mirror via radiation pressure, but the results extend to analogous systems [58]. A schematic drawing of an opto-mechanical system is given in Fig. 2.2a. The cavity under consideration consists of one highly reflective, large end mirror and another harmonically bound end mirror, which can oscillate due to small external forces. The optical field enters through the large mirror and the cavity bandwidth is κ. Under the single-mode approximation for the optical field, the light inside the cavity of length L is described by $H = \hbar\omega_0 a^\dagger a$, where $\omega_0 \propto L$ is the cavity resonance frequency and $a/a^\dagger$ are creation/annihilation operators for this optical mode. To derive the opto-mechanical coupling, a straightforward argument can be used [39]: The light inside the cavity interacts with the mechanical resonator via radiation pressure and changes its equilibrium position x. In this case, the optical resonance of the cavity is

changed, such that the new resonance frequency is given by $\omega_0 \propto (L+x)$. For $x/L \ll 1$, the expression can be expanded, which yields a modified Hamiltonian $H = \hbar\omega_0 a^\dagger a - \hbar\omega_0 (x/L) a^\dagger a$. Taking into account the harmonic evolution of the mechanical resonator with frequency ω_m, the overall Hamiltonian of this system becomes

$$H = \hbar\omega_0 a^\dagger a + \hbar\omega_m b^\dagger b - \hbar g_0 a^\dagger a X_m \,, \tag{2.1}$$

where $X_m = (b + b^\dagger)/\sqrt{2}$ is the mechanical quadrature and $g_0 = (\omega_0/L)x_0$ is the opto-mechanical coupling rate with the mechanical zero-point motion $x_0 = \sqrt{\hbar/m\omega_m}$. This Hamiltonian describes the interaction between a single optical mode (with respect to the instantaneous mirror position) and the movable end mirror of the cavity. A complete derivation of the opto-mechanical Hamiltonian has been performed by C.K. Law [48], where the classical Hamiltonian for the full electro-magnetic radiation with the boundary conditions of the cavity is derived and quantized to describe all optical modes. In the linearized regime, where the mirror displacement is small and the interaction is dominated by a single optical mode (i.e. the interaction does not induce scattering into other optical modes), the full Hamiltonian reduces to the expression (2.1) above.

To provide a full description of the opto-mechanical system, it is necessary to take the filling of the cavity and the decay of the optical field into account [59, 60]. In addition to the intra cavity dynamics, when light enters and leaves the cavity through the large end mirror the latter acts as a beam splitter between the modes c outside the cavity and the field a inside the cavity, described by the Hamiltonian $H_{ac} = i\hbar \int d\omega \tilde{\kappa}(\omega)(c_\omega a^\dagger - a c_\omega^\dagger)$. This takes into account the different frequency components through the bosonic operators c_ω of the driving field (with $[c_\omega, c_{\omega'}] = \delta(\omega - \omega')$) and the coupling $\tilde{\kappa}$ at the respective frequencies. In the Heisenberg picture, the operators c_ω evolve in time as $\dot{c}_\omega = -i\omega c_\omega + \tilde{\kappa} a$. The formal solution $c_\omega(t) = c_\omega(t') e^{-i\omega(t-t')} + \tilde{\kappa}(\omega) \int_{t'}^{t} ds e^{-i\omega(t-s)} a(s)$ can be used in the equation of motion for the intra-cavity field $\dot{a} = -i/\hbar\,[a(t), H] - \int d\omega \tilde{\kappa}(\omega) c_\omega(t)$. The field can be decomposed into an input- and output-contribution with respect to some fixed initial time $t' = t_0 < t$ and some final time $t' = t_1 > t$ (at which the outside fields take the values $c_\omega^{(0)}$ and $c_\omega^{(1)}$, respectively), defined through $a_{in}(t) = -1/\sqrt{2\pi} \int d\omega e^{-i\omega(t-t_0)} c_\omega^{(0)}$ and $a_{out}(t) = 1/\sqrt{2\pi} \int d\omega e^{-i\omega(t-t_1)} c_\omega^{(1)}$. Assuming the coupling to be approximately constant in the range of the relevant frequencies, one can set $\tilde{\kappa}^2(\omega) = \kappa/\pi$. In terms of these definitions, the dynamics of the intra cavity optical field becomes

$$\dot{a} = -(i/\hbar)\,[a, H] - \kappa a + \sqrt{2\kappa} a_{in} \tag{2.2}$$

and the optical field inside the cavity is related to the input light field and the output light field via $\sqrt{2\kappa}a = a_{out} + a_{in}$. The description in terms of input and output fields is convenient, since the input can be chosen arbitrarily. For coherent drive, the input is usually decomposed into a classical component with phase ω_L and the quantum noise: $a_{in} \rightarrow (E/\sqrt{2\kappa})e^{-i\omega_L} + a_{in}$, where E can be written in terms of the input power P as $E = \sqrt{2\kappa P/(\hbar\omega_L)}$. In this case, the classical drive can be directly incorporated into an effective Hamiltonian contribution $H_d = i\hbar(Ee^{-i\omega_L t}a^\dagger - E^* e^{i\omega_L t}a)$.

The phase of the drive, ω_L, can in principle be detuned from the cavity resonance frequency ω_0. The detuning is used in most opto-mechanical settings to cool the resonator [61–64] or to create entanglement between light and mechanics [53, 65, 66]. The detuning opens the route to access different interaction regimes between light and the mirror. Changing frame by an arbitrary operator U, the Hamiltonian changes according to $H \rightarrow i\hbar(\partial_t U)U^\dagger + UHU^\dagger$. In a frame rotating at ω_L, the opto-mechanical Hamiltonian thus changes to $H = -\hbar\Delta a^\dagger a + \hbar\omega_m b^\dagger b - \hbar g_0 a^\dagger a X + i\hbar(Ea^\dagger - E^* a)$, where $\Delta = \omega_L - \omega_0$ is the detuning of the laser with respect to the cavity frequency. The above Hamiltonian can be linearized (with respect to the optical field) when a strong coherent drive is used. Assuming the optical field inside the cavity varies only very slowly over the timescales of interest, it can be approximated by the semi-classical steady-state value $\alpha \approx E/(i\Delta + \kappa)$. One can choose a new frame that is displaced by α, neglect the contributions from vacuum fluctuations (since $|\alpha| \gg 1$) and then displace the frame back into the original picture, which yields the Hamiltonian $H \approx -\hbar\Delta a^\dagger a + \hbar\omega_m b^\dagger b - \hbar g_0(-|\alpha|^2 + \alpha a^\dagger + \alpha^* a)X$. This Hamiltonian is linearized in the vacuum contributions of the optical field. In the interaction picture the optical field and the mechanics interact via $H_{int} = -\hbar\sqrt{2}g_0(\alpha e^{i\Delta t}a^\dagger + \alpha^* e^{-i\Delta t}a)(be^{i\omega_m t} + b^\dagger e^{-i\omega_m t})$. In the sideband resolved regime, where $\omega_m \gg \kappa$, the optical field does not change appreciably on the timescale of the mechanics. In this case, the rotating wave approximation can be applied: For the particular choice of detuning $\Delta_- = -\omega_m$ and $\Delta_+ = \omega_m$, the Hamiltonian can be approximated as $H_- = -\hbar\sqrt{2}g_0(\alpha a^\dagger b + \alpha^* a b^\dagger)$ and $H_+ = -\hbar\sqrt{2}g_0(\alpha a^\dagger b^\dagger + \alpha^* a b)$, respectively. The former is a beam splitter Hamiltonian which allows for cooling and state transfer of the mechanical resonator [30, 67]. The latter can heat the mechanical resonator and is a 2-mode squeezing Hamiltonian which entangles the mechanics to the optical field [66]. These two interaction regimes are the main regimes currently considered in opto-mechanical systems. Cooling the resonator close to the ground state by driving the optical cavity at the red sideband has been achieved experimentally [63, 64]. However, full quantum state transfer between mechanics and the optical field remains a challenge, although significant experimental progress has been made [30]. The state

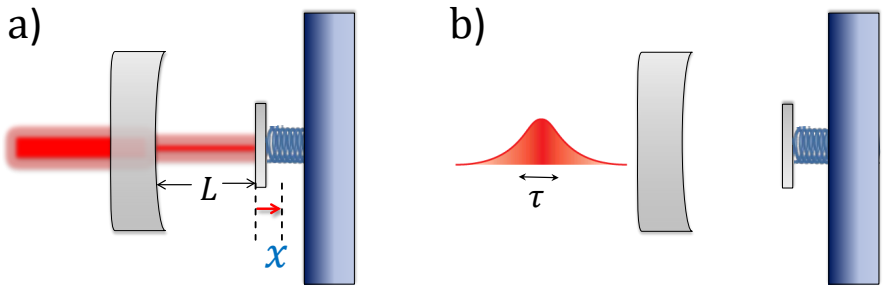

Figure 2.2: a) A typical opto-mechanical systems that consists of a one-sided cavity with a movable end mirror. The mirror is displaced by the light through radiation pressure, which in turn changes the resonance condition for the light. The interaction inside the cavity is governed by the Hamiltonian (2.1). b) In pulsed opto-mechanics an optical pulse of duration τ is interacting with the mechanical mirror. The pulse duration is much shorter than the mechanical period. The Hamiltonian for pulsed opto-mechanics is given in eq. (2.3).

transfer protocol requires the interaction to be on a timescale much longer than a single mechanical period, thus decoherence of non-classical states will strongly limit the fidelity of such a scheme. In contrast, a pulsed scheme [1] that operates on timescales less than a mechanical period provides access to a quantum non-demolition (QND) [68–70] type Hamiltonian, which allows in principle for arbitrary precise measurements of position. Such a pulsed regime can circumvent several current limitations in opto-mechanics for quantum state preparation and quantum state tomography.

2.2 Description of pulsed opto-mechanical systems

In pulsed opto-mechanics, the optical field interacts with the mechanical mirror on a timescale much shorter than the mechanical period (see Fig. 2.2b). This requires the bandwidth to be $\kappa \gg \omega_m$, which is the unresolved sideband regime, and is the opposite case as compared to the resolved sideband limit described above. In this limit, the light field interacts with the instantaneous mechanical position, and the mechanical motion during the interaction can be neglected. Even though the bandwidth is very large, the interaction with the mechanics can still be significant if the length of the cavity is reduced. Choosing the optical field to be on resonance with the cavity, the Hamiltonian is given by

$$H_{pulsed} = -\hbar g_0 a^\dagger a X_m \,. \tag{2.3}$$

This Hamiltonian has the form of a QND-interaction: the mechanical position can be read out directly and no backaction appears in the measurement, since $[H_{pulsed}, X_m] = 0$. Thus pulsed opto-mechanics is not limited by the so-called standard quantum limit [43], which is relevant for continuous read-out of the mechanical position and limits the precision of the measurement to the ground state extension of the mirror. In the following, the main results of the research of pulsed opto-mechanics are outlined [1].

The exact time scale and strength of the interaction can be found from considering the cavity dynamics. Since the bandwidth of the cavity is large, only the pulse shape is affected and the interaction takes place on the time scale $\tau \sim 1/\kappa$. For a strong coherent optical field $|\,\alpha\rangle$, the above Hamiltonian (2.3) can be linearized with respect to the optical field. Choosing α to be real for convenience (with respect to the phase of the local oscillator) and neglecting the vacuum contributions, this yields the linearized Hamiltonian $H = \hbar g_0 \alpha^2 X_m - \hbar g_0 \alpha \sqrt{2} X_L X_m$, where $X_L = (a + a^\dagger)/\sqrt{2}$ is the optical amplitude quadrature. The unitary operator can thus be written as

$$U(\tau) = e^{-i\Omega X_m}\, e^{i\chi X_L X_m}\,, \tag{2.4}$$

where $\chi = \sqrt{2} g_0 \alpha \tau$ and $\Omega = g_0 \alpha^2 \tau$. The mirror momentum is displaced by Ω and at the same time, its position becomes correlated with the optical quadrature. In particular, the mechanical position is imprinted onto the optical phase quadrature $P_L = i(a^\dagger - a)/\sqrt{2}$, since $P_L(\tau) = U^\dagger(\tau) P_L U(\tau) = P_L + \chi X_m$. To obtain precise information on the mechanical position, the phase quadrature of the light is therefore read-out after the opto mechanical interaction by balanced homodyne detection. In this detection scheme, a strong local oscillator coherent state (described by the annihilation operator a_{LO}) is mixed with the light signal on a 50-50 beam splitter. At the two output ports, the optical field becomes $a_1 = (a + i a_{LO})/\sqrt{2}$ and $a_1 = (ia + a_{LO})/\sqrt{2}$, respectively. These two fields are detected (with detection efficiency η) and the signal is subtracted. Writing $\langle a_{LO} \rangle = A e^{i\theta}$, the resulting differential signal is therefore $\langle n_1 \rangle - \langle n_2 \rangle = \sqrt{2}\eta A \left\langle X_L^{(\theta)} \right\rangle$, where $X_L^{(\theta)} = (a e^{-i\theta} + a^\dagger e^{i\theta})/\sqrt{2}$ is an arbitrary quadrature of the optical field of interest. Thus, any arbitrary optical quadrature can be measured with very high precision. In the case considered here, the local oscillator phase is chosen to give information about the phase of the optical field, i.e. $\theta = \pi/2$. The measurement can be optimized by mode-matching the local oscillator to the expected signal in the time domain, taking the cavity dynamics into account. The result can be approximated as an ideal measurement of the optical phase quadrature P_L, with corresponding quadrature eigenstate $|\,P_L\rangle$. Therefore, the overall pulsed opto mechanical interaction and subsequent

optical measurement can be described by the operator

$$\Upsilon(P_L) = \langle P_L \left| U(\tau) \right| \alpha \rangle \,, \tag{2.5}$$

which depends on the measurement outcome P_L. Note that Υ acts only on the Hilbert space of the mechanical mirror. Since the input state, the interaction and the measurement are all Gaussian, the above operation can be computed exactly. Inserting the optical x-quadrature basis gives $\Upsilon = e^{-i\Omega X_m} \int dx e^{-iP_L x} e^{i\chi x X_m} e^{-\alpha^2 + \sqrt{2}\alpha x - x^2/2} / \sqrt{2\pi^{3/2}}$. Noting that $\Omega = \alpha\chi/\sqrt{2}$, the resulting operator becomes

$$\Upsilon(P_L) = \frac{e^{-i\sqrt{2}\alpha P_L}}{\pi^{1/4}} D_m(i\Omega)\, e^{-\frac{1}{2}(P_L - \chi X_m)^2} \,, \tag{2.6}$$

where D_m is the displacement operator and the subscript m denotes action on the mechanical state. The above operation (2.6) captures the pulsed opto-mechanical interaction and subsequent read-out of the optics. It can be used to perform quantum state tomography of the mechanical state and to conditionally prepare a mechanical squeezed state, as will be shown below.

2.3 Quantum state tomography with pulsed opto-mechanics

Pulsed opto-mechanics can be used to reconstruct any arbitrary state ρ_m of the mirror, by only measuring the optical phase. The statistics of the optical phase are directly related to the statistics of the mechanical position. In particular, the mean of the measured optical phase is $\langle P_L(\tau) \rangle = \langle P_L \rangle + \chi \langle X_m \rangle$ and the variance of the optical phase is $\Delta^2 P_L(\tau) = \frac{1}{2} + \chi^2 \Delta^2 X_m$, assuming pure coherent optical input. To access other mechanical quadratures than the position, the free harmonic evolution of the mirror can be utilized. Before the pulsed interaction, the mechanical state is left to evolve freely by a fixed amount of time. After a fixed harmonic evolution with $\theta = \omega_m t$, the statistics of the phase measurement becomes

$$\Pr\left[P_L\right] = \mathrm{Tr}[\Upsilon \rho_m^{(\theta)} \Upsilon^\dagger] = \frac{1}{\sqrt{\pi}} \int dx\, e^{-(P_L - \chi x)^2} \langle x \left| \rho_m^{(\theta)} \right| x \rangle \,, \tag{2.7}$$

where $\rho_m^{(\theta)} = e^{-i\theta n_m} \rho_m e^{i\theta n_m}$ is the harmonically evolved mechanical state. Note that one can equivalently write $\langle x \left| \rho_m^{(\theta)} \right| x \rangle = \langle x_{-\theta} \left| \rho_m \right| x_{-\theta} \rangle$, which are the mechanical marginals with $\left| x_\theta \right\rangle = e^{-i\theta n_m} \left| x \right\rangle$. Thus the statistics of P_L depends directly on the mechanical marginals, convolved with a Gaussian of

width χ^{-2}. For sufficiently large χ, all mechanical marginals can therefore be obtained. Note that in the limit $\chi \to \infty$, the measurement becomes a perfect von-Neumann measurement of the mechanical marginals. For $\chi \gtrsim 1$, sub-Planck oscillations in the marginals can in principle be accessed.

Having access to mechanical marginals $\langle x_\theta \,|\rho_m|\, x_\theta \rangle$ provides a means to perform full quantum state tomography. Typically quantum mechanical operators are described in Hilbert space, but continuous variable systems can be equivalently described in phase space [71–74]. The one-to-one correspondence between operators and phase space functions is established by a Wigner-Weyl transformation. In the phase-space description, a density matrix is described by a quasi-probability distribution. Depending on the transformation used, the phase space representation is governed by different distributions, which are however all interrelated through convolution. The most popular representations are the Wigner function $W(\alpha, \alpha^*)$ [75], the Husimi Q function $Q(\alpha, \alpha^*)$ [76] and the Glauber-Sudarshan P function $P(\alpha, \alpha^*)$ [77, 78]. In general, the s-parameterized quasi-probability distribution $P(s, \alpha, \alpha^*)$ describing a quantum state ρ can be found from a 2-dimensional Fourier transform of the s-parameterized characteristic function $C(s, \xi, \xi^*)$ [74]. The latter is defined as

$$C(s, \xi, \xi^*) = \mathrm{Tr}[\rho e^{\xi a^\dagger - \xi^* a}] e^{s|\xi|^2/2}\,, \tag{2.8}$$

where $s = -1, 0, 1$ corresponds to the characteristic functions for the Husimi Q function, the Glauber-Sudarshan P function and the Wigner function, respectively. The quasi-probability distributions are then obtained from

$$P(s, \alpha, \alpha^*) = \frac{1}{\pi^2} \int d^2\xi C(s, \xi, \xi^*) e^{\alpha\xi^* - \alpha^*\xi}\,. \tag{2.9}$$

The exponential can be written as $\alpha\xi^* - \alpha^*\xi = -i2(\xi_i\alpha_r - \xi_r\alpha_i)$, where the subscripts i and r denote the imaginary and real parts, respectively. The above expression is therefore a 2-dimensional Fourier-transform of C. The specific quasi-probability distributions can be represented in more familiar forms:

$$\begin{aligned} P(-1, \alpha, \alpha^*) &= Q(\alpha, \alpha^*) = \frac{1}{\pi} \langle \alpha \,|\rho|\, \alpha \rangle \\ P(0, \alpha, \alpha^*) &= W(\alpha, \alpha^*) = \frac{2}{\pi^2} \int d^2\beta \langle \beta \,|D^\dagger(\alpha)\rho D(\alpha)|\, -\beta \rangle \\ P(1, \alpha, \alpha^*) &= P(\alpha, \alpha^*) \quad \text{with} \quad \rho = \int d^2\alpha P(\alpha, \alpha^*) |\, \alpha \rangle\langle \alpha \,|\,. \end{aligned} \tag{2.10}$$

The different distributions can be used to uniquely represent a quantum state, but they have different mathematical properties. The Husimi Q function ($s =$

-1) is always positive and can be used to directly compute anti-normal ordered correlation functions: $\left\langle a^p a^{\dagger q}\right\rangle = \mathrm{Tr}[\rho a^p a^{\dagger q}] = \pi^{-1}\int d^2\alpha \langle\alpha\,|a^{\dagger q}\rho a^p|\,\alpha\rangle = \int d^2\alpha\, Q(\alpha,\alpha^*)\alpha^{*q}\alpha^p$. The Glauber-Sudarshan P function, on the other hand, corresponds to normal-ordered correlation functions: $\left\langle a^{\dagger q}a^p\right\rangle = \mathrm{Tr}[a^p\rho a^{\dagger q}] = \int d^2\alpha\, P(\alpha,\alpha^*)\alpha^{*q}\alpha^p$. However, the P-representation is not always positive and for pure states is only defined through generalized functions (δ-functions and derivatives thereof). In contrast, the Wigner function is always well-defined, but can also have negative values. It can be used to directly compute symmetrically-ordered correlation functions, where expressions are symmetrized with respect to a and $a^\dagger$: $\left\langle (a^{\dagger q}a^p)_{sym}\right\rangle = \int d^2\alpha\, W(\alpha,\alpha^*)\alpha^{*q}\alpha^p$. The Wigner function has also the unique property that integrating out one variable yields the probability distribution for the conjugate variable. Using eq. (2.9) with $s = 0$ and $\alpha = x + ip$ and utilizing the delta-function representation $\delta(y-z) = (2\pi)^{-1}\int dq\, e^{iq(y-z)}$, a straightforward computation shows that $\int dx\, W(x,p) = \langle p\,|\rho|\,p\rangle = \Pr[p]$. In this respect, the Wigner function has the closest resemblance with a classical phase-space probability distribution. The negative parts of the Wigner function, however, have no classical counter part [71] and non-classicality is therefore often defined as negativity of the Wigner function [79]. All Gaussian states have fully positive Wigner functions. In quantum optics non-classicality is therefore often referred to in terms of the P-function, i.e. whether a state can be decomposed into a mixture of coherent states. A squeezed state, for example, has no Wigner negativity, but has a singular and highly oscillating P-function [80, 81]. An example for the quasi-probability distributions of some states is depicted in Fig. 2.3.

The various quasi-probability distributions are interrelated via Gaussian convolution. From eq. (2.8) it follows that characteristic functions of two different distributions are related via $C(s',\xi,\xi^*) = C(s,\xi,\xi^*)e^{(s'-s)|\xi|^2/2}$. The Fourier-transform of this expression is the s'-parameterized probability distribution as a function of the s-parameterized probability distribution. It can be computed in closed form by using the convolution theorem, which states that the Fourier transform $\mathcal{F}$ of the product of two functions g and f is a convolution of the corresponding transforms: $\mathcal{F}[f\cdot g] = \mathcal{F}[f] * \mathcal{F}[g]$, where the convolution is defined as $f(x) * g(x) = \int dy f(y)g(x-y)$. For the specific case here, the two-dimensional Fourier transform $\mathcal{F}^{(2)}$ gives $\mathcal{F}^{(2)}[C(s,\xi,\xi^*)] = P(s,\alpha,\alpha^*)$ and $\mathcal{F}^{(2)}[e^{-(s-s')|\xi|^2/2}] = 2/(\pi(s-s'))e^{-2|\alpha|^2/(s-s')}$, provided $s > s'$. Thus the relation between the s'- and s-parameterized probability distributions is

$$P(s',\alpha,\alpha^*) = \frac{2}{\pi(s-s')}\int d^2\beta P(s,\beta,\beta^*)e^{-2|\alpha-\beta|^2/(s-s')}\,. \tag{2.11}$$

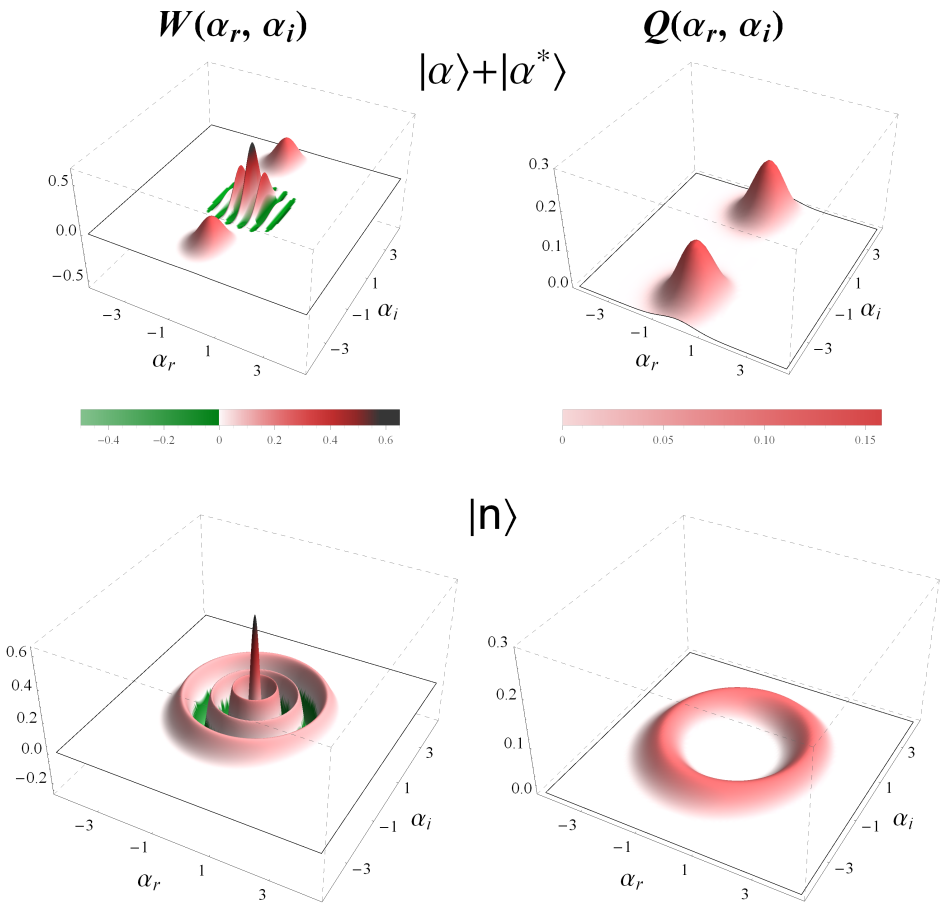

Figure 2.3: Comparison between the Wigner function (left) and the Husimi-Q-function (right) for two different states. The upper row shows the normalized superposition state $|\,\alpha\rangle + |\,\alpha*\rangle$ with $\alpha = i3$ [82, 83]. The lower row shows the Fock state $|\,n\rangle$ with $n = 6$ [72, 74]. While the Wigner function can have negative values, the Q-function remains always positive. Since quasi-probability distributions are interrelated by convolution, see eq. (2.11), the Q-function smoothes all features of the state as compared to the Wigner function. However, both distributions can be used to describe any quantum state.

The quasi-probability distribution fully describes the state of a system. It is also possible to experimentally measure the quasi-probability distribution. A common method relies on measurements of the marginals $M(X,\theta) = \Pr[X_\theta] = \langle X_\theta\,|\rho|\,X_\theta\rangle$, which have a one-to-one relation to the quasi-probability distributions [82]. The characteristic function for the marginals can be written as $C_m(\eta,\theta) = \mathrm{Tr}[\rho\, e^{i\eta X_\theta}]$ and the marginals can be found from the Fourier transform $M(X,\theta) = \mathcal{F}[C_m]$. Since $X_\theta = (ae^{-i\theta} + a^\dagger e^{i\theta})/\sqrt{2}$, the character-

istic function of quasi-probability distributions, eq. (2.8), can be written in terms of the characteristic function of the marginals as

$$C(s, \xi = i\eta e^{i\theta}/\sqrt{2}) = C_m(\eta, \theta) e^{s\eta^2/4}\,. \tag{2.12}$$

Thus there is a direct correspondence between the marginals and the quasi-probability distributions. Writing out explicitly the Fourier transforms yields the relation between quasi-probability and marginal distributions [82]:

$$P(s, \xi, \xi^*) = \frac{1}{\sqrt{2}\pi^2} \int_0^\infty d\eta \int_0^{2\pi} d\theta \int_{-\infty}^{\infty} dx M(x, \theta) \eta\, e^{s\eta^2/4 + i\sqrt{2}\eta(\sqrt{2}x - \xi_i \sin\theta - \xi_r \cos\theta)}. \tag{2.13}$$

The marginals $M(x, \theta)$ can in principle be obtained experimentally for all angles θ, and thus the state can be reconstructed. There are various numerical methods for such a quantum state tomography [84, 85], since a complete knowledge of all marginals is impossible to obtain. Quantum state tomography has been performed for various quantum systems [86–91]. In opto-mechanics, the ability to obtain information about the mechanical marginals through pulsed interactions, as described by eq. (2.7), opens the route for full reconstruction of an arbitrary quantum state of the mechanics. The fidelity depends only on the parameter χ, i.e., for large opto-mechanical coupling, the reconstruction can be sufficiently precise to measure quantum features of the mechanical state.

2.4 Quantum state preparation with pulsed opto-mechanics

Except for the ability to measure the quantum state of the mechanics, pulsed opto-mechanical interactions also allow for remote state preparation. The pulsed protocol yields an effective operation that acts on the mechanical state, described by eq. (2.6). After a single run, the mechanical state becomes the conditional state

$$|\,\Psi\rangle_m = \mathcal{N}\Upsilon|\,\Psi_0\rangle_m \tag{2.14}$$

where $\mathcal{N}^{-2} = \langle\Psi_0\,|\Upsilon^\dagger\Upsilon|\,\Psi_0\rangle$ is the renormalization factor. The renormalization is required since the state depends on the measurement outcome P_L and the operation Υ is non-unitary. The mechanics is projected onto a P_L-conditional state.

To see explicitly how Υ acts on a state, one can re-write eq. (2.6) in terms of the creation and annihilation operators $b^\dagger$ and b of the mechanics

and cast the result into a normal ordered form where all b stand to the right of $b^\dagger$. To this end, expression (2.6) is written as

$$\Upsilon = \frac{e^{-i\sqrt{2}\alpha P_L - P_L^2/2}}{\pi^{1/4}}\, e^{-\chi^2(b+b^\dagger)^2/4} e^{\chi P_L (b+b^\dagger)/\sqrt{2}} e^{i\Omega(b+b^\dagger)}\,. \tag{2.15}$$

Exponential operators, as the one above, can be cast into normal ordered form using exponential ordering theorems.

2.4.1 Exponential operator ordering

When considering exponential operators, convenient reformulations can be found from the general Baker-Campbell-Hausdorff expression. For any operators A and B, this expression takes the form [92–94]:

$$\begin{aligned} e^A B e^{-A} &= B + [A,B] + \frac{1}{2!}[A,[A,B]] + \frac{1}{3!}[A,[A,[A,B]]] + \dots \\ &= \sum_{k=0}^{\infty} \frac{1}{k!}\,[A,B]_k\ , \end{aligned} \tag{2.16}$$

where $[A,B]_k$ represent nested commutators, with $[A,B]_0 = B$. A related operator-ordering expression is the Zassenhaus-formula [95, 96]:

$$\begin{aligned} e^{A+B} =& e^A\, e^B\, e^{-\frac{1}{2}[A,B]}\, e^{\frac{1}{6}[A,[A,B]] + \frac{1}{3}[B,[A,B]]} \\ & e^{-\frac{1}{8}([B,[B,[A,B]]] + [B,[A,[A,B]]]) - \frac{1}{24}[A,[A,[A,B]]]} \dots \end{aligned} \tag{2.17}$$

These two relations are very convenient for computing quantum mechanical expressions. In the following, a few useful examples are derived.

Since $\left[a, a^\dagger\right] = 1$, for arbitrary complex numbers θ_+ and θ_- the following relation can easily be derived from eq. (2.17):

$$e^{\theta_+ b^\dagger - \theta_-^* b} = e^{\theta_+ b^\dagger} e^{-\theta_-^* b} e^{-\frac{1}{2}\theta_+\theta_-^*} = e^{-\theta_-^* b} e^{\theta_+ b^\dagger} e^{\frac{1}{2}\theta_+\theta_-^*}\,. \tag{2.18}$$

For $\theta_+ = \theta_-$ this expression reduces to the familiar relation for displacement operators $D(z) = e^{za^\dagger - z^* a} = e^{za^\dagger} e^{-z^* a} e^{-|z|^2/2}$. It also directly follows from eq. (2.16) that

$$\begin{aligned} e^{-\theta a^\dagger}\, a\, e^{\theta a^\dagger} &= a + \theta \\ e^{\theta a}\, a^\dagger\, e^{-\theta a} &= a^\dagger + \theta\,. \end{aligned} \tag{2.19}$$

The number operator $a^\dagger a$ induces rotations of the creation and annihilation operators. Since $\left[a^\dagger a, a^\dagger\right] = a^\dagger$, the nested commutator in eq. (2.16) becomes

$\left[a^\dagger a, a^\dagger\right]_k = a^{\dagger k}$. Thus any function $f(a, a^\dagger)$ that can be Taylor-expanded changes according to

$$e^{-\alpha a^\dagger a} f(a, a^\dagger) e^{\alpha a^\dagger a} = f(a e^\alpha, a^\dagger e^{-\alpha}) \,, \tag{2.20}$$

which holds for arbitrary α. For the more general case where the operators A and B satisfy $[A, B] = \omega A$, where ω is some complex number, one can derive the relation from eq. (2.17) [94]:

$$e^{A+B} = e^{\frac{1}{\omega}(1-e^{-\omega})A} e^B = e^B e^{-\frac{1}{\omega}(1-e^{\omega})A} \,. \tag{2.21}$$

In general, arbitrary exponentials with only quadratic terms in a and $a^\dagger$ can be cast into normal ordered form. Using new operators $K_+ = b^{\dagger 2}/2$, $K_- = b^2/2$ and $K_0 = (2b^\dagger b + 1)/4$, which obey the commutation relations $[K_0, K_\pm] = \pm K_\pm$ and $[K_+, K_-] = -2K_0$, one can use the relation (2.17) to show for arbitrary $f_\pm$, f_0 [74, 92–94]:

$$e^{f_+ K_+ + f_0 K_0 + f_- K_-} = e^{2\phi_+ K_+} \, e^{2\phi_0 K_0} \, e^{2\phi_- K_-} \,, \tag{2.22}$$

where

$$\begin{aligned} \phi_\pm &= \frac{f_\pm}{2\Gamma} \frac{\sinh(\Gamma)}{\cosh(\Gamma) - \frac{f_0}{2\Gamma}\sinh(\Gamma)} \\ \phi_0 &= -\ln\left[\cosh(\Gamma) - \frac{f_0}{2\Gamma}\sinh(\Gamma)\right] \\ \Gamma^2 &= \frac{f_0^2}{4} - f_+ f_- \,. \end{aligned} \tag{2.23}$$

The above relations are frequently used in quantum optics and are well-known. Here we derive two additional relations, which can be of help in quantum optical problems.

If in addition to $a^\dagger a$ only linear terms in a and $a^\dagger$ are present, the following relation holds for arbitrary complex numbers α, β_1 and β_2:

$$\begin{aligned} &e^{\alpha \, a^\dagger a + \beta_1 a + \beta_2 a^\dagger} = \\ &\quad = e^{-\frac{\beta_1\beta_2}{\alpha^2}(1+\alpha-e^\alpha)} \, e^{-\frac{\beta_2}{\alpha}(1-e^\alpha)a^\dagger} \, e^{\alpha a^\dagger a} \, e^{-\frac{\beta_1}{\alpha}(1-e^\alpha)a} = \\ &\quad = e^{-\frac{\beta_1\beta_2}{\alpha}\left(1-\frac{\sinh(\alpha)}{\alpha}\right)} \, e^{-\frac{1}{\alpha}[\beta_2(1-e^\alpha)a^\dagger - \beta_1(1-e^{-\alpha})a]} \, e^{\alpha a^\dagger a} \,. \end{aligned} \tag{2.24}$$

Both, the normal-ordered form and a form that resembles a displacement operator are given (the latter is convenient for some applications). To prove this

expression, one can write $e^{\alpha a^\dagger a+\beta_1 a+\beta_2 a^\dagger} = e^{\alpha(a^\dagger+\beta_1/\alpha)(a+\beta_2/\alpha)}e^{-\beta_1\beta_2/\alpha}$. One can see that the operators $a^\dagger$ and a are simply displaced. With the relations in eq. (2.19), this expression becomes $e^{-\beta_1\beta_2/\alpha}\, e^{-\beta_2 a^\dagger/\alpha}e^{\beta_1 a/\alpha}\, e^{\alpha a^\dagger a}\, e^{\beta_2 a^\dagger/\alpha}\, e^{-\beta_1 a/\alpha}$. Using eq. (2.20) it is now easy to move $e^{\alpha a^\dagger a}$ to the very left, such that one gets $e^{-\beta_1\beta_2(\alpha-1+e^\alpha)/\alpha}e^{\alpha a^\dagger a}\, e^{-\beta_2(1-e^{-\alpha})a^\dagger/\alpha}\, e^{-\beta_1(1-e^\alpha)a/\alpha}$. Swapping the second and third exponentials using again eq. (2.20) yields the desired normal-ordered expression.

A more general quadratic exponential can also be cast in normal ordered form. For arbitrary complex numbers α, β_1, β_2, γ_1, γ_2 the following relation holds:

$$\begin{aligned} &e^{\alpha a^\dagger a+\beta_1 a+\beta_2 a^\dagger+\gamma_1 a^2+\gamma_2 a^{\dagger 2}} = \\ &\quad e^{-\frac{\alpha}{2}+\frac{\phi_0}{2}-z_1 z_2\left(\alpha+1-e^{\phi_0}\right)-z_1^2(\gamma_2-\phi_+)-z_2^2(\gamma_1-\phi_-)}\times \\ &\quad e^{\phi_+ a^{\dagger 2}}\; e^{\left(\phi_+ z_1-z_2\left(1-e^{\phi_0}\right)\right)a^\dagger}\; e^{\phi_0 a^\dagger a}\; e^{\phi_- a^2}\; e^{\left(\phi_- z_2-z_1\left(1-e^{\phi_0}\right)\right)a}, \end{aligned} \tag{2.25}$$

where

$$\begin{aligned} z_1 &= \frac{\alpha\beta_1-2\gamma_1\beta_2}{\alpha^2-4\gamma_1\gamma_2} = \frac{\alpha\beta_1-2\gamma_1\beta_2}{\Gamma^2} \\ z_2 &= \frac{\alpha\beta_2-2\gamma_2\beta_1}{\alpha^2-4\gamma_1\gamma_2} = \frac{\alpha\beta_2-2\gamma_2\beta_1}{\Gamma^2} \\ \phi_\pm &= \frac{f_\pm}{2\Gamma}\frac{\sinh(\Gamma)}{\cosh(\Gamma)-\frac{\alpha}{\Gamma}\sinh(\Gamma)} \\ \phi_0 &= -\ln\left[\cosh(\Gamma)-\frac{\alpha}{\Gamma}\sinh(\Gamma)\right] \\ f_+ &= 2\gamma_2, \qquad f_- = 2\gamma_1, \qquad \Gamma^2 = \alpha^2-4\gamma_1\gamma_2\,. \end{aligned} \tag{2.26}$$

To prove this expression one can first eliminate the linear terms. This is achieved by including them as displacements of the quadratic terms, with the Ansatz $e^{\alpha a^\dagger a+\beta_1 a+\beta_2 a^\dagger+\gamma_1 a^2+\gamma_2 a^{\dagger 2}} = e^{z_1 a}e^{-z_2 a^\dagger}e^{\alpha a^\dagger a\gamma_1 a^2+\gamma_2 a^{\dagger 2}-\Omega}e^{-z_1 a}e^{z_2 a^\dagger}$. For this equality to be satisfied, the parameters z_1 and z_2 need to be determined using eq. (2.19). This yields $\Omega = \alpha z_1 z_2+\gamma_1 z_2^2+\gamma_2 z_1^2$, $\beta_1 = \alpha z_1+2\gamma_1 z_2$ and $\beta_2 = \alpha z_2+2\gamma_2 z_1$, from which it follows that $z_1 = \frac{\alpha\beta_1-2\gamma_1\beta_2}{\alpha^2-4\gamma_1\gamma_2}$ and $z_2 = \frac{\alpha\beta_2-2\gamma_2\beta_1}{\alpha^2-4\gamma_1\gamma_2}$. These expressions for z hold as long as the denominator is not zero. The remaining exponential $e^{\alpha a^\dagger a+\gamma_1 a^2+\gamma_2 a^{\dagger 2}}$ can be split using eq. (2.22), with $f_+ = 2\gamma_2$, $f_- = 2\gamma_1$, $f_0 = 2\alpha$, such that $\Gamma^2 = \alpha^2-4\gamma_1\gamma_2$. After defining for simplicity the numerical factors via $\tilde{\Omega} = -\phi_0/2+\Omega+\alpha_r/2$, this yields $e^{\alpha a^\dagger a+\beta_1 a+\beta_2 a^\dagger+\gamma_1 a^2+\gamma_2 a^{\dagger 2}} = e^{-\tilde{\Omega}}\, e^{z_1 a}e^{-z_2 a^\dagger}e^{\phi_+ a^{\dagger 2}}e^{\phi_0 a^\dagger a}e^{\phi_- a^2}e^{-z_1 a}e^{z_2 a^\dagger} = e^{-\tilde{\Omega}}\, e^{\phi_+(a^\dagger+z_1)^2}\, e^{\phi_0(a^\dagger a+z_1 a+z_2 a^\dagger+z_1 z_2)}\, e^{\phi_-(a+z_2)^2}$, where the relations (2.19) for

the displacements were used. As a last step, the exponential in the center can now be split using eq. (2.24), which yields $e^{\phi_0(a^\dagger a + z_1 a + z_2 a^\dagger + z_1 z_2 \phi_0)} = e^{-z_1 z_2(1-e^{\phi_0})} e^{-z_2(1-e^{\phi_0})a^\dagger} e^{\phi_0 a^\dagger a} e^{-z_1(1-e^{\phi_0})a}$. Collecting all numerical pre-factors yields the relation given in eq. (2.25) with the definitions as in (2.26).

2.4.2 Normal ordered form of the pulsing operator

Using the expressions for exponential ordering, it is straightforward to cast the pulsing operator $\Upsilon = \frac{e^{-i\sqrt{2}\alpha P_L - P_L^2/2}}{\pi^{1/4}}\, e^{-\chi^2(b+b^\dagger)^2/4} e^{\chi P_L (b+b^\dagger)/\sqrt{2}} e^{i\Omega(b+b^\dagger)}$ into normal ordered form. This form is convenient for computing the action of the operator onto a mechanical state. First, the linear terms can be rearranged using eq. (2.18) with the substitution $\theta_\pm = i\Omega \pm \chi P_L/\sqrt{2}$, which yields

$$e^{(i\Omega + \chi P_L/\sqrt{2})(b+b^\dagger)} = e^{\theta_+ b^\dagger} e^{-\theta_-^* b} e^{-\frac{1}{2}\theta_+\theta_-^*}\,. \tag{2.27}$$

The quadratic terms in eq. (2.15) can be split in terms of b and $b^\dagger$, using $X_m^2 = (b^2 + b^{\dagger 2} + 2b^\dagger b + 1)/2$ and the ordering theorem given in eq. (2.22). For the case here, the definitions in eq. (2.23) become $f_+ = f_- = -\chi^2/2$, $f_0 = -\chi^2$ and $\Gamma = 0$. Note that for $\Gamma = 0$ the relation given in eq. (2.25) does not hold, since the derivation of z_1, z_2 relied on $\Gamma \neq 0$. However, in this case the pulsing operator can be simplified since for $\Gamma = 0$ we have $\cosh(\Gamma) = \sinh(\Gamma)/\Gamma = 1$, and thus $\phi_\pm = \frac{f_\pm}{2 - f_0} = -\frac{1}{2}\frac{\chi^2}{2+\chi^2}$ and $\phi_0 = -\ln\left[1 - \frac{f_0}{2}\right] = -\ln\left[1 + \chi^2/2\right]$. Therefore the exponential with quadratic terms in eq. (2.15) becomes

$$e^{-\frac{1}{2}\chi^2 X_m^2} = e^{-\frac{1}{2}\frac{\chi^2}{2+\chi^2} b^{\dagger 2}}\; e^{-\ln\left[1+\frac{\chi^2}{2}\right](b^\dagger b + \frac{1}{2})}\; e^{-\frac{1}{2}\frac{\chi^2}{2+\chi^2} b^2} \tag{2.28}$$

Using eqs. (2.27) and (2.28), the total expression for the exponential operators is now of the form $(1+\chi^2/2)^{-1/2}\, e^{\phi_+ b^{\dagger 2}} e^{\phi_0 b^\dagger b} e^{\phi_- b^2} e^{\theta_+ b^\dagger} e^{-\theta_-^* b} e^{-\frac{1}{2}\theta_+\theta_-^*}$. To achieve normal ordering, one can use eq. (2.19) to pass $e^{\theta_+ b^\dagger}$ to the left side of the expression. The relevant exponentials for this procedure can be written as $e^{\theta_+ b^\dagger} e^{\Phi_+ b^{\dagger 2}} e^{\Phi_0(b^\dagger b + \theta_+ b^\dagger)} e^{\Phi_-(b+\theta_+)^2} e^{-\theta_-^* b}$. As a final step one is left with splitting $e^{\Phi_0(b^\dagger b + \theta_+ b^\dagger)}$. To this end, one can use the theorem in eq. (2.21) with $A = \Phi_0\theta_+ b^\dagger$, $B = \Phi_0 b^\dagger b$ and $\omega = -\Phi_0$, such that $e^{\Phi_0(b^\dagger b + \theta_+ b^\dagger)} = e^{-\theta_+ b^\dagger(1-e^{\Phi_0})} e^{\Phi_0 b^\dagger b}$. Using these results, and combining eqs. (2.15), (2.27) and (2.28), the Υ-operator in normal ordered form becomes

$$\begin{aligned}\Upsilon = &\sqrt{\frac{2}{\sqrt{\pi}(2+\chi^2)}}\; e^{-i\sqrt{2}\alpha P_L - P_L^2/2}\; e^{-\frac{1}{2}\theta_+\theta_-^*}\; e^{-\frac{1}{2}\frac{\chi^2}{2+\chi^2}\theta_+^2} \\ &e^{\frac{2\theta_+}{2+\chi^2} b^\dagger}\; e^{-\frac{1}{2}\frac{\chi^2}{2+\chi^2} b^{\dagger 2}}\; e^{-\ln\left[1+\chi^2/2\right] b^\dagger b}\; e^{-\frac{1}{2}\frac{\chi^2}{2+\chi^2}(b^2 + 2\theta_+ b)}\; e^{-\theta_-^* b}\,,\end{aligned} \tag{2.29}$$

where $\theta_\pm = i\Omega \pm \chi P_L/\sqrt{2}$.

2.4.3 Squeezed state preparation from an initial coherent state

In the following, the case of an initial mechanical coherent state $|\,\beta\rangle$ is considered, such that $|\,\Psi\rangle_m = \mathcal{N}\,\Upsilon|\,\beta\rangle_m = \mathcal{N}\,\Upsilon D(\beta)|\,0\rangle_m$.

First, the operator $D(\beta)$ can be included in the above expression (2.29) by using the property

$$e^{\alpha_+ b^\dagger - \alpha_-^* b} e^{\beta_+ b^\dagger - \beta_-^* b} = e^{(\alpha_+ + \beta_+) b^\dagger - (\alpha_-^* + \beta_-^*) b}\, e^{\frac{1}{2}(\alpha_+ \beta_-^* - \alpha_-^* \beta_+)}\,. \tag{2.30}$$

With the substitution $\alpha_\pm = i\Omega \pm \sqrt{2}\chi p$ and $\beta_\pm = \beta$ in the above expression, one can combine $D(\beta)$ with eq. (2.27). Therefore, the resulting mirror state is given by eq. (2.29) with $\theta_\pm = \beta + i\Omega \pm \chi P_L/\sqrt{2}$ and an additional factor $e^{(i\Omega + \chi P_L/\sqrt{2})\mathrm{Re}[\beta]}$. Since $b|\,0\rangle = 0$ the state of the mirror after the pulsed sequence becomes

$$\begin{aligned} |\,\Psi\rangle_m =& \frac{\sqrt{2}\mathcal{N} e^{-i\sqrt{2}\alpha P_L - P_L^2/2}}{\pi^{1/4}\sqrt{2+\chi^2}}\; e^{(i\Omega + \chi P_L/\sqrt{2})\mathrm{Re}\,[\beta]}\, e^{-\frac{1}{2}\theta_+\theta_-^*}\, e^{-\frac{1}{2}\frac{\chi^2}{2+\chi^2}\theta_+^2} \\ & e^{\frac{2\theta_+}{2+\chi^2} b^\dagger}\; e^{-\frac{1}{2}\frac{\chi^2}{2+\chi^2} b^{\dagger 2}}\; |\,0\rangle_m\,. \end{aligned} \tag{2.31}$$

This expression can be compared to a squeezed state $S(\zeta)|\,0\rangle$ with squeezing parameter $\zeta = re^{i\phi}$. Using the relations (2.22) and (2.23) with $f_+ = -\zeta$, $f_- = \zeta^*$ and $f_0 = 0$, the squeezing operator can be written in normal form as

$$\begin{aligned} S(\zeta) &= e^{-\frac{1}{2}(\zeta b^{\dagger 2} - \zeta^* b^2)} \\ &= e^{-\frac{1}{2}\tanh(r) e^{i\phi} b^{\dagger 2}} e^{-\ln[\cosh(r)](b^\dagger b + \frac{1}{2})} e^{\frac{1}{2}\tanh(r) e^{-i\phi} b^2}\,. \end{aligned} \tag{2.32}$$

Comparing this expression with the above mechanical state, (2.31), one can see that the state of the mechanics is related to a squeezed state. The squeezing parameter can be directly identified as

$$r = \frac{1}{2}\ln[1+\chi^2] \tag{2.33}$$

such that

$$\cosh(r) = \frac{1+\chi^2/2}{\sqrt{1+\chi^2}}; \quad \sinh(r) = \frac{\chi^2}{2\sqrt{1+\chi^2}}; \quad \tanh(r) = \frac{\chi^2}{2+\chi^2}\,. \tag{2.34}$$

In addition, one can include arbitrary functions of b acting on the vacuum state such that the squeezing operator is completed. This yields:

$$e^{-\frac{1}{2}\frac{\chi^2}{2+\chi^2}b^{\dagger 2}}\,|\,0\rangle = e^{-\frac{1}{2}\tanh(r)b^{\dagger 2}}\,|\,0\rangle = \sqrt{\cosh(r)}\,S(r)\,|\,0\rangle\,, \tag{2.35}$$

where eq. (2.32) was used.

Next, by the use the following property of the squeezing operator

$$S^{-1}(\zeta)b^\dagger S(\zeta) = b^\dagger\cosh(r) - be^{-i\phi}\sinh(r)\,, \tag{2.36}$$

which follows from eq. (2.16), and by completing the displacement operator one obtains

$$\begin{aligned} e^{\frac{2\theta_+}{2+\chi^2}\,b^\dagger}S(r)|\,0\rangle &= S(r)e^{\frac{2\theta_+}{2+\chi^2}(b^\dagger\cosh(r)\,-\,b\sinh(r))}|\,0\rangle \\ &= e^{-\frac{2\theta_+^2}{(2+\chi^2)^2}\cosh(r)\sinh(r)}\,S(r)\,e^{\frac{2\theta_+\cosh(r)}{2+\chi^2}\,b^\dagger}|\,0\rangle \\ &= e^{-\frac{1}{2}\frac{\chi^2}{(2+\chi^2)(1+\chi^2)}\,\theta_+^2}\,e^{\frac{|\theta_+|^2}{2(1+\chi^2)}}\,S(r)\,D(\mu)|\,0\rangle \end{aligned} \tag{2.37}$$

where

$$\mu = \frac{2\cosh(r)}{2+\chi^2}\,\theta_+ = \frac{1}{\sqrt{1+\chi^2}}\,(\beta + i\Omega + \chi P_L/\sqrt{2})\,. \tag{2.38}$$

Here eq. (2.18) was used to split the exponentials and the relations (2.34) were used to express the results in terms of the squeezing parameter.

After the combination of the above results with eq. (2.31), the mirror state becomes

$$\begin{aligned} |\,\Psi\rangle_m =& \frac{\mathcal{N}e^{-i\alpha\sqrt{2}P_L - P_L^2/2}}{\pi^{1/4}(1+\chi^2)^{1/4}}\,e^{(i\Omega\,+\,\chi P_L/\sqrt{2})\mathrm{Re}\,[\beta]}\,e^{-\frac{1}{2}\theta_+\theta_-^*}\,e^{-\frac{1}{2}\frac{\chi^2}{1+\chi^2}\theta_+^2} \\ & e^{\frac{|\theta_+|^2}{2(1+\chi^2)}}\,S(r)\,D(\mu)|\,0\rangle_m\,. \end{aligned} \tag{2.39}$$

Using $\theta_\pm = \beta + i\Omega \pm \chi P_L/\sqrt{2}$ explicitly in the above equation, the expression reduces to

$$|\,\Psi\rangle_m = \frac{\mathcal{N}e^{i\Phi(\beta)}}{\pi^{1/4}(1+\chi^2)^{1/4}}\,e^{-\frac{(\sqrt{2}\chi\mathrm{Re}[\beta]-P_L)^2}{2(1+\chi^2)}}\,S(r)\,D(\mu)|\,0\rangle\,, \tag{2.40}$$

where $\Phi(\beta) = (1+\chi^2)^{-1}\left(\Omega\beta_r + \Omega\chi P_L/\sqrt{2} + \beta_i\chi P_L/\sqrt{2} - \chi^2\beta_r\beta_i\right)$, with $\beta_r = \mathrm{Re}[\beta]$ and $\beta_i = \mathrm{Im}[\beta]$, is a global phase.

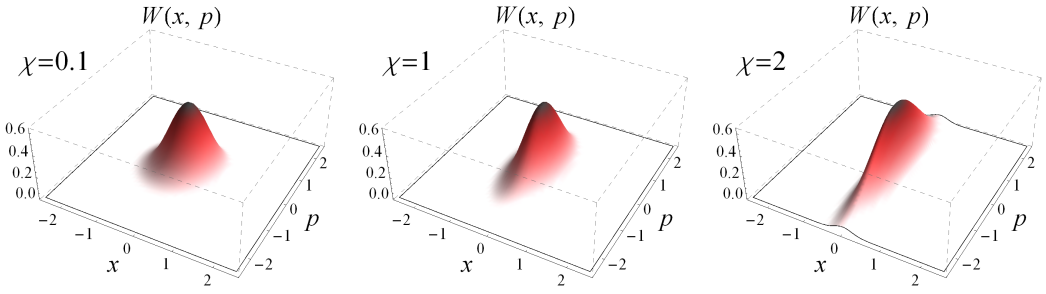

Figure 2.4: Wigner function of the mechanical state after a pulsed sequence. An initial coherent state becomes squeezed and displaced (the displacement is not shown here), see eq. (2.42). For interaction strength $\chi = 0.1$, the state is practically indistinguishable from a coherent state. For $\chi = 1$, the variance in the X_m-quadrature becomes $\Delta X_m^2 = 1/4$. The squeezing grows with increasing χ and is independent of the measurement outcome P_L.

To compute the normalization factor $\mathcal{N}$ one can use $D^\dagger(\beta) b\, D(\beta) = b + \beta$, such that $D^\dagger(\beta) X_m\, D(\beta) = X_m + \sqrt{2}\mathrm{Re}[\beta]$. With $|\langle 0\,|\,x\rangle|^2 = e^{-x^2}/\sqrt{\pi}$ the normalization factor becomes

$$\begin{aligned}
\mathcal{N}^{-2} &= \frac{1}{\sqrt{\pi}} \langle \beta\,|e^{-(\chi X_m - P_L)^2}|\,\beta\rangle = \frac{1}{\sqrt{\pi}} \langle 0\,|e^{-(\chi X_m + \sqrt{2}\chi\,\mathrm{Re}[\beta] - P_L)^2}|\,0\rangle \\
&= \frac{e^{-(\sqrt{2}\chi\,\mathrm{Re}[\beta] - P_L)^2}}{\pi} \int dx\, e^{-x^2(1+\chi^2)} e^{-2\chi x(\sqrt{2}\chi\,\mathrm{Re}[\beta] - P_L)} \\
&= \frac{e^{-(\sqrt{2}\chi\,\mathrm{Re}[\beta] - P_L)^2}}{\sqrt{\pi(1+\chi^2)}}\, e^{\frac{\chi^2(\sqrt{2}\chi\,\mathrm{Re}[\beta] - P_L)^2}{1+\chi^2}} \\
&= \frac{1}{\sqrt{\pi(1+\chi^2)}}\, e^{-\frac{(\sqrt{2}\chi\,\mathrm{Re}[\beta] - P_L)^2}{1+\chi^2}}\,.
\end{aligned} \tag{2.41}$$

Thus $\mathcal{N}$ cancels exactly all pre-factors in eq. (2.40). Omitting the global phase, the final result is

$$\begin{aligned}
&|\,\Psi\rangle_m = S(r) D(\mu)|\,0\rangle_m \\
&\text{with} \qquad r = \frac{1}{2}\ln[1+\chi^2]; \qquad \mu = e^{-r}\,(\beta + i\Omega + \frac{\chi P_L}{\sqrt{2}})\,.
\end{aligned} \tag{2.42}$$

By measurement of the optical phase quadrature P_L, the mirror is thus remotely projected into a squeezed displaced state. Therefore pulsed optomechanics can be used for measurement-based state preparation of the mechanical mirror.

2.4.4 State preparation from an initial thermal state

If the mirror is initially in a thermal state ρ_{th}, the pulsed scheme described above can still be used to remotely prepare a pure state of the mirror. In particular, with a single pulsed interaction, squeezing in the position of the mirror can be achieved. As will be discussed further below, even the preparation of a nearly pure squeezed state can be done, if two pulsed interactions are utilized.

As before, the state of the mirror after the pulsed protocol is computed by applying the operator Υ to the mechanical state. The marginals of the mirror state after the action of Υ are

$$\mathcal{N}^2\langle x\,|U_0(\theta)\Upsilon\rho_{th}\Upsilon^\dagger U_0^\dagger(\theta)|\,x\rangle \tag{2.43}$$

where Υ is given in eq. (2.6) and $U_0(\theta) = e^{-i\theta b^\dagger b}$ is the free evolution of the mirror. The thermal state, when written in the coherent state basis, is given by $\rho_{th} = (\pi\bar{n})^{-1}\int d^2\beta e^{-|\beta|^2/\bar{n}}|\,\beta\rangle\langle\beta\,|$, with $\bar{n} = (e^{\hbar\omega/k_BT} - 1)^{-1}$. In the previous section it was show how Υ acts onto a coherent state β. Before renormalization, the result is given by eq. (2.40). Applying additionally a subsequent harmonic evolution $U_0(\theta)$, the state becomes

$$U_0(\theta)\Upsilon|\,\beta\rangle = \frac{e^{i\Phi(\beta)}}{(\pi(1+\chi^2))^{1/4}}\, e^{-\frac{\chi^2}{(1+\chi^2)}(\beta_r - \frac{P_L}{\sqrt{2}\chi})^2} S(re^{-i2\theta})D(\mu e^{-i\theta})|\,0\rangle\,, \tag{2.44}$$

where $\beta_r = \mathrm{Re}[\beta]$. The marginals (2.43) for the thermal state after the pulsed sequence can therefore be written as

$$\begin{aligned}&\mathcal{N}^2\langle x\,|U_0(\theta)\Upsilon\rho_{th}\Upsilon^\dagger U_0^\dagger(\theta)|\,x\rangle = \\ &\frac{\mathcal{N}^2}{\pi\bar{n}\sqrt{\pi(1+\chi^2)}}\int d^2\beta\, e^{-|\beta|^2/\bar{n}} e^{-\frac{2\chi^2}{1+\chi^2}(\beta_r - \frac{P_L}{\sqrt{2}\chi})^2}|\langle x\,|S(re^{-i2\theta})D(\mu e^{-i\theta})|\,0\rangle|^2\end{aligned} \tag{2.45}$$

The last term can be written out explicitly by using [74]

$$|\langle x_\theta\,|D(\alpha)S(re^{i\varphi})|\,0\rangle|^2 = (2\pi\Delta x^2_{\theta,sq})^{-1/2}\, e^{-\frac{(x_\theta - \langle x_\theta\rangle_{sq})^2}{2\Delta x^2_{\theta,sq}}} \tag{2.46}$$

with

$$\begin{aligned}\langle x_\theta\rangle_{sq} &= \frac{1}{\sqrt{2}}(\alpha e^{-i\theta} + \alpha^* e^{i\theta}) \\ \Delta x^2_{\theta,sq} &= \frac{1}{2}\, e^{-2r}\cos^2(\theta - \varphi/2) + \frac{1}{2}\, e^{2r}\sin^2(\theta - \varphi/2)\end{aligned} \tag{2.47}$$

and using the relation

$$S(re^{i\varphi})D(\alpha) = D(\alpha\cosh r - \alpha^* e^{i\varphi}\sinh r)S(re^{i\varphi})\,. \tag{2.48}$$

In the case considered here, where $\varphi = -2\theta$ and $\alpha = \mu e^{-i\theta}$, the mean and variance of the state are given by

$$\begin{aligned}\langle x_\theta\rangle_{sq} &= \sqrt{2}(\mu_r\; e^{-r}\cos(\theta) + \mu_i\; e^{r}\sin(\theta))\\ \Delta x^2_{\theta,sq} &= \frac{1}{2}\; e^{-2r}\cos^2(\theta) + \frac{1}{2}\; e^{2r}\sin^2(\theta)\,.\end{aligned} \tag{2.49}$$

The normalization factor $\mathcal{N}^2$ is easily found, since all the integrals are Gaussian:

$$\mathcal{N}^2 = \frac{1}{\mathrm{Tr}[\Upsilon\hat{\rho}_{th}\Upsilon^\dagger]} = \sqrt{\pi(1+\chi^2(1+2\bar{n}))}\; e^{P_L^2/(1+\chi^2(1+2\bar{n}))}\,. \tag{2.50}$$

Using the above results in eq. (2.45) and performing the integrals over $\beta_r = \mathrm{Re}[\beta]$ and $\beta_i = \mathrm{Im}[\beta]$, the marginals become:

$$\mathcal{N}^2\langle x\,|U_0(\theta)\Upsilon(p)\,\hat{\rho}_{th}\Upsilon^\dagger(p)U_0^\dagger(\theta)|\,x\rangle = \frac{1}{\sqrt{2\pi\sigma_\theta^2}}\; e^{\frac{-(x-\langle x\rangle_\theta)^2}{2\sigma_\theta^2}}$$

where

$$\begin{aligned}2\sigma_\theta^2 &= \frac{\cos^2(\theta)}{\chi^2 + \frac{1}{1+2\bar{n}}} + (\chi^2 + 1 + 2\bar{n})\;\sin^2(\theta)\\ \langle x\rangle_\theta &= \sqrt{2}\,\Omega\;\sin(\theta) + \frac{\chi P_L}{\chi^2 + \frac{1}{1+2\bar{n}}}\;\cos(\theta)\,.\end{aligned} \tag{2.51}$$

Thus the resulting state is a Gaussian, with mean position and momentum

$$\begin{aligned}\langle x\rangle_{\theta=0} &= \frac{\chi P_L}{\chi^2 + \frac{1}{1+2\bar{n}}} = 2\sigma^2_{\theta=0}\;\chi P_L\\ \langle x\rangle_{\theta=\pi/2} &= \sqrt{2}\,\Omega\end{aligned} \tag{2.52}$$

and respective variances

$$\begin{aligned}2\sigma^2_{\theta=0} &= \frac{1}{\chi^2 + \frac{1}{1+2\bar{n}}} = \frac{1}{\chi^2 + \frac{1}{2\sigma^2_{th}}}\\ 2\sigma^2_{\theta=\pi/2} &= \chi^2 + 1 + 2\bar{n} = \chi^2 + 2\sigma^2_{th}\,,\end{aligned} \tag{2.53}$$

where $2\sigma^2_{th} = 1 + 2\bar{n}$. A single pusle and subsequent measurement thus changes the mechanical state: The mean of the momentum is changed by Ω,

which is deterministic, wheras the mean of the position is random, since it depends on the outcome P_L. A single pulse also reduces the uncertainty in the position of the mirror, depending on the interaction strength χ. However, the uncertainty in momentum remains unaffected, except for an anti-squeezing effect (as predicted by complementarity) captured by χ^2. This is consistent with the initial derivation of Υ, which describes the measurement of the mirror's position through measurement of the optical phase. No knowledge of the mirror's momentum is obtained, thus the uncertainty in momentum is only affected through quantum complementarity.

The total purity of the state can be estimated by considering the square root of the phase-space area covered by the two variances:

$$A = \sqrt{4\sigma^2_{\theta=0}\sigma^2_{\theta=\pi/2}} = \sqrt{\frac{\chi^2+1+2\bar{n}}{\chi^2+\frac{1}{1+2\bar{n}}}} \approx \sqrt{\frac{2\bar{n}}{\chi^2}}\,, \tag{2.54}$$

where the last approximation is valid for $\bar{n} \gg 1, \chi^2$. Thus the uncertainty of the initial thermal state, which is of order $\bar{n}$, is reduced after one pulsed sequence by $\sqrt{\bar{n}}$ if the parameter χ is of order 1. Based on the phase space area, one can define an effective temperature of the resulting state by comparison to an effective thermal state with the same area:

$$A = 1 + 2\bar{n}_{eff}\,. \tag{2.55}$$

Therefore, the effective temperature or occupation after the action of one pulse onto a thermal state is

$$\bar{n}_{eff} \approx \sqrt{\frac{\bar{n}}{2\chi^2}}\,. \tag{2.56}$$

2.4.5 Two-pulse sequence for state purification

The uncertainty in the state can be further reduced by utilizing another pulsed interaction. As discussed above, a single pulse does not affect the uncertainty in momentum. However, a second pulsed interaction can be introduced after the first pulsed measurement. By utilizing the mirror's harmonic evolution, one can therefore further purify the mirror state. If the two pulses are separated by exactly a quarter mechanical period, the purification is the strongest, since the second pulse affects the initial uncertainty in momentum in this case. The state of the mirror after the second pulsed measurement with outcome P_{L2} is described by

$$\rho^{(2)}_M = \mathcal{N}_2^2 \Upsilon(P_{L2}) \rho^{(1)}_M \Upsilon^\dagger(P_{L2}) \tag{2.57}$$

where

$$\rho_M^{(1)} = \mathcal{N}_1^2 U_0(\frac{\pi}{2})\Upsilon(P_{L1})\rho_{th}\Upsilon^\dagger(P_{L1})U_0^\dagger(\frac{\pi}{2}) \tag{2.58}$$

In the following, the marginals for the state $\rho_M^{(2)}$ are computed, where for simplicity the focus will be on the position and momentum distributions only.

Utilizing eq. (2.51) with eqs. (2.52) and (2.53) for the momentum distribution of the mirror after the first pulse, the X-distribution of the state $\rho_M^{(2)}$ after the second pulse is given by

$$\begin{aligned}
\langle X\,|\rho_M^{(2)}|\,X\rangle &= \mathcal{N}_2^2\langle X\,|\Upsilon(P_{L2})\mathcal{N}_1^2 U_0(\frac{\pi}{2})\Upsilon(P_{L1})\rho_{th}\Upsilon^\dagger(P_{L1})U_0^\dagger(\frac{\pi}{2})\Upsilon^\dagger(P_{L2})|\,X\rangle \\
&= \frac{\mathcal{N}_2^2}{\sqrt{\pi}}\,e^{-(\chi X - P_{L2})^2}\langle X\,|\mathcal{N}_1^2 U_0(\frac{\pi}{2})\Upsilon(P_{L1})\rho_{th}\Upsilon^\dagger(P_{L1})U_0^\dagger(\frac{\pi}{2})|\,X\rangle \\
&= \frac{\mathcal{N}_2^2}{\sqrt{\pi}}\,e^{-(\chi X - P_{L2})^2}\frac{1}{\sqrt{\pi(1+\chi^2+2\bar{n})}}\,e^{-\frac{(X-\sqrt{2}\,\Omega)^2}{1+\chi^2+2\bar{n}}} \\
&= \frac{\mathcal{N}_2^2\,e^{-\frac{(\frac{P_{L2}}{\chi}-\sqrt{2}\,\Omega)^2}{\chi^{-2}+1+\chi^2+2\bar{n}}}}{\sqrt{\pi}\sqrt{\pi(1+\chi^2+2\bar{n})}}\,e^{-(\chi^2+\frac{1}{1+\chi^2+2\bar{n}})(X-\frac{\chi P_{L2}+\frac{\sqrt{2}\Omega}{1+\chi^2+2\bar{n}}}{\chi^2+(1+\chi^2+2\bar{n})^{-1}})^2}.
\end{aligned} \tag{2.59}$$

The normalization factor $\mathcal{N}_2^2$ can be computed via $\mathcal{N}_2^2 = (\mathrm{Tr}[\rho_M^{(2)}])^{-1} = (\int dX\,\langle X\,|\hat{\rho}_M^{(2)}|\,X\rangle)^{-1}$. This yields

$$\mathcal{N}_2^2 = \sqrt{\pi}\sqrt{\chi^2(1+\chi^2+2\bar{n})+1}\;e^{\frac{(\frac{P_{L2}}{\chi}-\sqrt{2}\Omega)^2}{1+\chi^2+2\bar{n}+\chi^{-2}}}. \tag{2.60}$$

Thus the final result for the mechanical X-quadrature after the 2nd pulse is:

$$\langle X\,|\rho_M^{(2)}|\,X\rangle = \frac{1}{\sqrt{2\pi(\sigma_{\theta=0}^{(2)})^2}}\,e^{-\frac{\left(X-\langle X^{(2)}\rangle_{\theta=0}\right)^2}{2(\sigma_{\theta=0}^{(2)})^2}}$$

where

$$\begin{aligned}
2(\sigma_{\theta=0}^{(2)})^2 &= \frac{1}{\chi^2+\frac{1}{1+\chi^2+2\bar{n}}} = \frac{1}{\chi^2+\frac{1}{2(\sigma_{\theta=\pi/2}^{(1)})^2}} \\
\langle X^{(2)}\rangle_{\theta=0} &= \frac{\chi P_{L2}+\frac{\sqrt{2}\Omega}{1+\chi^2+2\bar{n}}}{\chi^2+\frac{1}{1+\chi^2+2\bar{n}}} = 2(\sigma_{\theta=0}^{(2)})^2\left(\chi P_{L2}+\frac{\langle X_1\rangle_{\pi/2}}{2(\sigma_{\theta=\pi/2}^{(1)})^2}\right)
\end{aligned} \tag{2.61}$$

Note that for large initial temperatures, i.e. $\bar{n} \gg 1, \chi^2$, the uncertainty in position becomes

$$2(\sigma_{\theta=0}^{(2)})^2 \to \frac{1}{\chi^2}. \tag{2.62}$$

Squeezing in the X-quadrature below the ground state extension (for which $2(\sigma^{(2)}_{\theta=0})^2 = 1$) can thus be achieved for $\chi > 1$.

To show that the state is indeed a squeezed state with an uncertainty close to the Heisenberg limit, the noise in the anti-squeezed p-quadrature of the mechanics needs to be considered as well. The marginals for the momentum distribution after the second pulse are given by

$$\begin{aligned}
\langle P\,|\rho^{(2)}_m|\,P\rangle &= \mathcal{N}_2^2\langle P\,|\Upsilon(P_{L2})\mathcal{N}_1^2 U_0(\frac{\pi}{2})\Upsilon(P_{L1})\rho_{th}\Upsilon^\dagger(P_{L1})U_0^\dagger(\frac{\pi}{2})\Upsilon^\dagger(P_{L2})|\,P\rangle \\
&= \mathcal{N}_2^2\mathcal{N}_1^2\,\frac{1}{\bar{n}\pi}\int d^2\beta\, e^{-\frac{|\beta|^2}{\bar{n}}}\left|\langle P\,|\Upsilon(P_{L2})U_0(\frac{\pi}{2})\Upsilon(P_{L1})|\,\beta\rangle\right|^2 \\
&= \frac{\mathcal{N}_2^2\mathcal{N}_1^2}{\bar{n}\pi}\int d^2\beta\, e^{-\frac{|\beta|^2}{\bar{n}}}\left|\int dX\frac{e^{-iXP}}{\sqrt{2\pi}}\frac{e^{-\frac{1}{2}(\chi X-P_{L2})^2}}{\pi^{1/4}}\langle X\,|U_0(\frac{\pi}{2})\Upsilon(P_{L1})|\,\beta\rangle\right|^2
\end{aligned} \tag{2.63}$$

where the overlap $\langle P\,|\,X\rangle = \frac{e^{-iXP}}{\sqrt{2\pi}}$ was used. With the expression (2.44), one needs to consider the squeezed displaced state in the position representation, which is given by [74]

$$\begin{aligned}
\langle x\,|S(re^{-i2\theta})D(\mu\,e^{-i\theta})|\,0\rangle &= \langle x\,|D(\mu\,e^{-i\theta}\cosh(r) - \mu^*\,e^{-i\theta}\sinh(r))S(re^{-i2\theta})|\,0\rangle \\
&= \frac{e^{i\Phi_{sq}}}{(2\pi\sigma^2_{sq})^{1/4}}\,e^{i\langle x_{\pi/2}\rangle_{sq}}\,e^{-\frac{(1+i\sin(2\theta)\sinh(2r))(x-\langle\hat{x}\rangle_{sq})^2}{4\sigma^2_{sq}}}
\end{aligned} \tag{2.64}$$

where the displaced squeezed state variance and mean are given by

$$\begin{aligned}
2\sigma^2_{sq} &= e^{2r}\sin^2(\theta) + e^{-2r}\cos^2(\theta) \\
\langle\hat{x}\rangle_{sq} &= \sqrt{2}(\mu_r e^{-r}\cos(\theta) + \mu_i e^{r}\sin(\theta)) \\
\langle\hat{x}_{\pi/2}\rangle_{sq} &= \sqrt{2}(\mu_i e^{r}\cos(\theta) + \mu_r e^{-r}\sin(\theta))\,.
\end{aligned} \tag{2.65}$$

Using these expressions in eq. (2.44) yields

$$\begin{aligned}
\langle X\,|U_0(\frac{\pi}{2})\Upsilon(P_{L1})|\,\beta\rangle = \frac{e^{i(\Phi_{sq}+\Phi(\beta))}}{\sqrt{\pi(1+\chi^2)}}\,e^{-\frac{\chi^2}{(1+\chi^2)}(\beta_r - \frac{P_{L1}}{\sqrt{2}\chi})^2} \\
e^{-i\frac{\sqrt{2}X}{1+\chi^2}(\beta_r + \frac{\chi P_{L1}}{\sqrt{2}})}\,e^{-\frac{(X-\sqrt{2}(\beta_i+\Omega))^2}{2(1+\chi^2)}}\,.
\end{aligned} \tag{2.66}$$

With the above expression in eq. (2.63) one obtains

$$\begin{aligned}
\langle P\,|\rho^{(2)}_m|\,P\rangle = \frac{\mathcal{N}_2^2\mathcal{N}_1^2}{\sqrt{\pi}(1+\chi^2)2\bar{n}\pi^3}\int d^2\beta\, e^{-\frac{|\beta|^2}{\bar{n}}}e^{-\frac{2\chi^2}{1+4\chi^2}(\beta_r-\frac{P_{L1}}{\sqrt{2}\chi})^2} \\
\left|\int dX e^{-iXP}e^{-\frac{1}{2}(\chi X-P_{L2})^2}e^{-i\frac{\sqrt{2}X}{1+\chi^2}(\beta_r+\frac{\chi P_{L1}}{\sqrt{2}})}\,e^{-\frac{(X-\sqrt{2}(\beta_i+\Omega))^2}{2(1+\chi^2)}}\right|^2\,.
\end{aligned} \tag{2.67}$$

The Gaussian integrals can now be computed, and the normalization factors are given in eq. (2.60) and eq. (2.50). The final result for the P-marginal of the mechanics after the second pulse is:

$$\langle P\,|\rho_M^{(2)}|\,P\rangle = \frac{1}{\sqrt{2\pi(\sigma^{(2)}_{\theta=\pi/2})^2}}\, e^{-\frac{\left(X-\langle X^{(2)}\rangle_{\theta=\pi/2}\right)^2}{2(\sigma^{(2)}_{\theta=\pi/2})^2}}$$

where

$$2(\sigma^{(2)}_{\theta=\pi/2})^2 = \chi^2 + \frac{1}{\chi^2+\frac{1}{1+2\bar{n}}} = \chi^2 + 2(\sigma^{(1)}_{\theta=0})^2$$

$$\langle X^{(2)}\rangle_{\theta=\pi/2} = \sqrt{2}\Omega - \frac{\chi P_{L1}}{\chi^2+\frac{1}{1+2\bar{n}}} = \sqrt{2}\Omega - \langle X^{(1)}\rangle_{\theta=0}\,. \tag{2.68}$$

One can see here that the variance in the P-quadrature of the mechanics is increased by χ^2 compared to its initial width. Thus this quadrature is anti-squeezed as compared to the position distribution, eq. (2.61), in accordance with quantum complementarity. The additional mean displacement $\sqrt{2}\Omega$ stems from the classical displacement due to the pulsed interaction, as captured by the parameter Ω.

As before, the purity of the resulting state can be quantified by the enclosed area in phase space, since the mechanical state remains Gaussian:

$$A^{(2)} = \sqrt{2(\sigma^{(2)}_{\theta=\pi/2})^2 2(\sigma^{(2)}_{\theta=0})^2} = \sqrt{\frac{\chi^2+\frac{1}{\chi^2+\frac{1}{1+2\bar{n}}}}{\frac{1}{\chi^2+\frac{1}{1+\chi^2+2\bar{n}}}}} \approx \sqrt{1+\frac{1}{\chi^4}}\,, \tag{2.69}$$

where the last approximation is valid for large $\bar{n}$. Note that the result is independent of initial temperatures. With the definition for an effective average phonon number through $A^{(2)} = 1 + 2\bar{n}^{(2)}_{eff}$, the uncertainty of the state after the second pulsed interaction is captured by

$$\bar{n}^{(2)}_{eff} = \frac{1}{2}\left(\sqrt{1+\frac{1}{\chi^4}} - 1\right) \approx \frac{1}{\chi^4}\,, \tag{2.70}$$

where the last approximation holds for $\chi \gg 1$. Since the result does not depend on the initial temperature, but is instead inversely proportional to χ^4, it is shown that one can obtain nearly pure states from any initial thermal distribution. After the action of two pulses with $\chi \approx 1$ an initially thermal mechanical state is purified to a state with an average mechanical phonon occupation of $\bar{n}^{(2)}_{eff} = \frac{1}{2}(\sqrt{2}-1) \approx 0.2$.

First experimental progress towards pulsed opto-mechanics for state preparation and state read-out has been made [97]. In the experiment, a pulsed scheme as discussed here was utilized, with the main difference being a lack of a cavity to enhance the opto-mechanical interaction. An effective coupling parameter $\chi \approx 10^{-4}$ was achieved. It was shown experimentally that an initial thermal distribution of the mechanical system is reduced to an effective temperature of $T_{eff} \approx 16$ K. Implementation of such a scheme with a cavity of Finesse $\mathcal{F} \gtrsim 10^4$ is expected to reach the quantum regime of pulsed opto-mechanics, with a parameter $\chi \sim 1$, as required for quantum state preparation and quantum state read-out of the mirror.

Chapter 3

Probing phenomenological models of quantum gravity with opto-mechanical systems

Opto-mechanical systems are ideally suited for the study of quantum phenomena in macroscopic systems. The ability to quantum mechanically control and read out a massive mechanical resonator through optical fields opens the route to probe quantum theory at unprecedented mass-scales. Opto-mechanical devices span a mass-range of about m$\sim$ 1 pg to m$\sim$ 100 kg [19–24]. A major driving force for developing opto-mechanical technologies was the proposal to test the transition from quantum behavior to classical behavior in such systems [52]. In particular, it was realized that opto-mechanical systems provide a means to test possible modifications of quantum theory in which a collapse of the wave function is caused by the mass of the system [98, 99]. These so-called gravitational collapse theories, developed by Penrose [98] and Diosi [99], predict that a superposition of sufficiently massive systems should not be sustainable even in principle. Today, large experimental efforts are made to experimentally test such proposals in opto-mechanical systems [52, 54, 57, 100].

However, opto-mechanics can also serve as a test-bed for other possible modifications of quantum theory. Even though the focus was largely on the transition to classicality, the precision and control achievable with opto-mechanical systems opens the route to probe various concepts and phenomena of quantum theory and to test whether those are modified in a novel mass-regime. In the following, it is shown that some phenomenological models of quantum gravity may be probed with opto-mechanical systems.

3.1 Modified uncertainty relations

In quantum theory, a fundamental concept is the uncertainty principle. Two observables A and B cannot be simultaneously known to arbitrary precision if they do not commute. The uncertainty relation is given by

$$\Delta A \Delta B \geq \frac{1}{2} |\langle [A, B] \rangle| . \tag{3.1}$$

The proof of the above relation is straightforward: defining the operators $A_0 = A - \langle A \rangle$ and $B_0 = B - \langle B_0 \rangle$ and the states $|\Phi_A\rangle = A_0 |\Psi\rangle$ and $|\Phi_B\rangle = B_0 |\Psi\rangle$, it follows from $\langle \Phi_A | \Phi_A \rangle \cdot \langle \Phi_B | \Phi_B \rangle \geq |\langle \Phi_A | \Phi_B \rangle|^2$ that $\Delta A^2 \Delta B^2 \geq |\langle [A, B]/2 + \{A, B\}/2 \rangle|^2 = |\langle [A, B] \rangle|^2/4 + |\langle \{A, B\} \rangle|^2/4$. For position and momentum, the uncertainty relation in quantum theory is

$$\Delta x \Delta p \geq \frac{\hbar}{2} . \tag{3.2}$$

This principle captures the inability to simultaneously determine the position and momentum of a particle. However, it is possible to measure any of the two to arbitrary precision. In particular, measurements and projections that are arbitrary close to a position eigenstate are allowed. Even though practically such measurements are restricted by experimental imperfections (current bounds on the precision of position measurements are around $\Delta x_{exp} \gtrsim 10^{-19}$ m [101]), there is no fundamental limit from quantum theory on measuring position.

In contrast, within a quantized framework of gravity the quantization of space-time is expected to lead to a fundamental limit on position measurements [102–106]. The dependence of the metric on the energy content given by Einstein's equations (1.3) suggests that the uncertainty principle in its current form is not viable at extreme scales. If the uncertainty in momentum can be sacrificed for a higher precision in position, as suggested by eq. (3.2), then $\Delta p \to \infty$ as $\Delta x \to 0$. However, a larger uncertainty in momentum implies a growth in the uncertainty in the energy-momentum tensor $T_{\mu\nu}$. From Einstein's field equations (1.3) it follows that uncertainty in the energy-momentum tensor causes back action onto the Einstein tensor $G_{\mu\nu}$ and thus onto the metric $g_{\mu\nu}$. Through the geodesic equation (1.2), the uncertainty in the metric causes an additional uncertainty in the position. Thus the back-action prevents the limit $\Delta x \to 0$ to be reached. This heuristic argument suggests that the uncertainty relation (3.2) is not fully compatible with general relativistic equations (1.3) and (1.2). In particular, the unmodified eq. (3.2) implies $\Delta x \gtrsim \hbar/\Delta p$, whereas the Schwarzschild radius suggests a fundamental limit of probing small regions of space through $\Delta x \gtrsim 2G\Delta p/c^3$.

This is in stark contrast to considerations that led to the quantization of the electro-magnetic field. The argument by Bohr and Rosenfeld [107] used the uncertainty relation (3.2) to derive quantum limits on the measurement of the electric and magnetic fields. These quantum limits, however, followed directly from the limits imposed due to the regular uncertainty principle. Any additional uncertainty in the electro-magnetic field that would be imparted by the measurement device could in principle be made arbitrary small or compensated. This is because in electro-magnetism the charge density can in principle be arbitrary large and the fields could be compensated by superposing fields of opposite sign. This is fundamentally different to measurements of gravitational fields, as was first realized by M. Bronstein [108]. In Bronstein's work, it was shown that the linearized equations of gravity obtained from the geodesic equation (1.2) could be consistently quantized, but that due to the fundamental back action from matter onto the gravitational field, a limit on measurements of gravitational fields should exist in the full theory of general relativity. Some modifications of the fundamental principles are therefore expected at some scale. This scale is typically assumed to be close to the Planck-scale [109, 110], defined through the fundamental constants $\hbar$, G and c as

$$\begin{aligned} L_p &= \sqrt{\frac{\hbar G}{c^3}} = 1.6 \times 10^{-35}\ \text{m}, \quad E_p = \sqrt{\frac{\hbar c^5}{G}} = 1.2 \times 10^{28}\ \text{eV}, \\ m_p &= \sqrt{\frac{\hbar c}{G}} = 2.2 \times 10^{-8}\ \text{kg}, \quad t_p = \sqrt{\frac{\hbar G}{c^5}} = 5.4 \times 10^{-44}\ \text{s}\,. \end{aligned} \tag{3.3}$$

Physical laws at this scale are assumed to be fundamentally different from our currently accepted theories. In particular, some or all the equations (1.1), (3.2), (1.3) and (1.2) will be modified. In particular, the above heuristic argument suggests a modified uncertainty of the order of $\Delta x \Delta p \gtrsim \hbar(1 + G\Delta p^2/(\hbar c^3)) = \hbar(1 + L_p^2 \Delta p^2/\hbar^2)$. Such heuristic arguments can only give a hint as to what to expect at these scales [111–114]. However, it seems plausible that a modification of the uncertainty principle may remain valid at least to some approximation and is, in fact, a feature of various models of quantum gravity. First suggested within string theory [102, 103], the following modified uncertainty principle is now widely believed to be a model-independent feature of quantum gravity [104, 114]:

$$\Delta x \Delta p \geq \frac{\hbar}{2}\left(1 + \beta_0 \frac{\Delta p^2}{m_p^2 c^2}\right)\,. \tag{3.4}$$

The numerical parameter β_0 in the above equation is a model-dependent parameter and captures the strength of the modification. If the uncertainty

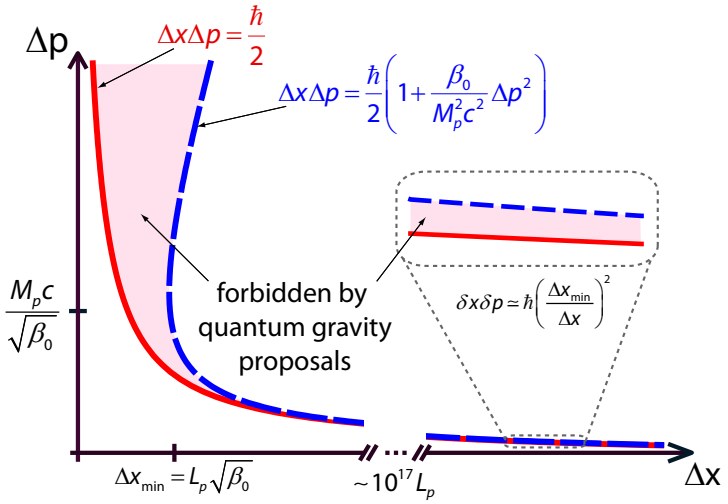

Figure 3.1: Reprint of a plot from Ref. [2]: The quantum mechanical minimum uncertainty given by eq. (3.2) as compared to the modified uncertainty, eq. (3.4). The modified uncertainty incorporates a minimal length scale $\Delta x_{min} = \sqrt{\beta_0} L_p$, below which no quantum state can be prepared or read out. For $\Delta x \gg \Delta x_{min}$ the modified uncertainty principle is practically indistinguishable from the quantum mechanical prediction.

relation is modified close to the Planck-scale, the parameter should be of order $\beta_0 \sim 1$. However, it can be considered as a free parameter that can be bounded by experiments, since a consistent theory of quantum gravity has yet to be formulated. Also, additional terms may also be present (such as terms proportional to Δx^2 to incorporate restrictions on the momentum, or higher-order contributions in $\Delta p/m_p c$), but the subsequent discussion is restricted to the above model. The inequality is minimized for the position uncertainty $\Delta x_{min} = \sqrt{\beta_0} L_p$. Thus the modified uncertainty principle captures a fundamental minimal length scale. For a comparison to the quantum uncertainty principle, see also Fig. 3.1.

The above modified uncertainty principle, eq (3.4), has motivated the study of theories with a modified algebraic structure. The relation (3.1) suggests, if it remains valid, that the canonical commutator is modified at a scale defined by β_0. A modification of the commutator algebra would entail that gravity in some way fundamentally acts back onto quantum systems. Maggiore has derived a very generic possible deformation of the canonical commutator [115, 116], under the assumptions that the rotation group for the angular momentum J remains undeformed (i.e. $[J_i, x_j] = i\hbar\epsilon_{ijk}x_k$ and

$[J_i, p_j] = i\hbar\epsilon_{ijk}p_k$, where ϵ_{ijk} is the Levi-Civita-symbol) and that the translation group is undeformed (i.e. $[p_i, p_j] = 0$). The resulting unique form of the algebra is that the positions do not commute between each other ($[x_i, x_j] = i2\mu_0\hbar\epsilon_{jik}J_k/(m_pc)^2$) and that the canonical commutator has the general form

$$[x_i, p_j] = i\hbar\delta_{ij}\sqrt{1 + 2\mu_0\frac{(|p|/c)^2 + m^2}{m_p^2}}\,, \tag{3.5}$$

where μ_0 is some numerical parameter and $|p|^2 = \sum_i^3 p_i^2$ is the square of the momentum operator. Curiously, the result above yields, to lowest order, the modified uncertainty relation (3.4) for $m \ll |p|/c \lesssim m_P$ and $\mu_0 = \beta_0$. The only difference to the uncertainty principle is the appearance of an additional term that is proportional to $\langle p\rangle^2$, which can be made arbitrary small. No assumptions about quantized gravity where made, rather, it was assumed that the fundamental algebra is deformed. Such an approach may phenomenologically capture the effect of quantized gravity on quantum systems. However, also other proposals for modified commutators have been put forward [117, 118]. The most commonly considered modification has been proposed by Kempf and colleagues [117, 119] and reads (in one spatial dimension)

$$[x, p] = i\hbar\left(1 + \beta_0\frac{p^2}{(m_pc)^2}\right)\,. \tag{3.6}$$

where β_0 is again a free numerical parameter. This deformation also yields the modified uncertainty relation, eq. (3.4), with an additional term proportional to $\langle p\rangle^2$. The deformed commutator (3.6) has been widely studied [120–129] and it was shown that a Hilbert space can be constructed with properly normalizable states [119]. In the momentum representation, the operator x can be written as $x = i\hbar(1 + \beta_0(p/m_pc)^2)\partial_p$, from which it follows that the momentum eigenstates obey $\langle p' \,|\, p\rangle = (1 + \beta_0(p/m_pc)^2)\delta(p - p')$ and that the completeness of the momentum basis is given by $1 = \int dp(1 + \beta_0(p/m_pc)^2)^{-1}$. In contrast, the position basis is no longer well defined, since position eigenstates are no longer part of the deformed theory, but it is possible to define a position representation with respect to some smeared distribution. Phenomenological models such as given in eq. (3.6) alter only the algebraic structure of ordinary quantum theory, but retain the formalism of the theory.

3.2 Scheme to probe deformations of the canonical commutator

Using a deformed canonical commutator such as given in eq. (3.6), it is possible to derive observable differences for quantum systems [128]. Investigations focused on the energy spectrum of harmonic oscillators [119, 123, 124], modified atomic spectra [121], tunneling of electrons (3.6) and electromagnetic radiation [130], to name a few. These phenomena were shown to put experimental bounds on the numerical parameter β_0, the best bound being $\beta_0 \lesssim 10^{33}$. It was also shown that under the additional assumption that the correspondence between canonical commutator and the classical Poisson bracket remains valid, stringent bounds can be found from the motion of planets from observations of their classical trajectories [131]. However, we do not know how the classical limit arises and the model given in eq. (3.4) does not seem to be applicable to classical systems. In the following, it is shown that without this assumption already with quantum mechanical systems it is possible to experimentally restrict the range for β_0. To this end, pulsed opto-mechanical systems are considered. The bounds are obtained directly from the deformation of the commutator, such as eq. (3.6), and the assumption that the commutator deformation applies to the center-of-mass of a system (a discussion of this assumption is given in Sec. 3.3.2).

Pulsed interaction between light and a mirror is described by the Hamiltonian (2.3). Therefore a single interaction gives rise to the unitary evolution $U = e^{i\lambda n_L X_m}$, where $\lambda = g_0\tau$ is the dimensionless interaction strength with the effective interaction time τ. The precise dependence of λ on the pulse and cavity parameters is found from the input-output formalism for the optical field. To probe a modification in the canonical commutator, a sequence of four subsequent pulsed interactions is considered:

$$\xi = e^{i\lambda n_L P_m}\, e^{-i\lambda n_L X_m}\, e^{-i\lambda n_L P_m}\, e^{i\lambda n_L X_m}\,. \tag{3.7}$$

These four interactions can be achieved by using one and the same pulse interacting with the mechanics every quarter mechanical period (for clarity, a subscript L is used to denote operators that act on the light). In quantum mechanics, the above operation can be rewritten as $\xi_{QM} = e^{-i\lambda^2 n_L^2}$ and yields a self-Kerr non-linear operation on the optical field. Similar schemes have been proposed [132, 133] and utilized [134] for implementing quantum gates in ions. Here it is shown that for opto-mechanical systems, models with a modified canonical commutator of the mechanics yield a measurable effect on the optical field. Even though we consider the limit where the quantum optical commutation relations hold, the operation on the light is altered due to

deformations of the mechanical commutator. Keeping the canonical commutator between the mechanical quadratures general, with only the assumption that it is a function of P_m, i.e. $[X_m, P_m] = f(P_m)$, the above expression (3.7) can be rewritten using the relation (2.16). The four-displacement-operator becomes

$$\begin{aligned}\xi &= e^{i\lambda n_L P_m}\, e^{-i\lambda n_L X_m}\, e^{-i\lambda n_L P_m}\, e^{i\lambda n_L X_m} \\ &= \exp\left(-i\lambda n_L \sum_{k=1}^{\infty} \frac{(-i\lambda n_L)^k}{k!} \left[X_m, P_m\right]_k\right) ,\end{aligned} \tag{3.8}$$

where $[X_m, P_m]_k = \left[X_m, [X_m, P_m]_{k-1}\right]$ and $[X_m, P_m]_1 = [X_m, P_m]$. Defining $C_k = [X_m, P_m]_k / i^k$ the four-displacement-operation thus becomes

$$\hat{\xi} = \exp\left(-i\lambda n_L \sum_{k=1}^{\infty} \frac{(\lambda n_L)^k}{k!} C_k\right) . \tag{3.9}$$

The optical field is therefore changed depending on the deformation parameters C_i. Consider, for example, the β_0-dependent deformation (3.6). Written in terms of quadratures and in terms of the zero-point fluctuations $p_0 = \sqrt{\hbar m \omega_m}$ and $x_0 = \sqrt{\hbar / m\omega_m}$, the commutator becomes $[X_m, P_m] = i\,(1 + \beta P_m^2)$, where

$$\beta = \beta_0 \frac{\hbar m \omega_m}{m_p^2 c^2} \ll 1 . \tag{3.10}$$

For this deformation, the C_k can be easily computed as an expansion in the parameter β. The first few are given by:

$$\begin{aligned}
C_1 &= 1 + \beta\, P_m^2 \\
C_2 &= \beta\, 2P_m + \beta^2 2P_m^3 \\
C_3 &= \beta\, 2 + \beta^2 8P_m^2 + \beta^3 6P_m^4 \\
C_4 &= \beta^2 16P_m + \beta^3 40P_m^3 + \beta^4 24P_m^5 \\
C_5 &= \beta^2 16 + \beta^3 136P_m^2 + \beta^4 240P_m^4 + \beta^5 120P_m^6 \\
C_6 &= \beta^3 272P_m + \beta^4 1232P_m^3 + \beta^5 1680P_m^5 + \beta^6 720P_m^7 \\
C_7 &= \beta^3 272 + \beta^4 3968P_m^2 + \beta^5 12096P_m^4 + \beta^6 13440P_m^6 + \beta^7 5040P_m^8 \\
&\dots
\end{aligned} \tag{3.11}$$

Note that the terms C_i for $i \geq 4$ are of order $O(\beta^2)$ and smaller. Collecting terms of the same order in β, the four-displacement-operator ξ can be rewritten as:

$$\xi = \exp\left(-i\lambda^2 n_L^2\right) \exp\left(-i\lambda n_L \sum_{k=1}^{\infty} \beta^k F_k(P_m,\, n_L)\right) , \tag{3.12}$$

where we defined

$$F_k(P_m, n_L) = \sum_{l=0}^{k+1} \beta_l^{(k)} \, (\lambda n_L)^{2k+1-l} \, P_m^l \,, \tag{3.13}$$

with $\beta_l^{(k)} \in \mathbb{Q}$ that appear in the expressions (3.11). Note that $\forall k$:

$$\beta_{k+1}^{(k)} = 1 \qquad \text{and} \quad \beta_0^{(k)} < 1 \,. \tag{3.14}$$

Explicitly, the first three operators F_k are given by

$$\begin{aligned} F_1 &= \lambda n_L P_m^2 + (\lambda n_L)^2 P_m + \frac{1}{3}(\lambda n_L)^3 \\ F_2 &= (\lambda n_L)^2 P_m^3 + \frac{4}{3}(\lambda n_L)^3 P_m^2 + \frac{2}{3}(\lambda n_L)^4 P_m + \frac{2}{15}(\lambda n_L)^5 \\ F_3 &= (\lambda n_L)^3 P_m^4 + \frac{5}{3}(\lambda n_L)^4 P_m^3 + \frac{17}{15}(\lambda n_L)^5 P_m^2 + \frac{17}{45}(\lambda n_L)^6 P_m + \frac{17}{315}(\lambda n_L)^7 \,. \end{aligned} \tag{3.15}$$

The first exponential on the RHS in eq. (3.12) is the self-Kerr nonlinear term that appears to zeroth order in β. The other exponential, written as an expansion in β with expressions F_k, captures the additional contributions due to deformations of the canonical commutator.

To probe possible deformations of the canonical commutator, it is sufficient to measure the optical field after the four-pulse-interaction. The optical field, described by the creation and annihilation operators $a_L^\dagger$ and a_L, changes according to $\xi^\dagger a_L \xi$. This expression can be computed exactly using the relation eq. (2.16) and the relation

$$[AB, C] = A\,[B, C] + [A, C]\,B \,, \tag{3.16}$$

which holds for arbitrary operators A, B and C. In particular, consider first the expression $e^{\varphi\, n_L^2}\, a_L\, e^{-\varphi\, n_L^2}$ for arbitrary φ. According to eq. (2.16) it is necessary to compute the nested commutators $[n_L^2, a_L]_k$. The first one is given by $[n_L^2, a_L] = n_L\,[n_L, a_L] + [n_L, a_L]\,n_L = -n_L a_L - a_L n_L = -(2n_L + 1)a_L$, where (3.16) was used. Thus the nested commutator becomes $[n_L^2, a_L]_k = (-1)^k (2n_L + 1)^k a_L$ and the change of the optical field due to the self-Kerr non-linearity is given by $e^{\varphi\, n_L^2}\, a_L\, e^{-\varphi\, n_L^2} = e^{-\varphi\,(2n_L+1)} a_L$. To first order in φ the optical field experiences an intensity-dependent phase rotation, whereas higher orders cause a non-Gaussian spread of the optical state [135, 136]. The additional terms in eq. (3.12) that arise due to a commutator deformation are higher order in n_L. Thus it is necessary to consider expressions of the form

$e^{\varphi n_L^j}\, a_L\, e^{-\varphi n_L^j}$ for arbitrary j. One finds $[n_L^3, a_L]_k = (-1)^k(1+3n_L+3\hat{n}^2)^k a_L$ and $[n_L^4, a_L]_k = (-1)^k(1+4n_L+6n_L^2+4n_L^3)^k a_L$. By direct inspection the general nested commutator $\left[n_L^j, a_L\right]_k$ can therefore be written as

$$\left[n_L^j, a_L\right]_k = (-1)^k \left((n_L+1)^j - n_L^j\right)^k a_L\,. \tag{3.17}$$

The above relation can easily be shown by induction: For the case $k=1$, the $j=1$ result follows immediately from $[n_L, a_L] = -a_L$ and according to eq. (3.16), the inductive step becomes $\left[n_L^{j+1}, a_L\right] = n_L\left[n_L^j, a_L\right] + [n_L, a_L]\, n_L^j = n_L\left[n_L^j, a_L\right] + \left[n_L^j, a_L\right] - n_L^j a_L = (n_L+1)\left[n_L^j, a_L\right] - n_L^j a_L$. With the above expression (3.17), this becomes $\left[n_L^{j+1}, a_L\right] = -\left((n_L+1)^j - n_L^j\right) a_L$, which proves the relation for $k=1$. The generalization to arbitrary k is straightforward. Therefore for arbitrary θ the optical field changes according to

$$e^{\theta n_L^j}\, a_L\, e^{-\theta n_L^j} = e^{-\theta\left((n_L+1)^j - n_L^j\right)} a_L\,. \tag{3.18}$$

With this result, and the expressions (3.12) and (3.13) for the four-displacement operator the change in the optical field after the pulsed sequence is given by

$$\begin{aligned}\xi^\dagger a_L \xi = &\exp\left(-i\lambda^2(2n_L+1)\right)\times \\ &\exp\left(-i\left(\sum_{k=1}^{\infty}\beta^k \sum_{l=0}^{k+1}\beta_l^{(k)}\lambda^{2k+2-l} P_m^l\left((n_L+1)^{2k+2-l} - n_L^{2k+2-l}\right)\right)\right) a_L\,.\end{aligned} \tag{3.19}$$

The above expression is exact and describes the change in the optical field if the canonical commutator of the mechanics is deformed according to eq. (3.6). Analogous expressions can be derived for other models of commutator deformations, such as for example eq. (3.5) and the deformation proposed in Ref. [118].

To obtain an estimate of the strength of the effect on the optical field, the change in the light is considered to lowest order in the small parameter β, given in eq. (3.10). For a typical opto-mechanical system with a ng-mirror oscillating at 1 MHz, this parameter is of the order of $\beta \sim 10^{-40}\beta_0$. Therefore an expansion in β is justified, especially since β_0 is assumed to be of order unity. However, the convergence of the total expression in eq. (3.19) is not guaranteed. Convergence will depend on the state of the mechanics. Higher order contributions in β^k may become more significant for some sufficiently large k, since the contributions $F_k(P_m, n_L)$ may grow exponentially or even faster for some initial states. The problem of convergence indicates that phenomenological models with deformed commutator relations, if taken at

face value, can cause some inconsistencies at some scales and that they can only approximate a more complete theory. Therefore, the model given in eq. (3.6), as well as other deformed commutator models, should be assumed to be only valid for low orders in β, with possible further modifications to the commutator or even a change in the basic structure of the theory at some higher order. Thus the exact result eq. (3.19) should only be considered as an approximation, valid only for low orders in β and for momenta lower than the Planck-momentum.

The change in the optical field, given in eq. (3.19) can be probed by measuring the phase of the light. The deformations in the commutator induce changes to all moments of the optical field, but already the mean of the phase is altered. Thus if the optical field is initially in some coherent state α, a measurement of its phase after the four-pulse interaction with the mechanics yields a measure of the commutator deformations. The mean phase is found from eq. (3.19) via $\langle\alpha\,|\xi^\dagger a_L \xi|\,\alpha\rangle$. For coherent states the following relations hold: $a_L|\,\alpha\rangle = \alpha|\,\alpha\rangle$, $e^{i\varphi n_L}|\,\alpha\rangle = |\,\alpha e^{i\varphi}\rangle$ and $\langle\alpha\,|\,\beta\rangle = e^{-(|\alpha|^2+|\beta|^2)/2}e^{\alpha^*\beta} = e^{-|\alpha-\beta|^2/2}e^{i\mathrm{Im}[\alpha^*\beta]}$. For $N_L = |\alpha|^2 \gg 1$, the change in phase to lowest order in β therefore becomes

$$\langle a_L\rangle \simeq \langle a_L\rangle_{qm}\; e^{-i\Theta}\,, \tag{3.20}$$

with

$$\langle a_L\rangle_{qm} = \alpha\, e^{-i\lambda^2 - N_L^2\left(1-e^{-i2\lambda^2}\right)} \tag{3.21}$$

being the quantum mechanical change in the optical field and

$$\Theta(\beta) \simeq \frac{4}{3}\beta N_L^3 \lambda^4\, e^{-i6\lambda^2} \tag{3.22}$$

being the additional phase contribution from the deformation of the mechanical commutator given by eq. (3.6). Precise measurements of the optical phase can therefore probe deformations of the commutator of the center-of-mass of the mirror. Analogous expressions can be derived for other models of deformed commutators, which yield an anomalous phase that differs from eq. (3.22) in its parameter-dependence.

3.3 Limitations of the scheme

3.3.1 Experimental limitations

Under ideal conditions, the change in the optical phase due to the four-pulsed-interaction can be precisely characterized and thus a possible anomalous phase can be probed. The sensitivity in measuring the phase scales with the

number of runs N_r and the number of photons N_p, with the Heisenberg limit given by $\delta \langle a_L \rangle \sim 1/\sqrt{N_p N_r}$. In practice, deleterious noise sources will affect the optical phase and thus make the measurement of a possible anomalous phase shift more challenging. For a specific experimental setup, a very careful analysis of its imperfections will therefore be necessary. However, some of the main noise sources which will affect any setup can be taken into account in general. The effects of pulse-shape distortions, optical losses, finite pulse duration and mechanical dissipation on the sensitivity of the setup have been analyzed. To this end, regular quantum theory is used, since the additional contributions from deformations of the commutator will be of lower order as compared to the signal in the ideal case, eq. (3.22).

One of the main challenges in the proposed scheme is to keep the effective interaction strength λ equal for all four interactions. The effective opto-mechanical interaction strength can vary from pulse to pulse, due to pulse shape deformation and the associated modified interaction time, and due to optical loss. This can be captured by the operator

$$\xi_\epsilon = e^{-i\lambda_4 n_L P_m} e^{-i\lambda_3 n_L X_m} e^{i\lambda_2 n_L P_m} e^{i\lambda_1 n_L X_m} \tag{3.23}$$

where λ_i is the interaction strength for the i-th pulse round trip. Defining $\epsilon_2 = \lambda_2 - \lambda_4$, $\epsilon_1 = \lambda_1 - \lambda_3$ and $\epsilon = \frac{1}{\sqrt{2}}(-\epsilon_2 + i\epsilon_1)$ one can write

$$\begin{aligned}
\xi_\epsilon &= e^{-i(\lambda_4-\lambda_2) n_L P_m} e^{-i(\lambda_3-\lambda_1) n_L X_m} e^{\lambda_2\lambda_3 n_L^2} \\
&= e^{i\epsilon_2 n_L P_m} e^{i\epsilon_1 n_L X_m} e^{\lambda_2\lambda_3 n_L^2} \\
&= e^{i(\epsilon_2 P_m + \epsilon_1 X_m) n_L} e^{(\frac{1}{2}\epsilon_1\epsilon_2 + \lambda_2\lambda_3) n_L^2} \\
&= e^{(\epsilon b^\dagger - \epsilon^* b) n_L} e^{(\frac{1}{2}\epsilon_1\epsilon_2 + \lambda_2\lambda_3) n_L^2}.
\end{aligned} \tag{3.24}$$

The first exponential in the above operator entangles the light to the mechanics, whereas the second exponential gives the expected Kerr-nonlinear term but with a modified strength $(\epsilon_1\epsilon_2 + \lambda_2\lambda_3)/2$. The resulting mean of the light for an initial coherent optical field $|\,\alpha\rangle$ and an initial thermal mechanical state $\rho_m^{\bar{n}}$ is

$$\begin{aligned}
\langle a_L \rangle_\epsilon &= \mathrm{Tr}[a_L\, \xi_\epsilon \rho_0\, \xi_\epsilon^\dagger] \\
&= \mathrm{Tr}[e^{-(\epsilon b^\dagger - \epsilon b) n_L} a_L\, e^{(\epsilon b^\dagger - \epsilon b) n_L} e^{i(\frac{1}{2}\epsilon_1\epsilon_2 + \lambda_2\lambda_3) n_L^2} |\,\alpha\rangle\langle\alpha\,| e^{-i(\frac{1}{2}\epsilon_1\epsilon_2 + \lambda_2\lambda_3) n_L^2} \otimes \rho_m^{\bar{n}}] \\
&= \mathrm{Tr}[a_L\, e^{\epsilon b^\dagger - \epsilon b} |\,\Psi_L^{(\epsilon)}\rangle\langle\Psi_L^{(\epsilon)}\,| \otimes \rho_m^{\bar{n}}] \\
&= \mathrm{Tr}_L[a_L |\,\Psi_L^{(\epsilon)}\rangle\langle\Psi_L^{(\epsilon)}\,|]\ \mathrm{Tr}_m[D_m(\epsilon)\rho_m^{\bar{n}}] \\
&= \langle a_L \rangle_{Kerr}^{(\epsilon)}\, e^{-\frac{|\epsilon|^2}{2}(1+2\bar{n})}
\end{aligned} \tag{3.25}$$

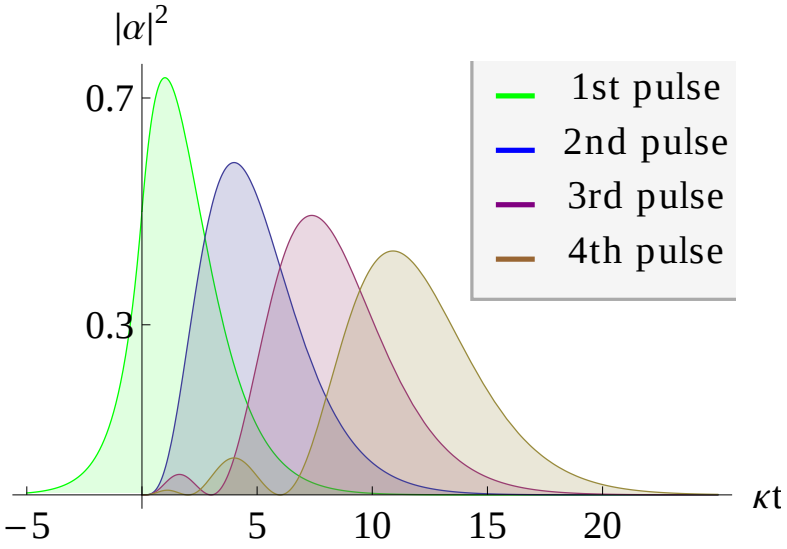

Figure 3.2: Change in the intra-cavity pulse shapes for the four subsequent interactions. An initial Lorentzian input pulse with $\alpha_{in}(t) = \sqrt{\kappa}e^{-\kappa|t|}$ is broadened after entering and leaving the cavity. This effect can be minimized by using pulses of duration much larger than the cavity ring-down time.

where the self-Kerr state $|\Psi_L^{(\epsilon)}\rangle = e^{i(\frac{1}{2}\epsilon_1\epsilon_2+\lambda_2\lambda_3)\hat{n}_L^2}|\alpha\rangle$ was introduced, which gives rise to a self-Kerr effect as in eq. (3.21) but with an modified strength $\lambda^2 \to (\epsilon_1\epsilon_2+\lambda_2\lambda_3)/2$. One can thus see that the varying interaction strength between the round-trips of the pulse reduces the mean of the outgoing light, and provides an modified Kerr-rotation. Both effects can be reduced: Since $\epsilon_i \lesssim \lambda_i$, the deleterious effect will be small as long as $\bar{n} \lesssim 1/\epsilon_i^2 \sim 1/\lambda_i^2$.

Many noise sources can be effectively incorporated into a change of the interaction strength. These include changes in the pulse shape due to the cavity dynamics and the loss of light in between the interactions. The former can be found from considering the input-output equations for the optical field, $\dot{a} = -i(\omega_0 - g_0 X_m)a - \kappa a + \sqrt{2\kappa}a_{in}$ where the optical field inside the cavity is related to the input light field and the output light field as $\sqrt{2\kappa}a = a_{out} + a_{in}$. For a Lorentzian optical input pulse of width $\tau = 1/\kappa$ (i.e. $\alpha_{in}(t) = \sqrt{\kappa}e^{-\kappa|t|}$ with $\int dt|\alpha_{in}(t)|^2 = 1$), the changes in pulse shapes of the intra-cavity field envelope during the four interactions are plotted in Fig. 3.2. A pulse duration of $\tau \gg 1/\kappa$ is required to minimize changes in the pulse shape. The loss of light can be incorporated by changing $\lambda \to \eta\lambda$ after each round trip of the pulse, where $\eta \leq 1$ is the loss parameter.

In addition to losses, a deviation from the QND-interaction of pulsed opto-mechanics yields a similar effect on the optical field. Within the pulsed

opto-mechanical regime, the harmonic evolution of the mirror during the interaction is neglected. However, a small harmonic contribution is expected which breaks the precise QND-nature of the interaction, and a spurious coupling to other mechanical quadratures occurs. To estimate such contributions, one can consider the full opto-mechanical Hamiltonian (in the rotating frame at the optical frequency):

$$H = \hbar\omega_m b^\dagger b - \hbar g_0 n_L (b + b^\dagger)/\sqrt{2}\,. \tag{3.26}$$

The unitary time evolution for this Hamiltonian can be cast in normal ordered form [49]: Application of the ordering theorem given in eq. (2.24) with the substitutions $\alpha = -i\omega_m t$ and $\beta_1 = \beta_2 = ig_0 t n_L/\sqrt{2}$ directly yields

$$U(t) = e^{i(\frac{g_0}{\sqrt{2}\omega_m})^2 n_L^2(\omega_m t - \sin\omega_m t)} e^{\frac{g_0}{\sqrt{2}\omega_m} n_L \left[b^\dagger\left(1-e^{-i\omega_m t}\right) - b\left(1-e^{i\omega_m t}\right)\right]} e^{-i\omega_m b^\dagger b t}. \tag{3.27}$$

Since for a short-pulse-interaction of duration τ we have $\omega_m\tau << 1$, the above expression can be expanded to first order in $\omega_m\tau$:

$$\begin{aligned} U(\tau) &\approx e^{\frac{g_0}{\sqrt{2}\omega_m} n_L \left[b^\dagger\left(i\omega_m\tau + \frac{\omega_m^2\tau^2}{2}\right) - b\left(-i\omega_m\tau + \frac{\omega_m^2\tau^2}{2}\right)\right]} e^{-i\omega_m b^\dagger b\,\tau} \\ &= e^{ig_0\tau n_L X_m - \frac{i}{2} g_0\omega_m\tau^2 n_L P_m} e^{-i\omega_m b^\dagger b\,\tau}. \end{aligned} \tag{3.28}$$

Defining the parameters $\lambda = g_0\tau$ and $\delta = \frac{1}{2}\omega_m\tau$, which measure the interaction strength and the QND-deviation, respectively, one gets

$$U(\tau) = e^{-\frac{1}{2}\delta\lambda^2 n_L^2} e^{i\lambda n_L X_m} e^{-i\delta\lambda n_L P_m} U_0(2\delta), \tag{3.29}$$

where $U_0(2\delta) = e^{-i2\delta b^\dagger b}$ describes the free mechanical harmonic evolution by 2δ. The above time-evolution operator is now used to described four subsequent pulsed interactions, with a quarter harmonic period in between. The resulting operator $\xi_\delta = U(\tau)\,U_0(\pi/2)\,U(\tau)\,U_0(\pi/2)\,U(\tau)\,U_0(\pi/2)\,U(\tau)$ becomes

$$\begin{aligned} \xi_\delta = U_0(\frac{3\pi}{2})\, & e^{-2\delta\lambda^2 n_L^2} e^{-i\lambda n_L P_m} e^{-i\delta\lambda n_L X_m} U_0(2\delta) e^{-i\lambda n_L X_m} \times \\ & e^{i\delta\lambda n_L P_m} U_0(2\delta) e^{i\lambda n_L P_m} e^{i\delta\lambda n_L X_m} U_0(2\delta) e^{i\lambda n_L X_m} e^{-i\delta\lambda n_L P_m} U_0(2\delta) \end{aligned} \tag{3.30}$$

One can now use $U_0(2\delta)^\dagger X_m U_0(2\delta) \approx X_m + 2\delta P_m$ and $U_0(2\delta)^\dagger P_m U_0(2\delta) \approx$

$P_m - 2\delta X_m$ and neglect all terms $O(\delta^2)$, i.e. $[\delta X_m, \delta P_m] \approx 0$. This yields

$$\begin{aligned}
\xi_\delta &= U_0(\frac{3\pi}{2})U_0(8\delta)\, e^{-2\delta\lambda^2 n_L^2} e^{-i\lambda n_L(P_m - 8\delta X_m)} e^{-i\delta\lambda n_L(X_m + 8\delta P_m)} e^{-i\lambda n_L(X_m + 6\delta P_m)} \times \\
&\quad e^{i\delta\lambda n_L(P_m - 6\delta X_m)} e^{i\lambda n_L(P_m - 4\delta X_m)} e^{i\delta\lambda n_L(X_m + 4\delta P_m)} e^{i\lambda n_L(X_m + 2\delta P_m)} e^{-i\delta\lambda n_L(P_m - 2\delta X_m)} \\
&\approx U_0(\frac{3\pi}{2})U_0(8\delta)\, e^{-8\delta\lambda^2 n_L^2} e^{-i\lambda n_L P_m} e^{-i\delta\lambda n_L X_m} e^{-i\lambda n_L X_m} e^{i\delta\lambda n_L P_m} \times \\
&\qquad e^{i\lambda n_L P_m} e^{i\delta\lambda n_L X_m} e^{i\lambda n_L X_m} e^{-i\delta\lambda n_L P_m} e^{i4\delta\lambda n_L X_m} e^{-i4\delta\lambda n_L P_m} \\
&= \xi \cdot\, U_0(8\delta)\, e^{-6\delta\lambda^2 n_L^2} e^{i4\delta\lambda n_L X_m} e^{-i4\delta\lambda n_L P_m},
\end{aligned} \tag{3.31}$$

where ξ is the original, unperturbed operator as in eq. (3.7). The above result shows two effects: one is an additional Kerr-nonlinear term with an opposite sign to the one in ξ, which however is by a factor δ smaller. The other effect is that the mechanics is no longer disentangled from the light, as in the case of distorted pulse shapes. Taking directly the result from the distorted pulse shape calculation, i.e. for $\xi_\epsilon = \xi\, e^{i\epsilon_2 n_L P_m} e^{i\epsilon_1 n_L X_m}$ the optical field changes according to $\langle a_L\rangle_\epsilon = \langle a_L\rangle_{Kerr}^{(\epsilon)} e^{-\frac{1}{4}(\epsilon_1^2+\epsilon_2^2)(1+2\bar{n})}$, where ϵ quantifies the difference of the λ-factors for two subsequent pulses. Substituting $\epsilon_1 = 4\delta\lambda$ and $\epsilon_2 = -4\delta\lambda$, and including the effect of finite mechanical evolution by 2δ, one thus obtains:

$$\langle a_L\rangle_\delta = \langle a_L\rangle_{Kerr}^{(\delta)}\, e^{-8\delta^2\lambda^2(1+2\bar{n})} \tag{3.32}$$

with $\langle a_L\rangle_{Kerr}^{(\delta)}$ being the ordinary mean of light due to a Kerr-nonlinearity with strength $6\delta\lambda^2$.

The noise sources discussed above impose additional constraints on the experimental parameters. In addition, noise affecting the mirror [137] can be taken into account as well. Dissipation of the mechanical state imposes constraints on the external temperature and the Q-factor of the setup, whereas non-linearities in the harmonic motion will have to be precisely characterized [138]. It will be necessary to perform the experiment at mK-temperatures with additional ground state cooling of the mechanical mode. The optical losses will have to be minimized and the finesse $\mathcal{F} = \frac{\pi c}{2\kappa L}$ of the cavity of length L needs to be of order $\mathcal{F} \gtrsim 10^5$. Despite these constraints, the scheme presented can provide a means to probe deformations of the canonical commutator to very high precision. In particular, for very challenging but still realistic system parameters, a sensitivity that allows to probe $\beta_0 \lesssim 1$ can in principle be achieved. For the other considered commutator deformations [115, 118], a similar sensitivity can be achieved with less stringent experimental parameters.

3.3.2 Conceptual limitations

In addition to experimental imperfections, the opto-mechanical scheme has a conceptual limitation. In particular, the scheme allows to probe possible deformations of the canonical commutator of the center-of-mass (cm) mode of the mirror to very high precision. The cm-mode has been shown to behave quantum mechanically [30, 31, 63] and is the center of studies within the field of opto-mechanics [19–24]. However, theories with a deformed commutator are ambiguous as to what degrees of freedom they apply to [114, 131, 139, 140]. No theoretical framework exists that would specify which systems or degrees-of-freedom are affected by deformations such as eqs. (3.5) and (3.6). Much has been speculated whether such deformations affect only elementary particles [114]. A main problem in models of modified canonical commutators is that the composition rule for many-body systems is not as straight-forward as in regular quantum theory. Consider, for example, the deformation (3.6). If applied to the center-of-mass, the deformation reads:

$$[x_{cm}, p_{cm}] = i\hbar \left(1 + \beta_0 \tilde{p}_{cm}^2\right) , \tag{3.33}$$

where $\tilde{p} = p/(M_P c)$. On the other hand, one can consider some N elementary particles with momenta p_i, position x_i and mass m_i and construct the center of mass mode via

$$x_{cm} = \frac{\sum_{i=1}^N m_i x_i}{\sum_{i=1}^N m_i} , \qquad p_{cm} = \sum_{i=1}^N p_i \, . \tag{3.34}$$

For particles with identical mass the position reduces to $x_{cm} = \sum_{i=1}^N x_i/N$. In this case, and using $[x_i, p_j] = 0$ for $i \neq j$, the effective commutator of the center of mass mode reads

$$[x_{cm}, p_{cm}]_{eff} = i\hbar \left(1 + \frac{\beta_0}{N} \sum_{i=1}^N \tilde{p}_i^2\right) = i\hbar \left(1 + \frac{\beta_0}{N} \left(\tilde{p}_{cm}^2 - \sum_{i \neq j} \tilde{p}_i \tilde{p}_j\right)\right) . \tag{3.35}$$

The difference between this commutator and the direct deformation, eq. (3.33) depends on the state of the system. For fully uncorrelated momenta, we have $\langle p_i p_j \rangle = 0$ and eq. (3.35) reduces to eq. (3.33), just with a rescaled deformation parameter $\beta_0 \to \beta_0/N$. If, instead, the whole system is perfectly entangled, the pairwise correlation is again vanishing. For example, in the EPR-case the entangled state for the N particles is given by $\rho = \int dp_1 \ldots \int dp_{N-1} |\, p_1\rangle \ldots |\, p_{cm} - \sum_{i=1}^{N-1} p_i\rangle\langle p_{cm} - \sum_{i=1}^{N-1} p_i \,| \ldots \langle p_1 \,|$, and the center of mass momentum is p_{cm}. In this case, one also has $\langle p_i p_j \rangle = 0$ and the result is the same as above.

On the other hand, if all particles move with the same momentum p_0, then $p_{cm} = Np_0$ and $\sum_{i\neq j} \tilde{p}_i\tilde{p}_j = N(N-1)p_0^2$. In this case, the effective commutator of the center of mass mode becomes $[x_{cm}, p_{cm}] = i\hbar\left(1 + \frac{\beta_0}{N^2}\tilde{p}_{cm}^2\right)$. This constitutes a reduction by N^2 as compared to a direct deformation of the center-of-mass, eq. (3.33).

The above examples show that models with modified commutation relation have an intrinsic ambiguity as to which degrees-of-freedom they apply to. In quantum theory, since the commutator is a constant, this problem does not arise. It has also been suggested that the composition rules given in eq. (3.34) should be modified [114, 140–143], in which case the relation between deformations of the center-of-mass and deformations of elementary constituents becomes different than discussed above. However, a lack of deformations for composite systems, as opposed to elementary systems, would entail that composite quantum systems can be localized arbitrary more precise than elementary systems. In addition, a problem arises in identifying the "correct" elementary constituents. The ambiguity of such phenomenological models cannot be resolved without a more fundamental theory. Therefore, experimental input in various parameter regimes can be helpful in probing the range and validity of such phenomenological models. Several other proposals for tests of other phenomenological models of quantum gravity also rely on testing possible anomalous behavior of the center-of-mass degree of freedom [144, 145]. Such experiments, as well as the opto-mechanical setup proposed here, will give bounds on the specific models in specific regimes. The scheme discussed here is particularly sensitive to deformations of the center-of-mass of a quantum system that has a mass close to the Planck mass. The experiment will also be able to put bounds on deformations of elementary particles that are possibly better than currently known bounds, however, these bounds will be less stringent than those for deformations of the center-of-mass. Together with other proposed experiments, such as observations of anomalous dispersion of light [146, 147] or tests of space-time fluctuations [144, 145], a significant experimental input for quantum gravity phenomenology can be expected in the near future.

Chapter 4

Time dilation in quantum systems

According to the theory of general relativity the motion of free particles is governed by the underlying geometry of space and time [148–154]. Gravitational attraction is the result of a curved space-time geometry. The theory correctly describes a vast range of phenomena ranging from our solar system to cosmological scales. General relativity is well-tested, but deviations from Newtonian theory are suppressed by powers of c and are therefore typically small. Therefore, and since quantum behavior is typically seen only in systems with small mass, phenomena that result from general relativity and quantum theory have not been observed so far. In the following, the weak field limit of general relativity is revised and it is shown how low-energy quantum systems are affected by general relativistic time dilation.

4.1 Space-time geometry and time dilation

An essential component in the theory of general relativity is the space-time metric $g_{\mu\nu}$, which describes the space-time geometry captured by the proper interval

$$ds^2 = -c^2 d\tau^2 = g_{\mu\nu} dx^\mu dx^\nu \,. \tag{4.1}$$

Here and in the following, Greek indices run from 0 to 3 and correspond to 4-vectors, whereas Latin indices run from 1 to 3 to describe the spatial three-vectors, and the Einstein summation convention is used. In general relativity, no global inertial frames can be found, however, all frames are locally inertial. That means that for any observer, local inertial coordinates ξ^μ can be found with respect to which the proper time is given by $\Delta\tau = \sqrt{-\eta_{\mu\nu} d\xi^\mu d\xi^\nu}/c$,

where $\eta_{\mu\nu}$ = diag[-1,1,1,1] is the Minkowski metric. However, these coordinates cannot be used to describe the time evolution at distant points, since the frame is only locally inertial (i.e. metric is only locally flat). Given some arbitrary coordinate system, the proper time interval $d\tau$ at any point is related to the coordinate time interval dt as

$$d\tau = \frac{1}{c}\sqrt{-g_{\mu\nu}dx^\mu dx^\nu} = \sqrt{-g_{00} - 2g_{i0}\frac{v^i}{c} - g_{ij}\frac{v^i v^j}{c^2}}dt\,, \tag{4.2}$$

where $dx^0 = cdt$ is the coordinate time component and $v^i = dx^i/dt$ is the coordinate velocity. The elapsed proper time at different points therefore depends on the metric. The operational meaning of the proper and coordinate times is the following: Any system's local time is the proper time τ, thus any clock can only measure time intervals in terms of the elapsed proper time. All clocks measure proper time and not coordinate time. To consider and compare measurements of distant systems, an observer can choose any coordinates. Since the elapsed proper time is in general different along different space-time trajectories, the coordinate time can be used to compute the other elapsed proper time in terms of the coordinate time. This allows the observer to compare distant time intervals to his local time. In this way time dilation between different space-time trajectories can be quantified. Comparing some two events or trajectories can only be performed by local measurements, i.e. two trajectories have to coincide at some point. Even if one uses other systems (such as light rays) to intersect between the two trajectories, they have to be prepared at some local point and then read-out locally at some other point in space-time. Otherwise the comparison of the times is meaningless, since no operational procedure exists that would compare the different proper times.

Even systems stationary with respect to the coordinates ($v^i = 0$) experience different time dilation depending on where in space they are situated. For a system at rest for time t at some fixed point, the accumulated proper time in terms of coordinate time is given by

$$\tau = \int dt\sqrt{-g_{00}} = \sqrt{-g_{00}}t\,. \tag{4.3}$$

The time dilation for stationary systems is therefore governed by the metric component g_{00}. In the weak field limit of the Schwarzschild metric, the change in frequency is therefore related to the gravitational potential $\Phi = -Gm/r$, since $g_{00} = -(1 + 2\Phi/c^2)$. In general, g_{00} will have a different magnitude at different points in space. However, locally inertial observes can only measure proper time τ, thus only a comparison of time measurements at different

points in space, at which the elapsed proper time (4.3) is different, shows time dilation. Note that g_{00} becomes η_{00} at $r \to \infty$, thus the coordinates correspond to clocks that measure time at infinity. These coordinates are useful to compare elapsed time at different points in space. According to eq. (4.3), at some point P_1 the coordinate time interval Δt corresponds to the proper time interval as $\Delta\tau^{(1)} = \sqrt{-g_{00}(P_1)}\Delta t$, while at point P_2 the same coordinate time interval corresponds to the proper time interval $\Delta\tau^{(2)} = \sqrt{-g_{00}(P_2)}\Delta t$. Setting $g_{00} = -(1 + 2\Phi/c^2)$ the time delay between the two is thus given by

$$\frac{\Delta\tau^{(1)}}{\Delta\tau^{(2)}} = \sqrt{\frac{g_{00}(P_1)}{g_{00}(P_2)}} = \sqrt{\frac{c^2 + 2\Phi(P_1)}{c^2 + 2\Phi(P_2)}} \approx 1 + \frac{\Phi(P_1)}{c^2} - \frac{\Phi(P_2)}{c^2} + O(c^{-4}) \quad (4.4)$$

The comparison between the proper times between two points can be made by using, for example, light signals. The proper interval, eq. (4.1), for null geodesics is 0, thus the coordinate time for light is given by $dt = -(cg_{00})^{-1}\left(g_{i0}dx^i - \sqrt{(g_{i0}g_{j0} - g_{00}g_{ij}dx^i dx^j)}\right)$. Integrating this expression along the light's trajectory yields the coordinate time for the light to take from point P_2 to point P_1. But if the two points are at rest and the metric is time independent, two successive signals emitted from point P_2 (separated by $\Delta\tau^{(2)}$) will travel the same amount of time to point P_1. Thus the time interval between the two signals measured at point P_1 will be given by $\Delta\tau^{(1)}$. The above formula (4.4) shows that the received time interval will be altered. In particular, if $\Phi(P_1) > \Phi(P_2)$, i.e. $r_1 > r_2$ for $\Phi = -Gm/r$, the received interval at r_1 is prolonged and thus the frequency of the emitter that is closer to the mass appears redshifted as compared to an observer further away from the mass.

Some other examples for systems that experience time dilation can easily be computed. Consider for example a local observer at some fixed space-time point P, measuring the local proper time in terms of coordinate time $\tau = t$. If another synchronized clock is taken from point P on a trajectory with a constant velocity v^i, then according to eq. (4.2) the proper time τ' on this trajectory is given in terms of the coordinate time of the stationary observer at P by $\tau' = \sqrt{-g_{00} - g_{ij}\frac{v^i v^j}{c^2}}t$, where a static metric was assumed. For the Minkowski metric $g_{\mu\nu} = \eta_{\mu\nu}$, this becomes $\tau' = \sqrt{1 - v^2/c^2}t < \tau$. Thus, the time elapses slower on a trajectory with velocity v as compared to a stationary clock. Of course to compare τ' to τ, the observers on the two trajectories must exchange information or meet at some later time. The difference in their time measurements will be given by the difference of the overall elapsed proper times along the two trajectories.

Another example is time dilation due to acceleration. For the case of constant proper acceleration $a^\mu = du^\mu/d\tau$, one has $a_\mu a^\mu = a = const.$ From $u_\mu u^\mu = -c^2$ it also follows that $a_\mu u^\mu = 0$. Assuming motion in one dimension only, the equations become $g_{00}(a^0)^2 + g_{11}(a^1)^2 = a^2$ and $g_{00}a^0u^0 + g_{11}a^1u^1 = 0$. Solving for a^μ yields $a^0 = a\sqrt{-\frac{g_{11}}{g_{00}}}\frac{u^1}{c}$ and $a^1 = a\sqrt{-\frac{g_{00}}{g_{11}}}\frac{u^0}{c}$. Since $a^\mu = d^2x^\mu/d\tau^2$ and $u^\mu = dx^\mu/d\tau$, these equations correspond to differential equations for x and t. In the case of a flat metric the solutions can be easily found, which are $t = c\sinh(a\tau/c)/a$ and $x = c^2\cosh(a\tau/c)/a$. These are the coordinates that describe uniformly accelerating systems, the function $t(\tau)$ describes the time dilation due to acceleration.

4.2 Dynamics on a curved space-time

Without any other external forces, particle motion is described by the geodesic equation (1.2). The geodesic equation can be derived directly from the equivalence principle, which states that effects of gravity are locally indistinguishable from acceleration. For free particles, according to the equivalence principle the motion in the local reference frame (described by coordinates ξ^μ) should be governed by Newton's second law with no forces, i.e. $d^2\xi^\mu/d\tau^2 = 0$. Here, the time component ξ^0/c measures the proper time, since the local reference frame is considered (i.e., in this reference frame one has $c^2d\tau^2 = -\eta_{\mu\nu}d\xi^\mu d\xi^\nu$, where $\eta_{\mu\nu} = \mathrm{diag}[-1,1,1,1]$ is the Minkowski metric). A transformation to arbitrary coordinates x^μ is given by the chain rule $d\xi^\mu = (\partial\xi^\mu/\partial x^\lambda)dx^\lambda = \partial_\lambda\xi^\mu dx^\lambda$, where the short hand notation $\partial_\lambda\xi^\mu = \partial\xi^\mu/\partial x^\lambda$ is used. Thus the equation of motion for free particles as seen from an arbitrary reference frame is given by $0 = \frac{d}{d\tau}(\partial_\lambda\xi^\mu\frac{dx^\lambda}{d\tau}) = \partial_\lambda\xi^\mu\frac{d^2x^\lambda}{d\tau^2} + \partial_\lambda\partial_\rho\xi^\mu\frac{dx^\lambda}{d\tau}\frac{dx^\rho}{d\tau}$. One can solve this equation for $\frac{d^2x^\lambda}{d\tau^2}$ by using the 'inverse' relation $\partial_\lambda\xi^\mu(\partial x^\nu/\partial\xi^\mu) = \delta^\nu_\lambda$. This yields

$$\frac{d^2x^\lambda}{d\tau^2} + \Gamma^\lambda_{\mu\nu}\frac{dx^\mu}{d\tau}\frac{dx^\nu}{d\tau} = 0\,, \tag{4.5}$$

where the symbol $\Gamma^\lambda_{\mu\nu}$ was defined as $\Gamma^\lambda_{\mu\nu} = (\partial x^\lambda/\partial\xi^\rho)\cdot\partial_\mu\partial_\nu\xi^\rho$. The above equation is exactly the geodesic equation (1.2). It can be shown from $g_{\mu\nu} = \eta_{\rho\sigma}\partial_\mu\partial_\nu d\xi^\rho d\xi^\sigma$ that $\Gamma^\lambda_{\mu\nu}$ is the Christoffel connection, which can be written in the more familiar form

$$\Gamma^\lambda_{\mu\nu} = \frac{1}{2}g^{\lambda\rho}(\partial_\mu g_{\nu\rho} + \partial_\nu g_{\rho\mu} - \partial_\rho g_{\mu\nu})\,. \tag{4.6}$$

Thus geodesic motion is derived by describing locally force free motion in arbitrary coordinates. Only the equivalence principle and the description of

space-time as a single four-dimensional entity are required. An alternative derivation involves the notion of parallel transport along some curve x^μ, governed by the covariant derivative ∇_μ. For scalars, the covariant derivative reduces to the partial derivative, but for vectors it takes the form $\nabla_\mu v^\nu = \partial_\mu + \Gamma^\nu_{\mu\lambda} v^\lambda$. The covariant derivative along some curve $x^\mu(\tau)$ is given by $D/D\tau = (dx^\mu/d\tau)\nabla_\mu$. In terms of the covariant derivative, the geodesic equation (4.5) therefore becomes $(D/D\tau)(dx^\mu/d\tau) = 0$.

The geodesic equation describes the change of the spatial coordinates x^i with respect to the system's proper time, as well as the change in the coordinate time $t = x^0/c$ with respect to proper time. The latter captures time dilation due to the space-time metric. The equations are used to find equations of motion with respect to the coordinate time, i.e. the functions $x^i(x^0)$ that describe the trajectories of particles in the chosen coordinates are found from the geodesic equation. Given any coordinate system, it is therefore possible to describe the dynamics of the particle in these coordinates and the proper time τ can be eliminated. The apparent dynamics for null-like curves (i.e. trajectories for light, for which $\tau = 0$) can be found by replacing τ with some affine parameter λ in the geodesic equation (4.6) and eliminating this parameter to find $x^i(x^0)$. In general, the dynamics of particles and light will differ when seen from different space-time points. The difference in the coordinate time x^0 is the reason for time dilation. However, quantities of the form $W = w_\mu w^\mu$ remain coordinate-invariant, i.e. they can be computed in any coordinates and remain invariant under coordinate transformations.

From eq. (4.5) one can see that apparent deviations from force-free motion are governed by the connection $\Gamma^\lambda_{\mu\nu}$. Denoting the proper four-velocity as $u^\mu = dx^\mu/d\tau$, the geodesic equation becomes:

$$\frac{du^\mu}{d\tau} = -\Gamma^\mu_{00}(u^0)^2 - 2\Gamma^\mu_{0k}u^0u^k - \Gamma^\mu_{nk}u^nu^k\,, \tag{4.7}$$

where the symmetric property $\Gamma^\mu_{0\nu} = \Gamma^\mu_{\nu 0}$ was used. In addition, the definition of the metric (4.1) yields the relation between the four-velocities

$$u_\mu u^\mu = -c^2 \quad \text{(for massive systems)}, \qquad u_\mu u^\mu = 0 \quad \text{(for light)}\,. \tag{4.8}$$

One can write out the four-velocity components explicitly as $u_0u^0 = -(sc^2 + g_{i\lambda}u^iu^\lambda)$, where $s = 1$ for massive particles and $s = 0$ for null rays. Note that $u^0 = cdt/d\tau$, since $x^0 = ct$. One can eliminate τ in favor of x^0 to obtain the equations of motions in terms of the coordinate velocity $v^i = dx^i/dt$. The explicit general expression for the coordinate acceleration in terms of the time coordinate t is found using eq. (4.5) for the spatial components of

the acceleration and using $\partial_\tau = (dt/d\tau)\partial_t$:

$$\begin{aligned} -\Gamma^i_{\mu\nu}\frac{dx^\mu}{d\tau}\frac{dx^\nu}{d\tau} = \frac{d^2x^i}{d\tau^2} &= \frac{d}{d\tau}\left(\frac{dx^i}{dt}\frac{dt}{d\tau}\right) = \frac{d^2x^i}{dt^2}\left(\frac{dt}{d\tau}\right)^2 + \frac{dx^i}{dt}\frac{d^2t}{d\tau^2} \\ &= \frac{d^2x^i}{dt^2}\left(\frac{dt}{d\tau}\right)^2 + \frac{dx^i}{dt}\left(-\frac{1}{c}\Gamma^0_{\mu\nu}\frac{dx^\mu}{d\tau}\frac{dx^\nu}{d\tau}\right) \\ &= \left(\frac{dt}{d\tau}\right)^2\left(\frac{d^2x^i}{dt^2} - \frac{1}{c}\frac{dx^i}{dt}\Gamma^0_{\mu\nu}\frac{dx^\mu}{dt}\frac{dx^\nu}{dt}\right), \end{aligned} \tag{4.9}$$

where $d^2t/d\tau^2 = c^{-1}d^2x^0/d\tau^2$ was rewritten using the zeroth component of the geodesic equation (4.5). The geodesic equation in terms of coordinate time is therefore given by

$$\frac{d^2x^i}{dt^2} = -\left(\Gamma^i_{\mu\nu} - \frac{1}{c}\frac{dx^i}{dt}\Gamma^0_{\mu\nu}\right)\frac{dx^\mu}{dt}\frac{dx^\nu}{dt}\,. \tag{4.10}$$

In the following, the motion of particles in the weak-field limit is considered.

4.3 General relativistic phenomena in the weak field limit

In the weak field limit of general relativity [149–154], the gravitational fields are assumed to be weak perturbations of the Minkowski metric such that $g_{\mu\nu} = \eta_{\mu\nu} + h_{\mu\nu}$. Considering the equations to first order in $h_{\mu\nu}$, the Christoffel symbols (4.6) become

$$\Gamma^\lambda_{\mu\nu} = \frac{1}{2}\left(\eta^{\lambda\rho} - h^{\lambda\rho}\right)\left(\partial_\mu h_{\nu\rho} + \partial_\nu h_{\rho\mu} - \partial_\rho h_{\mu\nu}\right). \tag{4.11}$$

The factor $h^{\lambda\rho}$ has been explicitly kept in the equation, even though it contributes to order $O(h^2)$. The factor is necessary to consistently compute the dynamics to lowest order in c^{-2}, as will be seen explicitly below. First, one can focus on the case of slow velocities $v^k \ll c$. Since $dx^0/dt = c$, and neglecting quadratic terms in v^k/c, the equation of motion (4.10) reduces to

$$\frac{dv^i}{dt} \approx -c^2\Gamma^i_{00} - 2c\Gamma^i_{0k}v^k \approx \frac{1}{2}c^2\partial^i h_{00} - cv^k(\partial_k h^i_0 - \partial^i h_{0k})\,, \tag{4.12}$$

where a static metric with $\partial_0 h_{\mu\nu} = 0$ was assumed. The above equation of motion is similar to a charged particle in the presence of the Lorentz-force. The first term on the RHS describes the gravitational potential whereas

the second term couples to the velocity and captures the gravito-magnetic effect. The limiting case can easily be found that reproduces Newton's law of gravitation. In the Newtonian limit, terms other than the h_{00} are neglected, since it is by order c larger than other components, if the velocity of the particle is small. Thus the velocity-dependent terms that are proportional to h_{oi} in the above equation are neglected and only the first term remains. This yields $dv^i/dt = -\partial^i\Phi$, or

$$\frac{d\vec{v}}{dt} = -\vec{\nabla}\Phi(|\vec{x}|)\,, \tag{4.13}$$

where v^i is the coordinate velocity of the system and the potential was defined in terms of the metric as $\Phi = -h_{00}c^2/2$. That Φ is indeed the correct Newtonian gravitational potential (i.e. $\Phi = -GM/|\vec{x}|$) can be verified through Einstein's equations (1.3), which yields the Poisson equation for Φ to lowest order.

General relativistic phenomena can be probed if one considers the theory beyond the Newtonian limit [151, 152]. All tests of general relativity, except of the production of gravitational waves in a binary star system [155] and

Weak field limit of general relativity		
Metric: $g_{\mu\nu} = \eta_{\mu\nu} + h_{\mu\nu}, \quad g^{\mu\nu} = \eta^{\mu\nu} - h^{\mu\nu}$		
Metric components	$\eta_{\mu\nu}$	$\mathrm{diag}[-1\,,1\,,1\,,1]$
	h_{00}	$-2\frac{\Phi(x)}{c^2} - 2\frac{\Phi^2(x)}{c^4}$
	h_{ii}	$-2\frac{\Phi(x)}{c^2}$
	$h_{ij},\ i \neq j$	0
	$h^{\mu\nu}$	$\eta^{\mu\rho}\eta^{\lambda\nu}h_{\rho\lambda}$
Connection: $\Gamma^\lambda_{\mu\nu} = \frac{1}{2}\left(\eta^{\lambda\rho} - \delta^\mu_0\delta^\nu_0 h^{\lambda\rho}\right)(\partial_\mu h_{\nu\rho} + \partial_\nu h_{\rho\mu} - \partial_\rho h_{\mu\nu})$		
Connection symbols	Γ^0_{00}	0
	Γ^i_{00}	$-\frac{1}{2}\partial^i h_{00} + \frac{1}{2}h^{ii}\partial^i h_{00}$
	Γ^0_{0n}	$-\frac{1}{2}\partial_n h_0^{\ 0}$
	Γ^i_{jk}	$\frac{1}{2}(\partial_j h_{ik}\delta^i_k + \partial_k h_{ij}\delta^i_j - \partial^i h_{jk}\delta_{jk})$

Table 4.1: Metric components and connection symbols in the weak field limit. A static metric with $\partial_0 h_{\mu\nu} = 0$ and $h_{0i} = h_{i0} = 0$ is assumed.

cosmological observations [156], are due to the weak-field approximation of general relativity, where corrections to Newtonian physics to order c^{-2} are included. Tests of weak field general relativity include measurements of the redshift [157] and time-dilation in a gravitational potential [158], deflection of light [159] and gravitational lensing [160], perihelion precession of Mercury, Shapiro delay [161] and the frame-dragging effect [162]. In the following, the focus will be on static metrics for which $\partial_0 g_{\mu\nu} = 0$ and $g_{0i} = 0$. Such a limit excludes the description of gravitational waves and the Lens-Thirring effect, which is related to the gravito-magnetic part found in eq. (4.12). However, all other phenomena described above are captured in this limit. In this static case the weak-field limit of the metric is $g_{\mu\nu} = \mathrm{diag}[-(1 + 2\Phi(x)/c^2 + 2\Phi^2(x)/c^4), 1 - 2\Phi(x)/c^2, 1 - 2\Phi(x)/c^2, 1 - 2\Phi(x)/c^2]$, i.e. $h_{00} = -2\Phi/c^2 - 2\Phi^2/c^4$ and $h_{ij} = -\delta_{ij}2\Phi/c^2$. The weak field limit describes the metric produced by a massive object to first order in c^{-2}. The c^{-4}-components in the h_{00}-component are necessary in this limit, since in the geodesic equation the Γ^{λ}_{00} component is multiplied by $(dx^0/dt)^2 = c^2$ (see for example eq. (4.12)). The Christoffel-symbols are computed from eq. (4.11), see table 4.1. The second term on the RHS of eq. (4.10) thus becomes $-c^{-1}v^i\Gamma^0_{\mu\nu}v^\mu v^\nu = -v^i(\partial_n h_{00})v^n/2$. In total, the equation of motion is

$$\frac{d^2\vec{x}}{dt^2} = -\vec{\nabla}\Phi(x)\left(1 + \frac{\vec{v}\cdot\vec{v}}{c^2}\right) - \frac{2}{c^2}\vec{\nabla}\Phi^2(x) + 4\frac{\vec{v}}{c^2}\left(\vec{v}\cdot\vec{\nabla}\Phi(x)\right) . \qquad (4.14)$$

The very first term survives in the Newtonian limit ($c \to \infty$) and stems from the h_{00}-component. In addition to the Newtonian term, one now has c^{-2}-order corrections to the dynamics. The term proportional to v^2/c^2 stems from the h_{ij} component and also couples to the Newtonian force. The gradient of the Φ^2 term stems from the c^{-4}-contribution of the h_{00}-component and the h_{ij}-component of the metric. This term highlights the non-linear nature of the gravitational coupling, i.e. gravity couples to the full energy of a system, including its own gravitational potential. The last term stems from the h_{ij} component and from the change of coordinates from τ to t, both contributions being equal in magnitude.

Note that the acceleration perpendicular to the velocity (neglecting the $\vec{\nabla}\Phi^2$-term) stems only from the first two terms, i.e. $\vec{a}_\perp = -\vec{\nabla}\Phi(x)\,(1 + \vec{v}\cdot\vec{v}/c^2)$. For light, this gives $\vec{a}_\perp = -2\vec{\nabla}\Phi(x)$. The perpendicular acceleration causes the well-known deflection of light due to a massive object. The magnitude of the effect is twice as large as compared to the result in the Newtonian limit, which is obtained by applying only the equivalence principle to light [163]. This is because in such a model (where light is treated as particles with effective mass $m = E/c^2$), the g_{ij}-components are neglected. In other

words, such a simple model does not take length-contraction of the coordinate system into account, which become relevant for relativistic speeds (thus this effect does not take place for massive non-relativistic particles, for which $v/c \ll 1$, as can be seen from eq. (4.14)). Nevertheless, the predictions obtained by the simple mass-energy equivalence argument give the correct order of magnitude. The full metric theory is needed to obtain the correct magnitude $\vec{a}_\perp = -2\vec{\nabla}\Phi(x)$.

A related effect for light is the apparent slow-down of the speed of light due to massive objects. This can be directly seen from the metric equation $g_{\mu\nu}u^\mu u^\nu = 0$. Changing coordinates to describe light rays in terms of the coordinate velocity gives $g_{00}v^0 = -g_{ij}v^i v^j$. Thus the coordinate-velocity of light is given by

$$\vec{v}_c = c\sqrt{-\frac{g_{00}}{g_{11}}}\vec{e}_c \approx c\left(1 + \frac{2\Phi}{c^2}\right)\vec{e}_c\,, \tag{4.15}$$

where the subscript c highlights that this is the coordinate velocity of light and the unit-vector $\vec{e}_c$ points into the direction of propagation of the light ray. The equation is directly analogous to propagation of light in a medium with a refractive index n_{eff} since the velocity changes as $c \to c/n$. To lowest order in c^{-2}, the effective refractive index is

$$v_c = \frac{c}{1 - 2\frac{\Phi(x)}{c^2}} = \frac{c}{n_{eff}}\,. \tag{4.16}$$

The coordinate velocity of light as seen from an outside observer is therefore effectively reduced. The time of propagation of light in the presence of a gravitational potential can be obtained from integrating eq. (4.15): $\Delta t = \int dx v_c^{-1}$. Note that this is the coordinate time of propagation, expressed in terms of the coordinate velocity. Note that the coordinate velocity can also be defined with respect to the proper spatial distance $dl = \sqrt{(-g_{0i}g_{0j}/g_{00} + g_{ij})dx^i dx^j}$ [148], which is more convenient in applications where the proper spatial distance of a trajectory is known (in terms of this velocity the light propagates at speed $dl/dt = \sqrt{g_{11}}v_c = c\sqrt{-g_{00}}$). If light travels from some distant coordinate point r_1 to r_2 in the presence of the gravitational potential $\Phi = -GM/|\vec{x}|$, to lowest (Newtonian) order it will follow a straight line with an impact parameter b. Since the velocity is already taken to first order in c^{-2}, one can approximate the trajectory as the non-relativistic straight trajectory. In this case $r^2 = x^2 + b^2$ and the integral

becomes

$$\begin{aligned} c\Delta t_{r_1\to r_2} &= \int_{r_1}^{r_2} dr \left(1 - \frac{2\Phi(r)}{c^2}\right) = \int_{r_1}^{r_2} dr \left(1 + \frac{2GM}{c^2\sqrt{r^2-b^2}}\right) \\ &= r_2 - r_1 + \frac{2GM}{c^2} \ln\left(\frac{r_2 + \sqrt{r_2^2-b^2}}{r_1 + \sqrt{r_1^2-b^2}}\right) , \end{aligned} \tag{4.17}$$

where the integral $\int dx(x^2 - b^2)^{-1/2} = \ln(x + \sqrt{x^2 - b^2})$ was used. The last term in the above equation is the general relativistic correction to the apparent speed of light, also called the Shapiro-delay [164].

As another example, one can compute the delay for a light signal travelling radially outwards from the surface of the Earth. Using the velocity with repsect to the proper spatial distance, $dl/dt = c\sqrt{-g_{00}}$, the time to reach height r_2 from r_1 is given by

$$\Delta t_{r_1\to r_2} = \frac{r_2 - r_1}{c} + \frac{GM}{c^3} \ln\left(\frac{r_2}{r_1}\right) . \tag{4.18}$$

If a light ray climbs up the potential by a proper spatial length l, and then returns to r_1, the total time of flight for this vertical trajecotry will be $t_v = \frac{2}{c}\left(l + \frac{G}{Mc^2} \ln\left(\frac{r_1+l}{r_1}\right)\right)$. In contrast, the time of flight for trajectory at a fixed radial distance r_1 with the same proper spatial length l is $t_h = \frac{2}{c}\left(l + \frac{GM}{c^2 r_1} l\right)$. Thus for $l \ll r_1$, the difference between the horizontal time of flight and the vertical time of flight is given by $\Delta t = t_h - t_v = \frac{GM}{c^3 r_1^2} l^2 = \frac{g}{c^3} l^2$, where $g = GM/r_1^2$ is the gravitational acceleration at distance z_1.

The Shapiro-delay has first been predicted in 1964 [164] and has subsequently been confirmed to high precision. Initial experiments in 1967 [161, 165] used radio signals that were emitted towards Mercury and Venus. The signals were reflected by the planet's atmosphere and the measurements revealed a delay due to the presence of the solar gravitational field. Today, the Shapiro delay has been confirmed to an accuracy of 10^{-5} with measurements involving spacecrafts such as the Cassini spacecraft [166]. The Shapiro-delay is considered the fourth classic test of general relativity, after tests of the gravitational deflection of light [159], the perihelion precession of Mercury and the redshift of light [157] (or similarly, the time dilation of clocks at different heights [158]).

Finally, it is also useful to see explicitly the relation between proper time τ and coordinate time t in the weak-field limit. Using eq. (4.2) and expanding the square root (to lowest order in c^{-4}, since the proper interval is $-c^2 d\tau^2$) yields:

$$d\tau = dt \left(1 + \frac{\Phi}{c^2} - \frac{1}{2}\frac{v^2}{c^2} - \frac{1}{8}\frac{v^4}{c^4} + \frac{1}{2}\frac{\Phi^2}{c^4} + \frac{3}{2}\frac{\Phi \cdot v^2}{c^4}\right) . \tag{4.19}$$

Note that this expression gives the Lagrangian for free systems in the presence of gravity. The action for a free massive particle is given by $S = -mc^2 \int d\tau$. When parameterized by x and t (assuming one spatial dimension for simplicity) this gives the Lagrangian through $S = \int L(x,t)dt = -mc^2 \int (d\tau/dt)dt$. The corresponding Hamiltonian is then $H = v(\partial L/\partial v) - L$, where $p = \partial L/\partial v = mv + mv^3/c^2 - 3m\Phi v/c^2$ is the canonical momentum. The resulting Hamiltonian is

$$H = mc^2 + m\Phi + \frac{p^2}{2m} - \frac{1}{8}\frac{p^4}{m^3c^2} + \frac{1}{2}\frac{m\Phi^2}{c^2} + \frac{3m}{2}\frac{\Phi p^2}{mc^2}\,. \tag{4.20}$$

This Hamiltonian governs the motion in one dimension of a particle with mass m in the gravitational field to first order in c^{-2}. In terms of the kinetic momentum $p_k = mv$, one can re-write the Hamiltonian as $H = mc^2 + m\Phi + p_k^2/2m + 3p_k^4/8m^3c^2 + m\Phi^2/2c^2 - 3\Phi p_k^2/2mc^2$. In three dimensions, the Lagrangian $L = -mc^2(d\tau/dt)$ or the corresponding Hamiltonian give the equations of motion as given in eq. (4.14).

4.4 Newtonian gravity in quantum mechanics

In non-relativistic quantum theory, external potentials are included in the Hamiltonian of a system. The Schrödinger equation can be formulated to include the Newtonian gravitational potential $\Phi(x)$ in the same way as when dealing with other potentials. At small distances x above the Earth, the force is approximately homogeneous and the interaction with gravity in the Schrödinger equation takes the form

$$H_{int} = mgx\,. \tag{4.21}$$

Here, $g \approx 9.81$ m/s^2 is the Earth acceleration, m the mass of the system of interest and x its height above the surface of the Earth. The potential above causes the accumulation of phase of the wavefunction, depending on the position of the particle. For example, a particle in superposition of two different heights acquires a relative phase between the superposition amplitudes (see Fig. 4.1). An initial superposition $|\,\psi(0)\rangle = |\,x_1\rangle + |\,x_2\rangle$ evolves under the above Hamiltonian to

$$|\,\Psi(t)\rangle = |\,x_1\rangle + e^{-img\Delta xt/\hbar}|\,x_2\rangle\,, \tag{4.22}$$

where $\Delta x = x_2 - x_1$. The relative phase caused by the Newtonian gravitational potential can be measured in interference experiments with quantum

systems. The first measurement was performed with neutrons in 1975 [167] and is known as the COW-experiment, named after the authors Colella, Overhauser and Werner. For an interferometer with height Δx and a length of the horizontal arms of s, the expected phase shift can be expressed in terms of the de-Broglie wavelength $\lambda = 2\pi\hbar t/(ms)$ as $\Delta\phi = 2\pi m^2 g \Delta x \lambda/(2\pi\hbar^2)$. It was shown that for thermal neutrons with $\lambda \sim 14.2$ nm and an interferometer of area $rs \approx 6$ cm^2, several full oscillations of the phase shift when rotating the setup are expected [168]. This has been confirmed in experiments, thus providing experimental evidence that Newtonian gravity affects quantum wave functions in the same way as any other potential would do. The phase shift can be considered as the gravitational analogue of the electric Aharonov-Bohm effect, since the effect depends only on the potential while the force is exactly the same on both arms of the interferometer.

Today, the Newtonian limit of gravity is explored in a variety of quantum experiments [169–171] and even technological applications are promising, since the gravitational acceleration g can be accurately measured in quantum interference experiments [172, 173].

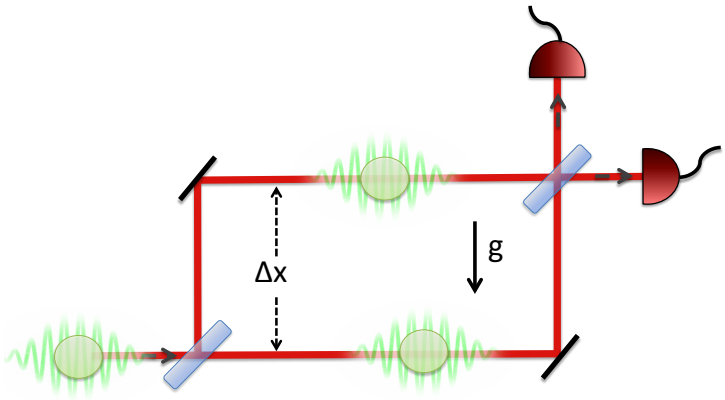

Figure 4.1: Schematic drawing of an interferometric setup where a particle is brought in superposition of two different heights. The matter-wave is coherently split on a beam splitter and the two amplitudes of the wave function evolve under the Newtonian gravitational potential (4.21). During the time spent at two different heights (with height difference Δx), the system acquires a relative phase as given in eq. (4.22). In the first experimental implementation [167], a neutron beam was coherently split using Bragg reflection from Si-crystals. The total area of the interferometer was 6 cm^2 and the neutrons were counted at the output ports using ^{3}He-detectors, confirming the gravitationally-induced relative phase of the wave function.

4.5 Quantum interference in the presence of time dilation

So far, only the Newtonian limit of gravity has been observed in quantum theory. This limit already shows that the Newtonian gravitational potential acts on quantum systems in the same way as any other potential. This means that the straightforward quantization of the position-dependence to lowest order in c^{-2} of the metric $g_{\mu\nu}(x)$ is consistent with experiments. Eq. (4.13) holds not only for the mean of a quantum wave function, but also causes quantum effects with no classical analogue, such as the accumulated relative phase shift described in eq. (4.22). It remains an experimental challenge to observe effects of general relativistic corrections to Newtonian gravity on quantum wave functions. To this end, research has mostly focused on corrections to the equation of motion, given in eq. (4.14). It was shown that quantum interference experiments with atomic fountains can in principle measure general relativistic corrections to the Newtonian potential in eq. (4.21) [174]. Thus the acquired relative phase $\Delta\phi$ in a gravitational potential includes c^{-2} contributions, which could in principle be resolved in high-accuracy measurements. Such an experiment would probe how the corrections to the Newtonian gravitational potential affect quantum systems.

However, general relativity not only gives effective corrections to the Newtonian potential, it also causes new effects that are not present in the Newtonian limit, such as time dilation. The latter is a distinct prediction of general relativity, which highlights that the theory is not simply a potential theory as any other force, but rather is of metric nature. This offers novel observable phenomena in quantum theory, with no classical analogue, that can be probed in quantum experiments. To probe time dilation, it is insufficient to test a change in relative phase between two amplitudes of a superposition [173], since such a relative phase always arises in the presence of a potential. It is necessary to consider evolution in time of internal degrees of freedom and thus to go beyond the point-particle approximation. In this way, it can be probed how time dilation due to the gravitational field, as given by eq. (4.19), enters quantum theory and how it affects quantum systems.

To include time dilation in quantum theory, it is necessary to describe the time evolution on a general background metric. To this end, geodesic motion governed by eq. (4.5) needs to be incorporated in the dynamics. Typically, quantum theory on curved space-time is formulated in the framework of quantum field theory [175]. This is the full relativistic treatment which describes the evolution of fields on curved space-time. In such an approach, the (special) relativistic equations of motions are formulated in

terms of co-variant derivatives, i.e. the Klein-Gordon and Dirac-equations are re-formulated with $\partial_\mu \to \nabla_\mu$, where $\nabla_\mu v^\nu = \partial_\mu + \Gamma^\nu_{\mu\lambda} v^\lambda$ is the covariant derivative that includes the connection when acting on a vector. Such replacement incorporates geodesic motion on a general metric. A Klein-Gordon field (describing particles with no spin) therefore evolves according to

$$(\hbar^2 \nabla_\mu \nabla^\mu - m^2 c^4)\Psi = 0\,, \tag{4.23}$$

where $\nabla_\mu \nabla^\mu \Psi = g^{\mu\nu}(\partial_\mu \partial_\mu - \Gamma^\lambda_{\mu\nu}\partial_\lambda)\Psi$ is the general relativistic d'Alembert operator. Such an equation has been extensively studied and gives a variety of novel phenomena [175]. A most prominent example is the production of Hawking radiation in the presence of a horizon [176, 177]. Quantum field theory on curved space-time offers a full framework for the description of fully relativistic phenomena. Even though the framework is in itself consistent and uncontroversial (as opposed to the attempts of fully quantizing Einstein's equations), so far there is no experimental evidence for quantum theory on curved space-time. Most phenomena considered so far involve very high energies or strong gravitational fields, and thus phenomena inherent to quantum field theory on curved space-time remain experimentally inaccessible. As a limiting case, one can consider the non-relativistic limit of the above equation, keeping only contributions to order $O(c^{-2})$. Such an approach yields an effective Hamiltonian for a point-particle that includes weak-field contributions of general relativity [178, 179]. Similarly, the Dirac equation can be considered on curved space-time and a non-relativistic limit can be obtained [180].

Here, however, we are interested in deriving the evolution of internal states in the presence of time dilation. To this end, the full quantum field theory approach is less suitable, since it is practically impossible to describe a complex, interacting system in this framework. The Hamiltonian formalism of non-relativistic theory is well-suited to describe atoms, molecules and other quantum systems with complex internal structure, since the interaction terms can be incorporated in the Hamiltonian. Such an approach is nevertheless a correct approximation, so long as full special relativistic effects can be neglected. Therefore, this approach is only valid in the low-energy limit, i.e. where particle velocities are very small and no particle creation occurs. In this limit inherent quantum field effects are negligible and the non-relativistic description is a good approximation. Despite this limit, it is possible to include general relativistic corrections in the weak-field limit. General relativity affects all systems, including "non-relativistic" systems. For example, a simple static clock in the gravitational field will experience time dilation according to eq (4.3) as compared to a clock at a different

height, and it is not necessary to describe this system in terms of relativistic fields.

Time dilation can be incorporated in low-energy quantum theory by considering any local evolution in terms of proper time. The time evolution of a system in its rest frame, given by the Schrödinger equation, needs to be replaced by the covariant derivative (along its trajectory) with respect to proper time:

$$i\hbar\frac{D}{D\tau}\Psi = H_{\text{rest}}\Psi. \tag{4.24}$$

The local dynamics, governed by H_{rest}, is given in terms of proper time, but the derivative can be expressed in terms of the 4-velocity as $D/D\tau = u^\mu\partial_\mu$. For a static observer the 4-velocity is proportional to the time translation Killing vector and has therefore only the component u^0 on a static metric. The above equation becomes $i\hbar\partial_t\Psi = (u^0/c)^{-1}H_{rest}\Psi$. The 4-velocity can now be expressed in terms of the metric via $u_\mu u^\mu = g_{\mu\nu}u^\mu u^\nu = -c^2$, such that for a static observer $(u^0/c)^{-1} = \sqrt{-g_{00}}$. Thus the time evolution for a static quantum state in terms of the coordinate time is given by

$$i\hbar\frac{\partial}{\partial t}\Psi = \sqrt{-g_{00}}H_{\text{rest}}\Psi. \tag{4.25}$$

This expression neglects velocity and special relativistic terms, but captures gravitational time dilation through the redshift factor $\sqrt{-g_{00}}$. Most importantly, the equation involves the full rest Hamiltonian that can include any internal evolution. Separating the rest mass contributions from any local dynamics governed by some Hamiltonian H_0, one can write $H_{\text{rest}} = mc^2 + H_0$. For the weak field limit, given in terms of the metric as in table 4.1 and where $g_{00} = -(1+2\Phi(x)/c^2+2\Phi^2(x)/c^4)$, the resulting expression can be expanded to lowest order in c^{-2} and one obtains an effective Schrödinger equation that includes general relativistic corrections due to time dilation:

$$i\hbar\frac{\partial}{\partial t}\Psi = \left(mc^2 + \left(1+\frac{\Phi(x)}{c^2}\right)H_0 + m\Phi(x) + m\frac{\Phi^2(x)}{2c^2}\right)\Psi\,. \tag{4.26}$$

This equation now includes a coupling term between the potential $\Phi(x)$ and the internal Hamiltonian H_0, which governs the internal dynamics of the particle. The approach presented here is valid only in the low-energy limit in which the Schrödinger equation can be used. The strength of this approach is that it explicitly takes any local time evolution of internal degrees of freedom, governed by H_0, into account. Thus the presented approach allows the study of composite low-energy quantum systems on arbitrary curved space-time. However, the equation of motion in (4.24) is not an invariant quantity, i.e., it

is not coordinate-invariant and thus only valid for specific observers. Thus the above equation only holds for static observers, but it captures time dilation in this limit and it can be generalized to include slow velocities (see below). The expression is therefore sufficiently general for the limit of interest, as long as the observers do not move at relativistic speeds.

One can compare eq. (4.26) with the expression for the proper time in the weak field limit given in eq. (4.19). The Hamiltonian can be seen as the generator of time evolution, i.e. $H \sim \partial_t$, whereas $H_{\text{rest}} \sim \partial_\tau$. The relation between the two is obtained by the change of variables through $\partial_t = (\partial\tau/\partial t)\partial_\tau$. Using eq. (4.19), the Hamiltonian is found as in the derivation of (4.20) with $mc^2 \to H_{rest}$. In this way the coupling of gravity to the rest Hamiltonian H_{rest} becomes explicit. The resulting classical expression can be canonically quantized for the position and momentum of the system. In addition, since the expression involves both x and p, the result will depend on the explicit ordering. The $\Phi(x)\cdot p$ cross-terms can be made to vanish [179], thus for simplicity we neglect these cross-terms here (note that the results presented here are not affected by these terms, since they do not couple to internal energy). The resulting quantum Hamiltonian for $H_{\text{rest}} = mc^2 + H_0$ to lowest order in c^{-2} becomes

$$H = H_0 + mc^2 + \frac{p^2}{2m} + m\Phi(x) + m\frac{\Phi^2(x)}{2c^2} - \frac{p^4}{8m^3c^2} + \left(\frac{\Phi(x)}{c^2} - \frac{p^2}{2m^2c^2}\right) H_0\,. \tag{4.27}$$

The result agrees exactly with the low energy limit obtained for point particles (with $H_0 = 0$) from eq. (4.23), found in ref. [178], apart from the above mentioned $\Phi(x)\cdot p$ cross-term ambiguity. The same result can also be obtained by considering eq. (4.24) for arbitrary non-static trajectories. The main feature of the Hamiltonian is the relativistic coupling to the internal Hamiltonian, governed by the interaction terms

$$H_{int} = \left(\frac{\Phi(x)}{c^2} - \frac{p^2}{2m^2c^2}\right) H_0\,. \tag{4.28}$$

This interaction term captures time dilation. The first term corresponds to the fact that the internal evolution is slowed down in the presence of a gravitational potential, the second term corresponds to the slow-down of the evolution due to particle motion. Neglecting the latter, the gravitational time dilation is governed by $H_{int} = H_0\Phi(x)/c^2$. This formulation now allows one to directly study quantum phenomena in the presence of time dilation. In quantum theory, the internal energy H_0 as well as the position x are operators. Thus, the time dilation term *entangles* the position of a particle to its internal dynamics. This causes novel effects to arise, with no analogue

in classical physics or considerations that approximate systems as point-particles without internal structure. The details of these novel phenomena and the implications for quantum experiments can be found in refs. [3–5]. In the following, a brief overview of these results are given.

4.5.1 Influence of time dilation on matter-wave interferometry with internal clocks

Time dilation in low-energy quantum theory, captured by the interaction Hamiltonian in eq. (4.28), can have measurable implications for matter wave interferometry. The difference as compared to the study of the Newtonian limit is the introduction of the internal Hamiltonian H_0. In Fig. 4.2 a schematic drawing of such a setup is shown. The clock represents the internal states of the wave function. For simplicity one can consider an initial superposition state $|\,\psi(0)\rangle = (|\,x_1\rangle + |\,x_2\rangle)|\,c\rangle$, where $|\,c\rangle$ is some arbitrary internal clock state that evolves in time. In the gravitational field, the Hamiltonian (4.28) acts on the system and thus the state evolves to

$$|\,\Psi(t)\rangle = |\,x_1\rangle|\,c_1(t)\rangle + e^{-i\varphi}|\,x_2\rangle|\,c_2(t)\rangle\,, \tag{4.29}$$

where $|\,c_i(t)\rangle = e^{-it\left(1+\Phi(x_i)/c^2-p^2/(2m^2c^2)\right)H_0/\hbar}|\,c\rangle$ is the evolved internal state in the presence of the gravitational potential and φ is the relative phase that

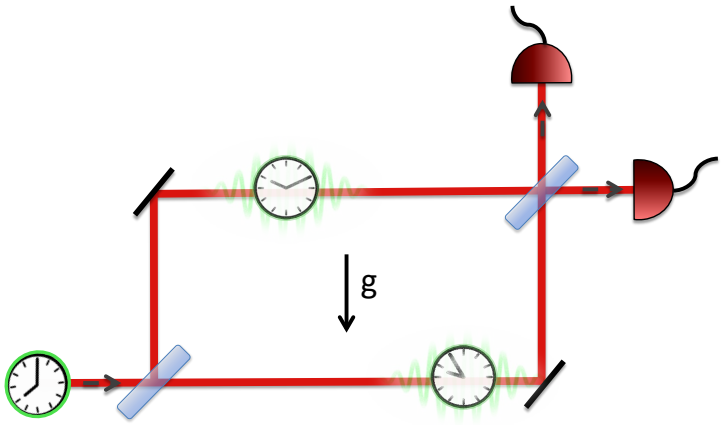

Figure 4.2: Schematic drawing of an interferometric setup where a matter wave with internal degrees of freedom is brought in superposition of two different heights. The matter-wave couples to gravity through the Hamiltonian (4.28), which captures time dilation. The internal degrees of freedom act as clocks. Thus, in addition to the relative phase as given in eq. (4.22), time dilation causes the wave function of the matter to become entangled to its internal clock states.

also includes the Newtonian potential and relativistic corrections stemming from eq. (4.27). The internal state now becomes entangled to the position x of the particle. If one performs an interference experiment, the internal state needs to be traced out. In this case, the interferometric visibility becomes

$$\mathcal{V} = |\langle c_1 \,|\, c_2 \rangle| \,. \tag{4.30}$$

In other words, the coherence of the position of the wave function is lost if the internal states become distinguishable. For example, the internal state can be a single 2-level internal degree of freedom which is in a clock-state, i.e. in a superposition of the ground and excited state with transition frequency ω and an arbitrary relative phase ϕ: $|\, c\rangle = |\, E_\phi\rangle = \frac{1}{\sqrt{2}} \big(|\, g\rangle + e^{i\phi} |\, e\rangle\big)$. The internal Hamiltonian for this state is $H_0 = E_g |\, g\rangle\langle g \,| + E_e |\, e\rangle\langle e \,|$ with $\hbar\omega = E_e - E_g$. According to (4.26), the internal state will acquire a different relative phase depending on the position x of the particle, or equivalently, the internal frequency gets redshifted to $\omega \to \omega(1 + \Phi(x)/c^2)$. In the homogeneous limit of the gravitational potential, $\Phi(x) = gx$, the visibility of the position of the particle thus becomes

$$\mathcal{V} = |\cos\left(\omega t \frac{g\Delta x}{2c^2}\right)| \,. \tag{4.31}$$

When the time dilation between the two arms matches exactly half a period of the internal oscillations, the visibility drops to 0. On the other hand, if the time dilation between the two arms is a multiple of the period of the clocks, no loss of visibility occurs. This is because the states become disentangled from the position, and no path information is available in the internal states.

Such a drop and revival of interference for matter waves with internal clocks can in principle be observed experimentally. To this end the accumulated time dilation between the two arms needs to be sufficiently large, i.e. one needs fast clock rates ω, large separations Δx or long time dilation accumulation times t. For example, for atomic clocks with $\omega \sim 10^{15}$ Hz and interferometers with $\Delta x = 1$ m, full loss of visibility is observed after keeping the superposition for about $t \sim 10$ s. The ability to maintain such a superposition or to perform interference experiments with larger separations may become experimentally feasible in the near future. Such an experiment would probe the interplay between general relativistic time dilation and quantum mechanics. This is conceptually different than probing time dilation for classical systems. It would allow to test quantum theory on a background space-time in the weak field limit to first order in c^{-2}, which has not been observed experimentally so far.

4.5.2 Shapiro-delay in single photon interference experiments

Quantum interference experiments with light can also be used to probe the effect of general relativity on quantum wave functions. General relativistic time dilation causes the slow-down of light in the presence of a gravitational potential, given by eq. (4.16). The quantum version of the Shapiro-delay experiment would be to send a single photon in a superposition of two different paths that differ in gravitational potential. The (coordinate) speed of light at different heights is given by $v_c(x) = c\sqrt{-g_{oo}/g_{xx}} \approx c(1 + 2\Phi(x)/c^2)$. If the interferometer is aligned in the same way as considered in previous sections (see Fig. 4.3), only the horizontal path with length L contributes to the Shapiro delay. However, this path length is not the coordinate length L_x: at a different height it is given by $L = \sqrt{g_{xx}}L_x \approx (1 - \Phi(x)/c^2)L_x$. Thus the photon traverses the path L_x with velocity $v_c(x)$ in a coordinate time $t = L_x/v_c(x) = (\sqrt{g_{00}})^{-1}L/c \approx (1 - \Phi(x)/c^2)L/c$. In the homogeneous limit, the photon in the lower arm is delayed (as compared to the upper arm) by

$$\Delta t = \frac{Lg\Delta x}{c^3} = \frac{Ag}{c^3}\,, \tag{4.32}$$

where A is the area of the interferometer. Thus $\Delta t \approx A \cdot 10^{-24}$ s/m^3 and a time shift of $\Delta t \sim 1$ fs is obtained in an interferometer of size $A \sim 10^3$ km^2. Such a large optical interferometer can in principle be implemented with optical fibres or with optical cavities. The signature of the delay would be

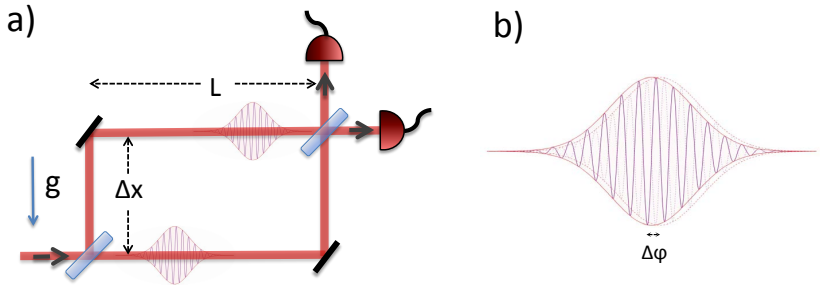

Figure 4.3: a) Schematic drawing of an interferometric setup where a photon travels in superposition at two different heights. The total area of the interferometer is $A = L\Delta x$. The Shapiro delay causes the amplitude on the lower paths to be delayed as compared to the upper path, given by eq. (4.32). If the delay Δt exceeds the pulse duration, the photon will not interfere. b) In the limit of very small delay as compared to the pulse length, the peak separation cannot be resolved and full interference is expected. However, the photon acquires a relative phase (dashed lines as compared to solid lines).

the loss of interference, since the two amplitudes of the photon would not fully overlap.

However, to lowest order (if the delay is much smaller than the pulse envelope of the light, see Fig. 4.3) the Shapiro-delay causes a phase shift between the two arms. In this case, the actual delay of the pulse would remain unobserved, but the influence of gravity on the photon would still be probed. For a photon wave packet with main frequency ν, the phase shift (in radians) is given by

$$\Delta\phi = \frac{Ag}{c^3}\nu\,. \tag{4.33}$$

The phase shift is a direct optical analogue of the Newtonian phase shift described in sec. 4.4. Observing such an optical shift would show that the Newtonian gravitational potential affects single photons in superposition in a coherent way. The phase shift according to eq. (4.33) has the value as one would expect from a "Newtonian" calculation, in which the photon of frequency ν is treated as giving rise to the mass $m_{eff} = \hbar\nu/c^2$. The factor 2 that is related to the g_{ij}-component and that appears in the bending of light, given in eq. (4.14), does not contribute to the effect described here. Even though the change in coordinate velocity of light changes according to eq. (4.15), which includes the factor of 2, the length of the interferometer L is also contracted in the gravitational field. Thus the additional contribution that stems from length contraction cancels, so long as the interferometer length was initially fixed.

The phase shift is much easier to observe than the full delay of the photon between the two arms. According to eq. (4.33), for $\nu = 10^{15}$ Hz an interferometer of size $A = 10^{-3}$ km^2 is sufficient to cause a phase shift of $\Delta\phi \approx 1$ rad. Even though the Shapiro delay is confirmed for classical electro-magnetic radiation, a quantum experiment as described here could probe the effect of Shapiro delay on a quantum wave function of a single photon and could in principle be performed in a laboratory experiment.

4.6 Universal decoherence due to gravitational time dilation

In the previous sections it was shown how simple quantum systems are affected by time dilation. Single photons in superposition are delayed due to gravity, whereas matter-waves with internal clock states lose coherence due to gravity-induced entanglement between position and internal clock-states. The latter can be generalized for any arbitrary composite quantum system. The relativistic interaction Hamiltonian (4.28) stemming from time dilation

couples *any* internal energy to the position of the system. The coupling is universal in the same sense as time dilation is universal: any dynamics will be slowed down in the presence of gravity, thus any composite system will be affected. As will be shown below, this causes decoherence of the centre-of-mass of all composite quantum system in the presence of time dilation.

Using the interaction Hamiltonian (4.27) one can derive an equation of motion for any composite quantum system in the presence of time dilation. We keep the internal Hamiltonian H_0 that governs the composition and the centre-of-mass Hamiltonian H_{cm} completely general. The overall Hamiltonian of the system is $H_{tot} = H_{cm} + H_0 + H_{int}$, where H_0 governs the evolution of the internal constituents and $H_{int} = H_0\Gamma(x,p)/c^2$ captures the time-dilation-induced coupling between internal degrees of freedom and the centre-of-mass to lowest order in c^{-2}. Since in this case the weak-field limit applies, the function $\Gamma(x,p)$ is given in eq. (4.28): $\Gamma(x,p) = \Phi(x) - p^2/2m^2$. Γ is a function of the centre-of-mass position x and momentum p to which the internal states couple due to special relativistic and general relativistic time dilation. The starting point is the von Neumann equation for the full quantum state of the system that includes both, the internal states and the external degrees of freedom:

$$\dot{\rho} = -\frac{i}{\hbar}\left[H_{tot}, \rho\right] \tag{4.34}$$

Writing $H_{tot} = H + H_{int}$, where $H = H_{cm} + H_0$, one can change frame to primed coordinates, which we define through $\rho'(t) = e^{it(H+h)/\hbar}\rho(t)e^{-it(H+h)/\hbar}$, where $h = h(x,p) = \Gamma(x,p)\bar{E}_0/c^2$. Here, $\bar{E}_0 = \langle H_0 \rangle$ is the average internal energy. The resulting von-Neumann equation in the primed frame is

$$\begin{aligned}\dot{\rho}'(t) &= \frac{i}{\hbar}\left[H'(t) + h'(t), \rho'(t)\right] - \frac{i}{\hbar}\left[H'(t) + H'_{int}(t), \rho'(t)\right] \\ &= -\frac{i}{\hbar}\left[H'_{int}(t) - h'(t), \rho'(t)\right] \ ,\end{aligned} \tag{4.35}$$

where $h'(t) = h(x'(t), p'(t))$. The formal solution of the above equation is $\rho'(t) = \rho'(0) - \frac{i}{\hbar}\int_0^t ds\,[H'_{int}(s) - h'(s), \rho'(s)]$. This can be inserted back into the equation above, which yields the integro-differential equation for the density matrix

$$\begin{aligned}\dot{\rho}'(t) = &-\frac{i}{\hbar}\left[H'_{int}(t) - h'(t), \rho'(0)\right] - \\ &- \frac{1}{\hbar^2}\int_0^t ds\left[H'_{int}(t) - h'(t), \left[H'_{int}(s) - h'(s), \rho'(s)\right]\right] \ .\end{aligned} \tag{4.36}$$

One can now trace over the internal degrees of freedom to obtain the dynamics of the center-of-mass. Assuming the state to be initially uncorrelated

(i.e. no prior time dilation) $\rho(0) = \rho_{cm}(0) \otimes \Pi_i^N \rho_i(0)$ and taking the Born approximation (keeping only terms to second order in H_{int}), the term $\rho'(s)$ can be replaced under the integral by $\rho'_{cm}(s) \otimes \rho_i(0)$. In this approximation the master equation for the centre-of-mass becomes

$$\begin{aligned}
&\dot{\rho}'_{cm}(t) = \Pi_{i=1}^N \mathrm{Tr}_i[\dot{\rho}'(t)] \\
&\approx -\frac{1}{\hbar^2}\Pi_{i=1}^N \int_0^t ds\, \mathrm{Tr}_i\Big\{ [H'_{int}(t) - h'(t), [H'_{int}(s) - h'(s), \rho'(s)]] \Big\} \\
&= -\left(\frac{1}{\hbar c^2}\right)^2 \Pi_{i=1}^N \int_0^t ds\, \mathrm{Tr}_i\Big\{ \left(H_0 - \bar{E}_0\right)^2 [\Gamma'(t), [\Gamma'(s), \rho'(s)]] \Big\} \\
&= -\left(\frac{\Delta E_0}{\hbar c^2}\right)^2 \int_0^t ds\, [\Gamma'(t), [\Gamma'(s), \rho'_{cm}(s)]] \,.
\end{aligned} \tag{4.37}$$

Here we used the notation $\Delta E_0^2 = \Pi_{i=1}^N \mathrm{Tr}_i \left\{ \rho_i \left(H_0 - \bar{E}_0\right)^2 \right\} = \langle H_0^2 \rangle - \langle H_0 \rangle^2$ for the energy fluctuations of the internal states and $\Gamma'(s) = \Gamma(x'(s), p'(s))$. The above equation is highly non-Markovian: the density matrix of the center-of-mass depends on the state and the trajectory of all previous times. This captures the accumulation of proper time difference. A Markovian approximation cannot be made.

Changing back to the original picture, and introducing $s \to t - s$ we obtain the integro-differential equation:

$$\begin{aligned}
\dot{\rho}_{cm}(t) = &-\frac{i}{\hbar}\left[H_{cm} + \Gamma(x,p)\frac{\bar{E}_0}{c^2}, \rho_{cm}(t)\right] - \\
&-\left(\frac{\Delta E_0}{\hbar c^2}\right)^2 \int_0^t ds \left[\Gamma(x,p), [\Gamma(x,p), \rho_{cm}(t-s)]\,\big|_s\right],
\end{aligned} \tag{4.38}$$

where $[\Gamma, \rho_{cm}]\,\big|_s = e^{-isH_{cm}/\hbar}\,[\Gamma, \rho_{cm}]\,e^{isH_{cm}/\hbar}$. This is the general equation of motion for a composite particle of arbitrary composition that undergoes time dilation. The first term is the unitary evolution due to the center-of-mass Hamiltonian H_{cm}. In addition, the unitary evolution includes the coupling between the mean internal energy to the position and momentum of the particle. This coupling comes about from the energy contribution of the internal states to the total mass. The second term is purely quantum mechanical and affects only off-diagonal elements of the density matrix. It causes decoherence of the system into a basis that is given by $\Gamma(x,p)$, i.e. a combination of position and momentum. In the case where general relativistic time dilation dominates, one has $\Gamma \approx gx$ and thus decoherence occurs into the position basis. The strength of the decoherence is governed by the system's internal energy spread ΔE_0. A larger energy distribution of internal states increases the decoherence rate.

The above integro-differential equation can be further simplified if the center-of-mass does not significantly change on the relevant timescale τ_d, on which coherence is lost. In this case, one can set $[\Gamma, \rho_{cm}]\big|_s \approx [\Gamma, \rho_{cm}]$ and the Master equation is significantly simplified:

$$\dot{\rho}_{cm}(t) = -\frac{i}{\hbar}\left[H_{cm} + \Gamma(x,p)\frac{\bar{E}_0}{c^2}, \rho_{cm}(t)\right] - \left(\frac{\Delta E_0}{\hbar c^2}\right)^2 t\left[\Gamma(x,p), [\Gamma(x,p), \rho_{cm}(t)]\right] . \tag{4.39}$$

To see the effect of time dilation more explicitly, one can model the composite system as consisting of $N/3$ non-interacting internal harmonic oscillators. In this case, the model for the internal structure is simply

$$H_0 = \hbar \sum_i^N \omega_i n_i \,, \tag{4.40}$$

where n_i are the number operators for each constituent. In the static case (i.e. neglecting special relativistic time dilation that stems from p^2-contributions), the interaction Hamiltonian (4.28) becomes

$$H_{int} = x\frac{\hbar g}{c^2}\sum_i^N \omega_i n_i \,. \tag{4.41}$$

Assuming all internal states to be thermal, the mean energy and energy variance are given in the high temperature limit ($k_B T \ll \hbar\omega_i$) as

$$\bar{E}_0 \approx N k_B T \,, \qquad \Delta E_0^2 \approx N (k_B T)^2 \,. \tag{4.42}$$

For this model, the master equation for the particle becomes

$$\dot{\rho}_{cm}(t) \approx -\frac{i}{\hbar}\left[\tilde{H}_{cm} + \left(m + \frac{N k_B T}{c^2}\right) g x, \rho_{cm}(t)\right] - Nt\left(\frac{k_B T g}{\hbar c^2}\right)^2 [x, [x, \rho_{cm}(t)]] \,, \tag{4.43}$$

In the unitary part the Newtonian gravitational potential was explicitly written out for clarity (i.e. $H_{cm} = \tilde{H}_{cm} + mgx$): It is evident that the potential couples to an effective total mass $m_{\text{tot}} = m + \bar{E}/c^2$ that includes the average internal energy $\bar{E} = \langle H_0 \rangle = N k_B T$. This is in accordance with the notion of heat in general relativity (in Einstein's words [181]: "a piece of iron weighs more when red-hot than when cool"). In the non-unitary part the coupling is now explicitly only to the position of the particle. In the position basis the term reads as $-Nt\left(k_B T g \Delta x/\hbar c^2\right)^2 \rho_{cm}(x,y,t)$, where $\rho_{cm}(x,y,t) = \langle x \,|\rho_{cm}|\, y\rangle$ and $\Delta x = x - y$. This term, responsible for the decoherence, scales with $\hbar^{-2}$ and therefore dominates over the Hamiltonian

term for the time evolution of the off-diagonal elements. The use of the above master equation (4.43) (instead of the integro-differential equation (4.38)) is therefore justified so long as the center-of-mass Hamiltonian H_{cm} does not induce significant changes to the off-diagonal elements on the time scale τ_d. This time scale is found from the solution to eq. (4.43), which to order $O(\hbar^{-2})$ is approximately

$$\rho_{cm}(x, y, t) \sim \rho_{cm}(x, y, 0)\, e^{-(t/\tau_d)^2}, \tag{4.44}$$

with

$$\tau_d = \sqrt{\frac{2}{N}} \frac{\hbar c^2}{k_B T g \Delta x}. \tag{4.45}$$

The above time scale gives the strength of decoherence due to gravitational time dilation. It affects all composite systems on Earth. Note that the decoherence is fully general and governed by eq. (4.38). Any composite quantum system will decohere if it is delocalized over a region of space that has time dilation. An estimate of the strength of the decoherence on Earth can easily be given: For a gram-scale object with $N \sim 10^{23}$ a superposition of size $\Delta x = 10^{-6}$ m, will decohere due to time dilation after

$$\tau_{\text{dec}} \approx 10^{-3} s\,. \tag{4.46}$$

Thus all macroscopic systems on Earth must have a purely classical position degree of freedom, in accordance with the quantum-to-classical transition. Time dilation therefore adds another decoherence mechanism which is relevant even in the weak-field limit of Earth for mesoscopic and macroscopic systems. Experimentally, this mechanism can be avoided only if superposition trajectories are chosen such that at the time of the read-out, no time dilation has been accumulated between the two paths. This can in principle be achieved, but the non-Markovian nature of the mechanism (i.e. the accumulation of time dilation throughout the whole experiment) makes such a cancellation increasingly challenging for larger objects. The reversibility of this effect also highlights the major conceptual difference to gravitationally-inspired collapse theories: while the latter postulate a modification of quantum theory at some scale [98, 99], the effect described here does not rely on any modification of either quantum theory or general relativity. Time dilation decoherence is therefore conceptually closer to decoherence due to interaction with gravitational waves [182–184]. However, decoherence due to time dilation takes place on static background metrics and follows directly from the low-energy limit of theory.

We note that the specific model for the internal states given by (4.40) is just an approximate model for the distribution of internal energy. It corresponds to the Einstein model for phonons. A more precise model would

be the Debye model, which has higher validity at low temperatures. In general, the decoherence time scale in the Master equation (4.39) depends only on ΔE_0. In thermodynamic equilibrium with the environment it is directly related to the heat capacity of a system [185]. A modelling of the internal structure is only required if the internal energy distribution cannot be measured accurately.

The decoherence effect described here can in principle be probed experimentally. To this end, it is necessary to bring relatively large objects into superposition. In recent years, quantum interference of large molecules has become accessible in experiments [186–188]. Opto-mechanical systems also offer the possibility to bring macroscopic systems into quantum superposition [49, 52, 54]. Another promising route is the optical control and read-out of micro- and nanospheres [189–192]. The development of experimental techniques to control quantum behaviour of larger and more massive objects is largely driven by the aim to probe possible gravitational collapse theories [52, 100, 193, 194]. As was shown above, even without any modification to quantum theory, gravity causes decoherence of larger systems due to time dilation. Thus it is expected that in future quantum experiments with large systems the effect predicted here will become dominant.

For an experiment to isolate the time-dilation-induced decoherence, all other sources of decoherence have to be negligible. For large systems, a dominant source of decoherence is the emission and scattering of radiation [195–197]. If the superposition size is much larger than the wavelength of the scattered radiation, $\Delta x \gg \lambda$, the decoherence is simply governed by the scattering rate γ. A single scattering event or emission of a single photon is sufficient to decohere the object. In the following, the discussion is restricted to when the wavelength is smaller than the superposition size. In this case, many events take place before full decoherence occurs. The decoherence in this case can be captured by the master equation [83, 137, 195–198] $\dot{\rho} = -i/\hbar\,[H,\rho] - \Lambda\,[x,[x,\rho]]$, where the localization rate Λ governs the strength of the decoherence. This master equation can be derived by considering the imparted momentum transfer from surrounding particles. For photons the localization rate is given by [83, 137]:

$$\Lambda = c\int_0^\infty dk k^2 N_k g(k)\sigma_{eff}(k)\,, \tag{4.47}$$

where k is the wave vector of radiation, N_k the number of particles with wave vector k, $g(k)$ the mode density and $\sigma_{eff}(k)$ the effective scattering cross section. To estimate these quantities, a careful analysis needs to be performed for any specific physical system [199]. For the simplified case of black-body radiation, the vacuum mode density is $g(k)dk = \pi^{-2}k^2 dk$.

However, it is possible to engineer a modified mode density (for example, by using cavities) with a "band gap", such that specific wavelengths cannot be emitted. For a black-body in equilibrium, the number of photons is given by the Planck distribution for the two polarization modes, i.e. $N_k = 2/(e^{\hbar ck/(k_B T)} - 1)$. However, this distribution is not applicable to a hot particle that is out of equilibrium, since the stimulated emission process is mostly absent [200]. In addition, the finite size of the system causes a dependence on the specific heat C_v of the system [200, 201]. In total, for hot particles that emit into the vacuum the corrected distribution is given by [200, 201] $N_k = 2e^{-\hbar ck/(k_B T) - (2C_v)^{-1} (\hbar ck/k_B T)^2}$. The second exponential can be neglected for large particle sizes for which $C_v \gg 1$. Finally, the effective cross-section depends on the type of processes and on the material properties of the particles. In particular, three main limits can be identified for the cross-section, in dependence on the size r of the particle as compared to the wave number k [199]:

$$\begin{aligned}
\sigma_{eff}(k) &\approx \sigma_g = \pi r^2 && (kr \gg 1, \quad \text{geometric scattering}) \\
\sigma_{eff}(k) &\approx \sigma_R = \frac{8\pi}{3} \left| \frac{\varepsilon(k) - 1}{\varepsilon(k) + 2} \right| k^4 r^6 && (kr \ll 1, \quad \text{Rayleigh scattering}) \\
\sigma_{eff}(k) &\approx \sigma_{abs} = 4\pi \mathrm{Im} \left[\frac{\varepsilon(k) - 1}{\varepsilon(k) + 2} \right] kr^3 && (kr \ll 1, \quad \text{absorption / emission}) ,
\end{aligned} \tag{4.48}$$

where ε is the (complex) dielectric constant of the material. The scattering for the case $kr \approx 1$ is more complicated and has to be described by the full Mie theory [199]. To include all the cases described in eq. (4.48), one can set $\sigma_{eff}(k) = \sigma_0 k^\delta r^{2+\delta}$ to obtain a general expression for Λ as a function of δ. In this case it is assumed that the dielectric properties do not appreciably change with wavenumber, $\varepsilon(k) \approx \varepsilon$, which is an oversimplification [202]. However, such an approximation allows one to find closed expressions for the localization rates. For $N_k = 2e^{-\hbar ck/(k_B T)}$ and the vacuum mode density one obtains

$$\begin{aligned}
\Lambda &= \frac{2c\sigma_0 r^{\delta+2}}{\pi^2} \int dk k^{4+\delta} e^{-\hbar ck/k_B T} = \\
&= \frac{2c\sigma_0 r^{\delta+2}}{\pi^2} \int dk \frac{d^{4+\delta}}{d(-\lambda_T)^{4+\delta}} e^{-\lambda_T k} = \\
&= \frac{2c\sigma_0 r^{\delta+2}}{\pi^2} \frac{(4+\delta)!}{\lambda_T^{5+\delta}} = \\
&= \frac{2c}{\pi^2} \sigma_0 \, (4+\delta)! \left(\frac{r}{\lambda_T} \right)^{\delta+2} \frac{1}{\lambda_T^3} ,
\end{aligned} \tag{4.49}$$

where $\lambda_T = \hbar c/(k_B T) \approx 2 \cdot 10^{-3} m \cdot K/T$ is the thermal de-Broglie wavelength up to order unity. Using eq. (4.48) for the scattering ($\delta = 4$) and the absorption ($\delta = 1$) of light with wavelengths larger than the particle size, the localization rates become

$$\begin{aligned} \Lambda_{scat} &= \frac{2 \cdot 10^5 c}{\pi} \left| \frac{\varepsilon - 1}{\varepsilon + 2} \right| \left(\frac{r}{\lambda_T} \right)^6 \frac{1}{\lambda_T^3} \\ \Lambda_{abs} &= \frac{960 c}{\pi} \mathrm{Im} \left[\frac{\varepsilon - 1}{\varepsilon + 2} \right] \left(\frac{r}{\lambda_T} \right)^3 \frac{1}{\lambda_T^3} \,. \end{aligned} \tag{4.50}$$

The numerical pre-factor is typically much larger for scattering than it is for absorption, since the latter depends only on the small imaginary component of $(\varepsilon - 1)/(\varepsilon + 2)$. However, the two decoherence effects scale very differently with the size of the particle. Since the limit considered here is $r/\lambda_T \ll 1$, decoherence due to absorption and emission will dominate for sufficiently large systems or low temperatures. For example, for a particle of size $r = 1$ μm interacting with radiation at room temperature ($T = 300K$, $\lambda_T \approx 10^{-5}$ m) $(r/\lambda_T)^3 \approx 10^{-3}$, whereas the same interaction at cryogenic temperatures ($\lambda_T \approx 10^{-3}$ m) gives $(r/\lambda_T)^3 \approx 10^{-9}$. Thus at low temperatures the dominant source of decoherence will be the absorption and emission of radiation. While the surrounding can be cooled to low temperatures, the particle itself will radiate and thus decohere. This decoherence source needs to be compared to the time dilation induced decoherence τ_d, which for the simple model (4.41) is given by eq. (4.45). Writing the particle number N in terms of the radius r by using the material density ρ and molecular mass m_0 as $N = 4\pi\rho r^3/(3m_0)$ one can compare the two decoherence sources:

$$\eta = \Lambda_{abs} \Delta x^2 \tau_d \approx 10^{31} \mathrm{Im} \left[\frac{\varepsilon - 1}{\varepsilon + 2} \right] \sqrt{\frac{m_0}{\rho}} \cdot \frac{1}{T^7} \cdot r^{3/2} \cdot \Delta x \,. \tag{4.51}$$

To observe time dilation induced decoherence, one requires $\eta \ll 1$. Emission of radiation is strongly suppressed at cryogenic temperatures and for low absorption coefficients. At cryogenic temperatures, the dominant range of the emitted radiation is in the microwave range. In this regime, materials can be found that have very low emission and absorption properties [202, 203]. In particular, it was shown that sapphire reaches values as low as $\mathrm{Im}[\varepsilon] \approx 10^{-9}$ at cryogenic temperatures in the microwave range [202, 204]. Thus, performing an interference experiment with sapphire microspheres at cryogenic temperatures should allow for the verification of decoherence due to gravitational time dilation.

Chapter 5

Reprints

5.1 Pulsed quantum optomechanics

In the work on pulsed opto-mechanics, conducted in close collaboration with the group of M. Aspelmeyer and M. S. Kim and with input from G. Milburn and K. Hammerer, we propose a scheme to realize quantum state tomography, squeezing, and state purification of a mechanical resonator using short optical pulses. The scheme allows observation of mechanical quantum features despite preparation from a thermal state and is shown to be experimentally feasible using optical microcavities. We studied the pulsed regime of the opto-mechanical interaction, where the pulse duration is on the order of the cavity ringdown time and is much shorter than a mechanical period. This allows for a novel interaction regime that goes beyond previously considered continuous interaction in opto-mechanics. Homodyne detection is used to determine the phase of the field emerging from the cavity, and thus to obtain a measure of the mechanical position. Measuring the optical phase at various times throughout a mechanical period provides access to arbitrary mechanical marginals and thus allows for full quantum state tomography. In addition, we show that the same experimental tools can also be used for remote preparation of a mechanical squeezed state and for state purification: The measurement of the phase of light projects the mechanics into a squeezed state, with the squeezing depending on the interaction strength. We show that for realistic experimental parameters the pulsed interaction can be sufficiently strong to prepare and to verify squeezed states.

I contributed to all aspects of the research project.

Pulsed quantum optomechanics

M. R. Vanner[a,1], I. Pikovski[a], G. D. Cole[a], M. S. Kim[b], Č. Brukner[a,c], K. Hammerer[c,d], G. J. Milburn[e], and M. Aspelmeyer[a]

[a]Vienna Center for Quantum Science and Technology (VCQ), Faculty of Physics, University of Vienna, Boltzmanngasse 5, A-1090 Vienna, Austria; [b]QOLS (Quantum Optics and Laser Science Group), Blackett Laboratory, Imperial College London, London SW7 2BW, United Kingdom; [c]Institute for Quantum Optics and Quantum Information (IQOQI) of the Austrian Academy of Sciences, A-1090 Vienna and A-6020 Innsbruck, Austria; [d]Institute for Theoretical Physics and Albert Einstein Institute, University of Hannover, Callinstrasse 38, D-30167 Hannover, Germany; and [e]School of Mathematics and Physics, University of Queensland, Saint Lucia 4072, Australia

Edited by Mikhail Lukin, Harvard University, Cambridge, MA, and accepted by the Editorial Board July 21, 2011 (received for review April 1, 2011)

Studying mechanical resonators via radiation pressure offers a rich avenue for the exploration of quantum mechanical behavior in a macroscopic regime. However, quantum state preparation and especially quantum state reconstruction of mechanical oscillators remains a significant challenge. Here we propose a scheme to realize quantum state tomography, squeezing, and state purification of a mechanical resonator using short optical pulses. The scheme presented allows observation of mechanical quantum features despite preparation from a thermal state and is shown to be experimentally feasible using optical microcavities. Our framework thus provides a promising means to explore the quantum nature of massive mechanical oscillators and can be applied to other systems such as trapped ions.

optomechanics | quantum measurement | squeezed states

Coherent quantum mechanical phenomena, such as entanglement and superposition, are not apparent in the macroscopic realm. It is currently held that on large scales quantum mechanical behavior is masked by decoherence (1) or that quantum mechanical laws may even require modification (2–5). Despite substantial experimental advances, see for example ref. 6, probing this regime remains extremely challenging. Recently however, it has been proposed to utilize the precision and control of quantum optical fields in order to investigate the quantum nature of massive mechanical resonators by means of the radiation-pressure interaction (7–13). Quantum state preparation and the ability to probe the dynamics of mechanical oscillators, the most rigorous method being quantum state tomography, are essential for such investigations. These important elements have been experimentally realized for various quantum systems, e.g., light (14, 15), trapped ions (16, 17), atomic ensemble spin (18, 19), and intracavity microwave fields (20). By contrast, an experiment realizing both quantum state preparation and tomography of a mechanical resonator is yet to be achieved. Also, schemes that can probe quantum features without full tomography [e.g., (9, 10, 21)] are similarly challenging. In nanoelectromechanics, cooling of resonator motion and preparation of the ground state have been observed (22, 23) but quantum state reconstruction (24) remains outstanding. In cavity optomechanics significant experimental progress has been made towards quantum state control over mechanical resonators (11–13), which includes classical phase-space monitoring (25, 26), laser cooling close to the ground state (27, 28), and low noise continuous measurement of mechanically induced phase fluctuations (29–31). Still, quantum state preparation is technically difficult primarily due to thermal bath coupling and weak radiation-pressure interaction strength, and quantum state reconstruction remains little explored. Thus far, a common theme in proposals for mechanical state reconstruction is state transfer to and then read-out of an auxillary quantum system (32–35). This technique is a technically demanding approach and remains a challenge.

In this paper we introduce an optomechanical scheme that provides direct access to all the mechanical quadratures in order to obtain full knowledge about the quantum state of mechanical motion. This quadrature access is achieved by observing the distribution of phase noise of strong pulses of light at various times throughout a mechanical period. We show that the same experimental tools used for quantum state tomography can also be used for squeezed state preparation and state purification, which thus provides a complete experimental framework. Our scheme does not require "cooling via damping" (11–13) and can be performed within a single mechanical cycle thus significantly relaxing the technical requirements to minimize thermal contributions from the environment.

Using a pulsed interaction that is very short compared to the period of an oscillator to provide a back-action-evading measurement of position was introduced in the seminal contributions of Braginsky and coworkers (36, 37), where schemes for sensitive force detection were developed. In our work, the quantum nature of a mechanical resonator is itself the central object of investigation. Here, the pulsed interaction is used to provide an experimentally feasible means to generate and fully reconstruct quantum states of mechanical motion. The proposed experimental setup is shown in Fig. 1. A pulse of duration much less than the mechanical period is incident upon an optomechanical Fabry-Pérot cavity which we model as being single sided. Due to the entanglement generated during the radiation-pressure interaction, the optical phase becomes correlated with the mechanical position while the optical intensity imparts momentum to the mechanical oscillator. Time-domain homodyne detection (15) is then used to determine the phase of the field emerging from the cavity, and thus to obtain a measurement of the mechanical position. For each pulse, the measurement outcome P_L is recorded, which for Gaussian optical states has mean and variance

$$\langle P_L\rangle = \chi\langle X_M^{\text{in}}\rangle, \qquad \sigma_{P_L}^2 = \sigma_{P_L^{\text{in}}}^2 + \chi^2\sigma_{X_M^{\text{in}}}^2, \qquad [1]$$

respectively. X_M^{in} is the mechanical position quadrature immediately prior to the interaction and P_L^{in} describes the input phase of light. The position measurement strength χ is an important parameter in this work as it quantifies the scaling of the mechanical position information onto the light field. A derivation of Eq. **1** including an optimization of χ by determining the input pulse envelope to gain the largest cavity enhancement is provided in the *Appendix*.

In order to describe and quantify the pulse interaction and measurement we use the nonunitary operator Υ that determines the new mechanical state via $\rho_M^{\text{out}} \propto \Upsilon\rho_M^{\text{in}}\Upsilon^\dagger$. This operator is mechanical state independent and can be determined from the probability density of measurement outcomes

$$\Pr(P_L) = \text{Tr}_M(\Upsilon^\dagger\Upsilon\rho_M^{\text{in}}). \qquad [2]$$

For pure optical input, it takes the form

Author contributions: M.R.V., I.P., G.D.C., M.S.K., Č.B., K.H., G.J.M., and M.A. designed research; M.R.V., I.P., G.D.C., M.S.K., Č.B., K.H., G.J.M., and M.A. performed research; and M.R.V., I.P., G.D.C., M.S.K., Č.B., K.H., G.J.M., and M.A. wrote the paper.

The authors declare no conflict of interest.

This article is a PNAS Direct Submission. M.L. is a guest editor invited by the Editorial Board.

Freely available online through the PNAS open access option.

[1]To whom correspondence should be addressed. E-mail: michael.vanner@univie.ac.at.

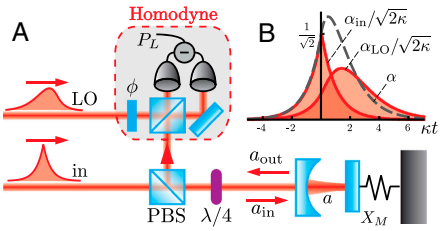

Fig. 1. (*A*) Schematic of the optical setup to achieve measurement based quantum state engineering and quantum state tomography of a mechanical resonator. An incident pulse (in) resonantly drives an optomechanical cavity, where the intracavity field *a* accumulates phase with the position quadrature X_M of a mechanical oscillator. The field emerges from the cavity (out) and balanced homodyne detection is used to measure the optical phase with a local oscillator pulse (LO) shaped to maximize the measurement of the mechanical position. (*B*) Scaled envelopes of the optimal input pulse, its corresponding intracavity field and the optimal local oscillator as computed in the *Appendix*.

$$\Upsilon = (\pi 2\sigma^2_{P_L^{\rm in}})^{-\frac{1}{4}} \exp\left[i\Omega X_M - \frac{(P_L - \chi X_M)^2}{4\sigma^2_{P_L^{\rm in}}}\right], \qquad [3]$$

where Ω quantifies the momentum transfer to the mechanics due to the pulse mean photon number. Υ can be readily understood by considering its action on a mechanical position wavefunction. This operator selectively narrows the wavefunction to a width scaling with χ^{-2} about a position which depends upon the measurement outcome. Moreover, the quantum non-demolition-like nature of Υ allows for back-action-evading measurements of X_M, i.e., the back-action noise imparted by the quantum measurement process occurs in the momentum quadrature only*. Other methods, such as the continuous variational measurement scheme (38), which has recently been considered for gravitational-wave detectors (39, 40), also allow for back-action-evading measurements. However, using short pulses offers a technically simpler route for quantum state tomography and is readily implementable, as will be discussed below.

In the following, we consider coherent drive i.e., $\sigma^2_{P_L^{\rm in}} = 1/2$. We first address the important challenge of how to experimentally determine the motional quantum state of a mechanical resonator. We then discuss how such a measurement can be used for quantum state preparation and finally we provide details for a physical implementation and analyze a thorough list of potential experimental limitations.

Mechanical Quantum State Tomography

Of vital importance to any experiment aiming to explore quantum mechanical phenomena is a means to measure coherences and complementary properties of the quantum system. Such measurement is best achieved by complete quantum state tomography, which despite being an important quantum optical tool has received very little attention for mechanical resonators†. Any measurement made on a single realization of a quantum state cannot yield sufficient information to characterize that quantum state. The essence of quantum state tomography is to make measurements of a specific set of observables over an ensemble of identically prepared realizations. The set is such that the measurement results provide sufficient information for the quantum state to be uniquely determined. One such method is to measure the marginals $\langle X|e^{-i\theta n}\rho e^{i\theta n}|X\rangle$, where n is the number operator, for all phase-space angles θ, see refs. 14, 15, 42 and e.g., ref. 43.

*No mechanical position noise is added as our measurement operator commutes with the mechanical position. This is because the mechanical evolution can be neglected during the short optomechanical interaction.

†During the submission process of this manuscript a scheme to perform tomography of the motional state of a trapped particle using a time-of-flight expansion was proposed (41).

Our scheme provides a means for precision measurement of the mechanical quadrature marginals, thus allowing the mechanical quantum state to be determined. Specifically, given a mechanical state $\rho_M^{\rm in}$, harmonic evolution of angle $\theta = \omega_M t$ provides access to all the quadratures of this mechanical quantum state which can then be measured by a subsequent pulse. Thus, reconstruction of any mechanical quantum state can be performed. The optical phase distribution Eq. **2**, including this harmonic evolution, becomes

$$\Pr(P_L) = \int \frac{dX_M}{\sqrt{\pi}} e^{-(P_L - \chi X_M)^2} \langle X_M|e^{-i\theta n}\rho_M^{\rm in} e^{i\theta n}|X_M\rangle, \qquad [4]$$

which is a convolution between the mechanical marginal of interest and a kernel that is dependent upon χ and the quantum phase noise of light. The effect of the convolution is to broaden the marginals and to smooth any features present.

Let us consider the specific example of a mechanical resonator in a superposition of two coherent states, i.e., $|\psi_\delta\rangle \propto |i\delta\rangle + |-i\delta\rangle$. The X_M marginal of this mechanical Schrödinger-cat state contains oscillations on a scale smaller than the ground state. The convolution scales the amplitude of these oscillations by $\exp(-\frac{2\delta^2}{\chi^2+1})$ and thus for small χ they become difficult to resolve in the optical phase noise distribution. Shown in Fig. 2 are marginals of the mechanical state $|\psi_\delta\rangle$ and the optical phase distributions that would be observed according to Eq. **4**. Scaling the phase distribution by using the variable P_L/χ provides an approximation to the mechanical marginals, which becomes more accurate with increasing χ and may even show the interference features in a superposition state. Indeed, the limiting case of infinite χ corresponds to a von-Neumann projective measurement of the mechanical position, such that the distribution obtained for P_L/χ becomes identical to the mechanical marginals. However, *the mechanical marginals can be recovered even for small measurement strength* χ. This recovery is achieved as follows: First, by fixing the length of the cavity the optical phase distribution can be observed without contributions from mechanical position fluctuations. This rigidity allows measurement of the convolution kernel for a particular χ (determined by the proper-

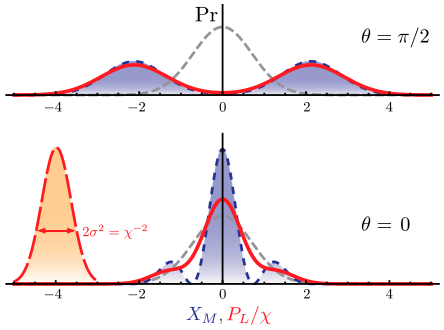

Fig. 2. The scheme presented here provides an experimentally feasible means to obtain direct access to the marginals of a quantum state of a mechanical resonator. Shown are complementary quadrature marginals of the mechanical coherent state superposition $|\psi_\delta\rangle \propto |i\delta\rangle + |-i\delta\rangle$, for $\delta = 1.5$ (blue dashed lines with fill, plotted with X_M). The mechanical ground state is shown for comparison in gray dashed lines. The two population components are seen for the quadrature angle $\theta = \pi/2$ and the quantum interference fringes for $\theta = 0$. A coherent optical pulse is used to probe the mechanical state where its phase quadrature becomes the convolution between the intrinsic phase noise, with variance scaling with χ^{-2}, and the mechanical marginal (red solid lines, plotted with P_L/χ where $\chi = 2$), see Eq. **4**. The convolution kernel can be observed by using a fixed length cavity, shown in the $\theta = 0$ plot (red dashed line with fill, fixed length with $X_M = -4$), which allows for accurate recovery of the mechanical marginals even for a weak measurement strength χ.

PHYSICS

ties of the mechanical resonator of interest, cavity geometry, and pulse strength, see Eq. **14**). With χ and the kernel known one can then perform deconvolution to determine the mechanical marginals. The performance of such a deconvolution is limited by experimental noise in the calibration of χ and the measurement of $\Pr(P_L)$. However, it is expected that these quantities can be accurately measured as quantum noise limited detection is readily achieved.

Mechanical Quantum State Engineering and Characterization

We now discuss how the measurement affects the mechanical state. First, we consider Υ acting on a mechanical coherent state $|\beta\rangle$. By casting the exponent of Υ in a normal ordered form, one can show that the resulting mechanical state, which is conditioned on measurement outcome P_L, is $\mathcal{N}_\beta \Upsilon|\beta\rangle = S(r)D(\mu_\beta)|0\rangle$. Here, $\mathcal{N}_\beta$ is a β-dependent normalization, D is the displacement operator for $\mu_\beta = (\sqrt{2}\beta + i\Omega + \chi P_L)/\sqrt{2(\chi^2+1)}$, and S is the squeezing operator, which yields the position width $2\sigma^2_{X_M} = e^{-2r} = (\chi^2+1)^{-1}$.

In most experimental situations, the initial mechanical state is in a thermal state $\rho_{\bar{n}} = \frac{1}{\pi\bar{n}}\int d^2\beta e^{-|\beta|^2/\bar{n}}|\beta\rangle\langle\beta|$, quantified by its average phonon occupation number $\bar{n}$. The marginals of the resulting state after the action of Υ are

$$\langle X_M|e^{-i\theta n}\Upsilon\rho_{\bar{n}}\Upsilon^\dagger e^{i\theta n}|X_M\rangle \propto \exp\left[-\frac{(X_M - \langle X_M^\theta\rangle)^2}{2\sigma_\theta^2}\right], \quad [5]$$

where

$$\langle X_M^\theta\rangle = \frac{\chi P_L}{\chi^2 + \frac{1}{1+2\bar{n}}}\cos(\theta) - \Omega\sin(\theta),$$
$$\sigma_\theta^2 = \frac{1}{2}\frac{\cos^2(\theta)}{\chi^2 + \frac{1}{1+2\bar{n}}} + \frac{1}{2}(\chi^2 + 1 + 2\bar{n})\sin^2(\theta) \quad [6]$$

are the mean and variance of the resulting conditional state, respectively. For large initial occupation (provided thermal fluctuations are negligible during the short interaction), the resultant position quadrature of the mechanics has mean $\langle X_M^{\theta=0}\rangle \simeq P_L/\chi$ and width $2\sigma^2_{\theta=0} \simeq \chi^{-2}$. Thus, squeezing in the X_M quadrature below the ground state is obtained when $\chi > 1$ and is *independent of the initial thermal occupation of the mechanics.* We have thus shown how the remarkable behavior of quantum measurement (also used in refs. 18–20, 44–47) can be experimentally applied to a mechanical resonator for quantum state preparation.

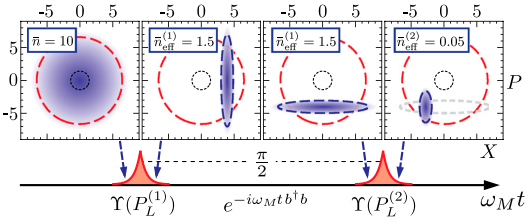

Fig. 3. Wigner functions of the mechanical state (above) at different times (indicated by arrows) during the experimental protocol (below). From left: Starting with an initial thermal state $\bar{n} = 10$, (this is chosen to ensure the figure dimensions are reasonable,) a pulsed measurement is made with $\chi = 1.5$ and outcome $P_L^{(1)} = 4\chi$ obtained, which yields an X_M quadrature squeezed state. The mechanical state evolves into a P_M quadrature squeezed state following free harmonic evolution of 1/4 of a mechanical period prior to a second pulse with outcome $P_L^{(2)} = -3\chi$ yielding the high-purity mechanical squeezed state. The effective thermal occupation of the mechanical states during the protocol is indicated. The final state's occupation can be reduced below unity even for large initial occupation, see Eq. **7** of the main text. Dashed lines indicate the 2σ-widths and the dotted lines show the ground state ($\bar{n} = 0$) for comparative purposes. The displacement Ω is not shown.

There is currently significant interest in the preparation of low entropy states of mechanical resonators as a starting point for quantum experiments, e.g., refs. 22, 23, 27, 28. The two main methods being pursued in optomechanics (11–13) are "passive cooling" which requires the stable operation of a (usually cryogenically compatible) high-finesse cavity, and "active cooling" which requires precision measurement and feedback. Closer in spirit to the latter, our pulsed measurement scheme provides a third method to realize high-purity states of the mechanical resonator. We quantify the state purity after measurement via an effective mechanical thermal occupation $\tilde{n}_{\rm eff}$, which we define through $1 + 2\tilde{n}_{\rm eff} = \sqrt{4\sigma^2_{\theta=0}\sigma^2_{\theta=\pi/2}}$. When acting on an initial thermal state, the measurement dramatically reduces uncertainty in the X_M quadrature, but leaves the thermal noise in the P_M quadrature unchanged: use of Eq. **6** for $\bar{n} \gg 1$ yields $\tilde{n}^{(1)}_{\rm eff} \simeq \sqrt{\bar{n}/2\chi^2}$. The purity can be further improved by a second pulse, which is maximized for pulse separation $\theta = \omega_M t = \pi/2$, where the initial uncertainty in the momentum becomes the uncertainty in position. Such a sequence of pulses[‡] is represented in Fig. 3, where the resulting state was obtained akin to Eq. **5**. The effective occupation of the final state after two pulses is

$$\tilde{n}^{(2)}_{\rm eff} \simeq \frac{1}{2}\left(\sqrt{1 + \frac{1}{\chi^4}} - 1\right), \quad [7]$$

which is also independent of initial occupation. For $\chi > 1$, $\tilde{n}^{(2)}_{\rm eff}$ is well below unity and therefore this scheme can be used as an alternative to "cooling via damping" for mechanical state purification.

Following state preparation, one can use a subsequent "read-out" pulse after an angle of mechanical free evolution θ to perform tomography. During state preparation however, the random measurement outcomes will result in random mechanical means Eq. **6**. This randomness can be overcome by recording and utilizing the measurement outcomes. One can achieve unconditional state preparation with use of appropriate displacement prior to the read-out pulse. Or, use postselection to analyze states prepared within a certain window. Alternatively, one may compensate during data analysis by appropriately adjusting each measurement outcome obtained during read-out. We now look at the latter option and consider a Gaussian mechanical state prepared by a prior pulsed measurement. The position distribution has variance σ^2 to be characterized and has a known mean $\langle X_M^{(p)}\rangle$, which is dependent upon the random measurement outcome. The read-out pulse will then have the distribution $\Pr(P_L) \propto \exp[(-(P_L - \chi\langle X_M^{(p)}\rangle)^2)/(1 + \chi^2 2\sigma^2)]$. For each read-out pulse, by taking $P_L|_p = P_L - \chi\langle X_M^{(p)}\rangle$ one can obtain the conditional variance $\sigma^2_{P_L|_p}$ for all θ to characterize the noise of the prepared Gaussian state. We note that this concept of compensating for a random but known mean can also be used to characterize non-Gaussian states.

Experimental Feasibility

We now provide a route for experimental implementation, discussing potential limitations and an experimentally feasible parameter regime. To ensure that the interaction time be much less than mechanical time scales the cavity decay rate κ must be much larger than the mechanical frequency. To this end, we consider the use of optical microcavities operating at $\lambda = 1{,}064$ nm, length 4λ and finesse of 7,000, which have an amplitude decay rate $\kappa/2\pi \simeq 2.5$ GHz. Such short cavity devices incorporating a micro-

[‡]We note that strong squeezing of an oscillator can also be achieved by using rapid modifications to the potential at quarter period intervals (48). However, we would like to emphasize that the squeezing we are discussing here does not arise from a parametric process, see e.g., ref. 49, rather it is due to the nonunitary action of measurement.

mechanical element as one of the cavity mirrors have previously been fabricated for tunable optical filters, vertical-cavity surface-emitting lasers and amplifiers (see for example ref. 50), but are yet to be considered for quantum optomechanical applications. Typically, these devices employ plane-parallel geometries, which places a severe constraint on the minimum lateral dimensions of the suspended mirror structure in order to minimize diffraction losses (51). Geometries using curved mirrors are required to reduce diffraction losses for the practical realization of high-finesse cavities. Presently, all realizations use a curved suspended mirror, see e.g., refs. 52, 53. However, in order to allow for enhanced freedom in the construction of the mechanical resonator, particularly with respect to the development of ultra-low loss mechanical devices (54), a flat suspended mirror is desired. In Fig. 4 our proposed fabrication procedure for such a device is shown. The small-mode-volume cavity considered here provides the bandwidth necessary to accommodate the short optical pulses and additionally offers a large optomechanical coupling rate. One technical challenge associated with these microcavities is fabrication with sufficient tolerance to achieve the desired optical resonance (under the assumption of a limited range of working wavelength), however this can be overcome by incorporating electrically controlled tunability of the cavity length (50, 52, 53).

For a mechanical resonator with eigenfrequency $\omega_M/2\pi =$ 500 kHz and effective mass $m = 10$ ng, the mechanical ground-state size is $x_0 = \sqrt{\hbar/m\omega_M} \simeq 1.8$ fm and optomechanical coupling proceeds at $g_0/2\pi = \omega_c(x_0/\sqrt{2}L)/2\pi \simeq 86$ kHz, where ω_c is the mean cavity frequency and L is the mean cavity length. The primary limitation in measurement strength is the optical intensity that can be homodyned before photodetection begins to saturate. Using pulses of mean photon number $N_p = 10^8$, which can be homodyned, yields $\Omega \simeq 10^4$ for the mean momentum transfer[§] and $\chi \simeq 1.5$. For this χ, the action of a single pulse on a large thermal state reduces the mechanical variance to $\sigma^2_{X_M} \simeq 0.2$, i.e., less than half the width of the ground state. With a second pulse after mechanical evolution the effective occupation [7] is $\bar{n}^{(2)}_{\rm eff} \simeq 0.05$.

In order to observe mechanical squeezing, i.e., $\sigma^2_{X_M} < 1/2$, the conditional variance must satisfy $\sigma^2_{P_{L|p}} < \sigma^2_{P^{\rm in}_L} + \chi^2/2$, where additional noise sources that do not affect the mechanical state, e.g., detector noise, can be subsumed into $\sigma^2_{P^{\rm in}_L}$. It is therefore necessary to have an accurate experimental calibration of χ to quantify the mechanical width. (Similarly, Ω must also be accurately known to determine the conditional mean, see Eq. **6**). This calibration can be performed in the laboratory as follows: For a fixed length cavity and a given pulse intensity, the length of the cavity is adjusted by a known amount (by a calibrated piezo for example) and the proportionality between the homodyne measurement outcomes and the cavity length is determined. The pulses are then applied to a mechanical resonator and χ is determined with knowledge of x_0 of the resonator. With χ known Ω can then also be measured by observing the displacement of the mechanical state after one-quarter of a period.

Finally we discuss practical limitations. Firstly, finite mechanical evolution during the interaction decreases the back-action-evading nature of the measurement, which is described in the *Appendix*. Such evolution is not expected to be a severe limitation in the proposed implementation considered here as $\omega_M/\kappa \simeq 10^{-4}$. Secondly, the optical measurement efficiency η, affected by optical loss, inefficient detection, and mode mismatch, yields a reduced measurement strength $\chi \to \sqrt{\eta}\chi$. And thirdly, in many situations coupling to other mechanical vibrational modes is expected. This coupling contributes to the measurement outcomes and yields a spurious broadening of the tomographic results for the mode of interest. In practice however, one can minimize these contributions by engineering mechanical devices with high effective masses for the undesired modes and tailoring the intensity profile of the optical spot to have good overlap with a particular vibrational profile (55).

[§]This momentum is comparable to the width of a thermal state, i.e., $\Omega/\sqrt{\bar{n}} < 10$ for room temperature. Thus the mechanical motion remains harmonic.

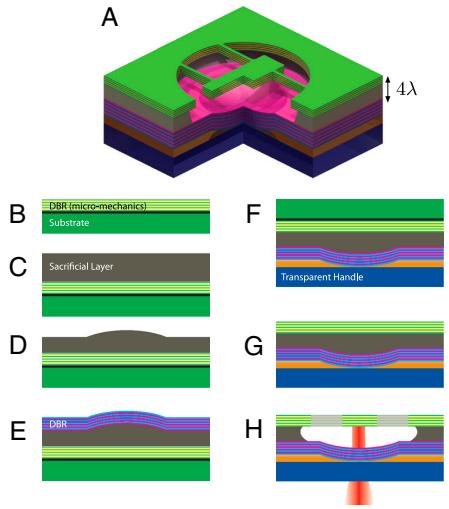

Fig. 4. Our proposed design and fabrication procedure for high-finesse optomechanical microcavities: Using microcavities provides optomechanical coupling rates many orders of magnitude larger than current millimeter or centimeter length scale implementations of optomechanical Fabry-Pérot cavities and can provide sufficient radiation-pressure interaction to resolve the small scale quantum properties of the mechanical resonator. (*A*) Cross-sectional view with a quarter of the device removed. Uppermost (colored green) is the mechanical resonator supported by auxiliary beams as was considered in ref. 54. The optical field is injected into the device from below through a transparent handle (colored blue) and the curved rigid input mirror (colored pink) and then resonates in the vacuum-gap between this and the mechanical device before being retroreflected. The design is a layered structure, fabricated in the following steps: (*B*) The base consists of a high-reflectivity distributed Bragg reflector (DBR) and an etch stop layer deposited on a suitable handle substrate. (*C*) First, a sacrificial film is deposited atop the DBR. (*D*) Next, a microlens pattern is transferred into the sacrificial layer through a reflow and reactive ion etching process. The radius of curvature of this structure is designed to match the phase front of the optical mode to minimize diffraction loss. (*E*) Following the microlens fabrication process a high reflectivity dielectric DBR is deposited over the sample surface. (*F*) The structure is then flipped and bonded to a transparent handle using a suitable low-absorption adhesive (e.g., spin on glass or UV-curable epoxy). (*G*) After mounting, the original growth substrate and etch stop are removed via chemo-mechanical etching. (*H*) Finally, the mechanical resonator is patterned and subsequently released via selective removal of the underlying sacrificial film. We remark that these integrated structures provide a platform for "on-chip" hybridization with other quantum systems.

Coupling to a Thermal Bath

For our tomography scheme the mechanical quantum state must not be significantly perturbed during the time scale ω_M^{-1}. To estimate the effect of the thermal bath following state preparation we consider weak and linear coupling to a Markovian bath of harmonic oscillators. For this model, assuming no initial correlations between the mechanics and the bath, the rethermalization scales with $\bar{n}\gamma_M$, where γ_M is the mechanical damping rate. It follows that an initially squeezed variance ($\chi > 1$) will increase to 1/2 on a time scale

$$\tau = \frac{Q}{\bar{n}\omega_M}\frac{1}{2}\left(1 - \frac{1}{\chi^2}\right). \qquad [8]$$

Thus, for the parameters above and mechanical quality $Q = \omega_M/\gamma_M \simeq 10^5$ a temperature $T \lesssim 1$ K is required for the observation of squeezing during one mechanical period.

The state purification protocol, as shown in Fig. 3, is affected by rethermalization between the two pulsed measurements. This thermal process increases the effective thermal occupation and [7] is modified to

$$\tilde{n}^{(2)}_{\rm eff}(T) \simeq \frac{1}{2}\left(\sqrt{1+\frac{1}{\chi^4}+\frac{\pi\tilde{n}}{Q\chi^2}}-1\right). \quad [9]$$

For the above system parameters $\tilde{n}^{(2)}_{\rm eff}(T = 1\ {\rm K}) \simeq 0.15$. Thus, mechanical state purification by measurement is readily attainable even at a modest bath temperature.

Moreover, we note that the position measurements of this scheme can be used to probe open system dynamics and thus provide an empirical means to explore decoherence and bath coupling models (56).

Conclusions

We have described a scheme to overcome the current challenge of quantum state reconstruction of a mechanical resonator, which provides a means to explore quantum mechanical phenomena on a macroscopic scale. Our experimental protocol allows for state purification, remote preparation of a mechanical squeezed state, and direct measurements of the mechanical marginals for quantum state reconstruction, thus providing a complete experimental framework. The experimental feasibility has been analyzed and we have shown that with the use of optomechanical microcavities this scheme can be readily implemented. The optomechanical entanglement generated by the pulsed interaction may also be a useful resource for quantum information processing. Moreover, the framework we have introduced can be built upon for further applications in quantum optomechanics and can be generalized to other systems, such as nanoelectromechanics and superconducting resonators, or used with dispersive interaction to study the motional state of mechanical membranes, trapped ions, or particles in a cavity.

Appendix

Model. The intracavity optomechanical Hamiltonian in the rotating frame at the cavity frequency is

$$H = \hbar\omega_M b^\dagger b - \hbar g_0 a^\dagger a(b+b^\dagger), \quad [10]$$

where a (b) is the optical (mechanical) field operator. The cavity field accumulates phase in proportion to the mechanical position and is driven by resonant radiation via the equation of motion

$$\frac{{\rm d}a}{{\rm d}t} = ig_0(b+b^\dagger)a - \kappa a + \sqrt{2\kappa}a_{\rm in}, \quad [11]$$

where κ is the cavity decay rate and $a_{\rm in}$ describes the optical input including drive and vacuum. During a pulsed interaction of time scale $\kappa^{-1} \ll \omega_M^{-1}$ the mechanical position is approximately constant. This constancy allows decoupling of Eq. **11** from the corresponding mechanical equation of motion and during the short interaction we have ${\rm d}b/{\rm d}t \simeq ig_0a^\dagger a$, where we neglect the mechanical harmonic motion, mechanical damping, and noise processes. We write $a_{\rm in}(t) = \sqrt{N_p}\alpha_{\rm in}(t) + \tilde{a}_{\rm in}(t)$, where $\alpha_{\rm in}(t)$ is the slowly varying envelope of the drive amplitude with $\int {\rm d}t\alpha^2_{\rm in} = 1$ and N_p is the mean photon number per pulse and similarly $a = \sqrt{N_p}\alpha(t) + \tilde{a}(t)$. Neglecting $ig_0(b+b^\dagger)\tilde{a}$ and approximating α as real, Eq. **11** becomes the pair of linear equations:

$$\frac{{\rm d}\alpha}{{\rm d}t} = \sqrt{2\kappa}\alpha_{\rm in} - \kappa\alpha, \quad [12]$$

$$\frac{{\rm d}\tilde{a}}{{\rm d}t} = ig_0\sqrt{N_p}(b+b^\dagger)\alpha + \sqrt{2\kappa}\tilde{a}_{\rm in} - \kappa\tilde{a}. \quad [13]$$

After solving for $\tilde{a}(t)$, the output field is then found by using the input-output relation $\tilde{a}_{\rm out} = \sqrt{2\kappa}\tilde{a} - \tilde{a}_{\rm in}$.

The mechanical position and momentum quadratures are $X_M = (b+b^\dagger)/\sqrt{2}$ and $P_M = i(b^\dagger - b)/\sqrt{2}$, respectively, the cavity (and its input/output) quadratures are similarly defined via $\tilde{a}$ ($\tilde{a}_{\rm in}/\tilde{a}_{\rm out}$). The statistics of the optical amplitude quadrature are unaffected by the interaction, however, the phase quadrature contains the phase dependent upon the mechanical position. The output phase quadrature emerging from the cavity is $P^{\rm out}_L(t) = \frac{g_0}{\kappa}\sqrt{N_p}\varphi(t)X^{\rm in}_M + 2\kappa e^{-\kappa t}\int^t_{-\infty}{\rm d}t' e^{\kappa t'}P^{\rm in}_L(t') - P^{\rm in}_L(t)$, where $\varphi(t) = (2\kappa)^{\frac{1}{2}}e^{-\kappa t}\int^t_{-\infty}{\rm d}t' e^{\kappa t'}\alpha(t')$ describes the accumulation of phase, $X^{\rm in}_M$ is the mechanical position prior to the interaction, and the last two terms are the input phase noise contributions. $P^{\rm out}_L$ is measured via homodyne detection, i.e., $P_L = \sqrt{2}\int {\rm d}t\alpha_{\rm LO}(t)P^{\rm out}_L(t)$. To maximize the measurement of the mechanical position the local oscillator envelope is chosen as $\alpha_{\rm LO}(t) = \mathcal{N}_\varphi\varphi(t)$, where $\mathcal{N}_\varphi$ ensures normalization. The contribution of $X^{\rm in}_M$ in P_L scales with $\chi = \sqrt{2}\frac{1}{\mathcal{N}_\varphi}\frac{g_0}{\kappa}\sqrt{N_p}$, which quantifies the mechanical position measurement strength. The mean and variance of P_L are given in Eq. **1** for pure Gaussian optical input and together with Ω and Eq. **2** are used to determine Υ, as given in Eq. **3**. We have thus arrived, for our physical setting, at an operator which is known from generalized linear measurement theory (see for example ref. 57). Also, we note that Eq. **3** is equivalent to $\Upsilon = e^{i\Omega X_M}\langle P_L|e^{i\chi X_L X_M}|0\rangle$, though the nonunitary process of cavity filling and decay is not explicit. We also remark that the construction of Υ can be readily generalized to include non-Gaussian operations.

The maximum χ is obtained for the input drive $\alpha_{\rm in}(t) = \sqrt{\kappa}e^{-\kappa|t|}$. This maximization can be seen by noting that $\mathcal{N}_\varphi^{-2} = \int {\rm d}t\varphi^2(t)$, which in Fourier space is $\mathcal{N}_\varphi^{-2} \propto \int {\rm d}\omega(\omega^2+\kappa^2)^{-2}|\alpha_{\rm in}(\omega)|^2$. Hence, for such cavity-based measurement schemes, the optimal drive has Lorentzian spectrum. This drive, $\alpha(t)$ obtained from Eq. **12** and the local oscillator are shown in Fig. 1*B*. The resulting optimal measurement strength is given by

$$\chi = 2\sqrt{5}\frac{g_0}{\kappa}\sqrt{N_p}, \quad [14]$$

and the mean momentum transfer due to α^2 is $\Omega = \frac{3}{\sqrt{2}}\frac{g_0}{\kappa}N_p$.

We note that this optimization of the driving field may also be applied to cavity-enhanced pulsed measurement of the spin of an atomic ensemble (18, 19, 58) or the coordinate of a trapped ion/particle (59–61). Particularly in the latter case, this approach will broaden the repertoire of measurement techniques available and may lead to some interesting applications.

Finite Mechanical Evolution During Interaction. In the model used above we have assumed that the mechanical position remains constant during the pulsed optomechanical interaction. Including finite mechanical evolution, the intracavity field dynamics Eq. **13** must be determined simultaneously with the mechanical dynamics. In the mechanical rotating frame with the conjugate quadratures $\overline{X}_M, \overline{P}_M$ these dynamics are solved to first order in ω_M/κ resulting in the input-output relations:

$$\overline{P}^{\rm out}_M = \overline{P}^{\rm in}_M + \Omega + \mathcal{N}_1\chi X_{C1},$$

$$\overline{X}^{\rm out}_M = \overline{X}^{\rm in}_M - \frac{\omega_M}{\kappa}\xi_1\Omega - \frac{\omega_M}{\kappa}\chi\mathcal{N}_2X_{C2},$$

$$P_L = P^{\rm in}_L + \chi(\overline{X}^{\rm in}_M + \frac{\omega_M}{\kappa}\xi_2\overline{P}^{\rm in}_M) + \chi\frac{\omega_M}{\kappa}\xi_3\Omega + \chi^2\frac{\omega_M}{\kappa}\mathcal{N}_3X_{C3}, \quad [15]$$

where P_L still represents the measurement outcome, $\mathcal{N}_{1,2,3}$ and $\xi_{1,2,3}$ are input drive-dependent dimensionless parameters of order unity, the former normalizing the nonorthogonal amplitude quadrature temporal modes $X_{C1,2,3}$. The main effects of the finite mechanical evolution can be seen in P_L. (*i*) The mechanical quadrature measured has been rotated, which in terms of the nonrotating quadratures is $\widetilde{X}_M \simeq X_M + \frac{\omega_M}{\kappa}\xi_2P_M$. Such a rotation poses no principle limitation to our scheme however this must be taken

into account for the measurement of a particular mechanical quadrature. (*ii*) Each pulsed measurement now has a nonzero mean proportional to Ω. This mean can be experimentally characterized and appropriately subtracted from the outcomes. (*iii*) P_L now includes a term proportional to the optical amplitude noise. This term decreases the back-action evading quality of the measurement and has arisen due to mechanical momentum noise gained from the optical amplitude quadrature evolving into position noise. The conditional variance of the rotated mechanical quadrature including these effects, for large initial occupation, is

$$\sigma^2_{\tilde{X}_M} \simeq \frac{1}{2}\left[\frac{1}{\chi^2} + \zeta^2\chi^2\left(\frac{\omega_M}{\kappa}\right)^2\right], \qquad [16]$$

where ζ is another drive-dependent parameter of order unity. The two competing terms here give rise to a minimum variance of $\zeta\omega_M/\kappa$ when $\chi^2 = \kappa/(\zeta\omega_M)$. Experimentally reasonable values of χ will lie much below this optimum point, however, as $\kappa \gg \omega_M$ for the parameters we consider, the broadening due to finite evolution is small and strong squeezing can be achieved.

ACKNOWLEDGMENTS. The kind hospitality provided by the University of Gdańsk (I.P.), the University of Queensland (M.R.V.) and the University of Vienna (G.J.M.) is acknowledged. We thank S. Hofer, N. Kiesel and M. Żukowski for useful discussion. We thank the Australian Research Council (ARC) (Grant FF0776191), United Kingdom Engineering and Physical Sciences Research Council (EPSRC) and the Royal Society, European Research Council (ERC) (StG QOM), European Commission (MINOS, Q-ESSENCE), Foundational Questions Institute (FQXi), Fonds zur Förderung der wissenschaftlichen Forschung (FWF) (L426, P19570, SFB FoQuS, START), Centre for Quantum Engineering and Space-Time Research (QUEST), and an ÖAD/MNiSW program for support. M.R.V. and I.P. are members of the FWF Doctoral Programme CoQuS (W 1210). M.R.V. is a recipient of a DOC fellowship of the Austrian Academy of Sciences. G.D.C. is a recipient of a Marie Curie Fellowship of the European Commission.

1. Zurek WH (2003) Decoherence, einselection, and the quantum origins of the classical. *Rev Mod Phys* 75:715–775.
2. Ghirardi GC, Rimini A, Weber T (1986) Unified dynamics for microscopic and macroscopic systems. *Phys Rev D* 34:470–491.
3. Diosi L (1989) Models for universal reduction of macroscopic quantum fluctuations. *Phys Rev A* 40:1165–1174.
4. Pearle P (1989) Combining stochastic dynamical state-vector reduction with spontaneous localization. *Phys Rev A* 39:2277–2289.
5. Penrose R (1996) On gravity's role in quantum state reduction. *Gen Relat Gravit* 28:581–600.
6. Hackermüller L, Hornberger K, Brezger B, Zeilinger A, Arndt M (2004) Decoherence of matter waves by thermal emission of radiation. *Nature (London)* 427:711–714.
7. Bose S, Jacobs K, Knight PL (1997) Preparation of nonclassical states in cavities with a moving mirror. *Phys Rev A* 56:4175–4186.
8. Bose S, Jacobs K, Knight PL (1999) Scheme to probe the decoherence of a macroscopic object. *Phys Rev A* 59:3204–3210.
9. Marshall W, Simon C, Penrose R, Bouwmeester D (2003) Towards quantum superpositions of a mirror. *Phys Rev Lett* 91:130401.
10. Kleckner D, et al. (2008) Creating and verifying a quantum superposition in a micro-optomechanical system. *New J Phys* 10:095020.
11. Kippenberg TJ, Vahala KJ (2008) Cavity optomechanics: back-action at the mesoscale. *Science* 321:1172–1176.
12. Marquardt F, Girvin S (2009) Optomechanics. *Physics* 2:40.
13. Aspelmeyer M, Groeblacher S, Hammerer K, Kiesel N (2010) Quantum optomechanics throwing a glance. *J Opt Soc Am B* 27:A189.
14. Smithey DT, Beck M, Raymer MG, Faridani A (1993) Measurement of the Wigner distribution and the density matrix of a light mode using optical homodyne tomography: application to squeezed states and the vacuum. *Phys Rev Lett* 70:1244–1247.
15. Lvovsky AI, Raymer MG (2009) Continuous-variable optical quantum-state tomography. *Rev Mod Phys* 81:299–332.
16. Leibfried D, et al. (1996) Experimental determination of the motional quantum state of a trapped atom. *Phys Rev Lett* 77:4281–4285.
17. Leibfried D, Blatt R, Monroe C, Wineland D (2003) Quantum dynamics of single trapped ions. *Rev Mod Phys* 75:281–324.
18. Kuzmich A, Mandel L, Bigelow NP (2000) Generation of spin squeezing via continuous quantum nondemolition measurement. *Phys Rev Lett* 85:1594–1597.
19. Appel J, et al. (2009) Mesoscopic atomic entanglement for precision measurements beyond the standard quantum limit. *Proc Natl Acad Sci USA* 106:10960–10965.
20. Deléglise S, et al. (2008) Reconstruction of non-classical cavity field states with snapshots of their decoherence. *Nature (London)* 455:510–514.
21. Armour A, Blencowe M, Schwab K (2002) Entanglement and decoherence of a micromechanical resonator via coupling to a cooper-pair box. *Phys Rev Lett* 88:148301.
22. Rocheleau T, et al. (2010) Preparation and detection of a mechanical resonator near the ground state of motion. *Nature (London)* 463:72–75.
23. O'Connell AD, et al. (2010) Quantum ground state and single-phonon control of a mechanical resonator. *Nature (London)* 464:697–703.
24. Rabl P, Shnirman A, Zoller P (2004) Generation of squeezed states of nanomechanical resonators by reservoir engineering. *Phys Rev B* 70:205304.
25. Tittonen I, et al. (1999) Interferometric measurements of the position of a macroscopic body: towards observation of quantum limits. *Phys Rev A* 59:1038–1044.
26. Briant T, Cohadon PF, Pinard M, Heidmann A (2003) Optical phase-space reconstruction of mirror motion at the attometer level. *Eur Phys J D* 22:131–140.
27. Groeblacher S, et al. (2009) Demonstration of an ultracold micro-optomechanical oscillator in a cryogenic cavity. *Nature Physics* 5:485–488.
28. Schliesser A, Arcizet O, Riviere R, Anetsberger G, Kippenberg TJ (2009) Resolved-sideband cooling and position measurement of a micromechanical oscillator close to the Heisenberg uncertainty limit. *Nature Physics* 5:509–514.
29. Teufel JD, Donner T, Castellanos-Beltran MA, Harlow JW, Lehnert KW (2009) Nanomechanical motion measured with an imprecision below that at the standard quantum limit. *Nat Nanotechnol* 4:820–823.
30. Anetsberger G, et al. (2010) Measuring nanomechanical motion with an imprecision below the standard quantum limit. *Phys Rev A* 82:061804(R).
31. Clerk AA, Girvin SM, Marquardt F, Schoelkopf RJ (2010) Introduction to quantum noise, measurement, and amplification. *Rev Mod Phys* 82:1155–1208.
32. Zhang J, Peng K, Braunstein S (2003) Quantum-state transfer from light to macroscopic oscillators. *Phys Rev A* 68:013808.
33. Woolley M, Doherty A, Milburn G, Schwab K (2008) Nanomechanical squeezing with detection via a microwave cavity. *Phys Rev A* 78:062303.
34. Singh S, Meystre P (2010) Atomic probe Wigner tomography of a nanomechanical system. *Phys Rev A* 81:041804(R).
35. Marek P, Filip R (2010) Noise-resilient quantum interface based on quantum nondemolition interactions. *Phys Rev A* 81:042325.
36. Braginsky VB, Vorontsov YI, Khalili FY (1978) Optimal quantum measurements in detectors of gravitation radiation. *JETP Lett+* 27:276–280.
37. Braginsky VB, Khalili FY (1992) *Quantum Measurement* (Cambridge University Press, United Kingdom).
38. Vyatchanin SP, Matsko AB (1993) Quantum limit on force measurements. *JETP Lett+* 77:218–221.
39. Mueller-Ebhardt H, et al. (2009) Quantum-state preparation and macroscopic entanglement in gravitational-wave detectors. *Phys Rev A* 80:043802.
40. Miao H, et al. (2010) Probing macroscopic quantum states with a sub-Heisenberg accuracy. *Phys Rev A* 81:012114.
41. Romero-Isart O, et al. (2011) Optically levitating dielectrics in the quantum regime: theory and protocols. *Phys Rev A* 83:013803.
42. Vogel K, Risken H (1989) Determination of quasiprobability distributions in terms of probability distributions for the rotated quadrature phase. *Phys Rev A* 40:2847–2849.
43. Dunn TJ, Walmsley IA, Mukamel S (1995) Experimental determination of the quantum-mechanical state of a molecular vibrational mode using fluorescence tomography. *Phys Rev Lett* 74:884–887.
44. Levenson MD, Shelby RM, Reid M, Walls DF (1986) Quantum nondemolition detection of optical quadrature amplitudes. *Phys Rev Lett* 57:24732476.
45. La Porta A, Slusher RE, Yurke B (1989) Back-action evading measurements of an optical field using parametric down conversion. *Phys Rev Lett* 62:28–31.
46. Roch J-F, et al. (1997) Quantum nondemolition measurements using cold trapped atoms. *Phys Rev Lett* 78:634–637.
47. Hammerer K, Aspelmeyer M, Polzik ES, Zoller P (2009) Establishing Einstein-Poldosky-Rosen channels between nanomechanics and atomic ensembles. *Phys Rev Lett* 102:020501.
48. Janszky J, Adam P (1992) Strong squeezing by repeated frequency jumps. *Phys Rev A* 46:6091–6092.
49. Walls DF (1983) Squeezed states of light. *Nature (London)* 306:141–146.
50. Cole GD, Behymer E, Bond TC, Goddard LL (2008) Short-wavelength MEMS-tunable VCSELs. *Opt Express* 16:16093–16103.
51. Riazi A (1981) Resonator equation relating Fresnel number, finesse, and number of beam transits. *Appl Optics* 20:3469–3470.
52. Tayebati P, et al. (1998) Half-symmetric cavity tunable microelectromechanical VCSEL with single spatial mode. *IEEE Photonic Tech L* 10:1679–1681.
53. Riemenschneider F, Aziz M, Halbritter H, Sagnes I, Meissner P (2002) Low-cost electrothermally tunable optical microcavities based on GaAs. *IEEE Photonic Tech L* 14:1566–1568.
54. Cole GD, Wilson-Rae I, Werbach K, Vanner MR, Aspelmeyer M (2010) Phonon-tunnelling dissipation in mechanical resonators. *Nature Communications* 2:231.
55. Pinard M, Hadjar Y, Heidmann A (1999) Effective mass in quantum effects of radiation pressure. *Eur Phys J D* 7:107–116.
56. Breuer H-P, Petruccione F (2002) *The Theory of Open Quantum Systems* (Oxford University Press, United Kingdom).
57. Caves CM, Milburn GJ (1987) Quantum-mechanical model for continuous position measurements. *Phys Rev A* 36:5543–5555.
58. Teper I, Vrijsen G, Lee J, Kasevich MA (2008) Backaction noise produced via cavity-aided nondemolition measurement of an atomic clock state. *Phys Rev A* 78:051803(R).
59. Jost JD, et al. (2009) Entangled mechanical oscillators. *Nature (London)* 459:683–685.
60. Chang DE, et al. (2010) Cavity opto-mechanics using an optically levitated nanosphere. *Proc Natl Acad Sci USA* 107:1005–1010.
61. Romero-Isart O, Juan ML, Quidant R, Cirac JI (2010) Toward quantum superposition of living organisms. *New J Phys* 12:033015.

5.2 Probing Planck-scale physics with quantum optics

One of the main ideas and results developed in my PhD is to show that the pulsed opto-mechanical scheme can be used for the study of quantum gravity phenomenology. In collaboration with the group of M. Aspelmeyer and M. S. Kim, we show that pulsed opto-mechanics provides a means to probe possible deformations of the canonical commutator, predicted in some models of quantum gravity phenomenology. The general argument for such a deformation is that a possible minimal length-scale is inconsistent with Heisenberg's uncertainty relation, which allows for arbitrary precise position measurements. Therefore the uncertainty relation is supplemented with an additional restriction on position. Such a modified uncertainty is found in many different models of quantum gravity, and can be phenomenologically incorporated into current quantum theory by modifying the canonical commutator. The resulting effects that were studied so far, such as modified spectra of atoms, were too small to be experimentally observable.

In our work we show that using pulsed opto-mechanics one can experimentally test such models for the center-of-mass of the resonator even if the commutator deformation is merely on the Planck-scale. The scheme builds upon the ability to precisely measure the phase of the light and utilizes a specifically chosen sequence of interactions that enhances the effect. A single pulse interacts with the mechanics four times, each interaction separated by a quarter mechanical period. The resulting unitary is independent of the mechanics and implements an optical self-Kerr-nonlinearity. However, possible commutator deformations of the mechanics are imprinted onto this operation and cause higher order non-linearities of the light. A strong optical light field can therefore enhance the small effect of the deformation, and the signal is imprinted onto the phase of the light as an additional perturbation. Depending on the model of commutator deformations, a different effect on the phase is expected, with a specific parameter-dependence that can be probed. It is shown that such a setup can reach unprecedented sensitivity even with current opto-mechanical setups. It therefore opens the route for table-top tests of some possible quantum gravitational predictions. Most importantly, the work shows that quantum control of massive, novel quantum systems can be very powerful in testing possible limits of our current physical theories.

I made leading contributions to all aspects of the research project.

nature physics

ARTICLES

PUBLISHED ONLINE: 18 MARCH 2012 | DOI: 10.1038/NPHYS2262

Probing Planck-scale physics with quantum optics

Igor Pikovski[1,2]*, Michael R. Vanner[1,2], Markus Aspelmeyer[1,2], M. S. Kim[3]* and Časlav Brukner[2,4]

One of the main challenges in physics today is to merge quantum theory and the theory of general relativity into a unified framework. Researchers are developing various approaches towards such a theory of quantum gravity, but a major hindrance is the lack of experimental evidence of quantum gravitational effects. Yet, the quantization of spacetime itself can have experimental implications: the existence of a minimal length scale is widely expected to result in a modification of the Heisenberg uncertainty relation. Here we introduce a scheme to experimentally test this conjecture by probing directly the canonical commutation relation of the centre-of-mass mode of a mechanical oscillator with a mass close to the Planck mass. Our protocol uses quantum optical control and readout of the mechanical system to probe possible deviations from the quantum commutation relation even at the Planck scale. We show that the scheme is within reach of current technology. It thus opens a feasible route for table-top experiments to explore possible quantum gravitational phenomena.

It is at present an open question whether our underlying concepts of space–time are fully compatible with those of quantum mechanics. The ongoing search for a quantum theory of gravity is therefore one of the main challenges in modern physics. A major difficulty in the development of such theories is the lack of experimentally accessible phenomena that could shed light on the possible route for quantum gravity. Such phenomena are expected to become relevant near the Planck scale, that is, at energies on the order of the Planck energy $E_{\rm P} = 1.2 \times 10^{19}$ GeV or at length scales near the Planck length $L_{\rm P} = 1.6 \times 10^{-35}$ m, where space–time itself is assumed to be quantized. However, such a minimal length scale is not a feature of quantum theory. The Heisenberg uncertainty relation, one of the cornerstones of quantum mechanics[1], states that the position x and the momentum p of an object cannot be simultaneously known to arbitrary precision. Specifically, the indeterminacies of a joint measurement of these canonical observables are always bound by $\Delta x \Delta p \geq \hbar/2$. Yet, the uncertainty principle still allows for an arbitrarily precise measurement of only one of the two observables, say position, at the cost of our knowledge about the other (momentum). In stark contrast, in many proposals for quantum gravity the Planck length constitutes a fundamental bound below which position cannot be defined. It has therefore been suggested that the uncertainty relation should be modified to take into account such quantum gravitational effects[2]. In fact, the concept of a generalized uncertainty principle is found in many approaches to quantum gravity, for example in string theory[3,4], in the theory of doubly special relativity[5,6], within the principle of relative locality[7] and in studies of black holes[8–10]. A generalized uncertainty relation also follows from a deformation of the underlying canonical commutator $[x,p] \equiv xp - px$ (refs 11–15), as they are related via $\Delta x \Delta p \geq (1/2)|\langle [x,p] \rangle|$.

Preparing and probing quantum states at the Planck scale is beyond today's experimental possibilities. Current approaches to test quantum gravitational effects mainly focus on high-energy scattering experiments, which operate still 15 orders of magnitude away from the Planck energy $E_{\rm P}$, or on astronomical observations[16,17], which have not found any evidence of quantum gravitational effects as of yet[18,19]. Another route would be to perform high-sensitivity measurements of the uncertainty relation, as any deviations from standard quantum mechanics are, at least in principle, experimentally testable[13–15]. However, with the best position measurements being of order $\Delta x/L_{\rm p} \sim 10^{17}$ (refs 20,21), at present sensitivities are still insufficient and quantum gravitational corrections remain unexplored.

Here we propose a scheme that circumvents these limitations. Our scheme allows one to test quantum gravitational modifications of the canonical commutator in a novel parameter regime, thereby reaching a hitherto unprecedented sensitivity in measuring Planck-scale deformations. The main idea is to use a quantum optical ancillary system that provides a direct measurement of the canonical commutator of the centre of mass of a massive object. In this way Planck-scale accuracy of position measurements is not required. Specifically, the commutator of a very massive quantum oscillator is probed by a sequence of interactions with a strong optical field in an optomechanical setting, which uses radiation pressure inside an optical cavity[22,23]. The sequence of optomechanical interactions is used to map the commutator of the mechanical resonator onto the optical pulse. The optical field experiences a measurable change that depends on the commutator of the mechanical system and that is nonlinearly enhanced by the optical intensity. Observing possible commutator deformations thus reduces to a measurement of the mean of the optical field, which can be performed with very high accuracy by optical interferometric techniques. We show that, already with state-of-the art technology, tests of Planck-scale deformations of the commutator are within experimental reach.

Modified commutation relations

A common modification of the Heisenberg uncertainty relation that appears in a vast range of approaches to quantum gravity[2–4,24,25] is $\Delta x \Delta p \geq \hbar(1 + \beta_0(\Delta p/(M_{\rm P}c))^2)/2$. Here, β_0 is a numerical parameter that quantifies the modification strength, c is the speed of light and $M_{\rm P} \simeq 22\,\mu$g is the Planck mass. The minimal measurable length scale appears as a natural consequence with $\Delta x_{\rm min} = L_{\rm P}\sqrt{\beta_0}$ (Fig. 1). Such a modification alters the allowed state-space and can

[1]Vienna Center for Quantum Science and Technology (VCQ), Boltzmanngasse 5, A-1090 Vienna, Austria, [2]Faculty of Physics, University of Vienna, Boltzmanngasse 5, A-1090 Vienna, Austria, [3]Quantum Optics and Laser Science (QOLS) group, Blackett Laboratory, Imperial College London, SW7 2BW, UK, [4]Institute for Quantum Optics and Quantum Information (IQOQI), Austrian Academy of Sciences, Boltzmanngasse 3, A-1090 Vienna, Austria.
*e-mail: igor.pikovski@univie.ac.at; m.kim@imperial.ac.uk.

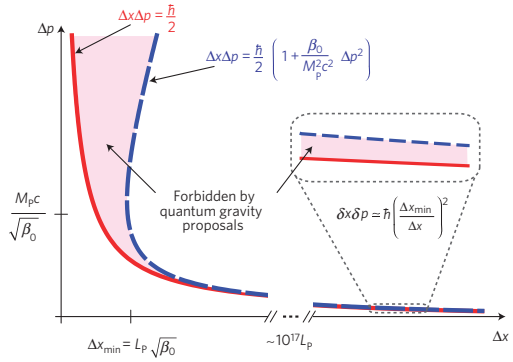

Figure 1 | The quantum uncertainty relation and a quantum gravitational modification. The minimum Heisenberg uncertainty (red curve) is plotted together with a modified uncertainty relation (dashed blue curve) with modification strength β_0. M_P and L_P are the Planck mass and Planck length, respectively. The shaded region represents states that are allowed in regular quantum mechanics but are forbidden in theories of quantum gravity that modify the uncertainty relation. The inset shows the two curves far from the Planck scale at typical experimental position uncertainties $\Delta x \gg \Delta x_{\min}$. An experimental precision of $\delta x \delta p$ is required to distinguish the two curves, which is beyond experimental possibilities at present. However, this can be overcome by our scheme, which allows one to probe the underlying commutation relation in massive mechanical oscillators and its quantum gravitational modifications.

be seen as a manifestation of a deformed canonical commutator, for example of the form[12]

$$[x,p]_{\beta_0} = i\hbar\left(1+\beta_0\left(\frac{p}{M_P c}\right)^2\right) \quad (1)$$

So far, no effect of a modified canonical commutator has been observed in experiments. At present the best available measurement precision (Table 1) allows one to put an upper bound on the magnitude of the deformation of $\beta_0 < 10^{33}$ (ref. 13). For theories that modify the commutator this rules out the existence of an intermediate fundamental length scale on the order of $x \sim 10^{-19}$ m. Note that the Planck-scale modifications correspond to $\beta_0 \sim 1$ and are therefore untested. Furthermore, the above modification of the commutator is not unique and experiments can, in principle, distinguish between the various theories. In particular, a generalized version of the commutator deformation is[11]

$$[x,p]_{\mu_0} = i\hbar\sqrt{1+2\mu_0\frac{(p/c)^2+m^2}{M_P^2}} \quad (2)$$

Here, m is the rest mass of the particle and μ_0 is again a free numerical parameter. For small masses $m \ll p/c \lesssim M_P$, and for $\mu_0 = \beta_0$, the above modified commutator reduces to equation (1). However, an important difference is that the commutation relation in equation (2) depends directly on the rest mass of the particle. In the limit $p/c \ll m \lesssim M_P$, the commutator reduces to $[x,p]_{\mu_0} \approx i\hbar(1+\mu_0 m^2/M_P^2)$, which can be seen as a mass-dependent rescaling of $\hbar$. It is worth noting that a modified, mass-dependent Planck constant $\hbar = \hbar(m)$ also appears in other theories, some of which predict that the value of Planck's constant can decrease with increasing mass ($\hbar \to 0$ for $m \gg M_P$), in contrast to the prediction above. Such a reduction would also account for a transition to classicality in massive systems or at energies close to the Planck energy[6,10].

Table 1 | Current experimental bounds on quantum gravitational commutator deformations.

System/experiment	$\beta_{0,\max}$	$\gamma_{0,\max}$	References
Position measurement	10^{34}	10^{17}	20,21
Hydrogen Lamb shift	10^{36}	10^{10}	13,15
Electron tunnelling	10^{33}	10^{11}	13,15

The parameters β_0 and γ_0 quantify the deformation strengths of the modification given in equation (1) and of the modification given in equation (3), respectively. For electron tunnelling an electric current measurement precision of $\delta I \sim 1$ fA was taken.

Among the various proposals for different commutator deformations, we choose as a last example the recently proposed commutator[14] which also accounts for a maximum momentum that is present in several approaches to quantum gravity[5,6]

$$[x,p]_{\gamma_0} = i\hbar\left(1-\gamma_0\frac{p}{M_P c}+\gamma_0^2\left(\frac{p}{M_P c}\right)^2\right) \quad (3)$$

Here, γ_0 is again a free numerical parameter that characterizes the strength of the modification. Experimental bounds on γ_0 are more stringent than in the case of equation (1) and were considered in ref. 15. The best bound at present can be obtained from Lamb shift measurements in hydrogen, which yield $\gamma_0 \lesssim 10^{10}$ (Table 1).

The strength of the modifications in all the discussed examples depends on the mass of the system. For a harmonic oscillator in its ground state the minimum momentum uncertainty is given by $p_0 = \sqrt{\hbar m \omega_m}$, where m is the mass of the oscillator and ω_m is its angular frequency. The deformations are therefore enhanced in massive quantum systems. We note that theories of deformed commutators have an intrinsic ambiguity as to which degrees of freedom it should apply to for composite systems (see Supplementary Information). For the centre of mass mode, the mass dependence of the deformations suggests that using massive quantum systems allows easier experimental access to the possible deformations of the commutator, provided that precise quantum control can be attained. Optomechanical systems, where the oscillator mass can be around the Planck mass and even larger, therefore offer a natural test-bed for probing commutator deformations of its centre of mass mode.

Scheme to measure the deformations

In the following we will outline a quantum optical scheme that allows one to measure deformations of the canonical commutator of a mechanical oscillator with unprecedented precision. For simplicity we use dimensionless quadrature operators X_m and P_m. They are related to the position and momentum operators via $x = x_0 X_m$ and $p = p_0 P_m$, where $x_0 = \sqrt{\hbar/(m\omega_m)}$ and $p_0 = \sqrt{\hbar m \omega_m}$.

The scheme relies on displacements of the massive mechanical oscillator in phase space, where the displacement operator is given by[26] $D(z/\sqrt{2}) = e^{i(\mathrm{Re}[z]X_m - \mathrm{Im}[z]P_m)}$. The action of this operator displaces the mean position and momentum of any state by $\mathrm{Im}[z]$ and $\mathrm{Re}[z]$, respectively. In quantum mechanics, two subsequent displacements provide an additional phase to the state, which can be used to engineer quantum gates[27–29]. Here we consider displacements of the mechanical resonator that are induced by an ancillary quantum system, the optical field, with an interaction strength λ. A sequence of four optomechanical interactions is chosen such that the mechanical state is displaced around a loop in phase space, described by the four-displacement operator

$$\xi = e^{i\lambda n_L P_m} e^{-i\lambda n_L X_m} e^{-i\lambda n_L P_m} e^{i\lambda n_L X_m} \quad (4)$$

In classical physics, after the whole sequence, neither of the two systems would be affected because the four operations cancel each other. However, for non-commuting X_m and P_m there is a change in the optical field depending on the commutator $[X_m, P_m] = iC_1$. We can rewrite equation (4) using the well-known relation[30] $e^{aX_m} P_m e^{-aX_m} = \sum_{k=0}^{\infty} (i^k a^k/k!) C_k$, where $iC_k = [X_m, C_{k-1}]$ and $C_0 = P_m$. This yields $\xi = \exp(-i\lambda n_L \sum_k (\lambda n_L)^k C_k/k!)$, which depends explicitly on the commutation relation for the oscillator, but not on the commutator of the optical field. For the quantum mechanical commutator, that is $C_1 = 1$, we obtain $\xi = e^{-i\lambda^2 n_L^2}$. In this case, the optical field experiences a self-Kerr nonlinearity, that is an n_L^2 operation, and the mechanical state remains unaffected. However, any deformations of the commutator would show in ξ, resulting in an observable effect in the optical field.

As an example we consider the modification given by equation (1). To first order in $\beta \equiv \beta_0 \hbar \omega_m m/(M_P c)^2 \ll 1$ one obtains $C_1 = 1 + \beta P_m^2$, $C_2 \approx \beta 2 P_m$, $C_3 \approx 2\beta$ and $C_k \approx 0$ for $k \geq 4$. Equation (4) thus becomes $\xi_\beta = e^{-i\lambda^2 n_L^2} e^{-i\beta(\lambda^2 n_L^2 P_m^2 + \lambda^3 n_L^3 P_m + (1/3)\lambda^4 n_L^4)}$ (this approximation has the physical meaning that one can neglect contributions which are higher order in β for the observables considered below). As one can see immediately, a deformed commutator affects the optical field differently owing to non-vanishing nested commutators $C_k, k > 1$. In addition to a Kerr-type nonlinearity the optical field experiences highly non-Gaussian n_L^3 and n_L^4 operations. The additional effect scales with β and therefore allows a direct measure of the deformations of the canonical commutator of the mechanical system via the optical field. To see that explicitly, let us denote the optical field by a_L, with the real and imaginary parts representing its measurable amplitude and phase quadratures, respectively. Also, for simplicity, we restrict the discussion to coherent states $|\alpha\rangle$ with real amplitudes of the optical input field and we neglect possible deformations in the commutator of the optical field during read-out[31,32] as those are expected to be negligible compared with the deformations of the massive mechanical oscillator (see refs 33,34 for schemes that can probe the non-commutativity of the optical field). For a large average photon number $N_p \gg 1$, and for a mechanical thermal state with mean phonon occupation $\bar{n} \ll \lambda N_p$, the mean of the optical field becomes (for $|\Theta| \ll 1$):

$$\langle a_L \rangle \simeq \langle a_L \rangle_{qm} e^{-i\Theta} \tag{5}$$

where $\langle a_L \rangle_{qm} = \alpha e^{-i\lambda^2 - N_p(1 - e^{-i2\lambda^2})}$ is the quantum mechanical value for the unmodified dynamics. The β-induced contribution causes an additional displacement in phase space by

$$\Theta(\beta) \simeq \frac{4}{3} \beta N_p^3 \lambda^4 e^{-i6\lambda^2} \tag{6}$$

The resulting optical state is represented in Fig. 2. We note that the magnitude of the effect is enhanced by the optical intensity and the interaction strength. For the μ- and the γ-deformation of the commutator, referring to equations (2) and (3), respectively, the effect on the optical field is similar, but shows a different scaling with the system parameters (see Table 2 and Supplementary Information for the derivation). Probing deviations from the quantum mechanical commutator of the massive oscillator thus boils down to a precision measurement of the mean of the optical field, which can be achieved with very high accuracy via interferometric means, such as homodyne detection.

Experimental implementation

We now discuss a realistic experimental scenario that can attain sufficient sensitivity to resolve the deformation-induced change in the optical field even for small values of β_0, μ_0 and γ_0, that is in a regime that can be relevant for quantum gravity.

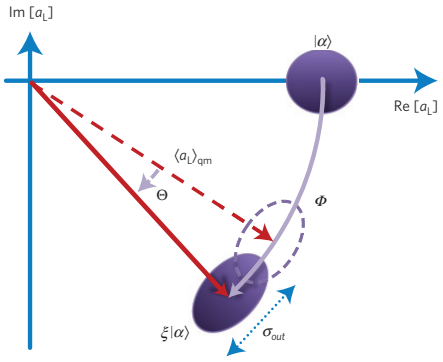

Figure 2 | Changes to the optical field following the pulsed optomechanical interactions. The effect of the four-displacement operation ξ onto an optical state for the experimentally relevant case $\lambda \ll 1$. In this case, an initial optical coherent state $|\alpha\rangle$ is rotated in phase-space through an angle Φ. A part Θ of the rotation is due to a possible quantum gravitational deformation of the canonical commutator of the mechanical resonator (see equation (6)). Measuring the mean of the optical field $\langle a_L \rangle$ and extracting the Θ-contribution allows one to probe deformations of the canonical commutator. Optical interferometric schemes can provide a measurement of the overall mean rotation with a fundamental imprecision $\delta\langle\Phi\rangle = \sigma_{out}/\sqrt{N_p N_r}$, ($N_r$: number of measurement runs, N_p: number of photons, σ_{out}: quadrature width of the optical state, which remains very close to the coherent state value 1/2). To resolve the Θ-contribution, the measurement imprecision must fulfill $\delta\langle\Phi\rangle < \Theta$, which we show can be achieved in quantum optomechanical systems even for deformations on the Planck scale.

The optomechanical scheme proposed here can achieve such a regime: it combines the ability to coherently control large masses with strong optical fields. From a more general perspective, optomechanical systems provide a promising avenue for preparing and investigating quantum states of massive objects ranging from a few picograms up to several kilograms[22,23]. Significant experimental progress has been recently made towards this goal, including laser cooling of nano- and micromechanical devices into their quantum ground state[35,36], operation in the strong-coupling regime[37–39] and coherent interactions[39,40]. Owing to their high mass they have also been proposed for tests of so-called collapse models[41,42], which predict a breakdown of the quantum mechanical superposition principle for macroscopic objects. For our purpose here, which is the high-precision measurement of the canonical commutator of a massive oscillator, we focus on the pulsed regime of quantum optomechanics[43].

We consider the set-up depicted in Fig. 3, where a mechanical oscillator is coupled to the optical input pulse via radiation pressure inside a high-finesse optical cavity. This is described by the intra-cavity Hamiltonian[44] $H = \hbar\omega_m n_m - \hbar g_0 n_L X_m$, where n_m is the mechanical number operator and $g_0 = \omega_c(x_0/L)$ is the optomechanical coupling rate with the mean cavity frequency ω_c and mean cavity length L. For sufficiently short optical pulses the mechanical harmonic evolution can be neglected and the intracavity dynamics can be approximated by the unitary operation $U = e^{i\lambda n_L X_m}$ (ref. 43). Here, the effective interaction strength is (see Supplementary Information) $\lambda \simeq g_0/\kappa = 4\mathcal{F}x_0/\lambda_L$, where κ is the optical amplitude decay rate, $\mathcal{F}$ is the cavity finesse and λ_L is the optical wavelength. To realize the desired displacement operation in phase-space it is also required to achieve a direct optomechanical coupling, with the same optical pulse, to the mechanical momentum (equation (4)). Such a momentum

Table 2 | Experimental parameters to measure quantum gravitational deformations of the canonical commutator.

$[X_m, P_m]$	Equation (2)	Equation (3)	Equation (1)
$\lvert\Theta\rvert$	$\mu_0 \frac{32\hbar\mathcal{F}^2 m N_p}{M_P^2 \lambda_L^2 \omega_m}$	$\gamma_0 \frac{96\hbar^2\mathcal{F}^3 N_p^2}{M_P c \lambda_L^3 m \omega_m}$	$\beta_0 \frac{1024\hbar^3\mathcal{F}^4 N_p^3}{3M_P^2 c^2 \lambda_L^4 m \omega_m}$
$\mathcal{F}$	10^5	2×10^5	4×10^5
m	10^{-11} kg	10^{-9} kg	10^{-7} kg
$\omega_m/2\pi$	10^5 Hz	10^5 Hz	10^5 Hz
λ_L	1,064 nm	1,064 nm	532 nm
N_p	10^8	5×10^{10}	10^{14}
N_r	1	10^5	10^6
$\delta\langle\Phi\rangle$	10^{-4}	10^{-8}	10^{-10}

The parameters are chosen such that a precision of $\delta\mu_0 \sim 1$, $\delta\gamma_0 \sim 1$ and $\delta\beta_0 \sim 1$ can be achieved, which amounts to measuring Planck-scale deformations.

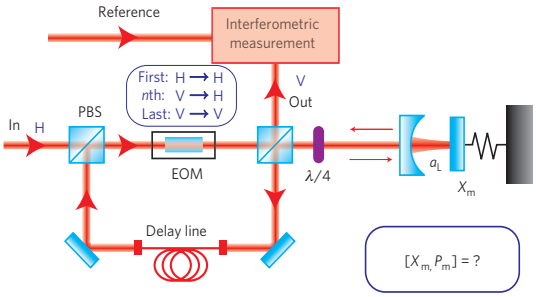

Figure 3 | Proposed experimental set-up to probe deformations of the canonical commutator of a macroscopic mechanical resonator. An incident pulse 'In' is transmitted through a polarizing beam splitter (PBS) and an electro-optic modulator (EOM) and then interacts with a mechanical resonator with position X_m via a cavity field a_L. The optical field is retro-reflected from the optomechanical system and then enters a delay line, during which time the mechanical resonator evolves for one quarter of a mechanical period. The optical pulse, now vertically polarized, is rotated by the EOM to be horizontally polarized and interacts again with the mechanical resonator. This is repeated for a total of four interactions, such that the canonical commutator of the resonator is mapped onto the optical field. Finally, the EOM does not rotate the polarization and the pulse exits in the mode labelled 'Out', where it is then measured interferometrically with respect to a reference field such that the commutator deformations can be determined with very high accuracy.

coupling could be achieved for example via the Doppler effect by using mirrors with a strongly wavelength-dependent optical reflectivity[45]. A more straightforward route is to use the harmonic evolution of the mechanical resonator between pulse round-trips (for example, ref. 43), which effectively allows X_m and P_m to be interchanged after a quarter of the oscillator period. In this case, the contribution from the commutator deformation has a different pre-factor, but remains of the same form (see Supplementary Information), and part of the phase-space rotation in the optical field is of classical nature. This has no effect on the ability to distinguish and observe the rotation due to the deformed commutator. After the four-pulse interaction has taken place the optical field can be analysed in an interferometric measurement, which yields the phase information of the light with very high precision.

As in previous approaches to measure possible modifications of the canonical commutator[13,15], the relevant question is which ultimate resolution $\delta\beta_0$, $\delta\mu_0$, $\delta\gamma_0$ the experiments can provide. In the case of a null result, these numbers would set an experimental bound for β_0, μ_0, γ_0 and hence provide an important empirical feedback for theories of quantum gravity. We restrict our analysis to the experimentally relevant case $\lambda < 1$, for which the effect of a deformed commutator resembles a pure phase-space rotation of the optical output state by angle Φ (Fig. 2). The inaccuracy $\delta\Phi$ of the measurement outcome depends on the quantum noise σ_{out} of the outgoing pulse along the relevant generalized quadrature and can be further reduced by quantum estimation protocols[46]. For our purposes we only require to measure the mean optical field, equation (5). The precision of this measurement is not fundamentally limited and is enhanced by the strength of the field and the number of experimental runs N_r via $\delta\langle\Phi\rangle = \sigma_{out}/\sqrt{N_p N_r}$, from which one directly obtains the fundamental resolutions $\delta\beta_0$, $\delta\mu_0$, $\delta\gamma_0$. For each of the discussed deformations it is possible to find a realistic parameter regime (Table 2) with markedly improved performance compared with existing bounds. In particular, we assume a mechanical oscillator of frequency $\omega_m/2\pi = 10^5$ Hz and mass $m = 10^{-11}$ kg, and an optical cavity of finesse $\mathcal{F} = 10^5$ at a wavelength of $\lambda_L = 1{,}064$ nm, which is in the range of current experiments[37,47–50]. To test a μ-modified commutator (equation (2)), a pulse sequence of mean photon-number $N_p = 10^8$ is sufficient to obtain a resolution $\delta\mu_0 \sim 1$ already in a single measurement run ($N_r = 1$). For the case of a γ-modified commutator (equation (3)), the same sequence would result in $\delta\gamma_0 \sim 10^9$. By increasing the photon-number to $N_p = 5\times10^{10}$, the finesse to $\mathcal{F} = 2\times10^5$ and the number of measurement runs to $N_r = 10^5$ (this would require stabilizing the experiment on a timescale of the order of seconds) one obtains $\delta\gamma_0 \sim 1$. Note that this would improve the existing bounds for γ_0 (ref. 15) by ten orders of magnitude. To obtain similar bounds for a β-modification is more challenging. The pulse sequence with the previous parameters yields $\delta\beta_0 \sim 10^{12}$, which already constitutes an improvement by about 20 orders of magnitude compared with the current bound for β_0 (ref. 13). This can provide experimental access to a possible intermediate length-scale or a meaningful feedback to theories of quantum gravity in the case of a null result. By further pushing the parameters to $N_p = 10^{14}$, $N_r = 10^6$, $\mathcal{F} = 4\times10^5$, $m = 10^{-7}$ kg and $\lambda_L = 532$ nm it is even possible to reach $\delta\beta_0 \sim 1$, that is, a regime where Planck-scale deformations are relevant and 33 orders of magnitude beyond current experiments. To achieve such experimental parameters is challenging, but is well within the reach of current technology.

The above considerations refer to the ideal case in which experimental noise sources can be neglected. Effects such as mechanical damping and distortions of the effective interaction strength impose additional requirements on the experimental parameters, which are discussed in detail in the Supplementary Information. In summary, being able to neglect the effects of pulse shape distortion and optical loss requires that the mechanical mode is optically cooled close to a thermal occupation of about $\bar{n} < 30$. Similarly, decoherence effects are negligible when the whole mechanical system is in a bath of temperature $T < 100$ mK for resonators with a quality factor of $Q > 10^6$, which can be achieved with dilution refrigeration. In general, the scheme is very robust against many noise sources, as it relies on the measurement of the mean of the optical field and the noise sources can be isolated by independent measurements. We also note that contributions from a modified commutator scale in a different way with the system parameters as compared with deleterious effects. It is therefore possible to distinguish these by varying the relevant parameters, such as optical intensity and the oscillator mass. The proposed scheme thus offers a feasible route to probe the possible effects of quantum gravity in a table-top quantum optics experiment and hence to provide important empirical feedback for theories of quantum gravity.

Received 4 November 2011; accepted 13 February 2012; published online 18 March 2012; corrected online 26 March 2012 and 10 April 2012

References

1. Heisenberg, W. Über den anschaulichen Inhalt der quantentheoretischen Kinematik und Mechanik. *Z. Phys.* **43,** 172–198 (1927).
2. Garay, L. G. Quantum gravity and minimum length. *Int. J. Mod. Phys.* **A10,** 145–165 (1995).
3. Amati, D., Ciafaloni, M. & Veneziano, G. Superstring collisions at planckian energies. *Phys. Lett. B* **197,** 81–88 (1987).
4. Gross, D. J. & Mende, P. F. String theory beyond the Planck scale. *Nucl. Phys. B* **303,** 407–454 (1988).
5. Amelino-Camelia, G. Doubly special relativity: First results and key open problems. *Int. J. Mod. Phys. D* **11,** 1643–1669 (2002).
6. Magueijo, J. & Smolin, L. Generalized Lorentz invariance with an invariant energy scale. *Phys. Rev. D* **67,** 044017 (2003).
7. Amelino-Camelia, G., Freidel, L., Kowalski-Glikman, J. & Smolin, L. Principle of relative locality. *Phys. Rev. D* **84,** 084010 (2011).
8. Maggiore, M. A generalized uncertainty principle in quantum gravity. *Phys. Lett. B* **304,** 65–69 (1993).
9. Scardigli, F. Generalized uncertainty principle in quantum gravity from micro-black hole gedanken experiment. *Phys. Lett. B* **452,** 39–44 (1999).
10. Jizba, P., Kleinert, H. & Scardigli, F. Uncertainty relation on a world crystal and its applications to micro black holes. *Phys. Rev. D* **81,** 084030 (2010).
11. Maggiore, M. The algebraic structure of the generalized uncertainty principle. *Phys. Lett. B* **319,** 83–86 (1993).
12. Kempf, A., Mangano, G. & Mann, R. B. Hilbert space representation of the minimal length uncertainty relation. *Phys. Rev. D* **52,** 1108–1118 (1995).
13. Das, S. & Vagenas, E. C. Universality of quantum gravity corrections. *Phys. Rev. Lett.* **101,** 221301 (2008).
14. Ali, A. F., Das, S. & Vagenas, E. C. Discreteness of space from the generalized uncertainty principle. *Phys. Lett. B* **678,** 497–499 (2009).
15. Ali, A. F., Das, S. & Vagenas, E. C. A proposal for testing quantum gravity in the lab. *Phys. Rev. D* **84,** 044013 (2011).
16. Amelino-Camelia, G., Ellis, J., Mavromatos, N. E., Nanopoulos, D. V. & Sarkar, S. Tests of quantum gravity from observations of gamma-ray bursts. *Nature* **393,** 763–765 (1998).
17. Jacob, U. & Piran, T. Neutrinos from gamma-ray bursts as a tool to explore quantum-gravity-induced Lorentz violation. *Nature Phys.* **7,** 87–90 (2007).
18. Abdo, A. A. *et al.* A limit on the variation of the speed of light arising from quantum gravity effects. *Nature* **462,** 331–334 (2009).
19. Tamburini, F., Cuofano, C., Della Valle, M. & Gilmozzi, R. No quantum gravity signature from the farthest quasars. *Astron. Astrophys.* **533,** A71 (2011).
20. Grote, H. & the LIGO Scientific Collaboration. The status of GEO 600. *Class. Quantum Grav.***25**, 114043 (2008).
21. Abbott, B. P. *et al.* LIGO: The Laser Interferometer Gravitational-wave Observatory. *Rep. Prog. Phys.* **72,** 076901 (2009).
22. Kippenberg, T. J. & Vahala, K. J. Cavity optomechanics: Back-action at the mesoscale. *Science* **321,** 1172–1176 (2008).
23. Aspelmeyer, M., Groeblacher, S., Hammerer, K. & Kiesel, N. Quantum optomechanics—throwing a glance. *J. Opt. Soc. Am. B* **27,** A189–A197 (2010).
24. Milburn, G. J. Lorentz invariant intrinsic decoherence. *New J. Phys.* **8,** 96 (2006).
25. Kempf, A. Information-theoretic natural ultraviolet cutoff for spacetime. *Phys. Rev. Lett.* **103,** 231301 (2009).
26. Barnett, S. M. & Radmore, P. M. *Methods in Theoretical Quantum Optics* (Oxford Univ. Press, 2002).
27. Milburn, G. J., Schneider, S. & James, D. F. V. Ion trap quantum computing with warm ions. *Fortschr. Phys.* **48,** 801–810 (2000).
28. Sørensen, A. & Mølmer, K. Entanglement and quantum computation with ions in thermal motion. *Phys. Rev. A* **62,** 022311 (2000).
29. Leibfried, D. *et al.* Experimental demonstration of a robust, high-fidelity geometric two ion-qubit phase gate. *Nature* **422,** 412–415 (2003).
30. Wilcox, R. M. Exponential operators and parameter differentiation in quantum physics. *J. Math. Phys.* **8,** 962–982 (1967).
31. Nozari, K. Some aspects of Planck scale quantum optics. *Phys. Lett. B.* **629,** 41–52 (2005).
32. Ghosh, S. & Roy, P. "Stringy" coherent states inspired by generalized uncertainty principle. Preprint at http://arxiv.org/hep-ph/11105136 (2011).
33. Parigi, V., Zavatta, A., Kim, M. S. & Bellini, M. Probing quantum commutation rules by addition and subtraction of single photons to/from a light field. *Science* **317,** 1890–1893 (2007).
34. Kim, M. S., Jeong, H., Zavatta, A., Parigi, V. & Bellini, M. Scheme for proving the bosonic commutation relation using single-photon interference. *Phys. Rev. Lett.* **101,** 260401 (2008).
35. Teufel, J. D. *et al.* Sideband cooling of micromechanical motion to the quantum ground state. *Nature* **475,** 359–363 (2010).
36. Chan, J. *et al.* Laser cooling of a nanomechanical oscillator into its quantum ground state. *Nature* **478,** 89–92 (2011).
37. Gröblacher, S., Hammerer, K., Vanner, M. R. & Aspelmeyer, M. Observation of strong coupling between a micromechanical resonator and an optical cavity field. *Nature* **460,** 724–727 (2009).
38. Teufel, J. D. *et al.* Circuit cavity electromechanics in the strong-coupling regime. *Nature* **471,** 204–208 (2011).
39. O'Connell, A. D. *et al.* Quantum ground state and single-phonon control of a mechanical resonator. *Nature* **464,** 697–703 (2010).
40. Verhagen, E., Deléglise, S., Weis, S., Schliesser, A. & Kippenberg, T. J. Quantum-coherent coupling of a mechanical oscillator to an optical cavity mode. *Nature* **482,** 63–67 (2012).
41. Marshall, W., Simon, C., Penrose, R. & Bouwmeester, D. Towards quantum superpositions of a mirror. *Phys. Rev. Lett.* **91,** 130401 (2003).
42. Romero-Isart, O. *et al.* Large quantum superpositions and interference of massive nanometer-sized objects. *Phys. Rev. Lett.* **107,** 020405 (2011).
43. Vanner, M. R. *et al.* Pulsed quantum optomechanics. *Proc. Natl Acad. Sci. USA* **108,** 16182–16187 (2011).
44. Law, C. K. Interaction between a moving mirror and radiation pressure: A Hamiltonian formulation. *Phys. Rev. A* **51,** 2537–2541 (1995).
45. Karrai, K., Favero, I. & Metzger, C. Doppler optomechanics of a photonic crystal. *Phys. Rev. Lett.* **100,** 240801 (2008).
46. Boixo, S. *et al.* Quantum-limited metrology and Bose–Einstein condensates. *Phys. Rev. A* **80,** 032103 (2009).
47. Corbitt, T. *et al.* Optical dilution and feedback cooling of a gram-scale oscillator to 6.9 mK. *Phys. Rev. Lett.* **99,** 160801 (2007).
48. Thompson, J. D. *et al.* Strong dispersive coupling of a high-finesse cavity to a micromechanical membrane. *Nature* **452,** 72–76 (2008).
49. Verlot, P., Tavernarakis, A., Briant, T., Cohadon, P-F. & Heidmann, A. Scheme to probe optomechanical correlations between two optical beams down to the quantum level. *Phys. Rev. Lett.* **102,** 103601 (2008).
50. Kleckner, D. *et al.* Optomechanical trampoline resonators. *Opt. Express* **19,** 19708–19716 (2011).

Acknowledgements

This work was supported by the Royal Society, by the Engineering and Physical Sciences Research Council, by the European Comission (Quantum InterfacES, SENsors, and Communication based on Entanglement (Q-ESSENCE)), by the European Research Council Quantum optomechanics: quantum foundations and quantum information on the micro- and nanoscale (QOM), by the Austrian Science Fund (FWF) (Complex Quantum Systems (CoQuS), START program, Special Research Programs (SFB) Foundations and Applications of Quantum Science (FoQuS)), by the Foundational Questions Institute and by the John Templeton Foundation. M.R.V. is a recipient of a DOC fellowship of the Austrian Academy of Sciences. I.P. and M.R.V are members of the FWF Doctoral Programme CoQuS and they are grateful for the kind hospitality provided by Imperial College London. The authors thank S. Das, S. Gielen, H. Grosse, A. Kempf, W. T. Kim and J. Lee for discussions.

Author contributions

I.P. and M.S.K. conceived the research, which was further developed by Č.B. and all co-authors. M.R.V. conceived the experimental scheme. M.A. analysed the feasibility of the scheme with input from all co-authors. All authors performed the research under the supervision of Č.B. and all authors wrote the manuscript.

Additional information

The authors declare no competing financial interests. Supplementary information accompanies this paper on www.nature.com/naturephysics. Reprints and permissions information is available online at www.nature.com/reprints. Correspondence and requests for materials should be addressed to I.P. or M.S.K.

CORRIGENDUM

Probing Planck-scale physics with quantum optics

Igor Pikovski, Michael R. Vanner, Markus Aspelmeyer, M. S. Kim and Časlav Brukner

Nature Physics http://dx.doi.org/10.1038/nphys2262 (2012); published online 18 March 2012; corrected online 26 March 2012.

In the version of this Article originally published online, ref. 5 should have read: Amelino-Camelia, G. Doubly special relativity: First results and key open problems. *Int. J. Mod. Phys. D* **11,** 1643–1669 (2002). This has been corrected in all versions of the Article.

CORRIGENDUM

Probing Planck-scale physics with quantum optics

Igor Pikovski, Michael R. Vanner, Markus Aspelmeyer, M. S. Kim and Časlav Brukner

Nature Physics http://dx.doi.org/10.1038/nphys2262 (2012); published online 18 March 2012; corrected online 10 April 2012.

In the version of this Article originally published online, the experimental parameters for testing equations (1) and (3) given in Table 2 and subsequently used in the text on the same page were incorrect. These errors have been corrected in all versions of the Article.

DOI: 10.1038/NPHYS2262

and $X'_m(t) = X'_m(0) + \frac{4}{3}\beta\omega_m t P'^3_m$. In the original frame, the result is thus

$$X_m(t) = X_m(0)\cos(\omega_m t) - P_m(0)\sin(\omega_m t) + \frac{4}{3}\beta\omega_m t\left(P_m(0)\cos(\omega_m t) + X_m(0)\sin(\omega_m t)\right)^3 . \tag{B.1}$$

Using four interactions separated by a quarter mechanical period, the four-displacement operator becomes $\xi = e^{i\lambda n_L(P_m - 2\beta\pi X_m^3)} e^{i\lambda n_L(-X_m - 4\beta\pi P_m^3/3)} e^{i\lambda n_L(-P_m + 2\beta\pi X_m^3/3)} e^{i\lambda n_L X_m}$. This expression can be simplified using the Zassenhaus formula [30] $\exp(X+Y) = \exp(X)\exp(Y)\prod_{i=1}^{\infty}\exp(Z_i)$, where $Z_1 = -[A,B]/2$, $Z_2 = [A,[A,B]]/6 + [B,[A,B]]/3$, $Z_3 = -\left([B,[A,[A,B]]] + [B,[B,[A,B]]]\right)/8 - [A,[A,[A,B]]]/24$ and Z_k, $k>3$ are functions of higher nested commutators. To leading order in n_L, the four-displacement operator becomes

$$\xi \simeq e^{-i\lambda^2 n_L^2}\, e^{i\beta\pi\frac{5}{3}\lambda^4 n_L^4}. \tag{B.3}$$

The optical field due to this operation is of the same form as in Eq. 5 with a modified numerical strength. The modified dynamics therefore does not alter the main conclusions.

C Additional requirements due to deleterious effects

In the following we analyze the experimental parameters necessary to overcome some additional deleterious effects in the opto-mechanical system. We analyze the cavity dynamics and its influence on the effective interaction, the effect of varying interaction strengths for each pulse round trip and the influence of mechanical decoherence. We neglect additional contributions from a modified commutator since these will be less prominent than that considered in the ideal case.

The Hamiltonian $H = \hbar\omega_m n_m - \hbar g_0 n_L X_m$ refers to the interaction between the optical field and the mechanics within the cavity [44]. To quantify the effects of cavity filling and decay for a short pulse we solve the optical Langevin equation

$$\frac{da_L}{dt} = (ig_0 X_m - \kappa)a_L + \sqrt{2\kappa}\left(a_L^{(in)} + \sqrt{N_p}\alpha_{\text{in}}\right) \tag{7}$$

with the boundary condition $a_L^{(in)} + a_L^{(out)} = \sqrt{2\kappa}a_L$ for the input and output optical fields and the incident cavity drive α_{in} that is normalized to the mean photon number per pulse, i.e. $\int \mathrm{d}t\, \alpha_{\text{in}}^2 = 1$. Since the mechanical motion can be neglected in the short pulse regime the overall effect on both the optical field and the mechanical oscillator can be described by the effective unitary operator $U = e^{i\lambda n_L X_m}$. The coupling strength λ depends on the intra-cavity field envelope and can be determined via the total momentum transfer onto the mechanics by the optical pulse $\langle P_m \rangle = g_0 \int dt\, \langle n_L(t) \rangle$, where $n_L(t)$ is obtained from Eq. 7. This yields $\lambda = \zeta\, g_0/\kappa$ with $\zeta = \int \mathrm{d}t e^{-2\kappa t}\kappa^2 \left[\int_{-\infty}^{t} \mathrm{d}t'\, e^{\kappa t'}\alpha_{\text{in}}(t')\right]^2$ for the effective unitary operator.

In general, the pulse shape of the output optical field is altered by the cavity. When such a distorted pulse is directed back for the i-th time into the cavity, the effective interaction time within the cavity will be different and will give rise to a modified opto-mechanical interaction strength λ_i. To minimize the distortion, one requires that the pulse duration τ is much longer than the intra-cavity lifetime, i.e. $\omega_m \ll \tau^{-1} \ll \kappa$, where κ is the cavity bandwidth. This ensures that the optical pulses are short

compared to the mechanical period and that the cavity is empty in between the pulsed interactions. In this regime we have $\zeta \simeq 1$ such that $\lambda \simeq g_0/\kappa$.

An additional effect that distorts the interaction strength λ from pulse to pulse is the loss of light. To include both loss and pulse shape change in the effective interaction, we define an overall distortion parameter η. With this parameter, the opto-mechanical interaction strength λ_i for the i-th interaction is approximately given by $\lambda_{i+1} = \eta\lambda_i$. We note that in the regime considered here the loss of light will be dominant and we assume a value of $\eta \sim 0.9$.

The effect of varying interaction strengths modifies the four-displacement operator to $\xi_\eta = e^{i\lambda_4 n_L P_m} \times e^{-i\lambda_3 n_L X_m} e^{-i\lambda_2 n_L P_m} e^{i\lambda_1 n_L X_m}$. Using $\lambda = \lambda_1$, it can be written as

$$\xi_\eta = \xi_0' \, e^{i\eta\lambda(1-\eta^2)n_L P_m} \, e^{i\lambda(1-\eta^2)n_L X_m} \,, \tag{8}$$

where ξ_0' is the four-displacement operator as considered previously, but with modified interaction strengths: For the β-, γ- and μ-deformations, the interaction strength is reduced to $\lambda^4 \to \eta^7\lambda$, $\lambda^3 \to \eta^5\lambda$ and $\lambda^2 \to \eta^3\lambda$, respectively. For $\eta \sim 0.9$ the $\Theta-$contribution to the optical mean by the β-modified commutator would therefore be reduced by a factor ~ 0.5, the contribution by the γ-modified commutator would be reduced by ~ 0.6 and the contribution by a μ-modified commutator would be reduced by ~ 0.7. Additionally, Eq. 8 contains a strong dependence of the outgoing optical field on the mechanical state. Given a thermal distribution of the mechanical center-of-mass mode with mean phonon occupation $\bar{n}$, the optical mean is reduced by $e^{-\bar{n}\lambda^2(1-\eta^2)(1-\eta^4)/2}$. For $\eta \sim 0.9$ and $\lambda \sim 1$, the mechanics therefore needs to be damped to $\bar{n} \lesssim 30$. This can be achieved by optical cooling of the mechanical mode, which has recently been demonstrated in Refs. [35, 36].

Finally, we discuss mechanical decoherence in between pulse interactions due to coupling of the mechanical mode to other degrees of freedom in the oscillator. We consider a linear coupling to an infinite bath of harmonic oscillators, which can be described by the interaction Hamiltonian

$$H_{int} = \sum_i \nu_i \left(b_i \, e^{-i\omega_i t} + b_i^\dagger \, e^{i\omega_i t} \right) X_m \,, \tag{9}$$

where b_i are operators for the i-th bath mode with frequency ω_i that interact with the mode of interest with interaction strength ν_i. Using the notation $B(t) = \sum_i \nu_i \left(b_i \, e^{-i\omega_i t} + b_i^\dagger \, e^{i\omega_i t} \right)$, the solutions for the position and momentum operators become

$$\begin{aligned} X_m(t) &= X_m^{(0)}(t,t_0) - \int_{t_0}^{t} \mathrm{d}t' B(t') \sin(\omega_m(t-t')) \\ P_m(t) &= P_m^{(0)}(t,t_0) + \int_{t_0}^{t} \mathrm{d}t' B(t') \cos(\omega_m(t-t')) \,, \end{aligned} \tag{10}$$

where $X_m^{(0)}(t,t_0) = \mathrm{Re}[A(t_0)e^{i\omega_m(t-t_0)}]$ and $P_m^{(0)}(t,t_0) = \mathrm{Im}[A(t_0)e^{i\omega_m(t-t_0)}]$ are the position and momentum operators without decoherence, respectively, with the initial value $A(t_0) = X_m(t_0) + iP_m(t_0)$. For a bath that is initially uncorrelated with the mechanical mode of interest, the ξ-operator changes to

$$\xi_B = \xi_0 \, e^{i\lambda n_L B_3} \, e^{i\lambda n_L B_2} \, e^{i\lambda n_L B_1} \tag{11}$$

where ξ_0 is the operator without decoherence as given in Eq. 4 and the bath degrees of freedom enter through the operators $B_1 = \int_0^{\pi/2\omega_m} dt B(t') \cos(\omega_m t)$, $B_2 = \int_0^{\pi/\omega_m} dt B(t') \sin(\omega_m t)$ and

DOI: 10.1038/NPHYS2262

$B_3 = -\int_0^{3\pi/2\omega_m} dt B(t')\cos(\omega_m t)$. We consider a Markovian bath with negligible bath correlation times such that $\langle B(t)\rangle = 0$ and $\langle B(t)B(t')\rangle = \gamma_m \coth(\hbar\omega_m/2k_BT)\delta(t-t')$, where the mechanical damping can be written in terms of the mechanical quality factor as $\gamma_m = \omega_m/Q$. To first order in T/Q the mean of the optical field becomes

$$\langle a_L\rangle_B \simeq \langle a_L\rangle_0 (1 - \lambda^2 \frac{k_B T}{\hbar\omega_m Q}), \tag{12}$$

where $\langle a_L\rangle_0$ is the mean of the optical field without decoherence. For $Q = 10^6$ one therefore requires $T \lesssim 100$ mK to keep the decoherence sufficiently weak. Such parameters can be achieved for kHz-resonators with dilution refrigeration.

5.3 Quantum interferometric visibility as a witness of general relativistic proper time

In this work, we consider how time dilation affects low energy quantum systems and show that novel phenomena arise with no counterpart in classical theory. Newtonian gravity has been shown to be fully consistent with quantum theory, as for example seen in observations of a quantum phase arising from the Newtonian gravitational potential. In our work on time dilation, conceived and conducted in collaboration with fellow PhD students M. Zych and F. Costa and our supervisor Č. Brukner, we go beyond the Newtonian limit and show how general relativistic time dilation affects quantum systems. Our results bring the interplay between quantum theory and classical general relativity into an experimentally accessible regime. In our approach we considered time dilation to lowest order as a perturbative correction to the evolution of matter-waves in a gravitational field. Due to the mass-energy equivalence, all energy contributes to the total weight of a system and gravity therefore couples also to the internal energy of a system. This is gravitational time dilation to lowest order and causes a position dependent internal evolution, also known as the redshift. Quantum mechanically, an additional phenomenon arises, which has been entirely overlooked so far and which is the core of the paper: internal oscillations entangle to the center-of-mass position of a particle. We consider matter waves with internal clocks, such as atomic clocks in atomic fountains, and show that the entanglement between the clock-states and the position causes suppression and revivals of the visibility of the interference pattern. This phenomenon can only be explained if both, quantum theory and general relativity, are taken into account.

I contributed to all aspects of the research project.

nature COMMUNICATIONS

OPEN

ARTICLE

Received 13 Jun 2011 | Accepted 5 Sep 2011 | Published 18 Oct 2011

DOI: 10.1038/ncomms1498

Quantum interferometric visibility as a witness of general relativistic proper time

Magdalena Zych[1], Fabio Costa[1], Igor Pikovski[1] & Časlav Brukner[1,2]

Current attempts to probe general relativistic effects in quantum mechanics focus on precision measurements of phase shifts in matter-wave interferometry. Yet, phase shifts can always be explained as arising because of an Aharonov–Bohm effect, where a particle in a flat space-time is subject to an effective potential. Here we propose a quantum effect that cannot be explained without the general relativistic notion of proper time. We consider interference of a 'clock'—a particle with evolving internal degrees of freedom—that will not only display a phase shift, but also reduce the visibility of the interference pattern. According to general relativity, proper time flows at different rates in different regions of space-time. Therefore, because of quantum complementarity, the visibility will drop to the extent to which the path information becomes available from reading out the proper time from the 'clock'. Such a gravitationally induced decoherence would provide the first test of the genuine general relativistic notion of proper time in quantum mechanics.

[1] Faculty of Physics, University of Vienna, Boltzmanngasse 5, 1090 Vienna, Austria. [2] Institute for Quantum Optics and Quantum Information, Austrian Academy of Sciences, Boltzmanngasse 3, 1090 Vienna, Austria. Correspondence and requests for materials should be addressed to M.Z. (email: magdalena.zych@univie.ac.at).

In the theory of general relativity, time is not a global background parameter but flows at different rates depending on the space–time geometry. Although verified to high precision in various experiments[1], this prediction (as well as any other general relativistic effect) has never been tested in the regime where quantum effects become relevant. There is, in general, a fundamental interest in probing the interplay between gravity and quantum mechanics[2]. The reason is that the two theories are grounded on seemingly different premises and, although consistent predictions can be extrapolated for a large range of phenomena, a unified framework is still missing and fundamentally new physics is expected to appear at some scale.

One of the promising experimental directions is to reveal, through interferometric measurements, the phase acquired by a particle moving in a gravitational potential[3,4]. Typically considered is a Mach–Zehnder type interferometer (Fig. 1), placed in the Earth's gravitational field, where a particle travels in a coherent superposition along the two interferometric paths γ_1, γ_2 that have different proper lengths. The two amplitudes in the superposition acquire different, trajectory-dependent phases Φ_i, $i=1,2$. In addition, the particle acquires a controllable relative phase shift φ. Taking into account the action of the first beam splitter and denoting by $|r_i\rangle$ the mode associated with the respective path γ_i, the state inside the Mach–Zehnder setup $|\Psi_{MZ}\rangle$, just before it is recombined, can be written as

$$|\Psi_{MZ}\rangle = \frac{1}{\sqrt{2}}\left(ie^{-i\Phi_1}|r_1\rangle + e^{-i\Phi_2+i\varphi}|r_2\rangle\right). \qquad (1)$$

Finally, the particle can be registered by one of the two detectors $D_\pm$ with corresponding probabilities $P_\pm$:

$$P_\pm = \frac{1}{2} \pm \frac{1}{2}\cos(\Delta\Phi + \varphi), \qquad (2)$$

where $\Delta\Phi := \Phi_1 - \Phi_2$. The phase Φ_i is proportional to the action along the corresponding (semiclassical) trajectory γ_i on which the particle moves. For a free particle on an arbitrary space–time background, the action can be written in terms of the proper time τ that elapsed during the travel, $S_i = -mc^2 \int_{\gamma_i} d\tau$. This might suggest that the measurement of $\Delta\Phi$ is an experimental demonstration of the general relativistic time dilation.

There is, however, a conceptual issue in interpreting experiments measuring a gravitationally induced phase shift as tests of the relativistic time dilation. The action S_i above can be written in terms of an effective gravitational potential on a flat space–time. Thus, all the effects resulting from such an action are fully described by the Schödinger equation with the corresponding gravitational potential and where the time evolution is given with respect to the global time. Note that a particle in a field of arbitrary nature is subject to a Hamiltonian where the potential energy is proportional to the field's charge and a position-dependent potential. Therefore, even in a homogeneous field, the particle acquires a trajectory-dependent phase although the force acting on it is the same at any point—the phase arises only because of the potential. For a homogeneous electric field, this relative phase is known as the electric Aharonov–Bohm effect[5]. The case of Newtonian gravity is directly analogous—the role of the particle's electric charge and of the Coulomb potential are taken by the particle's mass and the Newtonian gravitational potential, respectively[6]. All quantum interferometric experiments performed to date (see for example, refs 7–9) are fully explainable by this gravitational analogue of the electric Aharonov–Bohm effect. Moreover, even if one includes non-Newtonian terms in the Hamiltonian, this dichotomy of interpretations is still present. Again, one can interpret the phase shift $\Delta\Phi$ as a type of an Aharanov–Bohm phase, which a particle moving in a flat space–time acquires because of an effective, non-Newtonian, gravitational potential (at least for an effective gravitational potential arising from the typically considered Kerr or Schwarzschild space–times).

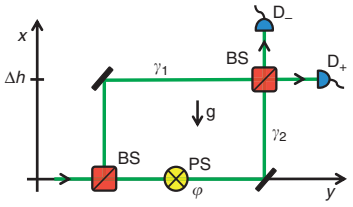

Figure 1 | Mach–Zehnder interferometer in the gravitational field. The setup considered in this work consists of two beam splitters (BS), a phase shifter (PS) and two detectors $D_\pm$. The PS gives a controllable phase difference φ between the two trajectories γ_1 and γ_2, which both lie in the $x-y$ plane. A homogeneous gravitational field (g) is oriented antiparallel to the x direction. The separation between the paths in the direction of the field is Δh. General relativity predicts that the amount of the elapsed proper time is different along the two paths. In our approach, we will consider interference of a particle (which is not in free fall) that has an evolving internal degree of freedom that acts as a 'clock'. Such an interference experiment will therefore not only display a phase shift, but also reduce the visibility of the interference pattern to the extent to which the path information becomes available from reading out the proper time of the 'clock'.

Here we predict a quantum effect that cannot be explained without the general relativistic notion of proper time and thus show how it is possible to unambiguously distinguish between the two interpretations discussed above. We consider a Mach–Zehnder interferometer placed in the gravitational potential and with a 'clock' used as an interfering particle. By 'clock' we mean some evolving internal degree of freedom of the particle. If there is a difference in proper time elapsed along the two trajectories, the 'clock' will evolve into different quantum states for the two paths of the interferometer. Because of quantum complementarity between interference and which-path information the interferometric visibility will decrease by an amount given by the which-way information accessible from the final state of the clock[10–12]. Such a reduction in the visibility is a direct consequence of the general relativistic time dilation, which follows from the Einstein equivalence principle. Seeing the Einstein equivalence principle as a corner stone of general relativity, observation of the predicted loss of the interference contrast would be the first confirmation of a genuine general relativistic effect in quantum mechanics.

One might sustain the view that the interference observed with particles without evolving degrees of freedom is a manifestation of some intrinsic oscillations associated with the particle and that such oscillations can still be seen as the ticking of a clock that keeps track of the particle's time. If any operational meaning was to be attributed to this clock, it would imply that which-way information is, in principle, accessible. One should then either assume that proper time is a quantum degree of freedom, in which case, there should be a drop in the interferometric visibility, or that the quantum complementarity relation (between which-path information and interferometric visibility) would be violated when general relativistic effects become relevant. Our proposed experiment allows to test these possibilities. The hypothesis that proper time is a degree of freedom has indeed been considered in various works[13–15].

The above considerations are also relevant in the context of the debate over ref. 16 (determination of the gravitational redshift by reinterpreting interferometric experiment[9] that measured the acceleration of free fall). It was pointed out in refs 17–20 that only states non-trivially evolving in time can be referred to as 'clocks'. In ref. 18, the interference in such a case was discussed, however, the role of the interferometric visibility as a witness of proper time in quantum mechanics and as a tool to test new hypotheses has not been previously considered.

In the present paper, we discuss an interferometric experiment in the gravitational field where the interfering particle can be operationally treated as a 'clock'. We predict that as a result of the quantum complementarity between interference and which-path information the general relativistic time dilation will cause the decrease in the interferometric visibility. The observation of such a reduction in the visibility would be the first confirmation of a genuinely general relativistic effect in quantum mechanics, in particular, it would unambiguously probe proper time as predicted by general relativity. The proposed experiment can also lead to a conclusive test of theories in which proper time is treated as a quantum degree of freedom.

Results

Which-way information from proper time. Consider an interferometric experiment with the setup as in Fig. 1, but in a situation where the particle in superposition has some internal degree of freedom that can evolve in time. In such a case, state (1) is no longer the full description of the system. Moreover, if this degree of freedom can be considered as a 'clock', according to the general relativistic notion of proper time it should evolve differently along the two arms of the interferometer in the presence of gravity. For a trajectory γ_i, let us call $|\tau_i\rangle$ the corresponding state of the 'clock'. The superposition (1) inside the interferometer now reads

$$|\Psi_{MZ}\rangle = \frac{1}{\sqrt{2}}\left(ie^{-i\Phi_1}|r_1\rangle|\tau_1\rangle + e^{-i\Phi_2+i\varphi}|r_2\rangle|\tau_2\rangle\right). \qquad (3)$$

In general, the state (3) is entangled and according to quantum mechanics interference in the path degrees of freedom should correspondingly be washed away. The reason is that one could measure the 'clock' degrees of freedom and in that way read out the accessible which-path information. Tracing out the 'clock' states in equation (3) gives the detection probabilities

$$P_{\pm} = \frac{1}{2} \pm \frac{1}{2}|\langle\tau_1|\tau_2\rangle|\cos(\Delta\Phi + \alpha + \varphi), \qquad (4)$$

where $\langle\tau_1|\tau_2\rangle = |\langle\tau_1|\tau_2\rangle|e^{i\alpha}$. When the ancillary phase shift φ is varied, the probabilities $P_{\pm}$ oscillate with the amplitude $\mathcal{V}$, called the visibility (contrast) of the interference pattern. Formally

$$\mathcal{V} := \frac{Max_{\varphi}P_{\pm} - Min_{\varphi}P_{\pm}}{Max_{\varphi}P_{\pm} + Min_{\varphi}P_{\pm}}.$$

Whereas without the 'clock' the expected contrast is always maximal (equation (2) yields $\mathcal{V}=1$), in the case of equation (4) it reads

$$\mathcal{V} = |\langle\tau_1|\tau_2\rangle|. \qquad (5)$$

The distinguishability $\mathcal{D}$ of the trajectories is the probability to correctly guess which path was taken in the two-way interferometer by measuring the degrees of freedom that serve as a which-way detector[12] (in mathematical terms it is the trace norm distance between the final states of the detectors associated with different paths). In our case, these are the 'clock' degrees of freedom and we obtain $\mathcal{D} = \sqrt{1-|\langle\tau_1|\tau_2\rangle|^2}$. The amount of the which-way information that is potentially available sets an absolute upper bound on the fringe visibility and we recover the well-known duality relation[10–12] in the form $\mathcal{V}^2 + \mathcal{D}^2 = 1$, as expected for pure states.

The above result demonstrates that general relativistic effects in quantum interferometric experiments can go beyond previously predicted corrections to the non-relativistic phase shift. When proper time is treated operationally we anticipate the gravitational time dilation to result in the reduction of the fringe contrast. This drop in the visibility is expected independently of how the proper time is measured and which system and interaction are used for the 'clock'. Moreover, when the information about the time elapsed is not physically accessible, the drop in the visibility will not occur. This indicates that the effect unambiguously arises because of the proper time as predicted by general relativity, in contrast to measurements of the phase shift alone. The gravitational phase shift occurs independently of whether the system can or cannot be operationally treated as a 'clock', just as the phase shift acquired by a system in the electromagnetic potential. Therefore, the notion of proper time is not probed in such experiments.

Massive quantum 'clock' in an external gravitational field. In the next paragraphs, we present how the above idea can be realized when the 'clock' degrees of freedom are implemented in internal states of a massive particle (neglecting the finite-size effects). Let $H_{\circlearrowleft}$ be the Hamiltonian that describes the internal evolution. In the rest reference frame, the time coordinate corresponds to the proper time τ, and the evolution of the internal states is given by $i\hbar(\partial/\partial\tau) = H_{\circlearrowleft}$. Changing coordinates to the laboratory frame, the evolution is given by $i\hbar(\partial/\partial t) = \dot{\tau}H_{\circlearrowleft}$, where $\dot{\tau} = \mathrm{d}\tau/\mathrm{d}t$ describes how fast the proper time flows with respect to the coordinate time. For a general metric $g_{\mu\nu}$, it is given by $\dot{\tau} = \sqrt{-g_{\mu\nu}\dot{x}^{\mu}\dot{x}^{\nu}}$, where we use the signature $(-+++)$ and summation over repeated indices is understood. The energy–momentum tensor of a massive particle described by the action S can be defined as the functional derivative of S with respect to the metric, that is, $T^{\mu\nu} := \delta S/\delta g_{\mu\nu}$ (see, for example, ref. 21). Since the particle's energy E is defined as the T_{00} component, it reads $E = g_{0\mu}g_{0\nu}T^{\mu\nu}$. In the case of a free evolution in a space–time with a stationary metric (in coordinates such that $g_{0j}=0$ for $j=1,2,3$), we have

$$E = mc^2\frac{-g_{00}}{\sqrt{-g_{\mu\nu}\dot{x}^{\mu}\dot{x}^{\nu}}}, \qquad (6)$$

where m is the mass of the particle. Space–time geometry in the vicinity of Earth can be described by the Schwarzschild metric. In isotropic coordinates (x,θ,ϑ) and with $\mathrm{d}\Omega^2 \equiv \mathrm{d}\theta^2 + \sin^2\theta\,\mathrm{d}\vartheta^2$ it takes the form[21]

$$c^2\mathrm{d}\tau^2 = \frac{(1+\frac{\phi(x)}{2c^2})^2}{(1-\frac{\phi(x)}{2c^2})^2}c^2\mathrm{d}t^2 - \left(1-\frac{\phi(x)}{2c^2}\right)^4\left(\mathrm{d}x^2 + x^2\mathrm{d}\Omega^2\right),$$

where $\phi(x) = -GM/x$ is the Earth's gravitational potential (G denotes the gravitational constant and M is the mass of Earth). We consider the limit of a weak field and of slowly moving particles. In the final result, we therefore keep up to quadratic terms in the kinetic and potential energy. In this approximation, the metric components read[21]

$$g_{00} \simeq -\left(1+2\frac{\phi(x)}{c^2}+2\frac{\phi(x)^2}{c^4}\right),\quad g_{ij} \simeq \frac{1}{c^2}\delta_{ij}\left(1-2\frac{\phi(x)}{c^2}\right),$$

so that

$$\dot{\tau} \simeq \sqrt{1+2\frac{\phi(x)}{c^2}+2\frac{\phi(x)^2}{c^4}-\left(\frac{\dot{x}}{c}\right)^2\left(1-2\frac{\phi(x)}{c^2}\right)}.$$

The total Hamiltonian in the laboratory frame is given by $H_{\mathrm{Lab}} = H_0 + \dot{\tau}H_{\circlearrowleft}$, where the operator H_0 describes the dynamics of the external degrees of freedom of the particle and is obtained by canonically quantizing the energy (6), that is, the particle's coordinate x and kinematic momentum $p = m\dot{x}$ become operators satisfying the canonical commutation relation $([x,p] = i\hbar)$. Thus, approximating up to the second order also in the internal energy,

$H_{\rm Lab}$ reads

$$H_{\rm Lab} \simeq mc^2 + H_{\circlearrowleft} + E_k^{GR} + \frac{\phi(x)}{c^2}\left(mc^2 + H_{\circlearrowleft} + E_{\rm corr}^{GR}\right), \qquad (7)$$

where

$$E_k^{GR} = \frac{p^2}{2m}\left(1 + 3\left(\frac{p}{2mc}\right)^2 - \frac{1}{mc^2}H_{\circlearrowleft}\right)$$

and

$$E_{\rm corr}^{GR} = \frac{1}{2}m\phi(x) - 3\frac{p^2}{2m}\,.$$

We consider a semiclassical approximation of the particle's motion in the interferometer. Therefore, all terms in $H_{\rm Lab}$, apart from the internal Hamiltonian $H_{\circlearrowleft}$, appear as purely numerical functions defined along the fixed trajectories.

In a setup as in Figure 1, the particle follows in superposition two fixed non-geodesic paths γ_1, γ_2 in the homogeneous gravitational field. The acceleration and deceleration, which the particle undergoes in the x direction, is assumed to be the same for both trajectories, as well as the constant velocity along the y axis. This assures that the trajectories have different proper length, but there will be no time dilation between the paths stemming from special relativistic effects. The particle inside the interferometer will thus be described by the superposition $|\Psi_{MZ}\rangle = \frac{1}{\sqrt{2}}\left(i|\Psi_1\rangle + e^{i\varphi}|\Psi_2\rangle\right)$, where the states $|\Psi_i\rangle$ associated with the two paths γ_i are given by applying the Hamiltonian (7) to the initial state, which we denote by $|x^{\rm in}\rangle|\tau^{\rm in}\rangle$. Up to an overall phase, these states read

$$|\Psi_i\rangle = e^{-\frac{i}{\hbar}\int_{\gamma_i} {\rm d}t \frac{\phi(x)}{c^2}\left(mc^2 + H_{\circlearrowleft} + E_{\rm corr}^{GR}\right)} |x^{\rm in}\rangle|\tau^{\rm in}\rangle. \qquad (8)$$

For a small size of the interferometer, the central gravitational potential $\phi(x)$ can be approximated to linear terms in the distance Δh between the paths:

$$\phi(R + \Delta h) = \phi(R) + g\Delta h + \mathcal{O}(\Delta h^2), \qquad (9)$$

where $g = GM/R^2$ denotes the value of the Earth's gravitational acceleration in the origin of the laboratory frame, which is at distance R from the centre of Earth.

For a particle having two internal states $|0\rangle$, $|1\rangle$ with corresponding energies E_0, E_1, the rest frame Hamiltonian of the internal degrees of freedom can be written as

$$H_{\circlearrowleft} = E_0|0\rangle\langle 0| + E_1|1\rangle\langle 1| \qquad (10)$$

and if we choose the initial state of this internal degrees to be

$$|\tau^{\rm in}\rangle = \frac{1}{\sqrt{2}}(|0\rangle + |1\rangle) \qquad (11)$$

the detection probabilities read

$$P_\pm(\varphi, m, \Delta E, \Delta V, \Delta T) = \frac{1}{2} \pm \frac{1}{2}\cos\left(\frac{\Delta E \Delta V \Delta T}{2\hbar c^2}\right)\cos\left(\left(mc^2 + \langle H_{\circlearrowleft}\rangle + \bar{E}_{\rm corr}^{GR}\right) + \frac{\Delta V \Delta T}{\hbar c^2} + \varphi\right), \qquad (12)$$

where ΔT is the time (as measured in the laboratory frame) for which the particle travels in the interferometer in a superposition of two trajectories at constant heights, $\Delta V := g\Delta h$ is the difference in the gravitational potential between the paths, $\bar{E}_{\rm corr}^{GR}$ represents the corrections $E_{\rm corr}^{GR}$ from equation (7) averaged over the two trajectories and $\Delta E := E_1 - E_0$. The expectation value $\langle H_{\circlearrowleft}\rangle$ is taken with respect to the state (11). The corresponding visibility (5) is

$$\mathcal{V} = \left|\cos\left(\frac{\Delta E \Delta V \Delta T}{2\hbar c^2}\right)\right|. \qquad (13)$$

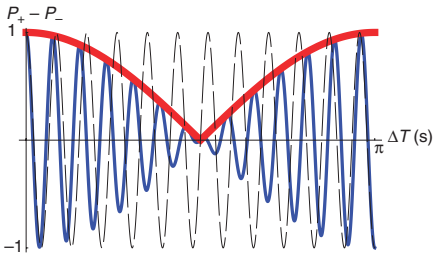

Figure 2 | Visibility of the interference pattern and the phase shift in the cases with and without the 'clock.' The plot of the difference between the probabilities $P_\pm(\varphi, m, \Delta E, \Delta V, \Delta T)$, equation (12), to find the particle in the output path of the Mach–Zehnder interferometer as a function of the time ΔT for which the particle travels in a superposition of two trajectories at constant heights (this corresponds to changing the length of the interferometric arms). The term proportional to the particle's mass is the phase originating from the Newtonian potential energy $m\Delta V$. General relativistic corrections stemming from external degrees of freedom are given by $\bar{E}_{\rm corr}^{GR}$, see for example, ref. 3. Without the 'clock' degrees of freedom, only these terms are present in the result (dashed, black line in the plot). In the situation with the 'clock' (blue line), we expect two new effects: the change of the interferometric visibility given by the absolute value of the first cosine (thick red line) and an extra phase shift proportional to the average internal energy of the 'clock'. The values for the energy gap ΔE and the gravitational potential difference ΔV between the interferometric paths are chosen such that $\Delta E \Delta V / 2\hbar c^2 = 1{\rm Hz}$. Whereas the phase shift alone can always be understood as an Aharonov–Bohm phase of an effective potential, the notion of general relativistic proper time is necessary to explain the decrease of the visibility.

The introduction of the 'clock' degrees of freedom results in two new quantum effects that cannot be explained without including general relativity: the change of the interferometric visibility and the extra phase shift proportional to the average internal energy (Fig. 2; equation (12)). The drop in the visibility is a consequence of a direct coupling of the particle's internal degrees of freedom to the potential in the effective Hamiltonian (7). Such a coupling is never found in Newtonian gravity, and it is the mathematical expression of the prediction that the 'clock' ticks at different rates when placed in different gravitational potentials. This coupling can directly be obtained from the Einstein equivalence principle. Recall that the latter postulates that accelerated reference frames are physically equivalent to those in the gravitational field of massive objects. When applied within special relativity, this exactly results in the prediction that initially synchronized clocks subject to different gravitational potentials will show different times when brought together. The proposed experiment probes the presence of such a gravitational time dilation effect for a quantum system—it directly shows whether the 'clock' would tick at different rates when taken along the two possible trajectories in the interferometer. On the other hand, to obtain the correct phase shift, it is sufficient to consider a semiclassical coupling of the average total energy of the system to the gravitational potential. With such a coupling, the time displayed by the 'clock' used in

the experiment will not depend on the path taken. This means that a gravitationally induced phase shift can probe general relativistic corrections to the Newtonian gravitational potential but is always consistent with having an operationally well-defined notion of global time, that is, with a flat space–time.

The effect described in our work follows directly from the Einstein equivalence principle, which is itself crucial for the formulation of general relativity as a metric theory[22]. Thus, the drop in the fringe contrast is not only genuinely quantum mechanical but also a genuine general relativistic effect that in particular unambiguously probes the general relativistic notion of proper time.

General 'clocks' and gravitational fields. Let us call $t_\perp$ the orthogonalization time of a quantum system, that is, the minimal time needed for a quantum state to evolve under a given Hamiltonian into an orthogonal one[23,24]. For the initial state (11) subject to the rest frame Hamiltonian $H_{\circlearrowleft}$ given by equation (10) we obtain

$$t_\perp = \frac{\pi\hbar}{\Delta E}. \tag{14}$$

A system with finite $t_\perp$ can be seen as a clock that ticks at a rate proportional to $t_\perp^{-1}$. Thus, the orthogonalization time gives also the precision of a considered 'clock'. From the expression for $\dot{\tau}$ in the approximation (9), it follows that the total time dilation $\Delta\tau$ between the trajectories is

$$\Delta\tau = \frac{\Delta V \Delta T}{c^2}. \tag{15}$$

We can, therefore, phrase the interferometric visibility $\mathcal{V}$ solely in terms of $t_\perp$ and $\Delta\tau$:

$$\mathcal{V} = \left|\cos\left(\frac{\Delta\tau}{t_\perp}\frac{\pi}{2}\right)\right|. \tag{16}$$

The total time dilation $\Delta\tau$ is a parameter capturing the relevant information about the paths, and $t_\perp$ grasps pertinent features of the 'clock'. It is only their ratio that matters for the fringe visibility. Equation (16) is a generalization of the result (13) to the case of an arbitrary initial state, 'clock' Hamiltonian and a non-homogeneous gravitational field: whenever the time dilation $\Delta\tau$ between the two trajectories through the Mach–Zehnder interferometer is equal to the orthogonalization time $t_\perp$ of the quantum mechanical system that is sent through the setup, the physically accessible proper time difference will result in the full loss of fringe contrast. There are several bounds on the orthogonalization time based on energy distribution moments[23,25,26]. Such bounds can through equation (16) give some estimates on the gravity-induced decoherence rates in more general situations. As an example, for mixed states one generally has[26]:

$$\frac{1}{t_\perp} \leq \frac{2^{\frac{1}{\alpha}}}{\pi\hbar}\langle (H - E_{gr})^\alpha \rangle^{\frac{1}{\alpha}},$$

$\alpha > 0$ (provided the initial state is in the domain of $(H - E_{gr})^\alpha$) where H denotes the internal Hamiltonian and E_{gr} the energy of its ground state.

Discussion

Current approaches to test general relativistic effects in quantum mechanics mainly focus on high precision measurements of the phase induced by the gravitational potential. Although such experiments would probe the potential and thus could verify non-Newtonian corrections in the Hamiltonian, they would not constitute an unambiguous proof of the gravitational time dilation, because they are also explainable without this concept by the Aharonov–Bohm effect: a trajectory-dependent phase acquired by a particle moving in a flat space–time in the presence of a position-dependent potential.

In our proposed experiment, the effects arising from general relativistic proper time can be separated and probed independently from the Aharonov–Bohm type of effects. Unlike the phase shift, which occurs independently of whether the interfering particle can be treated as a 'clock', the change of the interferometric visibility (equation (13)) is a quantum effect that arises if and only if general relativistic proper time has a well defined operational meaning. Indeed, if one prepares the initial state $|\tau^{in}\rangle$ as an eigenstate of the internal energy Hamiltonian $H_{\circlearrowleft}$, only the phase of such a state would change during the time evolution and, according to equation (16), interferometric visibility would be maximal. This 'clock' would not 'tick' (it has orthogonalization time $t_\perp = \infty$) so the concept of proper time would have no operational meaning in this case. Moreover, reasoning that any (even just an abstract) frequency which can be ascribed to the particle allows considering proper time as a physical quantity would imply that interference should always be lost, as the which-path information is stored 'somewhere'. This once again shows that, in quantum mechanics, it makes no sense to speak about quantities without specifying how they are measured.

The interferometric experiment proposed in this work can also be used to test whether proper time is a new quantum degree of freedom. This idea was discussed in the context of, for example, the equivalence principle in refs 13,14 and a mass–proper time uncertainty relation[15]. The equations of motion for proper time treated dynamically, as put forward in refs 13–15, are in agreement with general relativity. Therefore, the predictions of equation (5) would also be valid, if the states $|\tau_i\rangle$, introduced in equation (3), stand for this new degree of freedom. Already performed experiments, like

Table 1 | Discussion of possible outcomes of the proposed interferometric experiment.

Experimental visibility	Possible explanation	Current experimental status
$\mathcal{V}_m = 0$	Proper time: quantum d.o.f., sharply defined	Disproved in, for example, refs 7,9
$0 < \mathcal{V}_m < \mathcal{V}_{QM}$	Proper time: quantum d.o.f. with uncertainty σ_τ	Consistent with current data for $\sigma_\tau > \lvert\Delta\tau\rvert / \sqrt{-8\ln(1-\Delta\mathcal{V})}$
$\mathcal{V}_m = \mathcal{V}_{QM}$	Proper time: not a quantum d.o.f. or has a very broad uncertainty	Consistent with current data
$\mathcal{V}_m > \mathcal{V}_{QM}$	Quantum interferometric complementarity does not hold when general relativistic effects become relevant	Not tested

The measured visibility $\mathcal{V}_m$ is compared with the quantum mechanical prediction $\mathcal{V}_{QM}$ given by equation (13). Depending on their relation, different conclusions can be drawn regarding the possibility that proper time is a quantum degree of freedom (d.o.f.). Assuming that the distribution of the proper time d.o.f. is a Gaussian of the width σ_τ, current interferometric experiments give bounds on possible σ_τ in terms of the proper time difference $\Delta\tau$ between the paths and the experimental error $\Delta\mathcal{V}$ of the visibility measurement.

Table 2 | Comparison of different systems for the experimental observation of the reduced interferometric visibility.

System	'Clock'	ω (Hz)	ΔhΔT (ms) achieved	ΔhΔT (ms) required
Atoms	Hyperfine states	10^{15}	10^{-5}	10
Electrons	Spin precession	10^{13}	10^{-6}	10^{3}
Molecules	Vibrational modes	10^{12}	10^{-8}	10^{4}
Neutrons	Spin precession	10^{10}	10^{-6}	10^{6}

Several possible systems are compared on the basis of theoretically required and already experimentally achieved parameters, which are relevant for our proposed experiment. For a 'clock' with a frequency $\omega = \Delta E/\hbar$, the required value of the parameter $\Delta h \Delta T$ (Δh being the separation between the interferometers arms and ΔT the time for which the particle travels in superposition at constant heights) for the full loss of the fringe visibility (see equation (13)), is given in the rightmost column. In our estimations, we assumed a constant gravitational acceleration $g = 10(m/s^2)$. See section Methods for further discussion on possible experimental implementations.

in refs 7,16, which measured a gravitational phase shift, immediately rule out the possibility that the state of proper time was sharply defined in those tests, in the sense of $\langle\tau_1|\tau_2\rangle = \delta(\tau_1 - \tau_2)$. However, such experiments can put a finite bound on the possible uncertainty in the state of proper time. The phase shift measured in those experiments can be phrased in terms of the difference in the proper time $\Delta\tau$ between the paths. Denote by $\Delta\mathcal{V}$ the experimental error with which the visibility of the interference pattern was measured in those tests. As a result, a Gaussian state of the proper time degree of freedom of width σ_τ such that $\sigma_\tau > |\Delta\tau| / \sqrt{-8\ln(1-\Delta\mathcal{V})}$, is consistent with the experimental data. An estimate of the proper time uncertainty can be based on the Heisenberg uncertainty principle for canonical variables and the equation of motion for the proper time. In such an analysis, the rest mass m can be considered as a canonically conjugated momentum to the proper time variable τ, that is, one assumes $[\tau, mc^2] = i\hbar$[13–15]. In Table 1, we discuss what can be inferred about proper time as a quantum degree of freedom from an experiment in which the measured visibility would be $\mathcal{V}_m$ and where $\mathcal{V}_{QM}$ is the visibility predicted by quantum mechanics, as given by equation (13).

In conclusion, we predicted a quantum effect in interferometric experiments that, for the first time, allows probing general relativistic proper time in an unambiguous way. In the presence of a gravitational potential, we showed that a loss in the interferometric visibility occurs, if the time dilation is physically accessible from the state of the interfered particle. This requires that the particle is a 'clock' measuring proper time along the trajectories, therefore revealing the which-way information. Our predictions can be experimentally verified by implementing the 'clock' in some internal degrees of freedom of the particle (see Methods). The proposed experiment can also lead to a conclusive test of theories in which proper time is treated as a quantum degree of freedom. As a final remark, we note that decoherence due to the gravitational time dilation may have further importance in considering the quantum to classical transition and in attempts to observe collective quantum phenomena in extended, complex quantum systems because the orthogonalization time may become small enough in such situations to make the predicted decoherence effect prominent.

Methods

Systems for the implementation of the interferometric setup. Here we briefly discuss various systems for the possible implementation of the interferometric setup. Interferometry with many different massive quantum systems has been achieved, for example, with neutrons[7,8], atoms[16,27], electrons[28,29] and molecules[30,31]. In our framework, further access to an internal degree of freedom is paramount, as to initialize the 'clock' which measures the proper time along the interferometric path. Therefore, the experimental requirements are more challenging. To observe full loss of the interferometric visibility, the proper time difference in the two interferometric arms needs to be $\Delta\tau = t_\perp$. For a two level system, the revival of the visibility due to the indistinguishability of the proper time in the two arms occurs when $\Delta\tau = 2t_\perp$.

The best current atomic clocks operate at optical frequencies ω around 10^{15} Hz. For such systems, we have $t_\perp = \pi/\omega$, and one would therefore require an atomic superposition with $\Delta h \Delta T \sim 10$ ms to see full disappearance of the interferometric visibility. For example, the spatial separation would need to be of the order of 1 m, maintained for about 10 s. Achieving and maintaining such large superpositions of atoms still remains a challenge, but recent rapid experimental progress indicates that this interferometric setup could be conceivable in the near future. For neutrons, a separation of $\Delta h \sim 10^{-2}$ m with a coherence time of $t \sim 10^{-4}$ s has been achieved[8]. To implement our 'clock' in neutron interferometry, one can use spin precession in a strong, homogeneous magnetic field. However, such a 'clock' could reach frequencies up to $\omega \sim 10^9$ Hz (for a magnetic field strength of order of 10T (ref. 32)), which is still a few orders of magnitude lower than necessary for the observation of full decoherence owing to a proper time difference. Improvements in the coherence time and the size of the interferometer would still be necessary. Other systems, such as molecules, could be used as well and Table 2 summarizes the requirements for various setups (note again that the particles are assumed to travel at fixed height during the time ΔT).

The effect we predict can be measured even without achieving full orthogonalization of the 'clocks'. Note that even for $\Delta\tau \ll t_\perp$ the small reduction of visibility can already be sufficient to prove the accessibility of which-path information due to the proper time difference. With current parameters in atom interferometry, an accuracy of the measurement of the visibility of $\Delta\mathcal{V} = 10^{-6}$ would have to be achieved for the experimental confirmation of our predictions. A very good precision measurement of the interferometric visibility and a precise knowledge about other decoherence effects would therefore make the requirements for the other parameters less stringent.

References

1. Hafele, J. C. & Keating, R. E. Around-the-world atomic clocks: predicted relativistic time gains. *Science* **177,** 166–168 (1972).
2. Chiao, R. Y., Minter, S. J., Wegter-McNelly, K. & Martinez, L. A. Quantum incompressibility of a falling Rydberg atom, and a gravitationally-induced charge separation effect in superconducting systems. *Found. Phys.*1–19, DOI: 10.1007/s10701-010-9531-2 (2011).
3. Wajima, S., Kasai, M. & Futamase, T. Post-Newtonian effects of gravity on quantum interferometry. *Phys. Rev. D* **55,** 1964–1970 (1997).
4. Dimopoulos, S., Graham, P. W., Hogan, J. M. & Kasevich, M. A. General relativistic effects in atom interferometry. *Phys. Rev. D* **78,** 042003 (2008).
5. Aharonov, Y. & Bohm, D. Significance of electromagnetic potentials in the quantum theory. *Phys. Rev.* **115,** 485–491 (1959).
6. Ho, V. B. & Morgan, M. J. An experiment to test the gravitational Aharonov-Bohm effect. *Aust. J. Phys.* **47,** 245–253 (1994).
7. Colella, R., Overhauser, A. W. & Werner, S. A. Observation of gravitationally induced quantum interference. *Phys. Rev. Lett.* **34,** 1472–1474 (1975).
8. Zawisky, M., Baron, M., Loidl, R. & Rauch, H. Testing the world's largest monolithic perfect crystal neutron interferometer. *Nucl. Instrum. Methods Phys. Res. A* **481,** 406–413 (2002).
9. Peters, A., Chung, K. Y. & Chu, S. Measurement of gravitational acceleration by dropping atoms. *Nature* **400,** 849–852 (1999).
10. Wootters, W. K. & Zurek, W. H. Complementarity in the double-slit experiment: Quantum nonseparability and a quantitative statement of Bohr's principle. *Phys. Rev. D* **19,** 473–484 (1979).
11. Greenberger, D. M. & Yasin, A. Simultaneous wave and particle knowledge in a neutron interferometer. *Phys. Lett. A* **128,** 391–394 (1988).
12. Englert, B. G. Fringe visibility and which-way information: An inequality. *Phys. Rev. Lett.* **77,** 2154–2157 (1996).
13. Greenberger, D. M. Theory of particles with variable mass. I. Formalism. *J. Math. Phys.* **11,** 2329 (1970).
14. Greenberger, D. M. Theory of particles with variable mass. II. Some physical consequences. *J. Math. Phys.* **11,** 2341 (1970).
15. Kudaka, S. & Matsumoto, S. Uncertainty principle for proper time and mass. *J. Math. Phys.* **40,** 1237 (1999).
16. Müller, H., Peters, A. & Chu, S. A precision measurement of the gravitational redshift by the interference of matter waves. *Nature* **463,** 926–929 (2010).
17. Wolf, P. *et al.* Atom gravimeters and gravitational redshift. *Nature* **467,** E1 (2010).
18. Sinha, S. & Samuel, J. Atom interferometers and the gravitational redshift. *Class. Quantum Grav.* **28**, 145018 (2011).

19. Giulini, D. Equivalence principle, quantum mechanics, and atom-interferometric tests. arXiv:1105.0749v1 (2011).
20. Wolf, P. *et al.* Does an atom interferometer test the gravitational redshift at the Compton frequency? *Class. Quantum Grav.* **28**, 145017 (2011).
21. Weinberg, S. *Gravitation and Cosmology*, (John Wiley & Sons, 1972).
22. Will, C. M. *Theory and Experiment in Gravitational Physics*, (Cambridge University Press, 1993).
23. Mandelstam, L. & Tamm, I. The uncertainty relation between energy and time in non-relativistic quantum mechanics. *Journ. Phys. (USSR)* **9,** 249 (1945).
24. Fleming, G. N. A unitarity bound on the evolution of nonstationary states. *Nuovo Cim. A* **16,** 232–240 (1973).
25. Margolus, N. & Levitin, L. B. The maximum speed of dynamical evolution. *Physica D* **120,** 188–195 (1998).
26. Zielinski, B. & Zych, M. Generalization of the Margolus-Levitin bound. *Phys. Rev. A* **74,** 034301 (2006).
27. Müller, H., Chiow, S., Herrmann, S. & Chu, S. Atom interferometers with scalable enclosed area. *Phys. Rev. Lett.* **102,** 240403 (2009).
28. Neder, I., Heiblum, M., Mahalu, D. & Umansky, V. Entanglement, dephasing, and phase recovery via cross-correlation measurements of electrons. *Phys. Rev. Lett.* **98,** 036803 (2007).
29. Ji, Y. *et al.* An electronic Mach-Zehnder interferometer. *Nature* **422,** 415–418 (2003).
30. Arndt, M. *et al.* Wave-particle duality of C 60 molecules. *Nature* **401,** 680–682 (1999).
31. Gerlich, S. *et al.* Quantum interference of large organic molecules. *Nat. Commun.* 2:263 doi: 10.1038/ncomms1263 (2011).
32. Miller, J. R. The NHMFL 45-T hybrid magnet system: past, present, and future. *IEEE Trans. Appl. Supercond.* **13,** 1385–1390 (2003).

Acknowledgements

We thank M. Arndt, B. Dakic, S. Gerlich, D. M. Greenberger, H. Müller, S. Nimmrichter, A. Peters, and P. Wolf for insightful discussions. The research was funded by the Austrian Science Fund (FWF) projects: W1210, P19570-N16 and SFB-FOQUS, the Foundational Questions Institute (FQXi) and the European Commission Project Q-ESSENCE (No. 248095). F.C., I.P. and M.Z. are members of the FWF Doctoral Program CoQuS.

Author contributions

M.Z., F.C., I.P. and Č.B. contributed to all aspects of the research with the leading input from M.Z.

Additional information

Competing financial interests: The authors declare no competing financial interests.

Reprints and permission information is available online at http://npg.nature.com/reprintsandpermissions/

How to cite this article: Zych, M. *et al.* Quantum interferometric visibility as a witness of general relativistic proper time. *Nat. Commun.* 2:505 doi: 10.1038/ncomms1498 (2011).

5.4 General relativistic effects in quantum interference of photons

This project was developed as a follow-up on the study of time dilation in matter wave experiments, in collaboration with T. C. Ralph. We considered photons and how they could be used to probe the metric nature of space-time. Even though photons follow null geodesics, and therefore do not measure any proper time along their paths, they can nevertheless be used to probe general relativistic phenomena. We show that general relativistic slow-down of light, also known as Shapiro delay, can affect interference experiments with single photons. If the interferometer is sufficiently large, a single photon in superposition will experience a delay between the two arms such that no full quantum interference can be obtained. Even though Shapiro delay is well tested for classical electromagnetic radiation, a test of the delay for single photons in superposition allows one to probe the interplay between quantum theory and general relativity. In the manuscript we also discuss under what conditions an experiment of this kind is unambiguously of quantum and general relativistic nature. To highlight the difference to tests of general relativity with classical systems, we construct a simple model which would be consistent with all current experiments but which would predict a different outcome for the Shapiro delay of a single photon in superposition. In addition, it is shown that phase shift measurements on the light can reveal the influence of gravity on photons even in a regime where the slow-down along the different trajectories is vanishingly small.

I contributed to all aspects of the research project.

IOP PUBLISHING CLASSICAL AND QUANTUM GRAVITY

Class. Quantum Grav. **29** (2012) 224010 (18pp) doi:10.1088/0264-9381/29/22/224010

General relativistic effects in quantum interference of photons

Magdalena Zych[1], Fabio Costa[1], Igor Pikovski[1], Timothy C Ralph[2] and Časlav Brukner[1,3]

[1] Faculty of Physics, University of Vienna, Boltzmanngasse 5, A-1090 Vienna, Austria
[2] Department of Physics, University of Queensland, St. Lucia, Queensland 4072, Australia
[3] Institute for Quantum Optics and Quantum Information, Austrian Academy of Sciences, Boltzmanngasse 3, A-1090 Vienna, Austria

E-mail: magdalena.zych@univie.ac.it

Received 28 May 2012, in final form 12 August 2012
Published 18 October 2012
Online at stacks.iop.org/CQG/29/224010

Abstract
Quantum mechanics and general relativity have been extensively and independently confirmed in many experiments. However, the interplay of the two theories has never been tested: all experiments that measured the influence of gravity on quantum systems are consistent with non-relativistic, Newtonian gravity. On the other hand, all tests of general relativity can be described within the framework of classical physics. Here we discuss a quantum interference experiment with single photons that can probe quantum mechanics in curved space-time. We consider a single photon traveling in superposition along two paths in an interferometer, with each arm experiencing a different gravitational time dilation. If the difference in the time dilations is comparable with the photon's coherence time, the visibility of the quantum interference is predicted to drop, while for shorter time dilations the effect of gravity will result only in a relative phase shift between the two arms. We discuss what aspects of the interplay between quantum mechanics and general relativity are probed in such experiments and analyze the experimental feasibility.

PACS numbers: 03.65.−w, 04.20.−q, 42.50.−p, 04.62.+v

(Some figures may appear in colour only in the online journal)

1. Introduction

Quantum mechanics and Einstein's theory of gravity are the two pillars of modern physics. Since there are conceptual differences between the foundational principles of the two theories, new physics is expected to appear from their interplay at some scale [1]. However, even the regime in which *quantum* systems evolve on *classical*, curved space-time has never been

accessed experimentally: all experiments performed so far can be explained either by classical physics in curved background or by quantum mechanics in flat space-time. It is of fundamental interest to verify whether gravitational time dilation applies to single particles in quantum superposition. Likewise, it is important to probe quantum phenomena in regimes where general relativistic effects are present, for example, where time is not a common parameter for different amplitudes of a single quantum system in superposition. In this work we address such a regime and present a scheme which opens a feasible experimental route in this direction.

General relativity (GR) predicts that the flow of the time is altered by gravity. This yields several effects that have been independently tested. The gravitational redshift was first observed by Pound and Rebka [2], who verified that the frequency of electromagnetic radiation depends on the altitude difference between the emitter and the receiver. In a later experiment, Hafele and Keating [3] directly tested both the special and the general relativistic time dilation by comparing actual clocks at different heights moving at different speeds. Another classical test of GR was first proposed and performed by Shapiro [4]: the speed of light, as perceived by a laboratory observer, reduces for electromagnetic waves that travel across regions subject to a gravitational potential [5]. In these experiments, as well as for all other tests of GR, the degrees of freedom relevant for the observation of general relativistic effects can be fully described by the laws of classical physics: the Shapiro effect and the Pound–Rebka experiment can be modeled using classical electrodynamics in curved space-time, while the Hafele–Keating experiment can be described in terms of clocks measuring time along their classical (localized) trajectories.

The first experiment measuring the effect of gravity on the quantum wavefunction of a single particle was performed by Colella, Overhauser, and Werner (COW) [6]. In this experiment single neutrons travel in a superposition of two different heights. The different gravitational potential acting on the two paths induces a relative phase to the neutron wavefunction, which is observed from the quantum interference when the two superposed beams are recombined. Today, analogous experiments with atomic fountains are used to perform high-precision measurements of the gravitational acceleration g [7]. The phase-shifts observed in these interferometric experiments are fully compatible with non-relativistic quantum mechanics in the presence of the Newtonian gravitational potential. It is perhaps striking that the measurements of gravitationally induced phase-shifts are the only experiments performed to date where both quantum mechanics and gravity are relevant and still they cannot falsify non-metric, Newtonian gravity, which has so thoroughly been disproved for classical systems.

In a recent work [8], an experiment was proposed that allows probing general relativistic time dilation in conjunction with the quantum complementarity principle (which states that quantum interference is lost once which-way information becomes available). As in the COW experiment, one considers interference of matter waves. The novelty of the scheme is to use additionally some controllable time-evolving degree of freedom of the mater-wave as a clock [8, 9]. The system is brought in a coherent superposition of two locations at different gravitational potentials (e.g. at different heights above the earth). As a result of the general relativistic time dilation the rate of the time evolution of the clock will be different for each of the amplitudes of the superposition, depending on its location. Thus, according to quantum complementarity the coherence of such a spatial superposition will drop to the extent to which the information on the position becomes accessible from the state of the clock. In this setup one can therefore probe the general relativistic time dilation by observing the reduction of the visibility of quantum interference, in addition to the observation of the phase shift. The measurement of such a gravitationally induced decoherence (and revivals—for a periodic

clock) would be the first confirmation of a genuinely general relativistic effect in quantum mechanics.

Here we discuss a quantum-optics variation of this proposal where the function of the 'clock' is taken by the position of a single photon along the interferometer's arm. Because of general relativistic time dilation, the arrival time of the photon should depend on the altitude of its trajectory above the earth (consistently with the Shapiro delay). Thus, in an experiment with a single photon traveling in a superposition along two paths of an interferometer, each located at a different height above the earth, a reduction of the interferometric visibility is expected for relative time dilations larger than the photon's coherence time. This again can be understood in terms of quantum complementarity: if the which-path information of the photon can be read from its time of arrival, interference is lost.

The proposed effect depends simultaneously on GR and on quantum mechanics and therefore goes beyond previous experiments that probed the two theories independently. The experiment can distinguish between a semi-classical and a quantum extension of the mass–energy equivalence. To illustrate the differences between these two we present a toy model (appendix B) which incorporates such a semi-classical version of the mass–energy equivalence. The model is different than quantum mechanics in curved space-time, yet still in agreement with all current observations of either classical systems in curved space-time or quantum systems in Newtonian gravity.

The paper is organized as follows. In section 2 we review the quantum interferometry of clocks aimed at testing the general relativistic time dilation; in section 3 we derive the predicted outcomes for a photonic version of such an experiment; in section 4 the feasibility of the scheme is discussed; in section 5 we analyze which aspects of GR and quantum mechanics are tested in our proposal and in other experiments and address possible related interpretational issues; we conclude in section 6.

2. Quantum interference of clocks

2.1. The setup

In this section we briefly review the proposal given in [8]. A Mach–Zehnder interferometric setup for matter-waves is placed in the earth's gravitational field (see figure 1), and the massive particle is put in a coherent superposition of traveling along the two paths γ_1 and γ_2. The particle has additional internal degrees of freedom that can serve as a clock (e.g. a spin precessing in a magnetic field), which evolve into states $|\tau_i\rangle$, $i = 1, 2$ on the respective trajectories γ_i. Additionally, the particle acquires a trajectory dependent phase Φ_i and a controllable relative phase shift φ. The external modes associated with the paths are denoted by $|r_i\rangle$. After the superposition is recombined, the particle can be registered in one of the two detectors $D_\pm$. The state of the particle inside the interferometer reads

$$|\Psi\rangle = \tfrac{1}{\sqrt{2}}(\mathrm{i}\mathrm{e}^{-\mathrm{i}\Phi_1}|r_1\rangle|\tau_1\rangle + \mathrm{e}^{-\mathrm{i}\Phi_2+i\varphi}|r_2\rangle|\tau_2\rangle). \tag{1}$$

According to GR, time is not absolute but flows at different rates depending on the geometry of space-time. This means that the clock will evolve into different quantum states, depending on the path taken. The state (1) is then entangled and, according to quantum mechanics, interference in the path degrees of freedom should correspondingly be washed away. The reason is that one could measure the clock degrees of freedom and in that way access the which-path information. Indeed, tracing out the clock states in equation (1) gives the detection probabilities $P_\pm$ associated with the two detectors $D_\pm$:

$$P_\pm = \tfrac{1}{2} \pm \tfrac{1}{2}|\langle\tau_1|\tau_2\rangle|\cos(\Delta\Phi + \alpha + \varphi), \tag{2}$$

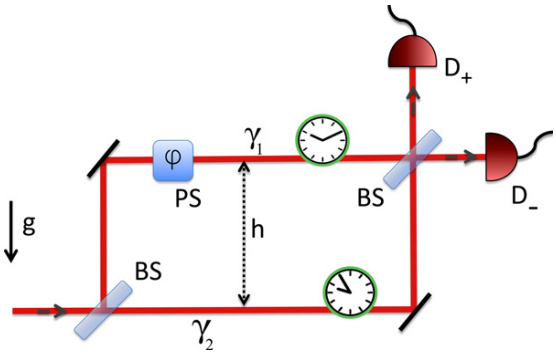

Figure 1. A Mach–Zehnder interferometer to measure the effect of general relativistic time dilation on a wavefunction of a single quantum system. The setup is placed in a homogeneous gravitational field (g) and it consists of two beam splitters (BS), two detectors $D_\pm$ and the phase shifter (PS) which gives a controllable phase difference φ between the two trajectories γ_1 and γ_2. The separation between the paths in the direction of the field is h. If the quantum particle that travels in superposition keeps track of time along its path, the visibility of the interference will be reduced since the which-way information becomes accessible due to the time dilation between the paths.

where $\langle\tau_1|\tau_2\rangle = |\langle\tau_1|\tau_2\rangle|\,\mathrm{e}^{\mathrm{i}\alpha}$ and $\Delta\Phi := \Phi_1 - \Phi_2$. When the ancillary phase shift φ is varied, the probabilities $P_\pm$ oscillate with the amplitude $\mathcal{V}$, called the visibility of the interference pattern. Formally $\mathcal{V} := \frac{\mathrm{Max}_\varphi P_\pm - \mathrm{Min}_\varphi P_\pm}{\mathrm{Max}_\varphi P_\pm + \mathrm{Min}_\varphi P_\pm}$ and for the case of equation (2) it reads

$$\mathcal{V} = |\langle\tau_1|\tau_2\rangle|. \tag{3}$$

The visibility of the interference pattern depends on the distinguishability of the clock states that followed different interferometric paths. If we quantify the amount of the which-way information $\mathcal{D}$ (distinguishability of the trajectories) as the probability to correctly guess which path was taken in the two-way interferometer [10], we obtain $\mathcal{D} = \sqrt{1 - |\langle\tau_1|\tau_2\rangle|^2}$. The complementarity principle can then be phrased in the form of the well-known duality relation $\mathcal{V}^2 + \mathcal{D}^2 = 1$, see [10, 12, 11].

In Newtonian gravity the expected visibility is (ideally) always maximal ($\mathcal{V} = 1$) because the rate of the time evolution of the clock is the same along both paths, i.e. $|\tau_1\rangle = |\tau_2\rangle$. In this limit the relative phase shift between the two amplitudes is the only effect of gravity and the internal clock is irrelevant. The phase Φ_i is proportional to the action along the corresponding (semiclassical) trajectory γ_i on which the particle moves. In the presence of the position dependent potential $V(x)$ this phase becomes trajectory dependent: $\Phi_i = m\int_{\gamma_i} V(x(t))\,\mathrm{d}t$ for a particle of mass m (assuming that contributions from the kinetic energy cancel out). Therefore, even in a homogeneous field the particle acquires a trajectory dependent phase although the force acting on it is the same at all points—the phase arises only due to the potential. For a homogeneous electric field such a relative phase is sometimes referred to as the electric Aharonov–Bohm effect [13]. The case of Newtonian gravity is directly analogous—the role of the particle's electric charge and of the Coulomb potential are taken by the particle's mass and the Newtonian gravitational potential, respectively [14].

Note that Newtonian gravity is a limiting case of Einstein's theory of gravity. Any Newtonian effect can therefore be equivalently described in the general relativistic framework. Within this framework, the action of a particle only subject to gravity is proportional to the proper time elapsed along the particle's trajectory: $S_i = -mc^2\int_{\gamma_i}\mathrm{d}\tau$. The low-energy limit of this expression is the action of a non-relativistic massive particle subject to the

Newtonian gravitational potential. Thus, even the Newtonian interferometric phase shift can be equivalently expressed as $\Delta\Phi = \frac{mc^2}{\hbar}\Delta\tau$ where $\Delta\tau$ is the proper time difference between the trajectories. Some authors interpret therefore the gravitational phase shift as the effect of gravitational time dilation [15]. Even though such an interpretation is consistent with GR, it cannot distinguish Newtonian (i.e. non-metric) gravity from genuine general relativistic effects as long as only the Newtonian limit of the phase shift, $\Delta\Phi = mght/\hbar$, is measured (as in the experiments performed so far). Similarly, any experiment that probes the acceleration of free fall, like Galilei's leaning tower experiment, cannot distinguish the effects of Newtonian gravity from general relativistic effects, although it can be interpreted as arising from gravitational time dilation when formulated within the general relativistic framework. An interpretation of these experiments as measuring the time dilation can only be sustained if the very existence of the time dilation is pre-assumed, i.e. by pre-assuming that the observed Newtonian effects are the low-energy limit of general relativistic effects.

Additionally, to sustain the general relativistic viewpoint it has been argued that, differently from classical free fall experiments, a massive quantum particle constitutes a 'clock' ticking at the Compton frequency, which causes the interference. The notion of such a 'Compton clock', however, is purely formal: no measurement on the particle within the interferometer can reveal the time of such a clock[4]. The phase shift observed is always just a relative phase between the two trajectories. In order to measure the frequency of the 'Compton clock', it would be necessary to measure the number of oscillations per unit time of the global phase of the wavefunction, in contradiction to the basic tenets of quantum mechanics. Moreover, any relative phase shift can be explained as arising due to an effective (possibly even non-Newtonian) gravitational potential within a non-metric theory, which does not predict the effect of time dilation. To conclude, such measurements can be used to test possible deviations from general relativity in the Newtonian limit [15, 16] but not to distinguish GR from Newtonian theory. When performed with higher precision, phase shift measurements alone can also reveal possible deviations from the Newtonian gravitational potential [17, 18], but will always be compatible with an absolute time (flat space-time). In contrast, the drop in the interferometric visibility (only observable when using *physical* clocks), cannot be explained without the general relativistic notion of proper time.

2.2. Interferometric visibility and which way-information

In order to explain the reduction in the interferometric visibility both quantum complementarity and the general relativistic time dilation are necessary. Here the which-way information becomes available only due to the gravitational time dilation. The time evolution of the upper amplitude of the clock precedes the lower one by $\Delta\tau$—the time dilation between the paths of the interferometer. The distinguishability, however, depends on how $\Delta\tau$ compares with the precision $t_\perp$ of the clock—i.e. the time that the quantum system needs to evolve between two distinguishable states. The expected visibility will thus depend only on the ratio of these two parameters and equation (3) will generally take the form:

$$\mathcal{V} = F_{\textcircled{L}}\left(\frac{\Delta\tau}{t_\perp}\right), \tag{4}$$

where the function $F_{\textcircled{L}}$ has the following properties: $F_{\textcircled{L}}: R_+ \to [0, 1]$ such that $F_{\textcircled{L}}(0) = 1$ and $F_{\textcircled{L}}(1) \ll 1$. Note that this conclusion is not limited to any particular physical implementation of the clock. The fact that the time dilation necessary to cause a loss of quantum interference only

[4] The claim that the measurement of the phase shift itself, being *proportional* to the Compton frequency, is a measurement of the latter is untenable: any measurement of the mass m is likewise proportional to the Compton frequency.

depends on the precision of the clock and not on its realization can be seen as a consequence of the universality of general relativistic time dilation: rates of all clocks are equally affected by gravity. Only the explicit form of the function $F_{\textcircled{L}}$ depends on the specific realization of the clock. For example, a clock with a finite dimensional Hilbert space has a periodic time evolution and thus one expects periodic modulations of the visibility with increasing time dilation between the two arms of the interferometer. For a clock implemented in a two-level quantum system the visibility reads [8]

$$\mathcal{V} = \left|\cos\left(\frac{\Delta\tau}{t_\perp}\frac{\pi}{2}\right)\right|. \tag{5}$$

For such a periodic clock, consecutive states at multiples of $t_\perp$ are mutually orthogonal (and in this case the parameter $t_\perp$ is known as the orthogonalization time), so the full loss of the visibility is expected for $\Delta\tau = t_\perp$. The period of a two-state clock is twice $t_\perp$, which explains the full revival of the visibility for $\Delta\tau = 2t_\perp$. Such a clock may be realized in hyperfine energy levels of an atom or with the spin of a neutron.

3. Testing general relativistic effects with single photons

We now consider a variation of the interferometric experiment that can be performed with single photons. In this case, the clock is implemented in the position degree of freedom of the photon (which has an infinite dimensional Hilbert space). We first consider the light-like geodesics within an interferometric setup as in figure 1 and then consider a single photon traveling in superposition along these geodesics. The interferometer is placed, vertically oriented, on the surface of the earth and the space-time is modeled by the Schwarzschild metric [19]. For a small size of the interferometer as compared to its radial coordinate r, all points on each of the horizontal paths are approximately at the same radial distance and the vertical distance h can be adjusted whilst keeping the horizontal path length l constant. We therefore restrict our attention to horizontal propagation in the x direction and describe the motion in an approximately flat $2D$ metric

$$\mathrm{d}s^2 = \mathrm{d}\tau_r^2 - \frac{1}{c^2}\,\mathrm{d}x_r^2, \tag{6}$$

where

$$\mathrm{d}\tau_r^2 = \left(1 + \frac{2V(r)}{c^2}\right)\mathrm{d}t^2, \quad \mathrm{d}x_r^2 = r^2\mathrm{d}\theta^2. \tag{7}$$

$V(r) = -\frac{GM}{r}$ is the gravitational potential, G is the universal gravitational constant and M is the earth's mass. The coordinates are defined as follows: $\mathrm{d}t$ is an infinitesimal time interval as measured by an observer far from the earth, θ is a polar coordinate that remains the same for the observer on earth and the far away observer, τ_r and x_r are the local time and the local cartesian coordinate, respectively, for an observer at radial coordinate r. We first focus on the coordinate time t_r of the photon's path along a horizontal trajectory at the radial distance r. Since the trajectory in this case is light-like, i.e. $\mathrm{d}s^2 = 0$, equation (6) results in $t_r = \frac{1}{c}\int_0^l \mathrm{d}x_r\left(1 + \frac{2V(r)}{c^2}\right)^{-1/2}$. By definition of the metric, the locally measured spatial intervals are independent of r and $\int_0^l \mathrm{d}x_r = l$, so that

$$t_r = \frac{l}{c\sqrt{1 + \frac{2V(r)}{c^2}}}. \tag{8}$$

According to equation (8), the time of the photon's flight along the horizontal path can be seen as a clock, which is subject to the gravitational time dilation as predicted by GR (which is

the Shapiro effect). Depending on the radial distance r of the path from the earth, the photon will arrive at the second beam splitter at different coordinate times. From the symmetry of the setup, the coordinate time of the photon's flight in the radial direction is the same for both trajectories γ_i. The total difference in photon arrival times as measured by the far away observer is therefore $t_r - t_{r+h}$. For the local observer at the upper path (at the radial distance $r + h$) this time dilation is given by

$$\Delta\tau = \sqrt{1 + \frac{2V(r+h)}{c^2}}\,(t_r - t_{r+h}) \approx \frac{lgh}{c^3}\,, \tag{9}$$

with $g = \frac{GM}{r^2}$. The approximation in equation (9) is valid for a small size of the interferometer, i.e. $h \ll r$, and when second order terms in the potential are neglected.

To probe quantum mechanics in curved space-time, we consider the above effect on single photons in superposition. The state of a photon moving in the $+x$ direction at the radial distance r in the space-time given by the metric (6) can be written as

$$|1\rangle_f = a_f^\dagger|0\rangle = \int \mathrm{d}\nu f(\nu)\,\mathrm{e}^{\mathrm{i}\frac{\nu}{c}(x_r - c\tau_r)} a_\nu^\dagger|0\rangle, \tag{10}$$

where $f(\nu)$ is the mode function with ν being the angular frequency defined with respect to a local observer at radial distance r and $a_\nu^\dagger$ being a single frequency bosonic creation operator. According to equation (9) the wave packet moves along each of the trajectories with a different group velocity with respect to a fixed observer. Therefore, the superposition states reaching the two detectors $D_\pm$ take the form $|1\rangle_{f\pm} \propto \int \mathrm{d}\nu f(\nu)\big(\mathrm{e}^{\mathrm{i}\frac{\nu}{c}(x_r - c\tau_r)} \pm \mathrm{e}^{\mathrm{i}\frac{\nu}{c}(x_r - c(\tau_r + \Delta\tau))}\big)a_\nu^\dagger|0\rangle$, with $\Delta\tau$ as given by equation (9). The probabilities of detecting the particle in $D_\pm$ read (see appendix A for a supplementary calculation)

$$P_{f\pm} = \frac{1}{2}\left(1 \pm \int \mathrm{d}\nu |f(\nu)|^2 \cos(\nu\Delta\tau)\right). \tag{11}$$

The mode function is normalized such that $\int \mathrm{d}\nu |f(\nu)|^2 = 1$. We can identify two limits of this expression, which in turn correspond to tests of two different physical effects.

(i) For $\Delta\tau$ small with respect to the frequency-width of the mode function $f(\nu)$ the cosine term will be approximately constant over the relevant range of ν and so can be taken outside the integral giving a phase shift term $\cos(\nu_0\Delta\tau)$, (where ν_0 is central frequency of the mode function) and the visibility remains maximal. Note that such a phase shift can be explained as arising from the coupling of the average energy of the photon to the Newtonian gravitational potential in the Euclidean space-time, where the time is absolute and no time dilation occurs—analogously to the case of a massive particle. The gravitational phase shift for a photon is also of the same form as the phase shift for a massive particle, with the photon's energy (divided by c^2) substituting the particle's mass. It thus constitutes an interesting test of the mass–energy equivalence and the resulting coupling to gravity, one of the conceptual pillars of GR. Although the measurement of a gravitational phase shift cannot be considered as a test of the time dilation, its observation with a single photon differs from a corresponding test for a massive particle because in the Newtonian limit of gravity no effect on a massless system would be expected (see table 2). In this sense in such an experiment both quantum and general relativistic effects could simultaneously be tested. Furthermore this proposal is particularly interesting as it seems feasible with current technology[5].

(ii) In the other limit, when the time dilation dominates over the pulse width, the oscillatory cosine term averages out the whole integrand, resulting in no interference. More precisely, the

[5] A similar experiment, where the gravitationally induced phase shift of classical light was considered, was first proposed in 1983 [20], but has not been performed yet.

amplitude of the phase shift term is given by the overlap between the modes associated with the two paths. For $\Delta\tau$ much larger than the coherence time of the photon wave packet (the pulse width) the interferometric visibility is lost as the two modes arrive at the second beam splitter at distinctly different times. Note that the slow-down of light is a direct consequence of the gravitational time dilation, and is absent in the non-metric Newtonian theory (see section 5 and appendix B for further discussion). The drop in the interferometric visibility is therefore probing a regime beyond the Newtonian limit. In this parameter regime the experiment directly tests the gravitational time dilation for superpositions of single photons.

The two limits can be clearly seen when considering the specific case of a Gaussian wave packet $f^{\nu_0}_{\sigma}(\nu) = (\frac{\sigma}{\pi})^{1/4} \exp\left[-\frac{\sigma}{2}(\nu-\nu_0)^2\right]$:

$$P_{f^{\nu_0}_{\sigma}\pm} = \tfrac{1}{2}(1 \pm \mathrm{e}^{-(\Delta\tau/2\sqrt{\sigma})^2}\cos(\nu_0\Delta\tau)). \tag{12}$$

The width σ of the gaussian mode function gives the precision $t_\perp$ of this clock. Defining distinguishable gaussian wave packets as such that their overlap is not larger than e^{-1}, the precision of the clock is given by $t_\perp = 2\sqrt{\sigma}$ and the visibility of the interference in equation (12) reads

$$\mathcal{V} = \mathrm{e}^{-(\frac{\Delta\tau}{t_\perp})^2}. \tag{13}$$

The clock implemented in the position degree of freedom of a photon is thus analogous to the clock implemented in an internal degree of freedom of a massive particle [8]: the interferometric visibility depends only on the ratio of the time dilation to the precision of the used clock[6] and the phase shift depends on the average energy of the clock, which is the mean frequency for the case of a photon.

4. Quantitative predictions

For a single photon in superposition, a full loss of the visibility can be obtained in a sufficiently large interferometer, such that $\Delta\tau > t_\perp$. Assuming the gravitational field to be homogeneous the corresponding area of the interferometer obtained from the equation (9) reads

$$A_\perp \approx t_\perp \frac{c^3}{g}. \tag{14}$$

For a clock of the same frequency but moving at a subluminal velocity v, the corresponding area of the interferometer necessary to observe the loss of the interferometric visibility is by v/c smaller than the area needed for the clock moving at velocity c. Thus, the size of the interferometer necessary for realizing the proposed experiment with the clock implemented in a photon is orders of magnitude larger than the setup needed for a massive clock. However, such an implementation can still be a feasible route for the observation of time dilation in a quantum system as an implementation with photons may provide some advantages. For example, the control over the exact length and separation between the interferometric paths would be easier with a photon clock since it could be confined in an optical fiber. Moreover, experiments were already performed confirming the high-fidelity transmission of polarization-encoded qubits from entangled photon pair sources over 100 km in a fiber [21]. For the preparation of a clock with a fixed precision one needs to control only the width of the photon's wave packet. The preparation of light pulses with duration on the order of 10 femtoseconds has already been achieved [22] and recent rapid progress in the preparation of attosecond optical pulses

[6] In general, demanding that the two wave packets are distinguishable when the absolute value of the amplitude between them is $1/n$ yields $\mathcal{V}_n = n^{-(\Delta\tau/t_{n\perp})^2}$ where $t_{n\perp} = 2\log(n)\sqrt{\sigma}$ is the corresponding clock's precision.

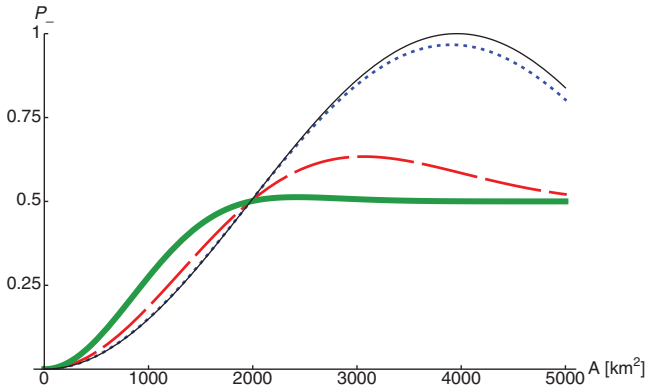

Figure 2. Probing the general relativistic slowdown of light in the proposed single photon interference experiments. The probabilities $P_{f_\sigma^{\nu_0}\_}$ (equation (12)) to find the photon in the detector D_- are shown as a function of the area A [km^2] of the interferometer in the vertical plane. The single-photon pulse has mean angular frequency $\nu_0 \approx 4 \times 10^{15}$ Hz. The four graphs correspond to different widths σ of the wave packet and thus to different coherence times $t_\perp = 2\sqrt{\sigma}$: $t_\perp = 0.05$ fs (thick green line), $t_\perp = 1$ fs (red dashed line), $t_\perp = 5$ fs (blue dotted line) and $t_\perp = \infty$ fs (black line), which is a limiting case of an infinitely long pulse (and thus with the clock effectively switched off). Observing a gravitational phase shift of a photon is within reach of current experimental capabilities.

Table 1. The size of the interferometer necessary to observe a loss of visibility due to the gravitational time dilation and to observe the gravitational phase shift. For the realization of the clock in the position degree of freedom of a photon the precision is given by the coherence time of the photon's wave packet. For the clock implemented in the internal degree of freedom of a massive particle—by the orthogonalization time (the shortest time after which the final state becomes orthogonal to the initial one). In both cases only the total energy of the system is relevant for the observation of the gravitational phase shift.

	System	**Clock**	$t_\perp$ **[s]**	$A_\perp$ **[km^2]**
Time dilation	Photon	position	10^{-15}	10^{3}
	Atom	hyperfine states	10^{-15}	10^{-7}
Phase shift	**Photon frequency [Hz]**			A_{ps} **[km^2]**
	10^{15}			10^{-3}

may provide a feasible route to such high-precision clocks [23, 24]. Finally, using slow light materials (e.g. with a suitable frequency dependent index of refraction) may allow reducing the necessary size of the interferometer.

The experimental parameters necessary to measure the gravitational phase shift for single photons are much less demanding than those required for full orthogonalization. (See table 1 for a comparison of the experimental parameters necessary to observe those effects and figure 2 for a plot of the detection probability P_-, equation (12), as a function of the interferometer's area.) For a photon with a central frequency ν_0, the gravitational phase shift in the considered interferometer is $\Delta\Phi \approx \nu_0 \frac{lgh}{c^3}$. Taking the angular frequency $\nu_0 = 10^{15}$ Hz, and the time dilation as used above ($\Delta\tau = 10^{-15}$ s) we get the phase shift of order of one radian. Since phase shifts that are at least six orders of magnitude smaller can be experimentally resolved [25], the area enclosed by the interferometer that would suffice to result in the measurable phase shift effect is correspondingly smaller: $A_{ps} = 10^3$ m^2. Such a size is feasible with

Table 2. Summary of the key interpretational aspects of our proposed experiments and of already performed experiments. In order to test the overlap between quantum mechanics and general relativity, the observed effect cannot be compatible neither with classical mechanics nor with the Newtonian limit of gravity. An experiment in a given entry of the table and the indicated coupling are compatible with both theories that label the entry's row and column. The coupling of the gravitational potential $V(\hat{r})$ to: mass m, average energy $\langle \hat{H}_s \rangle$, and the energy operator $\hat{H}_s$ can be interpreted as testing the gravitational coupling due to: Newton gravity, the semi-classical extension of the mass–energy equivalence, and the full quantum extension of the latter, respectively. Note that some of the experiments have more than one possible interpretation, and thus fit in several different slots of the table. In contrast, our proposed clock interferometry experiment can only be placed in the slot of the table at the intersection of general relativity and quantum mechanics. Its successful realization would thus probe general relativity and quantum mechanics in a hitherto untested regime.

			Gravity		
			non-metric, Newtonian	non-metric, Newtonian + semi-classical mass–energy equivalence	general relativity (time dilation)
Mechanics	classical	wave	*well-tested*		*Pound–Rebka* [2], *Shapiro delay* [5]
		particle	*well-tested*	*Pound–Rebka* [2]	*Shapiro delay* [5]
	quantum		*phase-shift of a matter wave* [6, 7] *(probes: $mV(\hat{r})$)*	*phase-shift of a single photon* ***(not yet tested)*** *(probes: $\langle \hat{H}_s \rangle \frac{V(\hat{r})}{c^2}$)*	*quantum interference of clocks* ***(not yet tested)*** *(probes: $\hat{H}_s \frac{V(\hat{r})}{c^2}$)*

current technology. One could also introduce some improvements to the proposed realization of the experiment. For example, by using multi-photon states or different interference schemes [26, 27] not only would it be possible to enhance the precision of the measured phase but, by observing an interference with no classical analogue, the interpretation of the experiment as testing the mass–energy equivalence in conjunction with quantum mechanics would be unambiguous.

5. Interpretation of photon experiments

The aim of the proposed experiment is to access a physical regime where the effects stemming from both quantum mechanics and GR cannot be neglected. To this end, experimental results should simultaneously falsify a model of quantum fields or particles evolving in a Newtonian potential *and* a model of classical fields or particles in curved space-time. Below we analyze in which sense and how this can be achieved. Finally, we show how with a modified experimental setup more general local realistic models of light in curved space-time can be ruled out.

5.1. General relativistic and quantum aspects of the proposal

In the absence of relativistic effects, clocks run at the same rate independently of their position with respect to a gravitational field. In the presently proposed experiment, the clock is implemented in the position of the photon in the direction parallel to the earth's surface. Since the gravitational field is constant in that direction, Newtonian gravity would not provide any measurable effect on the time evolution of the clock, i.e. on the displacement of the photon. A

difference in the arrival time for the two superposed wave packets of the photon is inconsistent with such a non-relativistic model and can therefore be considered as a genuine general-relativistic effect. Since in our current proposal the difference in the arrival time is measured by the drop in the interferometric visibility, the experiment needs to be able to discriminate between this effect and other sources of decoherence, which could also lead to the loss of interference. This can be done by rotating the interferometer from a vertical to a horizontal position, which should lead to a corresponding recovery of the interference; a correlation between the rotation angle and the visibility would imply that gravity is responsible for the effect. Another possibility is to use wave packets with a modulated profile in the time domain (e.g. with a double or multiple peak): by increasing the time delay the visibility should be partially recovered, as the two superposed wave packets start overlapping again. Since a revival of visibility cannot be attributed to decoherence, this possibility would be ruled out by the experiment.

As discussed above, the effect of gravity can also be detected by observing a shift in the relative phase between the superposed wave packets traveling along the two arms. The observation of the phase shift alone could not be directly interpreted as a test of the time dilation, since it can be understood in terms of a coupling between photons and a potential in a flat space-time, which would yield the same phase shift *without* the time dilation. The formal analogy of a massive particle in the Newtonian limit of gravity with a charged particle in a Coulomb electrostatic potential (where notions of proper time or space-time curvature unquestionably never enter) suggests that only those gravitational effects that have no electrostatic analogues can be seen as genuinely general relativistic. The gravitational phase shift effect does have an electrostatic counterpart (experimentally verified with electrons in a Coulomb potential, see e.g. [28]) and thus its measurements (such as in [6, 7]) do not contradict non-metric, Newtonian gravity and cannot be seen as tests of GR. The interaction of *photons* with the Newton potential, however, requires an additional ingredient: it is necessary to assign an effective gravitational mass to each photon, whereas massless particles or electromagnetic waves do not interact with gravity in non-relativistic mechanics. Such an interaction is a direct consequence of the mass–energy equivalence. More precisely, the interaction necessary to obtain the gravitational phase shift follows from postulating the equivalence between the system's mass and its average total energy, $mc^2 \to mc^2 + \langle \hat{H}_s \rangle$, where $\hat{H}_s$ is the non-gravitational Hamiltonian of the system. This would yield an interaction of the form

$$\hat{H}_{\text{phase}} = \langle \hat{H}_s \rangle \frac{V(\hat{r})}{c^2}, \tag{15}$$

which reduces to the Newtonian gravitational potential energy, $mV(\hat{r})$, in the non-relativistic limit. In this sense, observation of a gravitationally induced phase shift for a photon ($m = 0$) can already be considered as a test of GR. In particular, it probes a *semi-classical* version of the mass–energy equivalence, which endows photons with an effective gravitational mass *parameter*[7]: $\frac{\langle \hat{H}_s \rangle}{c^2} = \frac{\hbar \nu}{c^2}$. The interaction (15) results in a relative phase between the amplitudes of a wavefunction at different gravitational potentials, but it predicts no drop in

[7] Note that the Pound–Rebka experiment [2] probed the same aspect of GR: the redshift can be explained as each photon having a gravitational potential energy of ghE/c^2, with $E = \hbar\nu$. The redshift is then a consequence of the (semi-classical) mass–energy equivalence and energy conservation. However, the quantum nature of the photons was not probed directly in the Pound–Rebka experiment, which is thus still consistent with a classical description of light (more precisely, the experiment is consistent with classical waves on a curved background *or* with classical particles in a Newtonian potential, see table 2). Measuring the gravitational phase shift in single photon interference would allow probing this aspect of GR in a quantum regime. In simple terms, it would provide a quantum extension of the Pound–Rebka experiment in the same way as the COW experiment was a quantum extension of Galilei's free fall experiments.

the interferometric visibility (see appendix B). The latter effect is only present if the total Hamiltonian includes a direct coupling between the energy operator and the potential, a term of the form

$$\hat{H}_{\text{vis}} = \hat{H}_s \frac{V(\hat{r})}{c^2}. \tag{16}$$

Such a term follows from postulating the equivalence between mass and the energy *operator* $mc^2 \to mc^2 + \hat{H}_s$, which can be seen as a full *quantum* implementation of the mass–energy equivalence. Both couplings, (15) and (16), predict the same phase shift. In fact, all current observations are in agreement with effective theories, in which gravitational interactions of quantum particles do not include $\hat{H}_{\text{vis}}$, and which still correctly predict general relativistic effects in the classical limit and quantum effects in the Newtonian limit (see appendix B for such toy models and further discussion for their motivation). On the other hand, the experiment proposed in this work can distinguish the two couplings (15) and (16), which cannot be done through (even arbitrary precise) measurements of the phase shift alone. The physical motivation of making such a distinction is to answer how the mass–energy equivalence extends to quantum mechanics and in particular how it applies to superpositions of different energy eigenstates. A summary of the concepts that are tested in different experimental setups is given in table 2.

The proposed quantum optics experiment may also allow testing some other non-standard theories of quantum fields [31]. Some of these alternative models predict a difference in the time evolution of entangled states in a curved background as compared to predictions of standard quantum filed theory in the same space-time (for flat space-time, such models reduce to the standard quantum field theory and are thus only distinguishable in a curved background). For example, the model proposed in [31] predicts a decorrelation of entangled photons, which can have a measurable effect on the expected visibility in our setup.

In order to qualify as a genuine test of quantum mechanics, the results of the experiment should be incompatible with a classical model of light. It is not sufficient that an arbitrary part of the experiment shows some quantum property (in fact, quantum mechanics is necessary to explain the atomic transitions of the clocks used in already performed tests of GR). What should be stressed is that the experiments performed so far are still compatible with models where classical, localized degrees of freedom 'keep track of time' (see appendix B). Accessing the 'quantum domain' means showing experimentally that the degree of freedom keeping track of time was in a genuine quantum superposition, with each part of the superposition evolving at a different rate due to GR. In our case an analogous interference with a modulation in the visibility could also be observed in the intensity of classical electromagnetic wave packets following the paths of the interferometer. However, within such a picture the phase at each point of the electromagnetic wave is a classical degree of freedom that keeps track of time. An interference experiment in which a single photon source is utilized and single photons are detected is incompatible with this picture and thus would rule out an explanation of the experiment in terms of classical electromagnetic waves. The observation of quantum interference also rules out the model of photons as classical particles. As already noted, in the current proposal the signature of the general-relativistic time dilation is *the lack* of interference. Implementation of an additional, controllable delay in the upper arm compensating the general relativistic time dilation would result in a recovery of the interference, which would prove the quantum nature of the photons affected by general-relativistic time dilation.

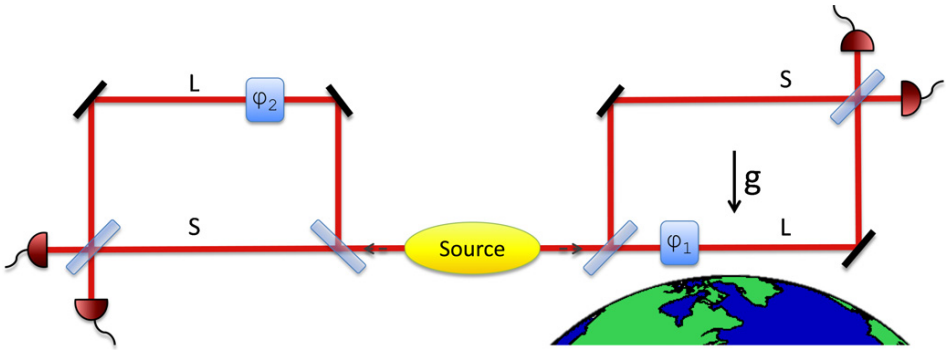

Figure 3. A Franson-type interferometer modified to test a local realistic description of photons undergoing gravitational time dilation. It consists of a source of photon pairs and two Mach–Zehnder setups with arms of different optical lengths S, L. On the right-hand side this difference is due to the general relativistic time dilation. This can be realized by utilizing a Mach–Zehnder setup as in figure 1, where the two paths of equal length are at different gravitational potentials, so that there will be a time dilation $\Delta\tau$ between them. The Mach–Zehnder interferometer on the left-hand side is placed such that both arms feel the same gravitational potential and the difference in their lengths is $L - S = c\Delta\tau$. In each of the interferometers a controllable phase shift φ_1, φ_2 is induced in the optically longer arm. By varying those phases it is possible to violate Bell's inequalities on a subensamble of coincident detected photons.

5.2. Disproving local-realistic description of the experiment

The experimental scheme discussed so far can rule out models where light is described by classical electromagnetic waves or by classical particles evolving on a curved space-time[8]. However, as any single photon experiment, it can still be described with a local realistic model. In order to rule out all local realistic models of photons in a curved background, a modified version of the experiment can be used. The idea is to use a Franson-type interferometer [29], where the difference in the optical length between the two arms on one side of the interferometer is produced by the general relativistic time dilation (see figure 3). In this version of the experiment, pairs of time-correlated photons are emitted by a source and fed into two separated Mach–Zehnder interferometers. The right-hand side interferometer has arms of equal length and is positioned vertically with respect to the surface of the earth, thus the arrival time of the lower arm is delayed by an amount $\Delta\tau$, as given by equation (9). The left-hand side interferometer is horizontal, thus insensitive to gravity, but the two arms differ in their optical lengths by an amount $\Delta l = c\Delta\tau$; in this way both interferometers effectively consist of a shorter and a longer arm, labelled by L and S respectively, which pairwise have the same optical length. Two additional, controllable phases, φ_1 and φ_2, are added to the longer arms of the right and left interferometer, respectively. The emission time of the two photons is correlated (to within their coherence time), but the specific emission time is unknown. For the coherence time of photons shorter than the time delay $\Delta\tau$, coincident photons will have the same time of flight. As a result, the state of the post-selected fraction of coincident photons (just before the beam splitter) is entangled:

$$|\psi\rangle = \tfrac{1}{\sqrt{2}}(\mathrm{e}^{\mathrm{i}(\varphi_1+\varphi_2)}|L\rangle_1|L\rangle_2 + |S\rangle_1|S\rangle_2). \tag{17}$$

[8] Note that classical models of light have already been extensively disproved experimentally, but only in regimes where no effect of GR is present.

By varying the phases φ_1 and φ_2, it is possible to violate Bell's inequalities (even when taking into account the post-selection procedure [30]). Thus, the scheme can provide a conclusive refutation of any model in which photons are described by local-realistic variables. At the same time, the violation of the inequalities is only possible if a photon traveling in the lower arm of the right-hand side interferometer is delayed by a time $\Delta\tau = \Delta l/c$. Since Δl (the length difference in the left arm) can be controlled independently, it can be used to measure the time dilation on the right-hand side and verify the prediction of GR.

6. Conclusion

Probing the effect of gravitational time dilation on quantum interfering particles is a promising path towards fundamental tests of the overlap between quantum mechanics and general relativity. Here we discussed a quantum optics realization of this general idea, where a single photon travels in a superposition along the two paths of a Mach–Zehnder interferometer placed in the gravitational field. The gravitational time dilation between the two paths will cause the lower part of the superposition to be delayed as compared to the upper one, leading to a loss of interference. For a total loss of interference a large-scale interferometer is required, which can be within reach in the near future. Already within reach of present-day technology is, however, the measurement of the gravitationally induced phase shift for single photons. Such an effect cannot be seen as a genuine test of gravitational time dilation, but it would probe a *semi-classical* extension of the mass–energy equivalence in which the *mean* energy couples to gravity, see equation (15). This feature was already observed in the Pound–Rebka experiment [2], here, however, we propose to use single photons that travel in superposition to probe this effect in a regime where no classical description of light is possible. In addition, observing the loss of quantum interference would corresponds to probing the full *quantum* extension of the mass–energy equivalence in which the energy *operator* couples to gravity, see equation (16). The observation of general relativistic time dilation for quantum interfering photons would represent an experimental test of the overlap between general relativity and quantum mechanics and would constitute a first step towards more advanced tests of the interplay between the two theories.

Acknowledgments

The authors thank S Ramelov, M Rupke and P Walther for insightful discussions. The research was funded by the Austrian Science Fund (FWF) projects W1210 and SFB-FOQUS, the Foundational Questions Institute (FQXi), the European Commission Project Q-ESSENCE (no. 248095) and by the John Templeton Foundation. MZ, FC and IP are members of the FWF Doctoral Program CoQuS. MZ acknowledges hospitality at the Center for Interdisciplinary Research (ZiF), University of Bielefeld in March 2012.

Appendix A. Evaluation of the expected photon number

Consider the light source for the interferometer to be an ideal single photon source, which produces pulses propagating in the $+x$ (horizontal) direction each containing only one photon. In the local shell-frame on the earth's surface this can be represented by the quantum state (10). The use of plane-wave propagation is assumed justified by the paraxial approximation of a Gaussian spatial mode.

Detection of the horizontal output mode of the interferometer is assumed to be broadband (i.e. a frequency band-width much greater than the source) and time integrated (detection time is much longer than the pulse width) and thus can be described by an operator

$$a_o^\dagger a_o = \int \frac{\mathrm{d}\tau_{r'}}{2\pi} \int \mathrm{d}\nu\, \mathrm{e}^{\mathrm{i}\frac{\nu}{c}(x_{r'}-c\tau_{r'})} b_\nu^\dagger \int \mathrm{d}\nu'\, \mathrm{e}^{-\mathrm{i}\frac{\nu'}{c}(x_{r'}-c\tau_{r'})} b_{\nu'} = \int \mathrm{d}\nu\; b_\nu^\dagger b_\nu, \tag{A.1}$$

where $b_{\nu'}$ are single wave-number boson annihilation operators for the output mode. We proceed by calculating the expectation value $\langle a_o^\dagger a_o\rangle$ against the initial state (10) by finding the Heisenberg evolution of the detection operators. Quite generally the evolved single wave-number operators are of the form

$$b_\nu = \tfrac{1}{2}a_\nu(\mathrm{e}^{-\mathrm{i}\nu\phi_1} - \mathrm{e}^{-\mathrm{i}\nu\phi_2}) + \tfrac{1}{2}v_\nu(\mathrm{e}^{-\mathrm{i}\nu\phi_1} + \mathrm{e}^{-\mathrm{i}\nu\phi_2}), \tag{A.2}$$

where v_ν are single wave-number boson annihilation operators from which the unoccupied input modes of the interferometer are constructed. Because they are initially in their vacuum state they will not contribute to the expectation value. The phases ϕ_i, $i = 1, 2$ are acquired propagating along the corresponding paths γ_i of the interferometer. We also require continuity at the mirror boundaries between the mode operator expressions along the different paths.

By symmetry, the contribution to the phases ϕ_i coming from the propagation along the radial part of the path is the same for both trajectories, as they are both evaluated over an equal time-interval and have the same lengths as measured by a distant observer. Because they are common they will be eliminated since only the phase difference $\Delta\phi := \phi_1 - \phi_2$ will contribute to the final expression. From equation (10) and the metric equation (6) follows that the phases read $\phi_1 = \frac{1}{c}(l - c\tau_{r+h})$, $\phi_2 = \frac{1}{c}(l - c\tau_r)$ and thus

$$\Delta\phi = \Delta\tau\,, \tag{A.3}$$

with $\Delta\tau$ given by the equation (9). Moreover, the locally measured radial distance h between the paths is found via

$$h_r = \int_r^{r+h} \frac{\mathrm{d}r'}{\sqrt{1-\frac{2M}{r'}}}\,. \tag{A.4}$$

Evaluating the photon number expectation value for the state $|1\rangle_f = \int \mathrm{d}\nu f(\nu)\,\mathrm{e}^{\mathrm{i}\frac{\nu}{c}(x_r - c\tau_r)} a_\nu^\dagger|0\rangle$, equation (10), yields

$$\langle a_o^\dagger a_o\rangle = \langle 1|_f \int \mathrm{d}\nu\; b_\nu^\dagger b_\nu\; |1\rangle_f = \int \mathrm{d}\nu |f(\nu)|^2 \frac{1}{4}|1 - \mathrm{e}^{\mathrm{i}\nu\Delta\tau}|^2\,, \tag{A.5}$$

which is the same result as that of equation (11) for a single photon normalized wave packet.

Appendix B. Toy models

Both experimental proposals discussed in this work are formulated within the framework of quantum mechanics in curved space-time. No effects specific to this theory have been experimentally verified so far—bridging this gap remains the principal motivation behind our work. Quite generally, new physics is expected only at the scale where gravity itself could no longer be described within a classical theory. However, the tension between quantum mechanics and general relativity is of conceptual nature. Both theories stress that only operationally well defined notions may have physical meaning and this concerns also the notion of time (or proper time in general relativity). However, in contrast to general relativity, in quantum mechanics any degree of freedom of a physical system can be in a superposition and thus becomes undefined (beyond the classical probabilistic uncertainty). More generally—the theory allows for physical states that cannot be described within any local realistic model. If this

applies to the degrees of freedom on which our operational treatment of time relies—the latter becomes classically undefined. This can be the case even when space-time itself can still be described classically, like in the proposals discussed in this paper. One could, however, take an opposite view and assume that whenever space-time itself is classical, the time for any system, that constitutes an operationally defined clock, should admit a classical description as well. The tension between these two views motivates the investigation of theoretical frameworks alternative to quantum mechanics in curved space time. Here we sketch an explicit example of such an alternative toy theory, which can be tested by the experiment proposed in this work.

Relevant for the present problem is how the physical degrees of freedom evolve on a curved background. In the standard approach such evolution results in entanglement between the spatial mode of the wavefunction and other degrees of freedom. There is no well-defined time that such degrees of freedom experience and even a Bell-type experiment can be designed in which any local realistic model of time can be refuted (the details of this study will be published elsewhere). This entanglement results from the coupling $\hat{H}_{\rm vis} = \hat{H}_s \frac{V(\hat{r})}{c^2}$, see equation (16), and is the reason for the drop in the interferometric visibility (for both massive and massless cases of the experimental proposal discussed in this work). All so far observed gravitational effects can, however, be explained with one of two possible effective forms of such an interaction, which reproduce only specific features of (16) and correspond to different physical effects.

The effective coupling $\hat{H}_{\rm phase} = \langle \hat{H}_s \rangle \frac{V(\hat{r})}{c^2}$, see equation (15), reproduces correctly the gravitational phase shift effect of the standard theory, but not the time dilation. Applying the operator (15) to the state of the clock degree of freedom $|\tau\rangle$ in a spatial superposition of two locations r_1 and r_2, $|\Psi\rangle = \frac{1}{\sqrt{2}}(|r_1\rangle + |r_2\rangle)|\tau\rangle$, we get

$$\hat{H}_{\rm phase}|\Psi\rangle = \frac{\langle \hat{H}_s \rangle}{\sqrt{2}} \left(\frac{V(r_1)}{c^2}|r_1\rangle + \frac{V(r_2)}{c^2}|r_2\rangle \right)|\tau\rangle,$$

where $\langle \hat{H}_s \rangle = \langle \tau | \hat{H}_s | \tau \rangle$. The full evolution in such a toy model is given by the Hamiltonian $\hat{H}_s + \hat{H}_{ps}$, which yields

$$|\Psi(t)\rangle = \mathrm{e}^{-\frac{\mathrm{i}}{\hbar}(\hat{H}_s + \hat{H}_{\rm phase})t}|\Psi\rangle = \frac{1}{\sqrt{2}}\left[\mathrm{e}^{-\frac{\mathrm{i}}{\hbar}(\langle \hat{H}_s \rangle \frac{V(r_1)}{c^2})t}|r_1\rangle + \mathrm{e}^{-\frac{\mathrm{i}}{\hbar}(\langle \hat{H}_s \rangle \frac{V(r_2)}{c^2})t}|r_2\rangle\right]|\tau(t)\rangle, \tag{B.1}$$

where $|\tau(t)\rangle = \mathrm{e}^{-\frac{\mathrm{i}}{\hbar}\hat{H}_s t}|\tau\rangle$ and thus the evolution of the clock degree of freedom $|\tau\rangle$ does not depend on the position r. Hence, the coupling (15) predicts no general relativistic time dilation and no drop in the interferometric visibility—the clock degree of the freedom remains factorized from the spatial modes. However, each mode acquires a phase proportional to the gravitational potential and an effective mass defined by $\langle \hat{H}_s \rangle$, hence this effective coupling reproduces the relative phase shift measured in interference experiments. For a particle of mass m, $\hat{H}_s = mc^2 + \hat{H}_{\rm int}$ (to first order in $1/c^2$), where $\hat{H}_{\rm int}$ is the Hamiltonian of the internal degrees of freedom and thus one obtains $m + \frac{\langle \hat{H}_{\rm int} \rangle}{c^2}$ for the effective mass. The first term is simply the Newtonian mass, while the second is a relativistic correction. For a single photon mode with a frequency ω, $\hat{H}_s = \hbar\omega a^\dagger a$ and therefore the whole contribution to the phase shift comes from $\frac{\langle \hat{H}_s \rangle}{c^2} = \frac{\hbar\omega}{c^2}$. Thus, any measurement of the gravitational phase shift for photons would represent a signature of a non-Newtonian effective mass. However, no measurement of the phase shift (in the massive or massless case) could represent a measurement of the time dilation, since the phase shifts are explainable by the coupling (15) which does not cause clocks at different potentials to tick at different rates.

A different effective coupling can explain all classical general relativistic effects observed so far. It includes an effective gravitational potential $\langle V(\hat{r}) \rangle$—gravitational potential smeared over the support of the wavefunction of a single physical system. Such a coupling reads

$$\hat{H}_{\rm loc} = \hat{H}_s \frac{\langle V(\hat{r}) \rangle}{c^2} \tag{B.2}$$

and it accounts for gravitational experiments in which the relevant degrees of freedom are sufficiently well localized. These include not only classical tests of general relativity [2–5], but also experiments measuring the time dilation between two *localized* atomic clocks, each at a different gravitational potential.

More generally, one can construct a toy model by combining the above effective couplings $\hat{H}_{\text{phase}}$ and $\hat{H}_{\text{loc}}$, for example

$$\hat{H}_i^{\text{eff}} = \hat{H}_s\left(1 + \frac{\langle V(\hat{r})\rangle}{c^2}\right) + \frac{\Delta N_i}{\langle \hat{N}_i\rangle}\left(\langle \hat{H}_s\rangle \frac{V(\hat{r})}{c^2} - \hat{H}_s\frac{\langle V(\hat{r})\rangle}{c^2}\right), \tag{B.3}$$

which governs the evolution of the ith mode of a quantum state (one can associate different modes to e.g., different paths of a Mach–Zehnder interferometer). $\hat{N}_i$ is the number operator in mode i and ΔN_i is its standard deviation. The parameter $\frac{\Delta N_i}{\langle \hat{N}_i\rangle}$ quantifies how well the quantum state is localized. It vanishes for Fock states (e.g. for a pair of atoms or photons, each in one, localized mode), and in the limit of large coherent states (for a coherent state $|\alpha\rangle$ in mode i we have $\frac{\Delta N_i}{\langle \hat{N}_i\rangle} = \frac{1}{|\alpha|} \to 0$ for $\alpha \to \infty$), which for photons corresponds to classical light. In both cases the Hamiltonian (B.3) reduces to $\hat{H}_s(1 + \frac{\langle V(\hat{r})\rangle}{c^2})$. In the other limit, when the parameter $\frac{\Delta N_i}{\langle \hat{N}_i\rangle} = 1$, which is the case for a single particle in a superposition of two modes, the effective Hamiltonian reduces to $\hat{H}_s + \langle \hat{H}_s\rangle \frac{V(\hat{r})}{c^2}$. The toy model (B.3) predicts no drop in the interferometric visibility for a particle in a spatial superposition (since in the relevant limit the energy *operator* $\hat{H}_s$ does not couple to the potential) but is still consistent with the experiments carried out so far. (Moreover, it can be generalized beyond the above weak energy limit.)

The difference between the standard extension of quantum mechanics to curved space-time and the toy model (B.3) can only be tested with a quantum system from which the time can be read out and which is put in a coherent spatial superposition at different gravitational potentials. Even though this model is artificial (e.g., it shares the difficulties of all quantum nonlinear models) it highlights the conceptual difference between gravitational phase shift experiments and measurements of the visibility loss. (While the former only probe the semi-classical coupling of energy to the gravitational potential, the latter directly test the full quantum form of such a coupling.) Most importantly, the toy model emphasizes the necessity of probing quantum mechanics in curved space-time: the results of current experiments cannot necessarily be extrapolated to this regime.

References

[1] Greenberger D M The disconnect between quantum mechanics and gravity arXiv:1011.3719v1 [quant-ph]
[2] Pound R V and Rebka G A 1960 Apparent weight of photons *Phys. Rev. Lett.* **4** 337
[3] Hafele J C and Keating R E 1972 Around-the-world atomic clocks: predicted relativistic time gains *Science* **177** 166–8
[4] Shapiro I I 1964 Fourth test of general relativity *Phys. Rev. Lett.* **13** 789–791
[5] Shapiro I I, Ash M E, Ingalls R P and Smith W B 1971 Fourth test of general relativity: new radar result *Phys. Rev. Lett.* **26** 1132–5
[6] Colella R, Overhauser A W and Werner S A 1975 Observation of gravitationally induced quantum interference *Phys. Rev. Lett.* **34** 1472–4
[7] Peters A, Chung K Y and Chu S 1999 Measurement of gravitational acceleration by dropping atoms *Nature* **400** 849–52
[8] Zych M, Costa F, Pikovski I and Brukner Č 2011 Quantum interferometric visibility as a witness of general relativistic proper time *Nature Commun.* **2** 505
[9] Sinha S and Samuel J 2011 Atom interferometers and the gravitational redshift *Class. Quantum Grav.* **28** 145018
[10] Englert B-G 1996 Fringe visibility and which-way information: an inequality *Phys. Rev. Lett.* **77** 2154–7

[11] Wootters W K and Zurek W H 1979 Complementarity in the double-slit experiment: quantum nonseparability and a quantitative statement of Bohr's principle *Phys. Rev.* D **19** 473–84
[12] Greenberger D M and Yasin A 1988 Simultaneous wave and particle knowledge in a neutron interferometer *Phys. Lett.* A **128** 391–4
[13] Aharonov Y and Bohm D 1959 Significance of electromagnetic potentials in the quantum theory *Phys. Rev* **115** 485–91
[14] Ho V B and Morgan M J 1994 An experiment to test the gravitational Aharonov–Bohm effect *Aust. J. Phys.* **47** 245–52
[15] Müller H, Peters A and Chu S A 2010 Precision measurement of the gravitational redshift by the interference of matter waves *Nature* **463** 926–9
[16] Fray S, Diez C A, Hänsch T W and Weitz M 2008 Atomic interferometer with amplitude gratings of light and its applications to atom based tests of the equivalence principle *Phys. Rev. Lett.* **93** 240404
[17] Dimopoulos S, Graham P W, Hogan J M and Kasevich M A 2008 General relativistic effects in atom interferometry *Phys. Rev.* D **78** 042003
[18] Müller H, Chiow S-W, Herrmann S and Chu S 2008 Atom-interferometry tests of the isotropy of post-Newtonian gravity *Phys. Rev. Lett.* **100** 031101
[19] Birrell N D and Davies P C W 1982 *Quantum Fields in Curved Space* (Cambridge: Cambridge University Press)
[20] Tanaka K 1983 How to detect the gravitationally induced phase shift of electromagnetic waves by optical-fiber interferometry *Phys. Rev. Lett* **51** 378–80
[21] Hübel H *et al* 2007 High-fidelity transmission of polarization encoded qubits from an entangled source over 100 km of fiber *Opt. Express* **15** 7853–62
[22] Mosley P J *et al* 2008 Heralded generation of ultrafast single photons in pure quantum states *Phys. Rev. Lett* **100** 133601
[23] Sansone G, Poletto L and Nisoli M 2011 High-energy attosecond light sources *Nature Photon.* **5** 655–63
[24] Gallmann L, Cirelli C and Keller U 2012 Attosecond science: recent highlights and future trends *Annu. Rev. Phys. Chem.* **63** 447–69
[25] Matsuda N *et al* 2009 Observation of optical-fibre Kerr nonlinearity at the single-photon level *Nature Photon.* **3** 95–8
[26] Xiang G Y *et al* 2011 Entanglement-enhanced measurement of a completely unknown optical phase *Nature Photon.* **5** 4347
[27] Ghosh R, Hong C K, Ou Z Y and Mandel L 1986 Interference of two photons in parametric down conversion *Phys. Rev.* A **34** 3962–8
[28] Neder I, Heiblum M, Mahalu D and Umansky V 2007 Entanglement, dephasing, and phase recovery via cross-correlation measurements of electrons *Phys. Rev. Lett.* **98** 036803
[29] Franson J D 1989 Bell inequality for position and time *Phys. Rev. Lett.* **62** 2205
[30] Aerts S, Kwiat P, Larsson J-Å and Żukowski M 1999 Two-photon Franson-type experiments and local realism *Phys. Rev. Lett.* **83** 2872
[31] Ralph T C, Milburn G J and Downes T 2009 Quantum connectivity of space-time and gravitationally induced de-correlation of entanglement *Phys. Rev.* A **79** 022121

5.5 Universal decoherence due to gravitational time dilation

This work describes one of the major results that I obtained during my PhD on the interplay between time dilation and quantum theory. It is shown that time dilation causes universal decoherence of all composite quantum systems. In contrast to our previous works, here we considered arbitrary composite systems with no internal clocks. Surprisingly, time dilation has a profound impact on sufficiently large quantum systems: all coherence is destroyed due to thermal internal oscillations. Time dilation induces a universal coupling between internal degrees-of-freedom and the centre-of-mass of a composite particle and we show that the resulting entanglement causes the particle's position to decohere. We derive the decoherence timescale and show that the weak time dilation on Earth is already sufficient to decohere micro-scale objects. The analysis includes a full master equation that describes any dynamic evolution of a composite system in the presence of gravity in the weak field limit. Completely isolated composite systems decohere in the presence of time dilation, since no coupling to an external environment is necessary and only the internal structure is responsible for the decoherence effect. In contrast to so-called gravitational collapse models, no modification of quantum theory is assumed and the decoherence arises entirely within the framework of quantum theory and weak gravity. General relativity therefore can account for the emergence of classicality. We show that it is challenging to experimentally isolate the effect but that it can in principle be tested in future matter wave interference experiments with large molecules or with microspheres.

Our overall results on time dilation, discussed in the three manuscripts, show that the interplay between quantum theory and general relativity affects even low-energy quantum systems and that it offers novel phenomena. Our works also pave the way for novel ways to explore this interplay in quantum optical experiments.

I made leading contributions to all aspects of the research project.

Universal decoherence due to gravitational time dilation

Igor Pikovski,[1,2,*] Magdalena Zych,[1,2] Fabio Costa,[1,2] and Časlav Brukner[1,2]

[1] *University of Vienna, Faculty of Physics, Vienna Center for Quantum Science and Technology (VCQ), Boltzmanngasse 5, A-1090 Vienna, Austria*

[2] *Institute for Quantum Optics and Quantum Information (IQOQI), Austrian Academy of Sciences, Boltzmanngasse 3, Vienna A-1090, Austria*

Phenomena inherent to quantum theory on curved space-time, such as Hawking radiation [1], are typically assumed to be only relevant at extreme physical conditions: at high energies and in strong gravitational fields. Here we consider low-energy quantum mechanics in the presence of weak gravitational time dilation and show that the latter leads to universal decoherence of quantum superpositions. Time dilation induces a universal coupling between internal degrees of freedom and the centre-of-mass of a composite particle and we show that the resulting entanglement causes the particle's position to decohere. We derive the decoherence timescale and show that the weak time dilation on Earth is already sufficient to decohere micro-scale objects. No coupling to an external environment is necessary, thus even completely isolated composite systems will decohere in the presence of time dilation. In contrast to gravitational collapse models [2, 3], no modification of quantum theory is assumed. General relativity therefore can account for the emergence of classicality and the effect can in principle be tested in future matter wave experiments with large molecules [4, 5] or with trapped microspheres [6–8].

The superposition principle is a major cornerstone of quantum mechanics. Quantum interference experiments have demonstrated superpositions of neutrons [9], atoms [10] and even large molecules [4, 5], however, quantum superpositions are not accessible on human scales. The origin of the quantum-to-classical transition is still an active field of research and a prominent role in this transition is commonly attributed to decoherence [11, 12]: due to interaction with an external environment, a particle loses its quantum coherence. Many specific models have been studied in which a particle interacts with its environment, such as for example scattering with surrounding phonons [13], photons [14] and gravitational waves [15–17]. A different approach in explaining classicality is taken in so-called "collapse models", in which macroscopic superpositions are prohibited without any external environment [2, 3]. Such models are often inspired by general relativity but they all rely on a postulated breakdown of quantum mechanics. In contrast, here we show the existence of decoherence due to general relativistic time dilation without any modification of quantum mechanics and which takes place even for isolated composite systems. We show that even the weak time dilation on Earth is already sufficient to decohere the position of micro-scale composite quantum systems.

To derive the decoherence we consider standard quantum mechanics in the presence of general-relativistic time dilation, which causes clocks to run slower near a massive object. A derivation of the quantum dynamics of a composite system on an arbitrary background space-time can be found in Appendix A. Here we consider weak gravitational fields (i.e. to lowest order in c^{-2}), in which case the results follow directly from the mass-energy equivalence [18]: any internal energy contributes to the total weight of a system and gravity couples to the total mass $m_{\rm tot} = m + H_0/c^2$, where the Hamiltonian H_0 generates the time evolution of the internal degrees of freedom of this particle and m is the remaining static rest mass. The interaction with the gravitational field is therefore $m_{\rm tot}\Phi(x) = m\Phi(x) + H_{int}$, where $H_{int} = \Phi(x)H_0/c^2$. For example, if the particle is a simple harmonic oscillator with frequency ω, the above interaction with gravity effectively changes the frequency according to $\omega \to \omega(1 + \Phi(x)/c^2)$. This is the well-known gravitational redshift to lowest order in c^{-2}. Classically, the time-dilation-induced interaction H_{int} yields only this frequency shift. On the other hand, in quantum mechanics the internal energy H_0 and the position x are quantized operators, thus time dilation causes an additional, purely quantum mechanical effect: entanglement between the internal degrees of freedom and the centre-of-mass position of the particle[19]. Even though the time dilation on Earth is very weak, the induced entanglement leads to a significant effect for composite quantum systems, as we will show below.

We consider composite particles subject to gravitational time dilation and model them by having $N/3$ constituents that are independent three dimensional harmonic oscillators. Such a model equivalently describes N internal harmonic modes of the particle. The internal Hamiltonian for this system is $H_0 = \sum_{i=1}^{N} \hbar\omega_i n_i$, where n_i are the number operators for the i-th mode with frequency ω_i. The centre-of-mass (with x and p being its vertical position and momentum, respectively) of the whole system is subject to the gravitational potential $\Phi(x)$. For a homogeneous gravitational field in the x-direction we can approximate $\Phi(x) = gx$, where $g = 9.81\ \mathrm{m/s^2}$ is the gravitational acceleration on earth. The total Hamiltonian is therefore $H = H_{cm} + H_0 + H_{int}$, where H_{cm} is the Hamiltonian for the centre-of-mass of the particle and the time-dilation-induced interaction (to

* igor.pikovski@univie.ac.at

lowest order in c^{-2}) between position and internal energy is

$$H_{int} = \Phi(x)\frac{H_0}{c^2} = \hbar\frac{gx}{c^2}\left(\sum_{i=1}^{N}\omega_i n_i\right). \quad (1)$$

Before deriving the resulting master equation that governs the full time evolution of the centre-of-mass of the particle, we first discuss a simplified case which already captures the time-dilation-induced decoherence: a particle at rest in superposition of two vertically distinct positions x_1 and x_2 and a height difference $\Delta x = x_2 - x_1$. The centre-of-mass is in the state $|\psi_{cm}(0)\rangle = \frac{1}{\sqrt{2}}(|x_1\rangle + |x_2\rangle)$. The internal degrees of freedom are in thermal equilibrium at temperature T, thus the i-th constituent is in the state $\rho_i = \frac{1}{\pi\bar{n}_i}\int d^2\alpha_i \exp(-|\alpha_i|^2/\bar{n}_i)|\,\alpha_i\rangle\langle\alpha_i\,|$, where we used the coherent state representation, $\bar{n}_i = (e^{\hbar\omega_i/k_BT}-1)^{-1}$ is the average excitation and k_B is the Boltzmann constant. The total initial state is thus given by $\rho(0) = |\,\psi_{cm}(0)\rangle\langle\psi_{cm}(0)\,| \otimes \prod_{i=1}^{N}\rho_i$. General relativistic time dilation now couples the centre-of-mass position of the system to the internal degrees of freedom ρ_i via the Hamiltonian in Eq. (1) (for now we consider the particle stationary in a Newtonian gravitational potential and neglect any additional dynamics of the centre-of-mass). The off-diagonal elements $\rho_{12} = \langle x_1\,|\rho|\,x_2\rangle = \rho_{21}^*$, responsible for quantum interference, therefore evolve in time as

$$\rho_{12}(t) = \frac{1}{2\pi\bar{n}_i}e^{img\Delta x t}\prod_{i=1}^{N}\int d^2\alpha_i e^{-|\alpha_i|^2/\bar{n}_i}|\,\alpha_i^{(1)}\rangle\langle\alpha_i^{(2)}\,| \quad (2)$$

where $\alpha_i^{(1)} = \alpha_i e^{-i\omega_i t(1+\frac{gx_1}{c^2})}$ and $\alpha_i^{(2)} = \alpha_i e^{-i\omega_i t(1+\frac{gx_2}{c^2})}$. The individual internal states can be seen as clocks (discussed in more detail in the Methods Section) and evolve at different frequencies according to gravitational time dilation (see also Fig. 1). To see decoherence of the centre-of-mass position, we trace out the internal degrees of freedom. The quantum coherence, quantified by the visibility $V(t) = 2|\rho_{cm}^{(12)}(t)| = 2|\Pi_{i=1}^{N}\mathrm{Tr}_i[\rho_{12}(t)]|$, becomes $V(t) = \left|\prod_{i=1}^{N}\left[1+\bar{n}_i\left(1-e^{-i\omega_i tg\Delta x/c^2}\right)\right]^{-1}\right|$. This expression can be simplified for the typical case $\omega_i tg\Delta x/c^2 \ll 1$. In the high temperature limit we also have $\bar{n}_i \approx \frac{k_BT}{\hbar\omega_i}$, so that the frequency-dependence completely drops out from the visibility. In this case, the reduction of quantum interference is given by

$$V(t) \approx \left(1+\left(\frac{k_BTg\Delta x t}{\hbar c^2}\right)^2\right)^{-N/2} \approx e^{-(t/\tau_{dec})^2}, \quad (3)$$

where we used $t^2 \ll N\tau_{\mathrm{dec}}^2$ and defined the decoherence time

$$\tau_{dec} = \sqrt{\frac{2}{N}}\frac{\hbar c^2}{k_BTg\Delta x}. \quad (4)$$

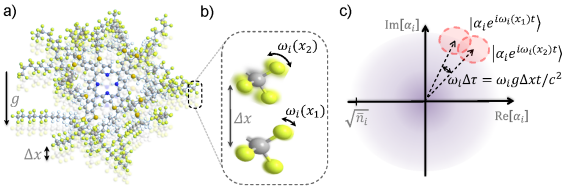

FIG. 1. Gravitational time dilation causes decoherence of composite quantum systems. a) Illustration of a TPPF20 molecule which has recently been used for matter-wave interference [5]. Here we illustrate a vertical superposition of size Δx in Earth's gravitational potential $\Phi(x) = gx$. b) The frequencies ω_i of internal oscillations get red-shifted in the gravitational field, i.e. $\omega_i \to \omega_i(1+gx/c^2)$. The internal oscillations entangle to the centre-of-mass position of the molecule. c) Phase-space representation of the i-th constituent which is in a thermal state with average occupation $\bar{n}_i \approx k_BT/\hbar\omega_i$. In the coherent state representation, the frequency of each coherent state depends on the position of the molecule and the internal states corresponding to the two superposition amplitudes evolve differently by an amount $\omega_i\Delta\tau$. Even for small time-dilations, this causes decoherence of the molecule with N constituents after a time τ_{dec}, given in eq. (4).

The above equation shows that gravitational time dilation causes superpositions of composite systems to decohere. The decoherence rate derived here scales linearly with the superposition size Δx, in contrast to other decoherence mechanisms that typically show a quadratic scaling [20]. Also, decoherence due to gravitational time dilation depends on the number of oscillating internal states of the system, N. Thus the suppression of quantum effects takes place even for completely isolated systems, provided that the superposition amplitudes acquire a proper time difference. In the high temperature limit the frequencies of the internal oscillations drop out entirely from the final expression, therefore it is not necessary to have fast-evolving internal states. Note that the decoherence derived here depends on the constants $\hbar$, c, k_B and the gravitational acceleration g: it can therefore be considered a relativistic, thermodynamic and quantum mechanical effect.

The arguments presented above can be made more rigorous by considering the full time evolution in the presence of relativistic time dilation. To this end, we derive in the Methods Section a master equation that describes the quantum dynamics of a composite system on a background space-time to lowest non-vanishing order in c^{-2}. The derivation is fully general and captures special and general relativistic time dilation for any space-time and any internal Hamiltonian H_0. The overall time-dilation-induced coupling between the internal Hamiltonian and the centre-of-mass is given by $H_{int} = H_0\Gamma(x,p)/c^2$, where $\Gamma(x,p) = \Phi(x) - p^2/2m^2$. For the composite par-

ticle as modelled here the master equation becomes

$$\dot{\rho}_{cm}(t) = -\frac{i}{\hbar}\left[H_{cm} + \frac{Nk_BT}{c^2}\Gamma(x,p), \rho_{cm}(t)\right] - N\left(\frac{k_BT}{\hbar c^2}\right)^2 \times \\ \times \int_0^t ds \left[\Gamma(x,p), e^{-iH_{cm}s/\hbar}\left[\Gamma(x,p), \rho_{cm}(t-s)\right] e^{iH_{cm}s/\hbar}\right]. \tag{5}$$

This equation describes the time evolution of the centre-of-mass of a composite particle in the presence of time dilation. The first term describes the unitary evolution of the centre-of-mass due to an arbitrary Hamiltonian H_{cm}, which is completely general and can also include external interactions (as for example those necessary for keeping the particle in superposition or realizing an interference experiment) as well as relativistic corrections to the centre-of-mass dynamics. The second term causes the suppression of off-diagonal elements of the density matrix and is responsible for the decoherence. The integral captures the fact that decoherence depends on the overall acquired proper time difference during a particle's evolution. For a stationary system, and if the centre-of-mass Hamiltonian H_{cm} does not induce significant changes to the off-diagonal elements on the decoherence time scale, the above equation can be approximated by

$$\dot{\rho}_{cm}(t) \approx -\frac{i}{\hbar}\left[\tilde{H}_{cm} + \left(m + \frac{Nk_BT}{c^2}\right) gx, \rho_{cm}(t)\right] - \\ - Nt\left(\frac{k_BTg}{\hbar c^2}\right)^2 [x,[x,\rho_{cm}(t)]]\,. \tag{6}$$

In the unitary part we have separated for clarity the Newtonian gravitational potential (i.e. $H_{cm} = \tilde{H}_{cm} + mgx$): It is evident that the potential couples to an effective total mass $m_{\rm tot} = m + \bar{E}/c^2$ that includes the average internal energy $\bar{E} = \langle H_0 \rangle = Nk_BT$. This is in accordance with the notion of heat in general relativity (in Einstein's words [21]: "a piece of iron weighs more when red-hot than when cool"). The non-unitary part now depends only on the stationary x-contributions (see also Fig. 2a). The decoherence time scale is found from the solution to eq. (6), which for the off-diagonal terms $\rho_{cm}^{(12)}$ is approximately (to order $O(\hbar^{-2})$): $\rho_{cm}^{(12)}(t) \sim \rho_{cm}^{(12)}(0)\, e^{-(t/\tau_{dec})^2}$, with $\tau_{\rm dec}$ as in eq. (4). The reduction of visibility is Gaussian and agrees with eq. (3). The master equation due to gravitational time dilation, eq. (6), is similar in form to other master equations typically studied in the field of decoherence [11, 20] but does not include any dissipative term. Thus time dilation provides naturally an "ideal" master equation for decoherence that suppresses off-diagonal terms in the position basis for stationary particles. For non-stationary systems, decoherence is governed by eq. (5) and the pointer basis derives from a combination of x and p. The master equation for gravitational time dilation differs from other decoherence mechanisms mainly by being inherently non-Markovian, since the overall acquired proper time difference is crucial. It causes a Gaussian decay (rather than an exponential decay in Markovian models) of the off-diagonal

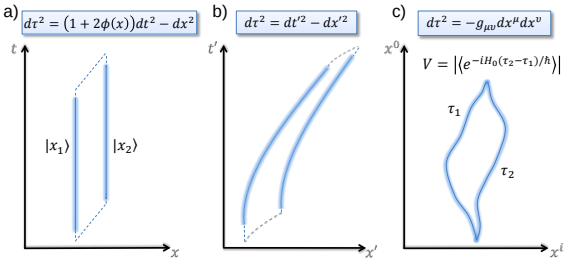

FIG. 2. A composite particle in superposition will decohere due to time dilation. The figure shows two superposed trajectories in different situations and space-times (here c=1). a) A particle in superposition at two different fixed heights above the earth, as considered in the main text (the dashed lines represent arbitrary small non-stationary contributions that would be necessary if one performs an interferometric experiment). The centre-of-mass will decohere after a time τ_{dec} as given in eq. (4). In general, the full evolution of the centre-of-mass is given by eq. (5). b) A particle undergoing uniform acceleration g in flat space-time will experience the same time dilation and thus the same decoherence. Equivalently, the diagram describes the previous situation from the point of view of a freely-falling observer. c) A composite particle with internal Hamiltonian H_0 in an arbitrary space-time will decohere if the two superposed trajectories differ in proper time (V is the interferometric visibility).

elements and yields a very specific form and parameter dependence of the decoherence time scale, eq. (4).

To estimate the strength of the decoherence due to time dilation, we consider a human-scale macroscopic system at room temperature. Assuming that the system has Avogadro's number of constituent particles which oscillate, we set $N \sim 10^{23}$, which amounts to a gram-scale system. For a superposition size of $\Delta x = 10^{-3}$ m, the decoherence time (4) becomes

$$\tau_{\rm dec} \approx 10^{-6} s\,. \tag{7}$$

Remarkably, even though the gravitational time dilation is very weak, its resulting decoherence is already substantial on human scales and not just for astrophysical objects. Macroscopic objects completely decohere on Earth on a short timescale due to gravitational time dilation. In contrast to other decoherence mechanisms, this effect cannot be shielded and decoherence will occur whenever there is time dilation between superposed amplitudes. Therefore future ground-based quantum interference experiments with large, complex systems can operate only if the superposed amplitudes have exactly vanishing proper time difference. In astrophysical settings, the decoherence can even be substantially stronger: the time scale (4) can be rewritten in terms of the Schwarzschild-radius $R_s = 2GM/c^2$ of the background space-time as $\tau_{\rm dec} = \sqrt{8/N}(\hbar R^2/k_BTR_s\Delta x)$, where R is the distance between the particle and the centre of the gravitating object (since the nature of the effect is gravitational, quantum mechanical and thermodynamic,

the decoherence time may also be written in terms of the Hawking-temperature [1] $T_H = \hbar c^3/8\pi k_B GM$ of the body with mass M, but the decoherence is not related to any horizon and the appearance of the Hawking temperature is solely a reformulation of the fundamental constants involved). The decoherence is stronger for high masses M and for small distances R to the mass, i.e. for stronger time dilation. At the horizon of a black hole with 5 solar masses, a nm-size superposition of a gram-scale object at $T = 1$ K would decohere after about $\tau_{\rm dec} \approx 1$ ns.

The effect predicted here is completely general and affects arbitrary quantum states on all space-time metrics: a composite quantum system in superposition between two arbitrary trajectories with proper time difference $\Delta\tau$ will decohere (see Fig. 2). For example, for a particle in superposition of semi-classical (i.e. well-localised) trajectories, the state of the centre-of-mass can easily be calculated as in the derivation of eq. (3) above: the visibility of the off diagonal elements will drop according to $V = \left|\left\langle e^{-iH_0\Delta\tau/\hbar}\right\rangle\right|$, where the mean is taken with respect to all internal states ρ_i. This holds for arbitrary internal states and proper time-differences $\Delta\tau$, so long as the individual trajectories are well-localised. Since time dilation is universal, all composite quantum systems are affected, independently of the nature and kind of their internal energy. The transition to classicality can only be avoided experimentally if paths with no time dilation are chosen or all internal degrees of freedom are frozen out.

We stress that the decoherence effect described here is not related to previously considered general relativistic models of decoherence [2, 3, 15–17, 22]. The mechanism here is time dilation, which arises already in stationary space-times and decoheres composite systems into the position basis, even if they are isolated from any external environment. This is conceptually different than previously considered scattering of gravitational waves [15–17], which causes decoherence into the energy basis. Our treatment, based on a Hamiltonian formulation of low-energy quantum systems on a fixed background space-time, allows for a direct description of composite quantum systems in weak, static gravitational fields and no assumptions about the matter field distribution or about a gravitational wave background are necessary. We also stress that the time-dilation-induced decoherence is entirely within the framework of quantum mechanics and classical general relativity. This is in stark contrast to hypothetical models where gravity leads to spontaneous collapse of the wave function and that require a breakdown of unitarity [2, 3] or include stochastic fluctuations of the metric [22]. Thus we show that general relativity can account for the suppression of quantum behavior for macroscopic objects without introducing any modifications to quantum mechanics or to general relativity.

We now discuss a possible direct experimental verification of the derived decoherence mechanism. The gravitational time dilation is well tested in classical physics but the quantized Hamiltonian has not yet been studied

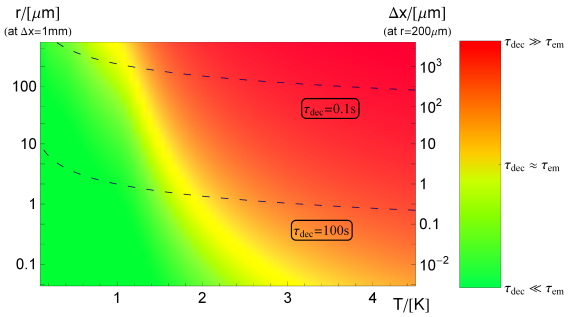

FIG. 3. Decoherence due to gravitational time dilation as compared to decoherence due to emission of thermal radiation for sapphire microspheres. In the green region time dilation is the dominant decoherence mechanism. The left axis shows various sphere radii r (corresponding to particle numbers $N = 10^7$ to $N = 10^{18}$) for a fixed superposition size Δx, whereas the right axis shows various superposition sizes for a fixed particle radius. The dashed lines correspond to the respective time dilation decoherence timescales. Sapphire was chosen for its low emission at microwave frequencies.

experimentally. In particular, an experiment to study the induced quantum entanglement of internal degrees of freedom with the centre-of-mass mode, first proposed in Ref. [19], has not yet been realised. To confirm this quantum mechanical interaction one can use controllable internal states in matter wave interferometry [19], or use Shapiro-delay in single photon interference [23]. Such an experimental verification of the quantum Hamiltonian (1) would be a strong indication for the presence of the decoherence described here. To test the decoherence due to time dilation directly it is necessary to bring relatively complex systems into superposition. This can in principle be achieved with molecule interferometry [4, 5], trapped microspheres [6–8] or with micromechanical mirrors [24, 25]. The latter, however, is currently restricted to very small separations only [25] (on the order of 1 pm) and is therefore less suitable. To see decoherence caused by time dilation, other decoherence mechanisms will need to be suppressed: The scattering with surrounding molecules and with thermal radiation requires such an experiment to be performed at liquid Helium temperatures and in ultra-high vacuum [14], which has no direct effect on the decoherence due to time dilation. However, the emission of thermal radiation by the system will be a directly competing decoherence source. The decoherence time due to photon emission is found to be [14, 26] $\tau_{\rm em} = (\int dk k^2 c\, g(k)\sigma_{\rm eff}(k)\Delta x^2)^{-1}$, where $g(k)$ is the mode density of the wave vectors k and $\sigma_{\rm eff}(k)$ the effective scattering cross section. To see the time-dilation-induced decoherence, we require that the decoherence due to emission of radiation is weaker than due to time dilation, i.e. $\tau_{\rm dec} \lesssim \tau_{\rm em}$. In Fig. 3 we show the parameter regime where time-dilation-induced decoherence can in principle be distinguished from decoherence

due to thermal emission, focussing on micro-scale particles at cryogenic temperatures (sapphire was chosen due to its low microwave emission at low temperatures [27]). The emission of radiation can be further suppressed if the mode density is reduced, which can ease the restrictions on temperature. Although an experiment to measure decoherence due to proper time is challenging, the rapid developments in controlling large quantum systems [5–8] for quantum metrology and for testing collapse-theories [24, 25, 28–30] will inevitably come to the regime where the time-dilation-induced decoherence predicted here will be of importance. In the long run, experiments on Earth will have to be specifically designed to avoid this decoherence mechanism.

As a final remark, we note that the presented estimate for the time-dilation-induced decoherence is likely to be an underestimation of the actual effect. The internal structure of the constituents is not taken into account and additional mechanisms, such as nuclear processes, may contribute to the decoherence effect. Additionally, special relativistic time dilation and the decoherence during the build-up of the superposition were neglected. We therefore expect that the actual decoherence due to time dilation is even stronger than predicted here.

ACKNOWLEDGMENTS

We thank M. Arndt, M. Aspelmeyer and M. Vanner for discussions and S. Eibenberger for providing us with the illustration of the TPPF20 molecule. This work was supported by the the Austrian Science Fund (FWF) through the doctoral program Complex Quantum Systems (CoQuS), the SFB FoQuS and the Individual Project 24621, by the Foundational Questions Institute (FQXi), the John Templeton Foundation and by the COST Action MP1209.

[1] Hawking, S. Black hole explosions. *Nature* **248**, 30 (1974).
[2] Penrose, R. On Gravity's role in Quantum State Reduction. *Gen. Relat. Gravit.* **28**, 581-600 (1996).
[3] Diósi, L. Models for universal reduction of macroscopic quantum fluctuations. *Phys. Rev. A* **40**, 1165-1174 (1989).
[4] Arndt, M. *et al.* Waveparticle duality of C60 molecules. *Nature* **401**, 680-682 (1999).
[5] Eibenberger, S., Gerlich, S., Arndt, M., Mayor, M. and Tüxen, J. Matter-wave interference with particles selected from a molecular library with masses exceeding 10 000 amu. *Phys. Chem. Chem. Phys.* **15**, 14696 (2013).
[6] Li, T., Kheifets, S. and Raizen, M. G. Millikelvin cooling of an optically trapped microsphere in vacuum, *Nature Phys.* **7**, 527-530 (2011).
[7] Kiesel, N., *et al.* Cavity cooling of an optically levitated submicron particle. *Proc. Natl. Acad. Sci. USA* **110**, 14180-14185 (2013).
[8] Asenbaum, P., Kuhn, S., Nimmrichter, S., Sezer, U. and Arndt, M. Cavity cooling of free Si nanospheres in high vacuum. *Nature Commun.* **4**, 2743 (2013).
[9] Colella, R., Overhauser, A. W. and Werner, S. A. Observation of Gravitationally Induced Quantum Interference. *Phys. Rev. Lett.* **34**, 1472-1474 (1975).
[10] Chu, S. Laser manipulation of atoms and particles. *Science* **253**, 861-866 (1991).
[11] Giulini, D. *et al. Decoherence and the appearance of a classical world in quantum theory.* Springer, Berlin (1996).
[12] Zurek, W. H. Decoherence, einselection, and the quantum origins of the classical. *Rev. Mod. Phys.* **75**, 715-775 (2003).
[13] Caldeira, A. O. and Leggett, A. J. Path integral approach to quantum Brownian motion. *Physica A* **121**, 587-616 (1983).
[14] Joos, E. and Zeh, H. D. The emergence of classical properties through interaction with the environment. *Z. Phys. B* **59**, 223-243 (1985).
[15] Anastopoulos, C. Quantum theory of nonrelativistic particles interacting with gravity. *Phys. Rev. D* **54**, 1600-1605 (1985).
[16] Lamine, B. and Hervé, R. and Lambrecht, A. and Reynaud, S. Ultimate Decoherence Border for Matter-Wave Interferometry. *Phys. Rev. Lett.* **96**, 050405 (2006).
[17] Blencowe, M. P. Effective Field Theory Approach to Gravitationally Induced Decoherence. *Phys. Rev. Lett.* **111**, 021302 (2013).
[18] Einstein, A. Über den Einfluß der Schwerkraft auf die Ausbreitung des Lichtes. *Ann. Physik* **340**, 898-908 (1911).
[19] Zych, M., Costa, F., Pikovski, I. and Brukner, Č. Quantum interferometric visibility as a witness of general relativistic proper time. *Nature Commun.* **2**, 505 (2011).
[20] Breuer, H.-P. and Petruccione, F. *The Theory of Open Quantum Systems.* Oxford University Press, Oxford (2002).
[21] Einstein, A. and Infeld, L. *The evolution of physics.* Simon and Schuster, New York (1938).
[22] Karolyhazy, F. Gravitation and quantum mechanics of macroscopic objects. *Nuovo Cimento* **42**, 390-402 (1966).
[23] Zych, M., Costa, F., Pikovski, I., Ralph, T. C. and Brukner, Č. General relativistic effects in quantum interference of photons. *Class. Quantum Grav.* **29**, 224010 (2012).
[24] Marshall, W., Simon, C., Penrose, R. and Bouwmeester, D. Towards quantum superpositions of a mirror. *Phys. Rev. Lett.* **91**, 130401 (2003).
[25] Kleckner, D., Pikovski, I. *et al.* Creating and verifying a quantum superposition in a micro-optomechanical system. *New J. Phys.* **10**, 095020 (2009).
[26] Pikovski, I. *On Quantum Superpositions in an Optomechanical System.* Diploma Thesis at Freie Universität Berlin, Berlin (2009).
[27] Lamb, J. W. Miscellaneous data on materials for millimetre and submillimetre optics. *Int. J. Infrared Millimeter*

Waves **17**, 1997-2034 (1996).
[28] Nimmrichter, S., Hornberger, K., Haslinger, P. and Arndt, M. Testing spontaneous localization theories with matter-wave interferometry. *Phys. Rev. A* **83**, 043621 (2011).
[29] Romero-Isart, O. *et al.* Large Quantum Superpositions and Interference of Massive Nanometer-Sized Objects. *Phys. Rev. Lett.* **107**, 020405 (2011).
[30] Bassi, A., Lochan, K., Satin, S., Singh, T. P. and Ulbricht, H. Models of wave-function collapse, underlying theories, and experimental tests. *Rev. Mod. Phys.* **85**, 471-527 (2013).
[31] Kiefer, C. and Singh, T. P. Quantum gravitational corrections to the functional Schrödinger equation. *Phys. Rev. D* **44**, 1067 (1991).
[32] Lämmerzahl, C. A Hamilton operator for quantum optics in gravitational fields. *Phys.Lett. A* **203**, 12-17 (1996).

APPENDIX

A. Hamiltonian for gravitational time dilation

We consider the time evolution of a composite quantum system in the low-energy limit on a generic space-time, described by a static metric $g_{\mu\nu}$ with signature $(-+++)$. For simplicity, we restrict the treatment to stationary metrics with $\partial_0 g_{0\mu} = 0$ and $g_{0i} = 0$, where latin indices refer to the 3-component. The rest energy E_{rest} of a system is invariant and is related to the momentum p_i and to the total energy $cp_0 = E$ by

$$p_\mu p^\mu = g^{\mu\nu} p_\mu p_\nu = -(E_{rest}/c)^2 \,. \tag{8}$$

For a static observer the 4-momentum has only the p_0 contribution and thus the energy of the particle is given by $cp_0 = \sqrt{-g_{00}} E_{rest}$. This expression corresponds to the red-shift, the factor $\sqrt{-g_{00}}$ captures the change in energy as compared to the rest frame of the particle. In other (primed) coordinates with a different metric $g'_{\mu\nu}(x')$, in which in general $p'_i \neq 0$, a different energy cp'_0 will be ascribed to the particle. However, what remains invariant is the scalar $p_\mu dx^\mu = p'_\nu dx'^\nu$. Choosing the unprimed coordinates to be the particles proper coordinates, we therefore have the very general expression $E_{rest} d\tau = p'_0 dx'^0 + p'_i dx'^i$. We stress again that since E_{rest} and the proper time τ are invariant, the energy $cp'_0 = E$ ascribed to the particle and the time evolution with respect to coordinate time are metric-dependent (the notions of time and energy in general relativity are observer-dependent).

Quantization on a curved space-time is achieved by replacing the 4-momenta with co-variant derivatives. For energies small compared to E_{rest} (such that particle creation is negligible), this yields directly a modified Schrödinger equation with the internal energy operator $E_{rest} \to H_0$ and total Hamiltonian $cp_0 \to H$, effectively replacing the time derivative $\partial/\partial t$ by the covariant derivative $D/D\tau$. Equivalently, one can first quantize the expression (8) to obtain a modified Klein-Gordon equation and derive (perturbatively in c^{-2}) the low energy limit of the dynamics of a scalar particle. For a point particle with rest energy mc^2 on a post-Newtonian background metric with $g_{00} = -(1 + 2\Phi(x)/c^2 + 2\Phi^2(x)/c^4)$ and $g_{ij} = \delta_{ij}(1 - 2\Phi(x)/c^2)$, this yields [32]:

$$\begin{aligned} H = mc^2 + \frac{p^2}{2m} + m\Phi(x) - \frac{p^4}{8m^3c^2} + \frac{m\Phi^2(x)}{2c^2} + \\ + \frac{3}{2mc^2}\left(\Phi(x)p^2 + [p\Phi(x)]\,p + \frac{1}{2}\left[p^2\Phi(x)\right]\right) , \end{aligned} \tag{9}$$

where $[p\Phi]$ acts only on the potential. For clarity, the rest mass contribution of the point particle is explicitly kept in the expression. For our purposes, we consider a composite system with an additional internal Hamiltonian that contributes to the rest energy. Since in general relativity there is no distinction between "rest mass" and "rest energy" (in fact, the largest contribution to the rest mass m of the systems we consider, e.g. a molecule, is already given by binding energies between atoms, nucleons, quarks, etc.), the dynamics of an internal degree of freedom can straightforwardly be incorporated into eq. (9): an eigenstate $|\,E_i\rangle$ of the internal dynamics with energy E_i will contribute to the rest energy, which becomes $mc^2 + E_i$. The composite particle will still obey eq. (9), but with $m \to m + E_i/c^2$. This is valid for arbitrary energy eigenstates of the internal Hamiltonian. Due to the linearity of quantum mechanics the full dynamics of the system is therefore given by the above Hamiltonian with the replacement $m \to m + H_0/c^2$, which holds for any arbitrary internal Hamiltonian H_0 (this can be seen as an extension of the mass-energy equivalence to quantum mechanics, discussed in more detail in Ref. [23]). Expanding the result to second order in $1/c^2$, we find

$$H = H_{cm} + H_0\left(1 + \frac{\Gamma(x,p)}{c^2}\right) \tag{10}$$

where H_{cm} includes all terms acting on the centre-of-mass to this order of approximation (and can also include any other interaction, such as the electromagnetic interaction [31]) and $\Gamma(x,p) = \Phi(x) - p^2/2m^2$. Eq. (10) describes in full generality the special and general relativistic corrections to the dynamics of a composite quantum system. Note that the coupling between internal and external degrees of freedom is completely independent of the nature of and kinds of interactions involved in the internal dynamics H_0. This is an expression of the universality of time dilation (or red-shift), which affects all kinds of clocks, irrespectively of their specific construction. The presented formalism allows the study of composite low-energy quantum systems on any fixed background space-time.

B. Master equation due to gravitational time dilation

Here we derive an equation of motion for a composite quantum system in the presence of time dilation. We keep the composition, the centre-of-mass Hamiltonian H_{cm} and the relativistic time dilation completely general. The overall Hamiltonian of the system is $H_{tot} = H_{cm} + H_0 + H_{int}$, where H_0 governs the evolution of the internal constituents and $H_{int} = H_0\Gamma(x,p)/c^2$ captures the time-dilation-induced coupling between internal degrees of freedom and the centre-of-mass to lowest order in c^{-2}. Γ is a function of the centre-of-mass position x and momentum p to which the internal states couple due to special relativistic and general relativistic time dilation (for the Schwarzschild metric in the weak-field limit we have $\Gamma(x,p) = \Phi(x) - p^2/2m^2$). We start with the von Neumann equation for the full state $\dot{\rho} = -i/\hbar\,[H_{tot},\rho]$ and write $H_{tot} = H + H_{int}$, where $H = H_{cm} + H_0$. We change frame to primed coordinates, which we define through $\rho'(t) = e^{it(H+h)/\hbar}\rho(t)e^{-it(H+h)/\hbar}$, where $h = h(x,p) = \Pi_{i=1}^N \mathrm{Tr}_i[H_{int}\rho_i(0)] = \Gamma(x,p)\bar{E}_0/c^2$ with the average internal energy $\bar{E}_0$. The resulting von-Neumann equation is

$$\begin{aligned}\dot{\rho}'(t) &= \frac{i}{\hbar}\left[H'(t)+h'(t),\rho'(t)\right] - \frac{i}{\hbar}\left[H'(t)+H'_{int}(t),\rho'(t)\right] \\ &= -\frac{i}{\hbar}\left[H'_{int}(t)-h'(t),\rho'(t)\right],\end{aligned} \tag{11}$$

where $h'(t) = h(x'(t),p'(t))$. The formal solution $\rho'(t) = \rho'(0) - \frac{i}{\hbar}\int_0^t ds\,[H'_{int}(s)-h'(s),\rho'(s)]$ is used in the equation above, which yields the integro-differential equation for the density matrix

$$\begin{aligned}\dot{\rho}'(t) = &-\frac{i}{\hbar}\left[H'_{int}(t)-h'(t),\rho'(0)\right] - \\ &-\frac{1}{\hbar^2}\int_0^t ds\left[H'_{int}(t)-h'(t),\left[H'_{int}(s)-h'(s),\rho'(s)\right]\right].\end{aligned} \tag{12}$$

We can now trace over the internal degrees of freedom. The state is initially uncorrelated $\rho(0) = \rho_{cm}(0)\otimes\Pi_i^N\rho_i(0)$ and we take the Born approximation, keeping only terms to second order in H_{int}. In this case $\rho'(s)$ can be replaced under the integral by $\rho'_{cm}(s)\otimes\rho_i(0)$ and the master equation for the centre-of-mass becomes

$$\begin{aligned}&\dot{\rho}'_{cm}(t) = \Pi_{i=1}^N\mathrm{Tr}_i[\dot{\rho}'(t)] \\ &\approx \frac{-1}{\hbar^2}\Pi_i\int_0^t ds\,\mathrm{Tr}_i\Big\{\left[H'_{int}(t)-h'(t),\left[H'_{int}(s)-h'(s),\rho'(s)\right]\right]\Big\} \\ &= -\left(\frac{1}{\hbar c^2}\right)^2\Pi_i\int_0^t ds\,\mathrm{Tr}_i\Big\{\left(H_0-\bar{E}_0\right)^2\left[\Gamma'(t),\left[\Gamma'(s),\rho'(s)\right]\right]\Big\} \\ &= -\left(\frac{\Delta E_0}{\hbar c^2}\right)^2\int_0^t ds\,\left[\Gamma'(t),\left[\Gamma'(s),\rho'_{cm}(s)\right]\right].\end{aligned} \tag{13}$$

Here we used the notation $\Delta E_0^2 = \Pi_{i=1}^N\mathrm{Tr}_i\left\{\left(H_0-\bar{E}_0\right)^2\right\} = \left\langle H_0^2\right\rangle - \left\langle H_0\right\rangle^2$ for the energy fluctuations of the internal states and $\Gamma'(s) = \Gamma(x'(s),p'(s))$. Changing back to the original picture, and introducing $s \to t-s$ we obtain the integro-differential equation:

$$\begin{aligned}\dot{\rho}_{cm}(t) = &-\frac{i}{\hbar}\left[H_{cm}+\Gamma(x,p)\frac{\bar{E}_0}{c^2},\rho_{cm}(t)\right] - \\ &-\left(\frac{\Delta E_0}{\hbar c^2}\right)^2\int_0^t ds\left[\Gamma(x,p),\left[\Gamma(x,p),\rho_{cm}(t-s)\right]\big|_s\right],\end{aligned} \tag{14}$$

where $[\Gamma,\rho_{cm}]\big|_s = e^{-isH_{cm}/\hbar}\left[\Gamma,\rho_{cm}\right]e^{isH_{cm}/\hbar}$. This is the general equation of motion for a composite particle of arbitrary composition that undergoes time dilation. The decoherence of its off-diagonal elements is governed by its internal energy spread ΔE_0 and by the metric-dependent coupling Γ. The former is $\Delta E_0^2 \approx N(k_BT)^2$ in the high-temperature limit for $N/3$ non-interacting internal harmonic oscillators and the latter is $\Gamma = \Phi(x) \approx gx$ for stationary particles in the homogeneous weak-field limit of the Schwarzschild metric.

C. Internal degrees of freedom as clocks

The time dilation induced coupling between internal degrees of freedom and the centre-of-mass causes decoherence of the latter. The complementarity principle between the visibility V of interference and the which-path information D is given by the inequality $V^2 + D^2 \leq 1$. The equal sign holds for pure states, i.e. for well-defined clocks as considered in Ref. [19]. For mixed states, it is possible to have loss of visibility with no accessible which-path information, as is the case here (as well as in most other decoherence models such as in quantum Brownian motion [13, 20]). The thermal state of the internal degrees of freedom can be seen as a mixture of clock-states that each measure the proper time along their path. To highlight this, consider for example a particle with a single 2-level internal degree of freedom which is in a clock-state, i.e. in a superposition of the ground and excited state with transition frequency ω and an arbitrary relative phase ϕ: $|\,E_\phi\rangle = \frac{1}{\sqrt{2}}\left(|\,g\rangle + e^{i\phi}|\,e\rangle\right)$. If the particle moves along a path with overall proper time τ, the internal state will evolve to $|\,E_\phi(\tau)\rangle = \frac{1}{\sqrt{2}}\left(|\,g\rangle + e^{i\phi+\omega\tau}|\,e\rangle\right)$. For the particle in superposition along two paths with proper time difference $\Delta\tau$, the internal clock state will therefore acquire which-path information, thus leading to a loss in visibility given by $|\langle E_\phi(\tau_1)\,|\,E_\phi(\tau_2)\rangle| = |\cos(\omega\Delta\tau/2)|$, independent of the phase ϕ. For a fully mixed internal state (analogous to a thermal state),

$$\rho = \frac{1}{2}\left(|\,E_\phi\rangle\langle E_\phi\,| + |\,E_{\phi+\pi}\rangle\langle E_{\phi+\pi}\,|\right), \tag{15}$$

the relative phase between $|\,g\rangle$ and $|\,e\rangle$ is unknown and thus no which-path information is available, but it still

results in a drop in visibility. The above state can be equivalently written in the basis

$$\rho = \frac{1}{2} \left(|\, g\rangle\langle g\,| + |\, e\rangle\langle e\,| \right). \tag{16}$$

Since it represents the same state, it will cause the same loss of visibility, the two situations (15) and (16) cannot be discriminated. The states $|\, g\rangle$ and $|\, e\rangle$ individually, however, are not clock-states, thus no time dilation can be read out directly. The interpretation of the visibility drop in this representation is the phase scrambling between $|\, g\rangle$ and $|\, e\rangle$ due to the red shift, since the states $|\, e\rangle$ acquire a different phase than the states $|\, g\rangle$. Irrespective of the state representation, time dilation will cause decoherence of composite particles with internal degrees of freedom.

Acknowledgements

During my doctoral studies in Vienna, I have received a great deal of support from a variety of people. Most importantly, I am grateful to my supervisor Časlav Brukner for the support and guidance throughout the years. Časlav gave me the unique opportunity to pursue my own scientific ideas, and was always excited and supportive to explore new directions. The many discussions with Časlav have often resulted in completely new insights and his passion for fundamental questions with experimental relevance have been inspirational throughout the years. I am also deeply grateful to Myungshik Kim, who has given me guidance and has been extremely supportive during my doctoral studies. I had been fortunate to work with Myungshik on several projects and have been inspired by his intuition and deep knowledge of quantum optics. His encouragement and deep insights have been a major driving force for my work.

In my doctoral studies I had the exceptional opportunity to interact closely and to collaborate with experimental groups. In particular, I am very grateful to Markus Aspelmeyer with whom I have been working on several projects. Markus' excitement for fundamental questions of physics and his passion for new ideas and novel experiments have led to many stimulating discussions. I am very thankful for his support to pursue new unorthodox ideas. In addition, I would like to thank Anton Zeilinger and Markus Arndt for their assistance and encouragement. Anton served as my thesis advisor and has encouraged me to study new regimes of quantum science. Markus Arndt has always been open for discussions and eager to help with any problem. I am grateful to all three and I feel fortunate to have been able to profit from their great experience and knowledge in quantum research. I also thank Dirk Bouwmeester for introducing me to the fascinating fields of optomechanics, quantum foundations and gravitational phenomena in quantum experiments.

On my first day in Vienna I have met Michael Vanner and we became friends and have been closely working together ever since. In our countless discussions we have explored numerous ideas in great depth and have helped

each other on lots of occasions. I have greatly benefitted from these discussions and have learned a great deal from Michael's unique physical intuition. Working with Michael has helped me to better connect with experiments and I have developed a better intuition for physics in general. I would also like to thank fellow PhD students Magdalena Zych and Fabio Costa, with whom I have worked on several projects. Exploring, developing and working out new ideas with Fabio and Magdalena was a lot of fun and has been very fruitful. We have shared the passion for fundamental physics and I have benefitted from their insights and creativity.

In Vienna, I was also fortunate to be part of the 'quantum family'. The possibility to interact with PhD students and postdocs from various groups that work on quantum science has been tremendously inspirational. The Vienna doctoral program CoQuS offered many unique opportunities and helped to establish connections between the various groups. It would not have been possible without the endless efforts by Markus Arndt, Canan Göser and Christiane Losert. The many interesting discussions with other young researchers in the kitchen, in the park, on the retreats and during journal clubs have greatly broadened my knowledge and interest in theoretical and experimental quantum research. Among the many fellow researchers in Vienna, I would like to particularly thank Mateus Araújo, Garrett Cole, Borivoje Dakic, Adrien Feix, Robert Fickler, Sebastian Hofer, Johannes Kofler, Radek Lapkiewicz, Stefan Nimmrichter, Ognyan Oreshko, William Plick, Sven Ramelow, Jonas Schmöle, Philip Walther and Johannes Wilms.

A PhD in physics is a long endeavor with many ups and downs on the dissertation road. I was extremely fortunate to share the journey and the life in Vienna with my wife Henrietta. I am forever grateful for her endless support, her patience and her devotion throughout the whole time. Without her encouragement this dissertation would not have been possible. I also thank my brother and my parents for their assistance, advice and interest in my work.

Bibliography

[1] M. R. Vanner, I. Pikovski, et al., "Pulsed Quantum Optomechanics", Proc. Natl. Acad. Sci. U.S.A. **108**, 16182–16187 (2011).

[2] I. Pikovski, M. R. Vanner, M. Aspelmeyer, M. Kim, and Č. Brukner, "Probing planck-scale physics with quantum optics", Nature Physics **8**, 393–397 (2012).

[3] M. Zych, F. Costa, I. Pikovski, and Č. Brukner, "Quantum interferometric visibility as a witness of general relativistic proper time", Nature communications **2**, 505 (2011).

[4] M. Zych, F. Costa, I. Pikovski, T. C. Ralph, and Č. Brukner, "General relativistic effects in quantum interference of photons", Classical and Quantum Gravity **29**, 224010 (2012).

[5] I. Pikovski, M. Zych, F. Costa, and C. Brukner, "Universal decoherence due to gravitational time dilation", arXiv preprint arXiv:1311.1095 (2013).

[6] M. P. Bronstein, "K voprosu o vozmozhnoy teorii mira kak tselogo,(on a possible theory of the world as a whole)", Osnovnye problemy kosmicheskoy fiziki (Basic problems of cosmic physics). Kiev, ONTI, 186–218 (1934).

[7] G. Gorelik, "The first steps of quantum gravity and the planck values", Studies in the history of general relativity, 364–379 (1992).

[8] L. B. Okun, "The fundamental constants of physics", Soviet Physics Uspekhi **34**, 818 (1991).

[9] M. Planck, "Ueber das gesetz der energieverteilung im normalspectrum", Annalen der physik **309**, 553–563 (1901).

[10] N. Bohr, "I. on the constitution of atoms and molecules", The London, Edinburgh, and Dublin Philosophical Magazine and Journal of Science **26**, 1–25 (1913).

[11] W. E. Lamb and R. C. Retherford, "Fine structure of the hydrogen atom by a microwave method", Physical Review **72**, 241–243 (1947).

[12] J. Schwinger, "Quantum electrodynamics. i. a covariant formulation", Physical Review **74**, 1439 (1948).

[13] R. P. Feynman, "Space-time approach to quantum electrodynamics", Physical Review **76**, 769 (1949).

[14] R. J. Glauber, "Coherent and incoherent states of the radiation field", Physical Review **131**, 2766 (1963).

[15] E. T. Jaynes and F. W. Cummings, "Comparison of quantum and semiclassical radiation theories with application to the beam maser", Proceedings of the IEEE **51**, 89–109 (1963).

[16] B. W. Shore and P. L. Knight, "The jaynes-cummings model", Journal of Modern Optics **40**, 1195–1238 (1993).

[17] J. P. Dowling and G. J. Milburn, "Quantum technology: the second quantum revolution", Philosophical Transactions of the Royal Society of London. Series A: Mathematical, Physical and Engineering Sciences **361**, 1655–1674 (2003).

[18] N. J. Cerf, G. Leuchs, and E. S. Polzik, *Quantum information with continuous variables of atoms and light* (World Scientific, 2007).

[19] T. J. Kippenberg and K. J. Vahala, "Cavity opto-mechanics", Optics Express **15**, 17172–17205 (2007).

[20] F. Marquardt and S. M. Girvin, "Optomechanics (a brief review)", arXiv preprint arXiv:0905.0566 (2009).

[21] I. Favero and K. Karrai, "Optomechanics of deformable optical cavities", Nature Photonics **3**, 201–205 (2009).

[22] M. Aspelmeyer, S. Gröblacher, K. Hammerer, and N. Kiesel, "Quantum optomechanicsthrowing a glance [invited]", JOSA B **27**, A189–A197 (2010).

[23] G. J. Milburn and M. J. Woolley, "An introduction to quantum optomechanics", Acta Physica Slovaca. Reviews and Tutorials **61**, 483–601 (2011).

[24] P. Meystre, "A short walk through quantum optomechanics", Annalen der Physik **525**, 215–233 (2013).

[25] D. Kleckner, W. Marshall, et al., "High finesse opto-mechanical cavity with a movable thirty-micron-size mirror", Physical review letters **96**, 173901 (2006).

[26] O. Arcizet, P.-F. Cohadon, T. Briant, M. Pinard, and A. Heidmann, "Radiation-pressure cooling and optomechanical instability of a micromirror", Nature **444**, 71–74 (2006).

[27] S. Gröblacher, J. B. Hertzberg, et al., "Demonstration of an ultracold micro-optomechanical oscillator in a cryogenic cavity", Nature Physics **5**, 485–488 (2009).

[28] J. D. Teufel, J. W. Harlow, C. A. Regal, and K. W. Lehnert, "Dynamical backaction of microwave fields on a nanomechanical oscillator", Physical review letters **101**, 197203 (2008).

[29] T. Rocheleau, T. Ndukum, et al., "Preparation and detection of a mechanical resonator near the ground state of motion", Nature **463**, 72–75 (2010).

[30] T. A. Palomaki, J. W. Harlow, J. D. Teufel, R. W. Simmonds, and K. W. Lehnert, "Coherent state transfer between itinerant microwave fields and a mechanical oscillator", Nature **495**, 210–214 (2013).

[31] A. D. OConnell, M. Hofheinz, et al., "Quantum ground state and single-phonon control of a mechanical resonator", Nature **464**, 697–703 (2010).

[32] H. Rokhsari, T. Kippenberg, T. Carmon, and K. J. Vahala, "Radiation-pressure-driven micro-mechanical oscillator", Optics Express **13**, 5293–5301 (2005).

[33] A. Schliesser, O. Arcizet, R. Riviere, G. Anetsberger, and T. J. Kippenberg, "Resolved-sideband cooling and position measurement of a micromechanical oscillator close to the heisenberg uncertainty limit", Nature Physics **5**, 509–514 (2009).

[34] E. Verhagen, S. Deléglise, S. Weis, A. Schliesser, and T. J. Kippenberg, "Quantum-coherent coupling of a mechanical oscillator to an optical cavity mode", Nature **482**, 63–67 (2012).

[35] A. H. Safavi-Naeini, T. P. M. Alegre, M. Winger, and O. Painter, "Optomechanics in an ultrahigh-q two-dimensional photonic crystal cavity", Applied Physics Letters **97**, 181106 (2010).

[36] J. D. Thompson, B. M. Zwickl, et al., "Strong dispersive coupling of a high-finesse cavity to a micromechanical membrane", Nature **452**, 72–75 (2008).

[37] V. B. Braginskii, Y. I. Vorontsov, and F. Y. Khalili, "Optimal quantum measurements in detectors of gravitation radiation", JETP Lett **27** (1978).

[38] C. M. Caves, K. S. Thorne, R. W. P. Drever, V. D. Sandberg, and M. Zimmermann, "On the measurement of a weak classical force coupled to a quantum-mechanical oscillator. i. issues of principle", Reviews of Modern Physics **52**, 341 (1980).

[39] A. F. Pace, M. J. Collett, and D. F. Walls, "Quantum limits in interferometric detection of gravitational radiation", Physical Review A **47**, 3173 (1993).

[40] T. Corbitt, Y. Chen, et al., "An all-optical trap for a gram-scale mirror", Physical review letters **98**, 150802 (2007).

[41] V. B. Braginskii and Y. I. Vorontsov, "Quantum-mechanical limitations in macroscopic experiments and modern experimental technique", Physics-Uspekhi **17**, 644–650 (1975).

[42] C. M. Caves, "Quantum-mechanical noise in an interferometer", Physical Review D **23**, 1693 (1981).

[43] V. B. Braginskii and F. Y. Khalili, *Quantum measurement* (Cambridge University Press, 1995).

[44] K. Jacobs, P. Tombesi, M. J. Collett, and D. F. Walls, "Quantum-nondemolition measurement of photon number using radiation pressure", Physical Review A **49**, 1961 (1994).

[45] S. Mancini and P. Tombesi, "Quantum noise reduction by radiation pressure", Physical Review A **49**, 4055 (1994).

[46] A. Heidmann and S. Reynaud, "Photon noise reduction by reflection from a movable mirror", Physical Review A **50**, 4237 (1994).

[47] A. Heidmann, Y. Hadjar, and M. Pinard, "Quantum nondemolition measurement by optomechanical coupling", Applied Physics B **64**, 173–180 (1997).

[48] C. K. Law, "Interaction between a moving mirror and radiation pressure: a hamiltonian formulation", Physical Review A **51**, 2537–2541 (1995).

[49] S. Bose, K. Jacobs, and P. L. Knight, "Preparation of nonclassical states in cavities with a moving mirror", Physical Review A **56**, 4175 (1997).

[50] S. Bose, K. Jacobs, and P. L. Knight, "Scheme to probe the decoherence of a macroscopic object", Physical Review A **59**, 3204 (1999).

[51] S. Mancini, D. Vitali, V. Giovannetti, and P. Tombesi, "Stationary entanglement between macroscopic mechanical oscillators", The European Physical Journal D-Atomic, Molecular, Optical and Plasma Physics **22**, 417–422 (2003).

[52] W. Marshall, C. Simon, R. Penrose, and D. Bouwmeester, "Towards quantum superpositions of a mirror", Physical Review Letters **91**, 130401 (2003).

[53] D. Vitali, S. Gigan, et al., "Optomechanical entanglement between a movable mirror and a cavity field.", Physical review letters **98**, 030405 (2007).

[54] D. Kleckner, I. Pikovski, et al., "Creating and verifying a quantum superposition in a micro-optomechanical system", New Journal of Physics **10**, 095020 (2008).

[55] C. Genes, D. Vitali, and P. Tombesi, "Simultaneous cooling and entanglement of mechanical modes of a micromirror in an optical cavity", New Journal of Physics **10**, 095009 (2008).

[56] M. Arndt, M. Aspelmeyer, and A. Zeilinger, "How to extend quantum experiments", Fortschritte der Physik **57**, 1153–1162 (2009).

[57] B. Pepper, R. Ghobadi, E. Jeffrey, C. Simon, and D. Bouwmeester, "Optomechanical superpositions via nested interferometry", Physical review letters **109**, 023601 (2012).

[58] K. J. Vahala, "Optical microcavities", Nature **424**, 839–846 (2003).

[59] M. J. Collett and C. W. Gardiner, "Squeezing of intracavity and traveling-wave light fields produced in parametric amplification", Physical Review A **30**, 1386 (1984).

[60] C. Gardiner and P. Zoller, *Quantum noise: a handbook of markovian and non-markovian quantum stochastic methods with applications to quantum optics*, Vol. 56 (Springer, 2004).

[61] I. Wilson-Rae, N. Nooshi, W. Zwerger, and T. J. Kippenberg, "Theory of ground state cooling of a mechanical oscillator using dynamical backaction", Physical Review Letters **99**, 093901 (2007).

[62] F. Marquardt, J. P. Chen, A. A. Clerk, and S. M. Girvin, "Quantum theory of cavity-assisted sideband cooling of mechanical motion", Physical Review Letters **99**, 093902 (2007).

[63] J. Chan, T. P. M. Alegre, et al., "Laser cooling of a nanomechanical oscillator into its quantum ground state", Nature **478**, 89–92 (2011).

[64] J. D. Teufel, T. Donner, et al., "Sideband cooling of micromechanical motion to the quantum ground state", Nature **475**, 359–363 (2011).

[65] S. Mancini, V. Giovannetti, D. Vitali, and P. Tombesi, "Entangling macroscopic oscillators exploiting radiation pressure.", Physical review letters **88**, 120401 (2002).

[66] S. G. Hofer, W. Wieczorek, M. Aspelmeyer, and K. Hammerer, "Quantum entanglement and teleportation in pulsed cavity optomechanics", Physical Review A **84**, 052327 (2011).

[67] J. Zhang, K. Peng, and S. L. Braunstein, "Quantum-state transfer from light to macroscopic oscillators", Physical Review A **68**, 13808 (2003).

[68] V. B. Braginskii, Y. I. Vorontsov, and K. S. Thorne, "Quantum nondemolition measurements", Science **209**, 547–557 (1980).

[69] V. B. Braginskii and F. Y. Khalili, "Quantum nondemolition measurements: the route from toys to tools", Reviews of Modern Physics **68**, 1 (1996).

[70] P. Grangier, J. A. Levenson, and J.-P. Poizat, "Quantum non-demolition measurements in optics", Nature **396**, 537–542 (1998).

[71] M. O.S. M. Hillery, R. F. Oconnell, M. O. Scully, and E. P. Wigner, *Distribution functions in physics: fundamentals* (Springer, 1997).

[72] W. P. Schleich, *Quantum optics in phase space* (John Wiley & Sons, 2001).

[73] M. O. Scully, *Quantum optics* (Cambridge university press, 1997).

[74] S. M. Barnett and P. M. Radmore, *Methods in theoretical quantum optics*, Vol. 15 (Oxford University Press, 2002).

[75] E. Wigner, "On the quantum correction for thermodynamic equilibrium", Physical Review **40**, 749 (1932).

[76] K. Husimi, "Some formal properties of the density matrix", in Proc. phys. math. soc. jpn, Vol. 22, 264 (1940), p. 123.

[77] R. J. Glauber, "Coherent and incoherent states of the radiation field", Physical Review **131**, 2766 (1963).

[78] E. C. G. Sudarshan, "Equivalence of semiclassical and quantum mechanical descriptions of statistical light beams", Physical Review Letters **10**, 277–279 (1963).

[79] C.-W. Lee and H. Jeong, "Quantification of macroscopic quantum superpositions within phase space", Physical review letters **106**, 220401 (2011).

[80] D. F. Walls, "Squeezed states of light", Nature **306**, 141–146 (1983).

[81] G. Leuchs, "Squeezing the quantum fluctuations of light", Contemporary Physics **29**, 299–314 (1988).

[82] K. Vogel and H. Risken, "Determination of quasiprobability distributions in terms of probability distributions for the rotated quadrature phase", Physical Review A **40**, 2847–2849 (1989).

[83] I. Pikovski, *On quantum superpositions in an optomechanical system.* (Diploma Thesis at Freie Universität Berlin, 2009).

[84] A. I. Lvovsky, "Iterative maximum-likelihood reconstruction in quantum homodyne tomography", Journal of Optics B: Quantum and Semiclassical Optics **6**, S556 (2004).

[85] A. I. Lvovsky and M. G. Raymer, "Continuous-variable optical quantum-state tomography", Reviews of Modern Physics **81**, 299 (2009).

[86] U. Leonhardt, "Quantum-state tomography and discrete wigner function", Physical review letters **74**, 4101 (1995).

[87] A. I. Lvovsky, H. Hansen, et al., "Quantum state reconstruction of the single-photon fock state", Physical Review Letters **87**, 050402 (2001).

[88] R. T. Thew, K. Nemoto, A. G. White, and W. J. Munro, "Qudit quantum-state tomography", Physical Review A **66**, 012303 (2002).

[89] E. Skovsen, H. Stapelfeldt, S. Juhl, and K. Mølmer, "Quantum state tomography of dissociating molecules", Physical review letters **91**, 090406 (2003).

[90] M. Hofheinz, H. Wang, et al., "Synthesizing arbitrary quantum states in a superconducting resonator", Nature **459**, 546–549 (2009).

[91] C. R. Müller, B. Stoklasa, et al., "Quantum polarization tomography of bright squeezed light", New Journal of Physics **14**, 085002 (2012).

[92] J. Wei and E. Norman, "On global representations of the solutions of linear differential equations as a product of exponentials", Proceedings of the American Mathematical Society **15**, 327–334 (1963).

[93] K. Kumar, "On expanding the exponential", Journal of Mathematical Physics **6**, 1928–1934 (1964).

[94] R. M. Wilcox, "Exponential operators and parameter differentiation in quantum physics", Journal of Mathematical Physics **8**, 962–982 (1967).

[95] H. Zassenhaus, "Ein verfahren, jeder endlichen p-gruppe einen lie-ring mit der charakteristik p zuzuordnen", in Abhandlungen aus dem mathematischen seminar der universität hamburg, Vol. 13, 1 (Springer, 1939), pp. 200–207.

[96] W. Magnus, "On the exponential solution of differential equations for a linear operator", Communications on pure and applied mathematics **7**, 649–673 (1954).

[97] M. R. Vanner, J. Hofer, G. D. Cole, and M. Aspelmeyer, "Cooling-by-measurement and mechanical state tomography via pulsed optomechanics", Nature communications **4** (2013).

[98] R. Penrose, "On gravity's role in quantum state reduction", General relativity and gravitation **28**, 581–600 (1996).

[99] L. Diosi, "Models for universal reduction of macroscopic quantum fluctuations", Physical Review A **40**, 1165 (1989).

[100] O. Romero-Isart, A. C. Pflanzer, et al., "Large quantum superpositions and interference of massive nanometer-sized objects", Physical review letters **107**, 020405 (2011).

[101] B. P. Abbott, R. Abbott, et al., "Ligo: the laser interferometer gravitational-wave observatory", Reports on Progress in Physics **72**, 076901 (2009).

[102] D. J. Gross and P. F. Mende, "String theory beyond the planck scale", Nuclear Physics B **303**, 407–454 (1988).

[103] T. Yoneya, "On the interpretation of minimal length in string theories", Modern Physics Letters A **4**, 1587–1595 (1989).

[104] L. J. Garay, "Quantum gravity and minimum length", International Journal of Modern Physics A **10**, 145–165 (1995).

[105] E. Witten, "Reflections on the fate of spacetime", Physics today **49**, 24–30 (1996).

[106] N. Seiberg and E. Witten, "String theory and noncommutative geometry", Journal of High Energy Physics **1999**, 032 (1999).

[107] N. Bohr and L. Rosenfeld, "Zur frage der messbarkeit der elektromagnetischen feldgrössen", (1933).

[108] M. P. Bronstein, "Quantentheorie schwacher gravitationsfelder", Physikalische Zeitschrift der Sowietunion **9**, 140–157 (1936).

[109] C. Rovelli, *Quantum gravity* (Cambridge university press, 2004).

[110] C. Kiefer, *Why quantum gravity?* (Springer, 2007).

[111] G. Amelino-Camelia, "Testable scenario for relativity with minimum length", Physics Letters B **510**, 255–263 (2001).

[112] S. Hossenfelder, "A note on theories with a minimal length", Classical and Quantum Gravity **23**, 1815 (2006).

[113] G. Amelino-Camelia, "Quantum gravity phenomenology", Approaches to quantum gravity, 427 (2009).

[114] S. Hossenfelder, ""minimal length scale scenarios for quantum gravity", Living Reviews in Relativity **16** (2013).

[115] M. Maggiore, "A generalized uncertainty principle in quantum gravity", Physics Letters B **304**, 65–69 (1993).

[116] M. Maggiore, "Quantum groups, gravity, and the generalized uncertainty principle", Physical Review D **49**, 5182 (1994).

[117] A. Kempf, "Uncertainty relation in quantum mechanics with quantum group symmetry", Journal of Mathematical Physics **35**, 4483–4496 (1994).

[118] A. F. Ali, S. Das, and E. C. Vagenas, "Discreteness of space from the generalized uncertainty principle", Physics Letters B **678**, 497–499 (2009).

[119] A. Kempf, G. Mangano, and R. B. Mann, "Hilbert space representation of the minimal length uncertainty relation", Physical Review D **52**, 1108 (1995).

[120] A. Kempf and G. Mangano, "Minimal length uncertainty relation and ultraviolet regularization", Physical Review D **55**, 7909 (1997).

[121] F. Brau, "Minimal length uncertainty relation and the hydrogen atom", Journal of Physics A: Mathematical and General **32**, 7691 (1999).

[122] F. Scardigli, "Generalized uncertainty principle in quantum gravity from micro-black hole gedanken experiment", Physics Letters B **452**, 39–44 (1999).

[123] L. N. Chang, D. Minic, N. Okamura, and T. Takeuchi, "Exact solution of the harmonic oscillator in arbitrary dimensions with minimal length uncertainty relations", Physical Review D **65**, 125027 (2002).

[124] I. Dadić, L. Jonke, and S. Meljanac, "Harmonic oscillator with minimal length uncertainty relations and ladder operators", Physical Review D **67**, 087701 (2003).

[125] C. Quesne and V. M. Tkachuk, "Deformed algebras, position-dependent effective masses and curved spaces: an exactly solvable coulomb problem", Journal of Physics A: Mathematical and General **37**, 4267 (2004).

[126] C. Quesne and V. M. Tkachuk, "Dirac oscillator with nonzero minimal uncertainty in position", Journal of Physics A: Mathematical and General **38**, 1747 (2005).

[127] K. Nozari and T. Azizi, "Some aspects of gravitational quantum mechanics", General Relativity and Gravitation **38**, 735–742 (2006).

[128] S. Das and E. C. Vagenas, "Universality of quantum gravity corrections", Physical review letters **101**, 221301 (2008).

[129] S. Das and R. B. Mann, "Planck scale effects on some low energy quantum phenomena", Physics Letters B **704**, 596–599 (2011).

[130] K. Nozari, "Some aspects of planck scale quantum optics", Physics Letters B **629**, 41–52 (2005).

[131] C. Quesne and V. M. Tkachuk, "Composite system in deformed space with minimal length", Physical Review A **81**, 012106 (2010).

[132] G. J. Milburn, S. Schneider, and D. F. V. James, "Ion trap quantum computing with warm ions", Fortschritte der Physik **48**, 801–810 (2000).

[133] A. Sørensen and K. Mølmer, "Entanglement and quantum computation with ions in thermal motion", Physical Review A **62**, 022311 (2000).

[134] D. Leibfried, B. DeMarco, et al., "Experimental demonstration of a robust, high-fidelity geometric two ion-qubit phase gate", Nature **422**, 412–415 (2003).

[135] B. Yurke and D. Stoler, "Generating quantum mechanical superpositions of macroscopically distinguishable states via amplitude dispersion", Physical review letters **57**, 13 (1986).

[136] B Yurke and D Stoler, "Quantum behavior of a four-wave mixer operated in a nonlinear regime", Physical Review A **35**, 4846 (1987).

[137] H.-P. Breuer and F. Petruccione, *The theory of open quantum systems* (Oxford university press, 2002).

[138] M. Plenio, "Private communication",

[139] F. Girelli and D. Poulin, "Quantum reference frames and deformed symmetries", Physical Review D **77**, 104012 (2008).

[140] G. Amelino-Camelia, L. Freidel, J. Kowalski-Glikman, and L. Smolin, "Relative locality and the soccer ball problem", Physical Review D **84**, 087702 (2011).

[141] N. R. Bruno, G. Amelino-Camelia, and J. Kowalski-Glikman, "Deformed boost transformations that saturate at the planck scale", Physics Letters B **522**, 133–138 (2001).

[142] J. Magueijo and L. Smolin, "Lorentz invariance with an invariant energy scale", Physical Review Letters **88**, 190403 (2002).

[143] S. Hossenfelder, "Deformed special relativity in position space", Physics Letters B **649**, 310–316 (2007).

[144] C. J. Hogan, "Measurement of quantum fluctuations in geometry", Physical Review D **77**, 104031 (2008).

[145] J. D. Bekenstein, "Is a tabletop search for planck scale signals feasible?", Physical Review D **86**, 124040 (2012).

[146] G. Amelino-Camelia, J. Ellis, N. E. Mavromatos, D. V. Nanopoulos, and S. Sarkar, "Tests of quantum gravity from observations of gamma-ray bursts", Nature **393**, 763–765 (1998).

[147] G. Amelino-Camelia and L. Smolin, "Prospects for constraining quantum gravity dispersion with near term observations", Physical Review D **80**, 084017 (2009).

[148] L. D. Landau and E. M. Lifshits, *The classical theory of fields*, Vol. 2 (Butterworth-Heinemann, 1975).

[149] S. Weinberg, "Gravitation and cosmology: principles and applications of the general theory of relativity", (1972).

[150] C. Misner, K. Thorne, and J. A. Wheeler, *Gravitation* (Freeman, 1973).

[151] C. M. Will, *Theory and experiment in gravitational physics* (Cambridge University Press, 1993).

[152] E. Bertschinger, "Gravitation in the weak-field limit", Physics 8.962 (MITs GR course) lecture notes **22**.

[153] S. M. Carroll, *Spacetime and geometry. an introduction to general relativity*, Vol. 1 (2004).

[154] H. C. Ohanian and R. Ruffini, *Gravitation and spacetime* (Cambridge University Press, 2013).

[155] J. H. Taylor, L. A. Fowler, and P. M. McCulloch, "Measurements of general relativistic effects in the binary pulsar psr 1913+ 16", Nature **277**, 437–440 (1979).

[156] M. Tegmark, "Measuring spacetime: from the big bang to black holes", Science **296**, 1427–1433 (2002).

[157] R. V. Pound and G. A. Rebka Jr., "Gravitational red-shift in nuclear resonance", Physical Review Letters **3**, 439 (1959).

[158] J. C. Hafele and R. E. Keating, "Around-the-world atomic clocks: observed relativistic time gains", Science **177**, 168–170 (1972).

[159] F. W. Dyson, A. S. Eddington, and C. Davidson, "A determination of the deflection of light by the sun's gravitational field, from observations made at the total eclipse of may 29, 1919", Philosophical Transactions of the Royal Society of London. Series A, Containing Papers of a Mathematical or Physical Character, 291–333 (1920).

[160] S. S. Shapiro, J. L. Davis, D. E. Lebach, and J. S. Gregory, "Measurement of the solar gravitational deflection of radio waves using geodetic very-long-baseline interferometry data, 1979–1999", Physical review letters **92**, 121101 (2004).

[161] I. I. Shapiro, G. H. Pettengill, et al., "Fourth Test of General Relativity: Preliminary Results", Physical Review Letters **20**, 1265–1269 (1968).

[162] C. W. F. Everitt, D. B. DeBra, et al., "Gravity probe b: final results of a space experiment to test general relativity", Physical Review Letters **106**, 221101 (2011).

[163] A. Einstein, "Über den einfluß der schwerkraft auf die ausbreitung des lichtes", Annalen der Physik **340**, 898–908 (1911).

[164] I. I. Shapiro, "Fourth Test of General Relativity", Physical Review Letters **13**, 789–791 (1964).

[165] I. I. Shapiro, M. E. Ash, et al., "Fourth Test of General Relativity: New Radar Result", Physical Review Letters **26**, 1132–1135 (1971).

[166] B. Bertotti, L. Iess, and P. Tortora, "A test of general relativity using radio links with the Cassini spacecraft", Nature **425**, 374–376 (2003).

[167] R. Colella, A. W. Overhauser, and S. A. Werner, "Observation of gravitationally induced quantum interference", Physical Review Letters **34**, 1472–1474 (1975).

[168] A. W. Overhauser and R. Colella, "Experimental test of gravitationally induced quantum interference", Physical Review Letters **33**, 1237 (1974).

[169] M. Kasevich and S. Chu, "Measurement of the gravitational acceleration of an atom with a light-pulse atom interferometer", Applied Physics B **54**, 321–332 (1992).

[170] A. Peters, K. Y. Chung, and S. Chu, "Measurement of gravitational acceleration by dropping atoms", Nature **400**, 849–852 (1999).

[171] V. V. Nesvizhevsky, H. G. BoÈrner, et al., "Quantum states of neutrons in the earth's gravitational field", Nature **415**, 297–299 (2002).

[172] A. Peters, K. Y. Chung, B. Young, J. Hensley, and S. Chu, "Precision atom interferometry", Philosophical Transactions of the Royal Society of London. Series A: Mathematical, Physical and Engineering Sciences **355**, 2223–2233 (1997).

[173] H. Müller, A. Peters, and S. Chu, "A precision measurement of the gravitational redshift by the interference of matter waves", Nature **463**, 926–929 (2010).

[174] S. Dimopoulos, P. W. Graham, J. M. Hogan, and M. A. Kasevich, "Testing general relativity with atom interferometry", Physical review letters **98**, 111102 (2007).

[175] N. D. Birrell and P. C. W. Davies, *Quantum fields in curved space*, 7 (Cambridge university press, 1984).

[176] S. W. Hawking, "Black hole explosions", Nature **248**, 30–31 (1974).

[177] S. W. Hawking, "Particle creation by black holes", Communications in mathematical physics **43**, 199–220 (1975).

[178] C. Lämmerzahl, "A hamilton operator for quantum optics in gravitational fields", Physics Letters A **203**, 12–17 (1995).

[179] R. J. Adler and P. Chen, "Gravitomagnetism in quantum mechanics", Physical Review D **82**, 025004 (2010).

[180] R. J. Adler, P. Chen, and E. Varani, "Gravitomagnetism and spinor quantum mechanics", Physical Review D **85**, 025016 (2012).

[181] A. Einstein and L. Infeld, *The evolution of physics: the growth of ideas from early concepts to relativity and quanta* (CUP Archive, 1961).

[182] C. Anastopoulos, "Quantum theory of nonrelativistic particles interacting with gravity", Physical Review D **54**, 1600 (1996).

[183] M. P. Blencowe, "Effective field theory approach to gravitationally induced decoherence.", Physical review letters **111**, 021302 (2013).

[184] C. Anastopoulos and B. L. Hu, "A master equation for gravitational decoherence: probing the textures of spacetime", Classical and Quantum Gravity **30**, 165007 (2013).

[185] M. Wieśniak, V. Vedral, and Č. Brukner, "Heat capacity as an indicator of entanglement", Physical Review B **78**, 064108 (2008).

[186] M. Arndt, O. Nairz, et al., "Wave–particle duality of c60 molecules", nature **401**, 680–682 (1999).

[187] S. Gerlich, S. Eibenberger, et al., "Quantum interference of large organic molecules", Nature communications **2**, 263 (2011).

[188] S. Eibenberger, S. Gerlich, M. Arndt, M. Mayor, and J. Tüxen, "Matter–wave interference of particles selected from a molecular library with masses exceeding 10000 amu", Physical Chemistry Chemical Physics **15**, 14696–14700 (2013).

[189] P. F. Barker and M. N. Shneider, "Cavity cooling of an optically trapped nanoparticle", Physical Review A **81**, 023826 (2010).

[190] T. Li, S. Kheifets, and M. G. Raizen, "Millikelvin cooling of an optically trapped microsphere in vacuum", Nature Physics **7**, 527–530 (2011).

[191] P. Asenbaum, S. Kuhn, S. Nimmrichter, U. Sezer, and M. Arndt, "Cavity cooling of free silicon nanoparticles in high vacuum", Nature communications **4** (2013).

[192] N. Kiesel, F. Blaser, et al., "Cavity cooling of an optically levitated submicron particle", Proceedings of the National Academy of Sciences **110**, 14180–14185 (2013).

[193] S. Nimmrichter, K. Hornberger, P. Haslinger, and M. Arndt, "Testing spontaneous localization theories with matter-wave interferometry", Physical Review A **83**, 043621 (2011).

[194] A. Bassi, K. Lochan, S. Satin, T. P. Singh, and H. Ulbricht, "Models of wavefunction collapse, underlying theories, and experimental tests", Reviews of Modern Physics **85**, 471 (2013).

[195] E. Joos and H. D. Zeh, "The emergence of classical properties through interaction with the environment", Zeitschrift für Physik B Condensed Matter **59**, 223–243 (1985).

[196] M. R. Gallis and G. N. Fleming, "Environmental and spontaneous localization", Physical Review A **42**, 38 (1990).

[197] K. Hornberger and J. E. Sipe, "Collisional decoherence reexamined", Physical Review A **68**, 012105 (2003).

[198] R. Alicki, "Search for a border between classical and quantum worlds", Physical Review A **65**, 034104 (2002).

[199] C. F. Bohren and D. R. Huffman, *Absorption and scattering of light by small particles* (John Wiley & Sons, 2008).

[200] K. Hansen and E. E. B. Campbell, "Thermal radiation from small particles", Physical Review E **58**, 5477 (1998).

[201] K. Hornberger, J. E. Sipe, and M. Arndt, "Theory of decoherence in a matter wave talbot-lau interferometer", Physical Review A **70**, 053608 (2004).

[202] J. W. Lamb, "Miscellaneous data on materials for millimetre and submillimetre optics", International Journal of Infrared and Millimeter Waves **17**, 1997–2034 (1996).

[203] O. V. Mazurin, M. V. Streltsina, and T. P. Shvaiko-Shvaikovskaya, "Handbook of glass data. part a. silica glass and binary silicate glasses", Elsevier Science Publishers B. V., 1983, xv+ 669, 1983 (1983).

[204] J. Krupka, K. Derzakowski, M. Tobar, J. Hartnett, and R. G. Geyer, "Complex permittivity of some ultralow loss dielectric crystals at cryogenic temperatures", Measurement Science and Technology **10**, 387 (1999).